New Techniques for the Measurement of Radiated Emissions in a Screened Room for Frequencies up to 200MHz

Submitted for the degree of D.Phil

by

Linda Dawson

Department of Electronics

University of York

August 1989

LIST OF CONTENTS

LIST OF CONTENTS

LIST OF CONTENTS

LIST OF FIGURES

LIST OF FIGURES

LIST OF FIGURES

LIST OF FIGURES

LIST OF TABLES

SUMMARY

This thesis describes the work carried out to develop measurement techniques for the assessment of electromagnetic emissions within screened rooms for frequencies up to 200 MHz.

A general introduction into the techniques presently used to assess the radiated emissions from a piece of equipment is given. Improved models to describe propagation mechanisms in a screened room in the frequency range below 30MHz are described. These are then used to develop two measurement techniques for describing a small source in terms of its equivalent dipole moment for the frequency range up to 30 MHz. This includes techniques to identify the type of source present (i.e. magnetic or electric dipole).

The propagation mechanisms in a screened room in the frequency range 30 to 200 MHz are then discussed and the effect of the cavity resonances on the measured fields is shown. A technique for reducing the Q of the resonances is presented and the results of measurements using this technique with two types of material are given.

This thesis concludes that it is possible to obtain the moment of an equivalent dipole for sources below 30 MHz and that is possible to reduce the effect of resonances on measurements made at frequencies where the screened room acts as a cavity resonator. The measurements are also more repeatable because there is a reduced dependence on source and antenna positioning.

DECLARATION

The following papers have been presented at conferences and published in the associated proceedings.

1. 'New screened room techniques for the measurement of RFI', presented at 5th IERE International Conference on EMC, October 1986. Joint author with Dr. A.C.Marvin

2. 'Efficient use of absorber in shielded enclosures used for emission measurement', presented at Enigma Variations Conference, June 1987. Joint author with Dr. A.C.Marvin. Reprinted in Enigma Variations News.

3. 'Alternative methods of damping resonances in a screened room in the frequency range 30 to 200MHz', presented at 7th IERE International Conference on EMC, September 1988. Joint author with Dr. A.C.Marvin.

4. 'Techniques for damping resonances in screened rooms in the frequency range 30 to 200 MHz', presented at Enigma Variations Conference, May 1989. Joint author with Dr. A.C.Marvin.

The following two papers have been published.

1. 'Improved techniques for the measurement of radiated emissions inside a screened room', IEE Electronics Letters, Vol.22 No.2, Jan 1986. Joint author with Dr. A.C.Marvin.

2. 'New screened room techniques for the measurement of RFI', J.IERE, Vol.58 No.1, Jan/Feb 1988. Joint author with Dr. A.C.Marvin

All the papers are included in Appendix F

ACKNOWLEDGEMENTS

Thanks are due to the SERC who funded the major part of this work and to Emerson and Cuming Ltd who funded the work carried out on magnetic materials. In particular thanks are due to Eddie Weston and Hugo Pues of Emerson and Cuming for their help during the latter part of the work.

Grateful thanks also go to Andy Marvin, who set this project up and supervised the work, for his help and encouragement throughout the project.

In addition grateful thanks go to my mother (Valerie Steele) and Maryon Marshman for their help with the proof reading and improvement of the English. Thanks also go to the rest of my colleagues for their help and encouragement over the last few months.

Finally, many thanks go to my husband John for the help and encouragement he has given me and for putting up with me panicking over this thesis.

GLOSSARY OF SYMBOLS AND ABBREVIATIONS

ABBREVIATIONS

ANSI	American National Standards Institute
BSI	British Standards Institute
CISPR	Commite International Special des Perturbations Radioelectriques
DC	Direct Current
DOD	Department of Defence
DTI	Department of Trade and Industry
EMC	Electromagnetic Compatibility
EMI	Electromagnetic Interference
EUT	Equipment Under Test
FCC	Federal Communications Commission
FTZ	Fernmelde-technisches Zentralamt
IEC	International Electrotechnical Commission
RAM	Radio Absorbent Material
RF	Radio Frequency
TE	Transverse Electric
TM	Transverse Magnetic
TEM	Transverse Electromagnetic
VDE	Verbandes Deutscher Electrotechniker

SYMBOLS

a,b,d	dimensions of waveguide and cavity resonator
B	
C	capacitance
E	electric field
f	frequency
H	magnetic field
I	current
j	complex operator
L	length
l	height of radiating monopole
M	moment
m,n,p	mode numbers for waveguides and cavity resonators
Q	quality factor
R	resistance
U	Eulers constant
V	voltage
X	reactance
x,y,z	distance in the x,y,z directions
Y	admittance
Z	impedance

γ	propagation constant
ϵ	permitivity
η	intrinsic impedance
λ	wavelength
μ	permeability
π	pi
σ	conductivity
ω	angular frequency

1. INTRODUCTION

1.1 Introduction

The use of electronic equipment has become more widespread and the speed at which digital equipment works has become faster; subsequently the electromagnetic spectrum is getting increasingly congested with spurious electromagnetic emissions as well as intended ones (e.g. broadcast). Any piece of equipment which has wires carrying a varying electric current will radiate to some extent and likewise will also act as a receiving antenna being susceptible to pickup from any external electromagnetic field [Hyde and Leak 1986]. This may cause problems with the reception of wanted electromagnetic signals [Schildt 1979]. However, excessive pickup may also cause equipment to fail, possibly with catastrophic consequences [Deb and Mukherjee 1985]. It is therefore necessary to design electronic equipment so that two or more items may operate in the same environment without detrimental effect to the operation of either.

The ability of two or more pieces of electronic equipment to exist in the same electromagnetic environment, without degradation of the operation of either, is termed Electromagnetic Compatibility (EMC). The impairment of operation caused by electromagnetic disturbance is termed Electromagnetic Interference (EMI).

The effects of EMI were first noticed as long ago as the 1920s [Webb 1985] and the first EMC standards were published during the second world war [JAN-1-222]. Since then there has been an ever increasing problem with interference resulting in a proliferation of standards to cover both military and civilian (domestic, medical and industrial) applications.

There are two aspects to the specifications :-

a) regulation of susceptibility of equipment so that it will operate correctly in specified field levels;

b) regulation of the spurious emissions from equipment to enable other equipment to operate in the same environment and to prevent/reduce interference with communications systems.

It is therefore necessary to create known fields for susceptibility testing and to be able to measure emissions accurately. Various specifications describe test set-ups and limits, the use of which depends on several factors:-

a) type and use of equipment (e.g military, domestic, medical);

b) size of equipment;

c) frequency range;

Limits are established by bodies such as:-

a)BSI British Standards Institute;

b)DOD Department of Defence - US Military standards;

c)VDE Verbandes Deutscher Electrotechniker - West Germany;

d)ANSI American National Standards Institute;

The limits are based on recommendations from CISPR (Commite International Special des Perturbations Radioelectriques) a part of the IEC (International Electrotechnical Commission).

Limits are enforced by bodies such as :-

a)DTI Department of Trade and Industry (UK)

d)FTZ West German Post Office

a)FCC Federal Communications Commission (USA)

Various methods are available for the measurement of radiated emissions, the most commonly used ones are as follows:-

a) Open field test site;

b) Screened room;

c) Anechoic chamber;

d) Stirred mode (reverberating) chamber;

e) TEM cell (Crawford cell);

Each method has its own strengths and weaknesses and no one method is ideal for all measurements. Emission test methods [BS 6527, VDE 0877, FCC/OST MP-4] are often defined separately from the radiation limits [VDE 0871, FCC CFR47 part 15], although some standards specify both [BS 800, DEF-STAN 59/41]. Two papers which compare some or all of these methods are by Donaldson, Free, Robertson and Woody 1972; Ma, Kanda, Crawford and Larsen 1985. The major measurement methods are described below and the limitations of each are explained.

1.2 Open Field Test Site

The open field test site is the basic test site specified for frequencies above 30 MHz, by the FCC and VDE. The site layout and quality are themselves the subjects of various specifications [e.g. VDE 0877, FCC OST 55].

An open field test site (which is defined by CISPR) has dimensions shown in Fig.1.2.1 . The area within the ellipse should be flat (to within 5cm [OST 55]) and clear of any obstructions. The area around this should also be clear of any large reflecting objects for as great

a distance as is practical. The distance d between the source and measuring antenna is usually 3, 10 or 30m depending on the specification in use and the equipment under test. The site attenuation, which is defined as the ratio of input power to a source antenna to the power induced in the load impedance connected to the receiving antenna, must fall within set limits (e.g +/- 3 dB from the calculated response) to allow comparison between different sites [FCC docket 21371, 1977: Kawana and Miyajima 1979 : Fitzgerrell 1986]. A conducting ground plane is usually required to ensure that the attenuation is within the specified limits. The procedure for site attenuation measurement may vary according to the specification being used [FCC OST 55, VDE 0877].

Fields are measured using standard antennas with known antenna factors. However, these antenna factors (which are calculated by the manufacturers or measured by standards laboratories) assume far field radiation patterns from the source. This is not always the case at the lower frequencies (e.g below 50 MHz at 3m separation) [Smith, German and Pate 1982]. There is some degree of near field coupling between the source and sensing antenna [Kawana and Miyajima 1979 : Fitzgerrell 1986]. The antenna factors also assume conditions of free space which is not the case when there is a ground plane present [FCC docket 21371, 1977]. Reflections from the ground plane also cause errors in the field which is calculated from measured results [Fitzgerrell 1983, Feh and Bianchi 1979].

The receiving antenna is raised on a mast (over a specified range of heights) to find the maximum received signal caused by the reflected and direct waves adding in phase. The positions of the field maxima are a function of the frequency of the emissions, the distance

between the source and the antenna and also the height of the source. The size of a source determines its position as small items are placed on a non-conducting table while larger items are placed on the ground plane.

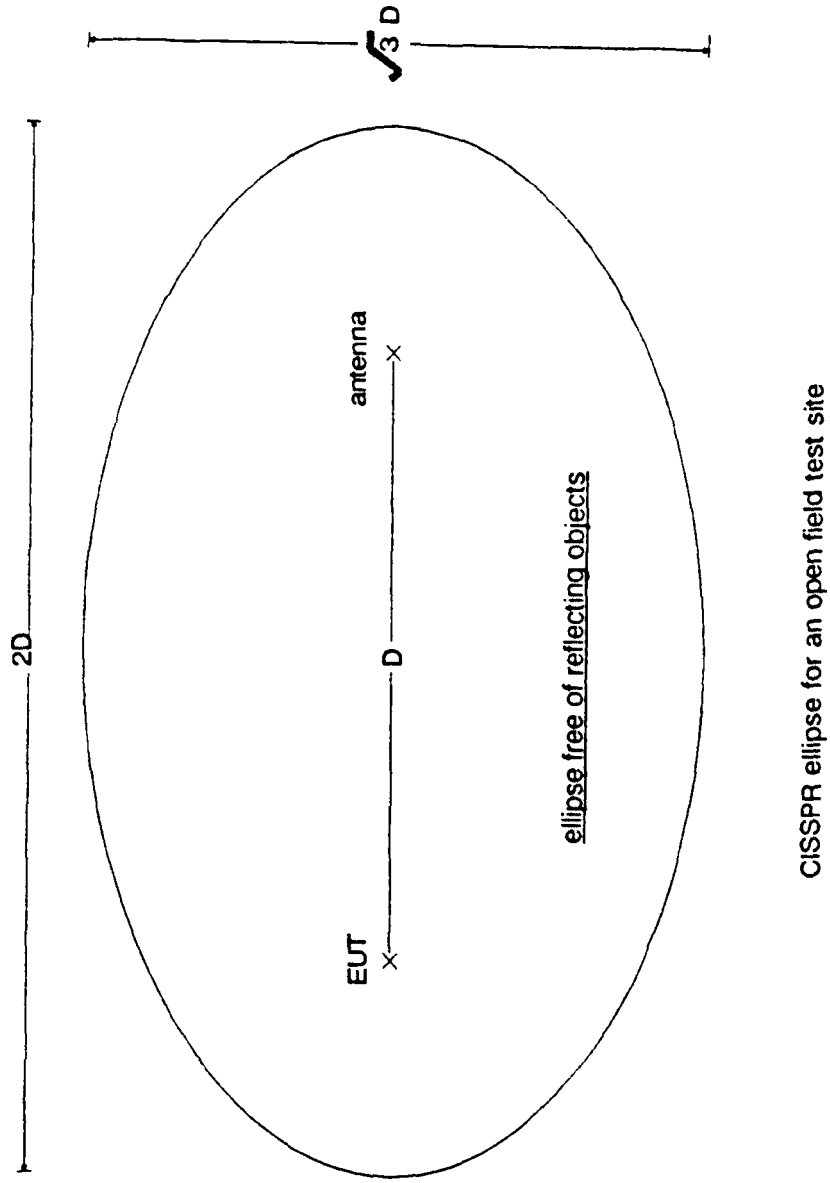

Fig.1.2.1 The open field test site (showing the CISPR ellipse)

Other papers which investigate the effect of these and other parameters on the site attenuation and accuracy of the resulting measurements are [Mis and Visek 1986, Heisman 1987, Bronaugh 1987, Tang and Gunn 1987, Pavlasek and Mishra 1987, Bennet 1983]

Since open field measurements are mostly far field it is impossible to distinguish between electric and magnetic dipole sources as the wave impedance for both source types is 377Ω. Knowledge of the type of electromagnetic source causing radiation from a piece of equipment could assist in determining the optimum technique for reducing the emissions as the methods of screening electric (high impedance) and magnetic (low impedance) sources are different.

The open field test site is widely used by test houses carrying out commercial emission testing. Unfortunately, environmental considerations mean that it is not always possible to use such a site. A large area of open ground is needed, 52 × 60m for a 30m test site, which is expensive and rare in densely populated countries. Also the ambient electromagnetic environment is of a high level in urban areas. Finally, the British climate presents practical difficulties for outdoor testing and large investment is required if the site is to be covered with a suitable building.

When constructing an open site it is also necessary to provide an enclosure for the test equipment to isolate it from the test environment. This should be close but should not interfere with the test setup (therefore it is often below ground). The test distance is specified as being the perpendicular distance from the antenna to the front of the equipment under test; which is defined as a vertical plane through the part of the equipment which is closest to the

antenna. With large test objects the measured signal may be heavily dependent on the relative positions of the source and the sensing antenna, particularly if they are too close together. The minimum test distance allowed is calculated using the dimensions of the equipment under test in order to minimise the effect of the relative positions of the source and the sensing antenna.

The biggest advantage of open site measurements is that the equipment under test is not limited in size by the test environment, only by the practicality of moving it to the site.

1.3 Screened Rooms

A screened room is basically a large metal box (e.g 3m × 4m × 5m) which shields equipment within it from the external ambient environment. As such, a screened room takes up relatively little space compared to an open field test site and is less expensive to purchase than an open field test site. A screened room can be installed within an existing test facility which may simplify the logistics of EMC testing compared with open field testing where the test site may be at some distance from other test facilities. A screened room is available for testing in all weather conditions whereas clement conditions are required for open field testing unless an expensive 'transparent' building covers the site.

Although screened rooms overcome two problems of the open field test site they do introduce others. The metallic construction of the room means that it acts as a waveguide cavity resonator with a cut-off frequency below which fields do not propagate very efficiently

[Harrington 1961], and above which exhibit a series of high Q resonances [Keiser 1987]. As well as the high Q of the resonances the fields of the individual modes change significantly over a relatively small distance, particularly for higher order modes. Several modes with the same resonant frequency may exist in rooms where the dimensions have specific ratios. It is then possible for a position inside the room, in which individual modes have non zero fields, to have a zero field because the sum of the individual mode fields is zero. This means that measurements are very sensitive to the position of both the sensing antenna and the source [Magnuson 1982]; it is therefore very difficult to repeat measurements on the same piece of equipment and get the same results. It is also difficult to compare the results from different rooms due to the dependence of the resonances on the room dimensions. Apart from the problems associated with the nature of the room itself, it is also a mistake to rely on antenna correction factors to give values for the field strength at a point within a screened room. The fields within a screened room are not 'plane wave' which means that antenna factors measured under plane wave conditions are unlikely to be correct. The proximity of the conducting walls will also provide another source of errors in the antenna factors due to a capacitive loading of the antenna.

These limitations also make it difficult to relate screened room measurements to open field measurements.

A typical screened room test setup for frequencies up to 30 MHz is shown in Fig. 1.3.1; with this arrangement a series of TEM mode resonances may also exist on the conducting bench and extension [Marvin 1984].

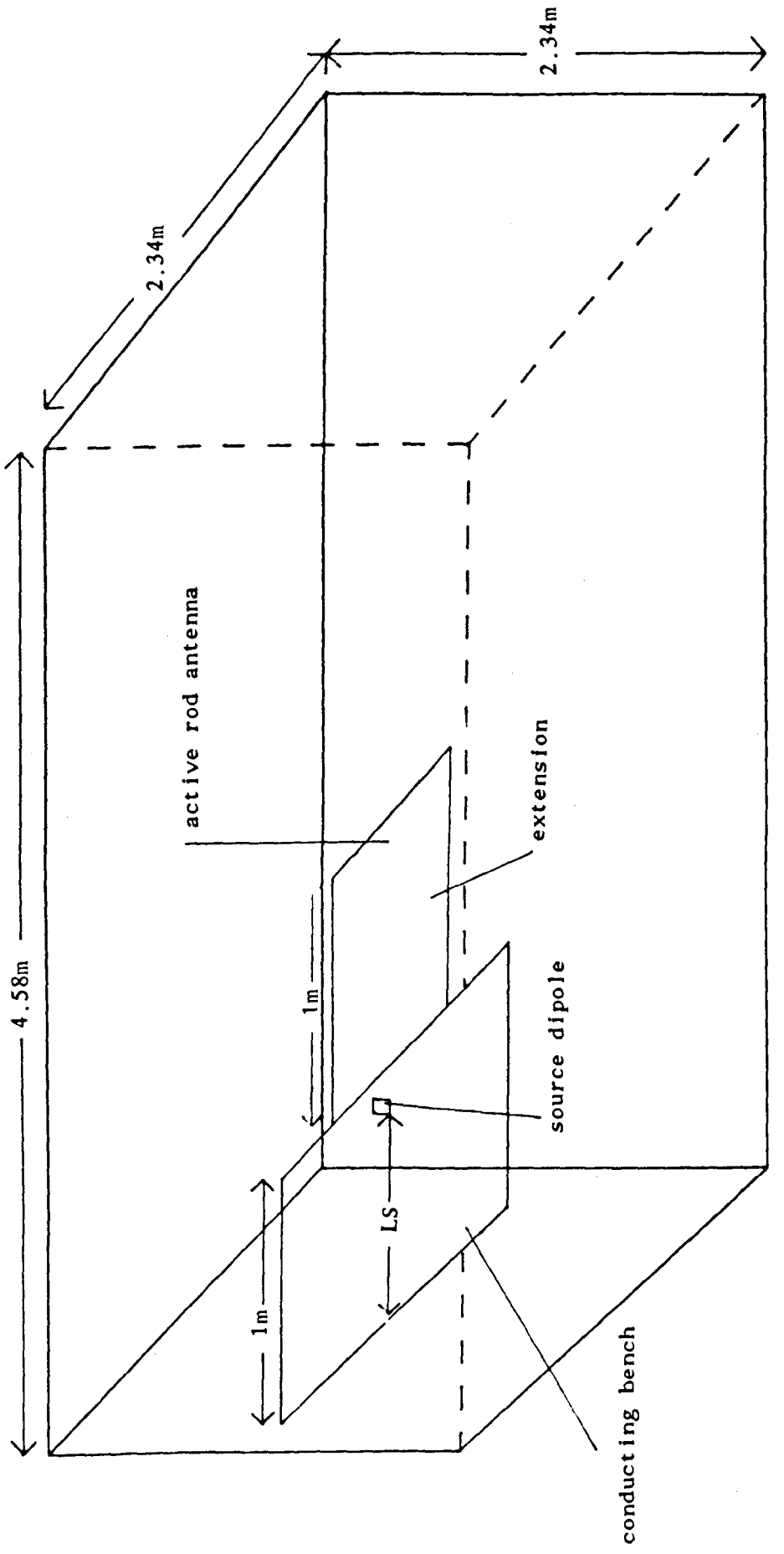

Fig.1.3.1 Typical screened room test setup

Large screened enclosures can be constructed out of wire mesh to give screening at low frequencies as this is cheaper than sheet metal. However, if the room is large there will also be a corresponding drop in the cut off frequency (i.e it will start to resonate at much lower frequencies). It will not give such high screening of the ambient signals, particularly at higher frequencies where the mesh size approaches the order of a wavelength.

The problems associated with screened rooms mean that the screened room is considered unsuitable for amplitude measurements by many aurthorities. It is generally only used to obtain the frequencies of emissions whose amplitudes are then measured more accurately on an open field test site. Where measurements are made inside a room the uncertainty in the results can be very large (up to +/- 40dB) [Donaldson, Free, Robertson and Woody 1972]. Screened room measurements are called for in various military specifications due to the low level of ambient signals inside the room. Conducted emission measurements are made in them to make use of the filtered power supply and minimise pickup of external signals by the cables.

Two methods of improving the accuracy of measurements made within a screened room have been suggested. The first of these is to use a 'hooded antenna' [Free 1967] which entails surrounding an antenna with a shielded box lined with absorbent tiles. The box is open in the direction of the EUT (equipment under test) only. The aim is to reduce reflections from the conducting walls etc, which the antenna receives so that only the direct wave is measured. Unfortunately, this method does not work well below about 200 MHz as the ferrite tile absorbers used are not effective at low frequencies. This is the frequency range which has greatest problems due to the depth and cost of absorber

required to make the room anechoic (see next section). The second method which has been suggested is to build rooms underground without metal walls [Donaldson, Free, Robertson, Woody 1978]. The suggestion is that the earthen walls of such a chamber will be lossy and the Q of such a cavity will be low. A suitable depth of soil above the room will give the required shielding to the external electromagnetic environment. However, as far as can be determined no such chambers have actually been built and tested. If this type of construction did work the major problem would be to find a suitable site which would then not need supporting with a metal structure.

1.4 Anechoic Chambers

An anechoic chamber consists of a screened room with its walls, ceiling and floor lined with radio absorbent material (RAM) to reduce reflections of the incident wave. The chamber then models free space with no reflections of the emitted wave and therefore no resonances. The RAM is usually a carbon loaded foam with a defined conductivity. At microwave frequencies a multilayer foam can be used. In this type of absorber the conductivity is increased with depth into the material to obtain a gradual reduction in the wave impedance with increasing depth into the absorber so that a plane wave hitting the surface of the block is absorbed rather than reflected. The absorber is designed to work best with a metal backing so must be mounted on conducting walls to be most effective as a plane wave absorber. At lower frequencies carbon loaded foam with a uniform loading is shaped into pyramids to have the same effect. The depth of the pyramids must be greater than $\lambda/4$ to work effectively. The RAM is also most efficient

for a wave whose direction of propagation is perpendicular to the plane of the absorber, not at any other angle (the absorption at other angles varies depending on the type of absorber). As the absorbers are all designed to be most effective on waves with 377Ω impedance they are not as efficient when they are within the near field of the source where the wave impedance can have any value.

The depth of absorber required for an anechoic chamber means that for frequencies lower than 100/ 200 MHz it is very expensive to build such a chamber as the room will need to be very large and a great deal of absorber will be required. For example at 30 MHz the pyramids would need to be 2.5m deep giving a minimum dimension for the room of 5m without being able to get into it. For all the absorber to be in the far field of the source at this frequency the internal dimensions must then be 3.3m before any allowance is made for the sensing antenna; giving minimum dimensions of 8.3m for a point source.

Even in the best anechoic chamber only a relatively small portion of the room is a 'quiet zone' (i.e is free from reflections from the walls) which means that the source and sensing antenna must be carefully positioned. As with free space measurements, the sensing antenna is not always in the far field region of the source and the room must be calibrated for each different test layout to be used. When the room is well designed and operated at high enough frequencies for the far field conditions to be valid it can provide conditions which approximate to free space. Such rooms can also be used for susceptibility measurements when an antenna is used to produce the incident field. The room provides the shielding necessary to prevent the test causing a nuisance to other equipment or broadcast users. As it approximates free space the fields generated can be calculated

using known free space antenna factors.

Semi anechoic chambers are also used. In these the floor is not lined with absorber. They are not as good as full anechoic chambers due to the reflections which occur from the floor but are less resonant than an empty screened room. The reflections from the floor will give a measurement which is closer to that of the open field test site than a fully anechoic chamber and will mean that the sensing antenna has to be scanned over a range of heights as with the open field test site.

Further descriptions of anechoic chambers and comparisons with other types of test site are given by Mishra and Kashyap 1987, Emerson 1973 and 1977; Donaldson, Free, Robertson and Woody 1978; Hofman 1983; German 1982; Gonschorek and Kohling 1984 and Tsaliovich 1987

1.5 Stirred Mode (Reverberating) Chambers

Stirred mode chambers are screened rooms which are operated well above cut-off so that they are heavily overmoded. They have at least one large rotating paddle (Fig.1.5.1) which is used to 'stir' the modes in the room [Liu, Chang and Ma 1983 : Corona, Latmiral, Paolini and Piccioli 1986]. The effect of the rotating paddle is to adjust the resonant frequencies and positions of field maxima so that the average of the radiated power received by the measuring antenna is proportional to the power radiated by the source into the room. It is assumed that this is the same as the total power which would be radiated by the source into free space. The average power measured in

the chamber is independent of the gain of the receiving antenna but does depend upon the dimensions and geometry of the room [Corona, Latmiral and Paolini 1980]. This means that it is particularly important to calibrate a room with a known source if measurements from different facilities are to be compared meaningfully. The average received power is also independent of the gain and orientation of the source.

It is necessary for the power to be averaged over a period which is greater than the period of one rotation of the paddle at each frequency of interest. This means that a measurement may take longer than with other test methods. If more than one paddle is used it is necessary to ensure that the paddles rotate at different speeds to ensure that standing patterns which may effect the measurements are not set up between the paddles.

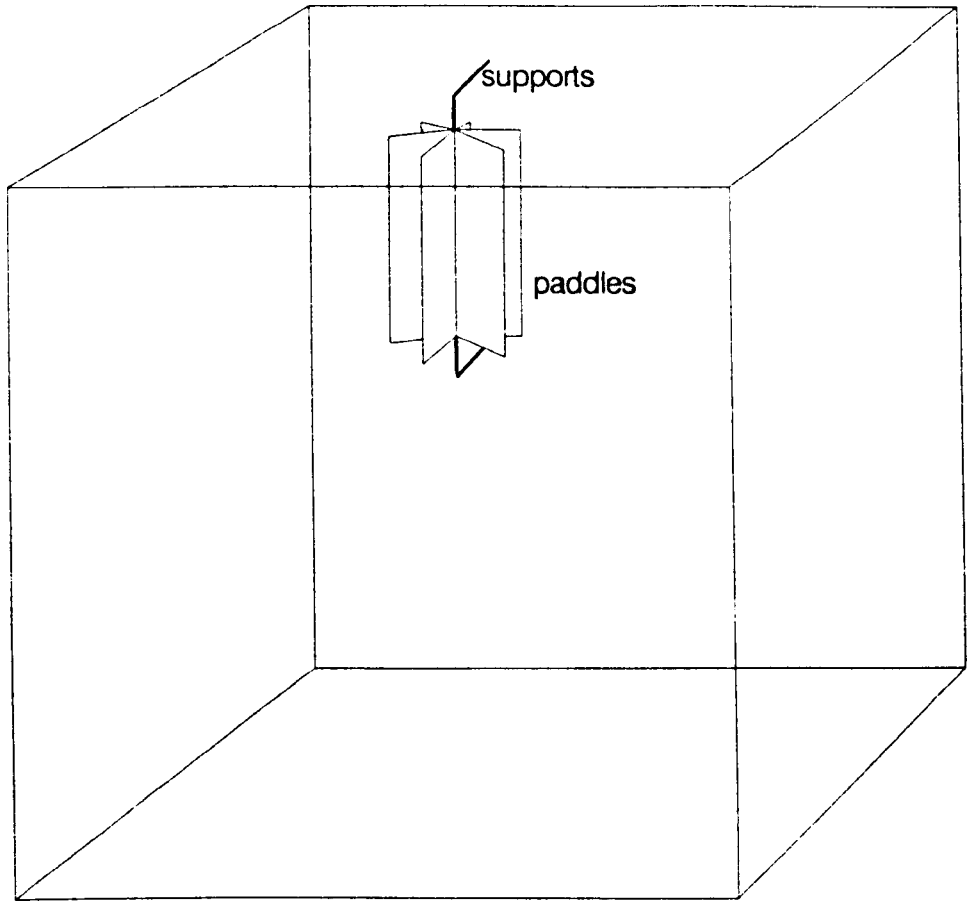

Fig.1.5.1 Stirred mode chamber showing the rotating paddles.

Stirred mode measurements can only work where the mode density is high, so that as the paddle rotates every frequency becomes resonant at some point in its rotation. For this reason stirred mode techniques cannot be used at low frequencies; the lowest frequency available will depend on the size of the room. These techniques are used mostly at microwave frequencies (e.g. to measure the harmonics of microwave ovens which may interfere with satellite communications) [Sugiura and Okamura 1987].

1.6 The TEM Cell (Crawford Cell)

The TEM cell is basically an expanded coaxial transmission with a defined impedance (usually 50Ω)[NBS tech note 1011 1979 : Tippet and Chang 1976]. The dimensions of the cell and the conducting bench, which forms the inner conductor (Fig.1.6.1), are chosen to give the required characteristic impedance and range of operating frequencies.

An electrically small source can be described in terms of 3 pairs of orthogonal dipoles [Sreenivasiah, Chang and Ma 1981] (1 electric and 1 magnetic in each pair, see Fig. 1.6.2). For emission measurements the EUT is placed on the bench so that components of the source dipoles which line up with the TEM fields which will propagate along the transmission line couple into the line and appear as a voltage at the coaxial terminals at the ends of the cell. This technique can be used (after calibration) to give the six dipole moments of the source. The relative phases between the dipoles cannot be measured so that it is not possible to give a full description of the source. This will prevent the actual fields generated in a particular location from being calculated but the fields due to each dipole may be predicted.

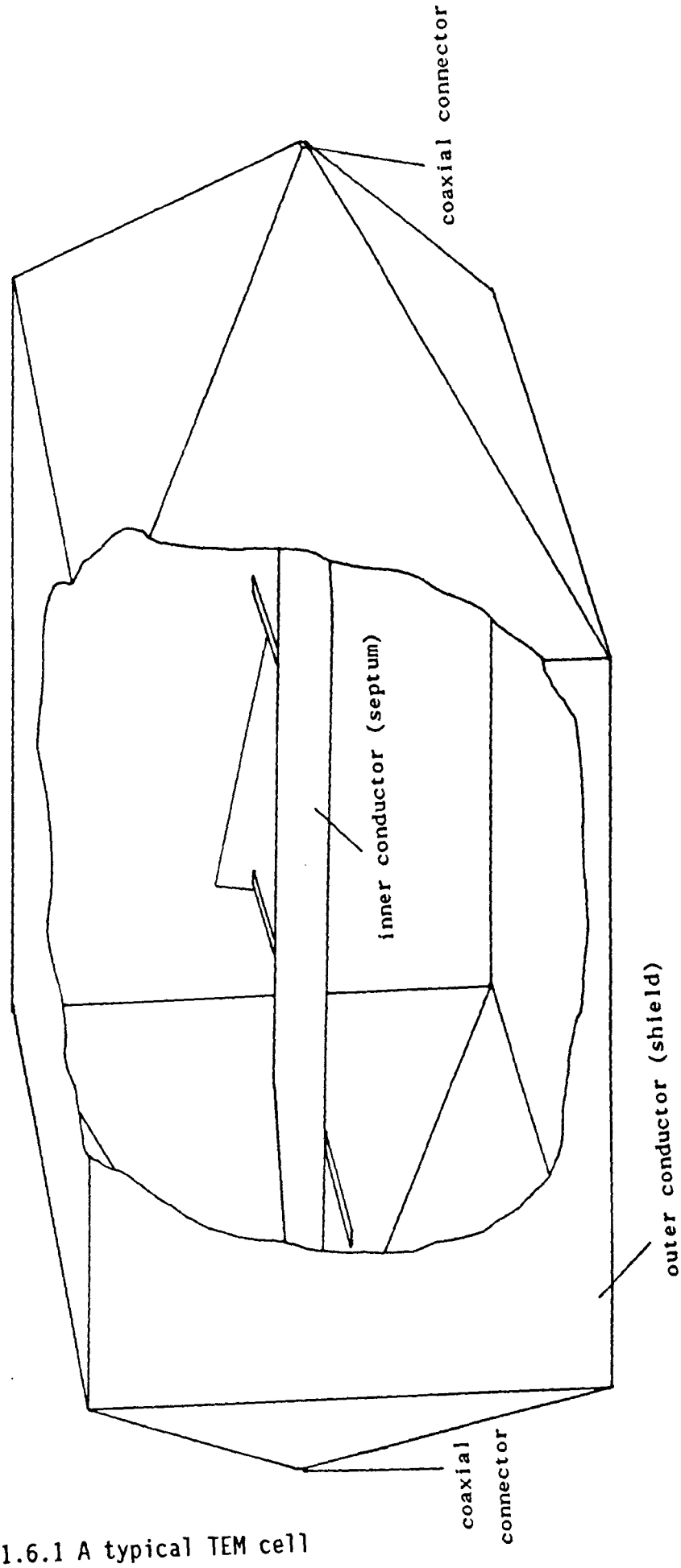

Fig.1.6.1 A typical TEM cell

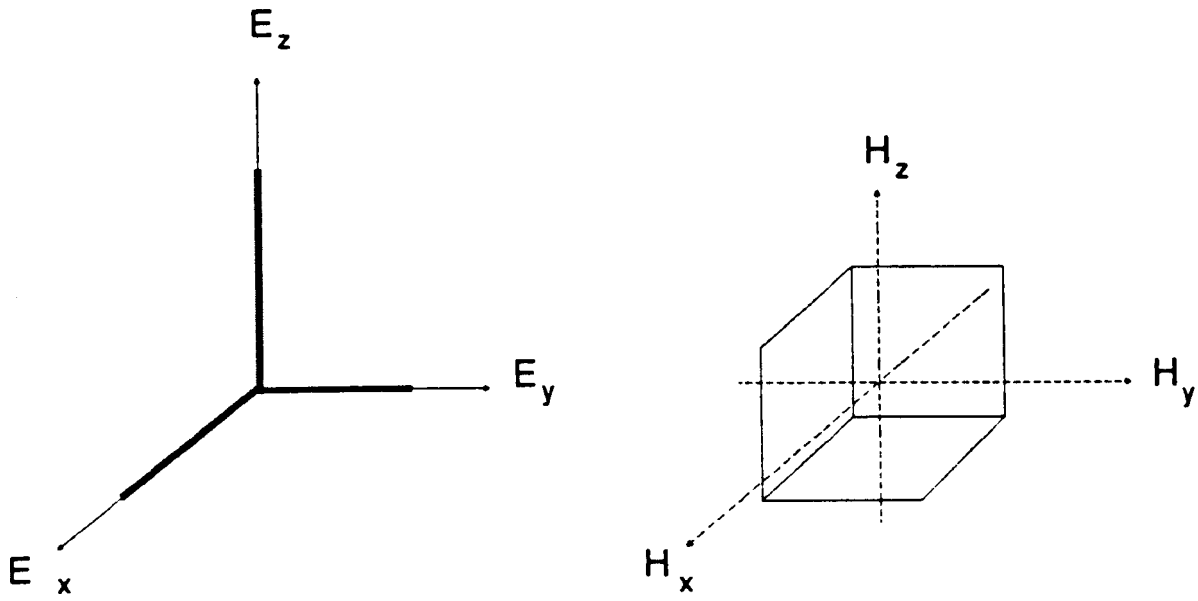

Fig. 1.6.2 A set of orthogonal dipoles to describe a small source

For the TEM cell to work accurately the source must be small to minimise the perturbation the fields within the line [Ma, Kanda, Crawford and Larsen 1985]. The cell can only be operated in the frequency region below the first cavity resonance; this limits its size for a particular frequency range and hence the size of the EUT is limited [Crawford 1974 : Meyer 1981; Hill 1983; Gruner 1967]. Investigations have been carried out into methods of increasing the bandwidth of such cells but it is beyond the scope of this introduction to describe them [Crawford, Workman and Thomas 1988].

The TEM cell can also be used to generated known fields for susceptibility measurements [Crawford 1974] and also to measure the screening effectiveness of materials or apertures [Burbridge, Edwards, Morrison and Williams 1988; Wilson and Ma 1986 (a)].

Other papers which describe the TEM cell are [Crawford et al 1980; Crawford and Workman 1979; Chang and Ma; Konigstein and Hansen 1987]

1.7 Aims and Objectives

The objective of the research was to develop emission test methods for use in a screened room in the frequency range below 200MHz (i.e below the frequency where it is easy to construct an anechoic chamber; particularly in a small room). This frequency range can be divided into two regions where different test methods are presently used:-

a) up to 30MHz where the room is acting as a cutoff waveguide and the major mode of propagation is a TEM wave between the bench and the walls, ceiling and floor.

b) 30-200MHz where the room starts to act as a resonant cavity but the mode density is not high enough to use stirred mode techniques

The frequency break of 30MHz is used in present test specifications and for some antennas but with larger rooms the cavity resonances may start to occur below this frequency and may cause errors in the results. The results included in this thesis assume that the first cavity resonance is above 30 MHz.

The aim was to devise quantitative measurement techniques, for these two frequency ranges, which would be simple to carry out and without complex mathematical manipulation of the results. The tests should also be repeatable and, with suitable calibration, the results from different rooms should be directly comparable. The room should not need adaptations which would be costly or make it unusable for other purposes. A technique which could be used to obtain the moments of the individual dipoles which make up the source was also desirable.

1.8 Format of the Thesis

The work on the lower frequency range is described in the first section of this thesis (Chapters 2 to 5).

Chapter 2 describes two simple, equivalent circuit, models which describe the coupling between the source and sensing antenna and were used to verify and describe the mechanisms present at these frequencies.

Chapters 3 and 4 investigate adaptations to the standard test setup, first predicting the effect of changes using the equivalent circuit models and then comparing them with practical measurements. These three chapters also describe a technique for distinguishing between electric and magnetic dipole sources. The effect of the orientation of the source on the measurements for each adaptation of the test setup is also investigated.

As stated in Section 1.7 one of the aims of the research is to devise a test method which can be used to obtain the moment of the dipole sources which can describe a source. Chapter 5 defines the moment of electric and magnetic dipoles. The results of theoretical and practical investigations into the effect of a change in the length of an electric dipole source on its moment are presented. Also presented are the results of a practical investigation into the effect of this change in the length of the electric dipole on the measured voltage for three of the test set-ups discussed in the previous three chapters.

Chapters 6 to 9 describe the work for the higher frequency range.

Chapter 6 describes the theory of the propagation mechanisms in this frequency range and discusses the possibility of modelling the fields.

Chapter 7 investigates how carbon loaded absorber can be used to damp the resonances in a screened room, therefore enabling a smooth or slowly changing frequency response to be obtained for an empty room. The effect of placing a bench in the room (when loaded and unloaded) and how to minimise this effect is described. The effect of using a practical antenna and its position in the damped and undamped rooms are examined.

Chapters 8 and 9 describe work carried out to investigate the feasibility of using magnetic absorbers to reduce the Q of cavity mode resonances within the room as well as the bench resonances. Chapter 8 compares various magnetic absorbers on the first resonance of a model room and investigates changes which could be made to the characteristics of the absorbers to try to increase the energy absorbed. Chapter 9 describes the performance of a full magnetic load within the model room, including loading of the bench resonances. It also compares the results for the first resonance within the model room with measurements carried out in the full sized room.

Chapter 10 draws conclusions for both frequency ranges and also suggests how the setups for the two frequency ranges can be merged to remove the need for changing the room configuration for the different frequency ranges.

NOTE

The measured results are generally given on plotted graphs. The reference level of the graph is given at the top. This refers to the line which is arrowed on the left hand side. The scale is also given at the top of the graph and is given as x/ which indictes x per division where x is a figure (e.g. 10 dB). The stop and start frequencies are given at the bottom of the graph.

2. EQUIVALENT CIRCUITS FOR MIL STD 461 SETUP

2.1 Equivalent Circuits

The test set-up used as the basis for this work is shown in Fig. 1.3.1. It is a configuration commonly used for military work [Marvin 1984 : DEF STAN 59/41] due to the low ambient noise level in a screened room but there is no reason why it should not be adapted for civilian work if the problems described in chapter 1 can be overcome. In this case it consists of a screened room (2.34 x 2.34 x 4.58 m) containing a copper bench (1m deep by 1.63m wide) bonded to the back wall with copper straps at three points. The test object is placed 10cm from the front of the bench. The relevant standards specify a 41inch active rod antenna placed on a conductive extension to the bench 1m away from the EUT. Due to the size of the room, the antenna used was limited to a height of 1m which gave adequate clearance from the ceiling, as defined in the specifications.

The sources used for the experimental work were small electric and magnetic dipoles as it is possible to calculate the dipole moments of these known sources. The construction and dimensions of the dipoles are shown in Fig. 2.1.1. The magnetic loop has an electrostatic shield so that it acts as a purely magnetic dipole source. The test source was excited using the RF output of a network analyser as shown in Fig. 2.1.2. The DC power to the active rod antenna was provided via a bias box along the same cable used for the output of the RF voltage (the circuits are shown in Fig. 2.1.3). The signal from the antenna was then amplified and measured with the network analyser.

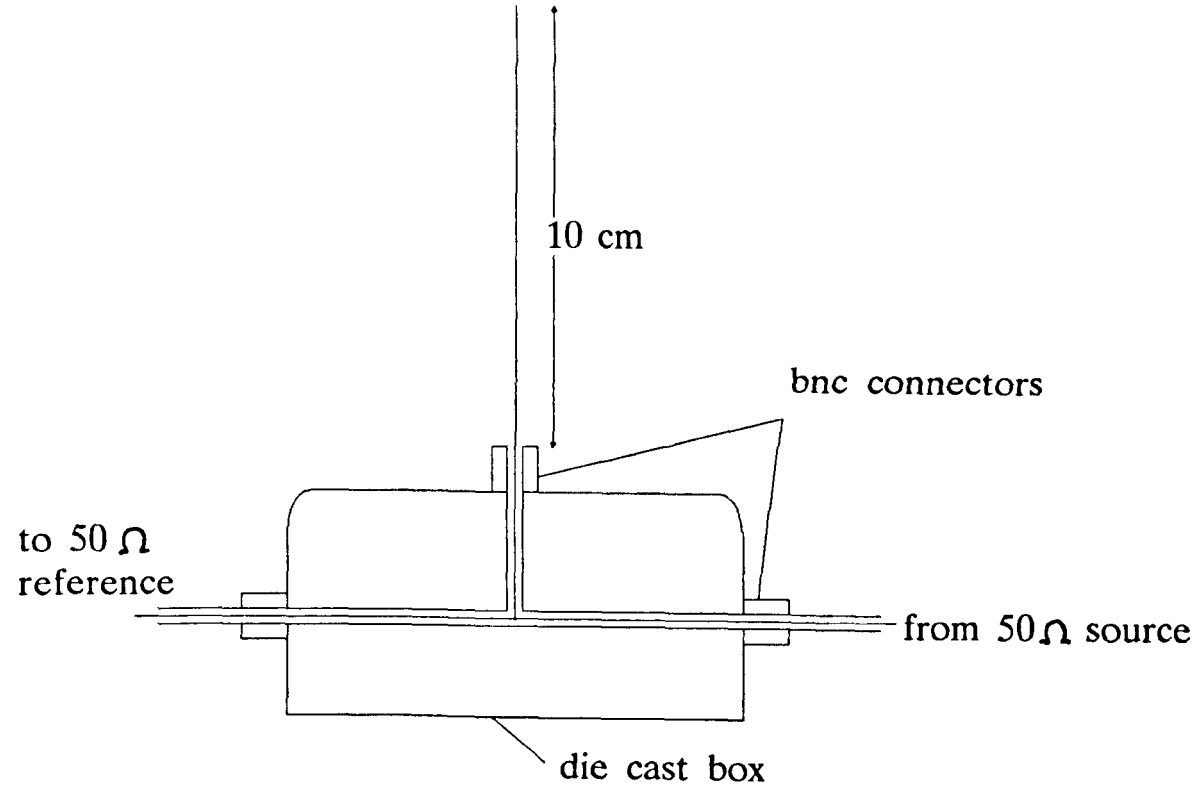

a) electric dipole source

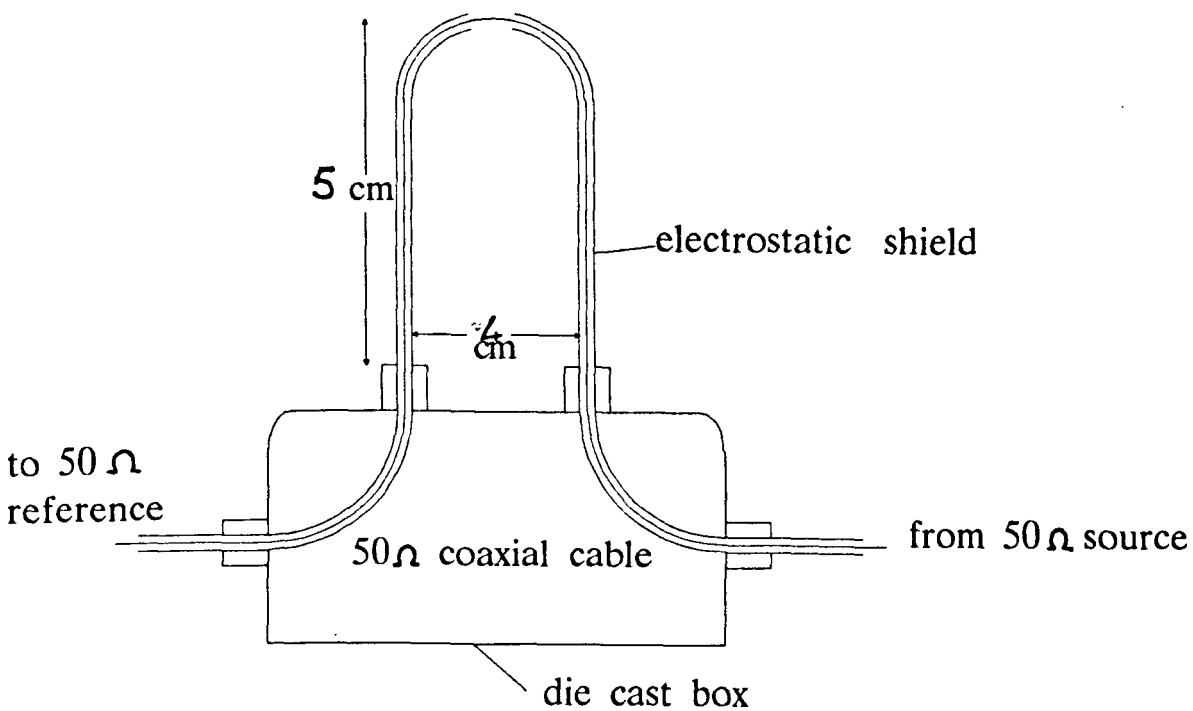

b) magnetic dipole source

Fig. 2.1.1 Construction of small dipole sources

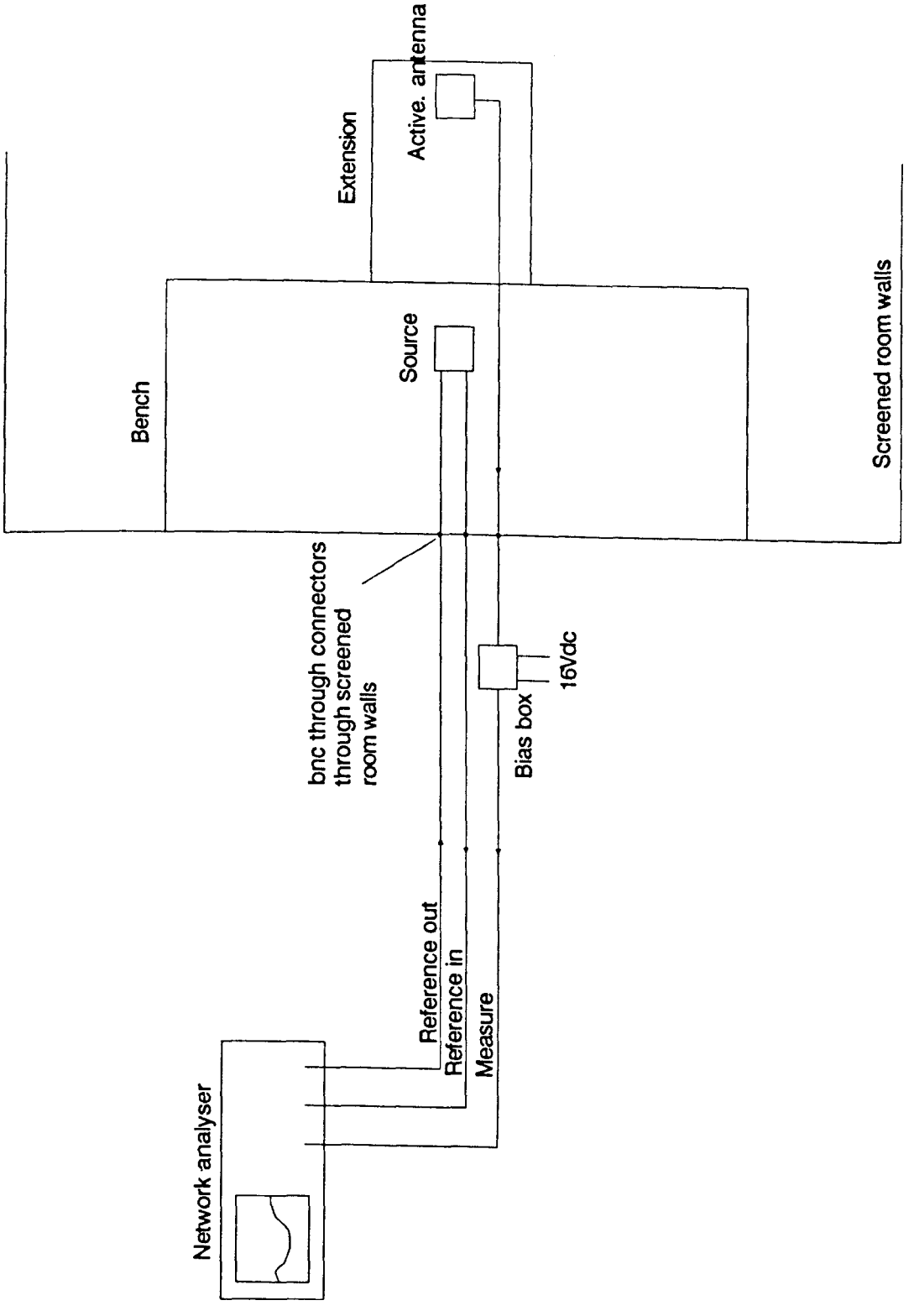

Fig. 2.1.2 Method of measurements

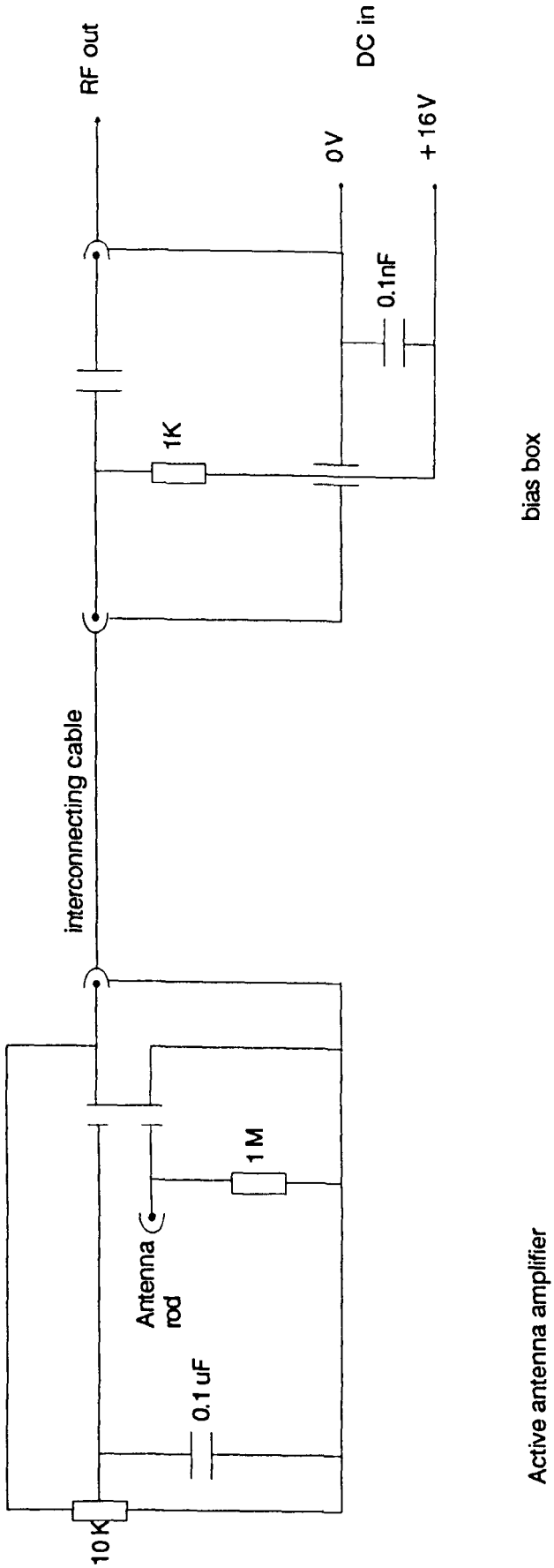

Fig. 2.1.3 Circuits of antenna amplifier and bias network

The reference signal for the network analyser was taken from the point at which the source antenna was fed (see Fig. 2.1.2). This avoided unecessary standing wave effects on the cables which would produce errors in the measurements. The effects of the cables and amplifiers on the phase and amplitude of the measurements were calibrated out using functions available on the network analyser. The measurements given in this Thesis are the measured voltage relative to the feed voltage at the source (i.e. the gain of the system) except where otherwise specified.

Initially ordinary braided sheath coaxial cable was used but this proved to be 'leaky' and at certain frequencies the stray coupling that occurred between the cable inside the screened room and the sensing antenna dominated the measurements. There was also stray coupling between the cables outside the room. This caused measurements to contain unexpected resonances. By moving the cables and watching the resonances shift in frequency and amplitude cable coupling was shown to be the cause. The cables were replaced with 'super screened' cables which have a mu-metal screen between the two layers of braided screen. This gives about 40dB reduction in the leakage fields compared to the ordinary cable. This improved the measurements although a small resonance in the measurements at about 48MHz can still be attributed to systematic errors (see Chapter 4 Section 2).

Simple models were put forward [Marvin 1984] to describe the test set-up shown in Fig. 1.3.1. They are for the frequency region below the first cavity resonance of the room where the source is electrically small. These models were based on a coaxial TEM transmission line. Although they did successfully model the resonance

that occurs when the bench and transmission line are approximately 1/4 wavelength long, they did not model the response completely and in particular did not predict the deep null that occurs with an electric source (Fig. 2.1.4). The models have been improved to give a good prediction of the voltages on the sensing antenna, while still retaining the basic simplicity which enables them to be used as a tool to aid the understanding of the propagation mechanisms involved. The frequency range for these tests is specified as up to 30MHz but the models and measurements have been carried up to 51MHz so that the resonances which occur on the bench are included in the work being a useful guide as to whether the models are accurate.

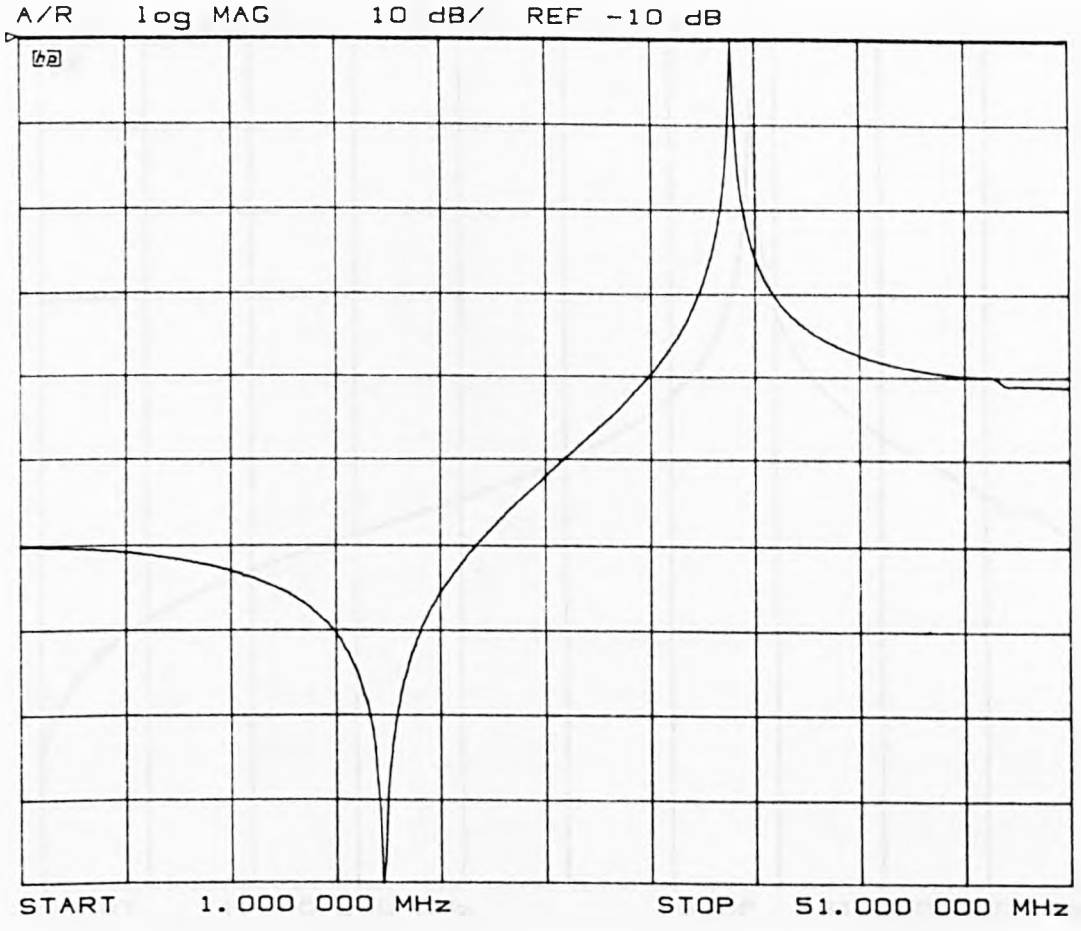

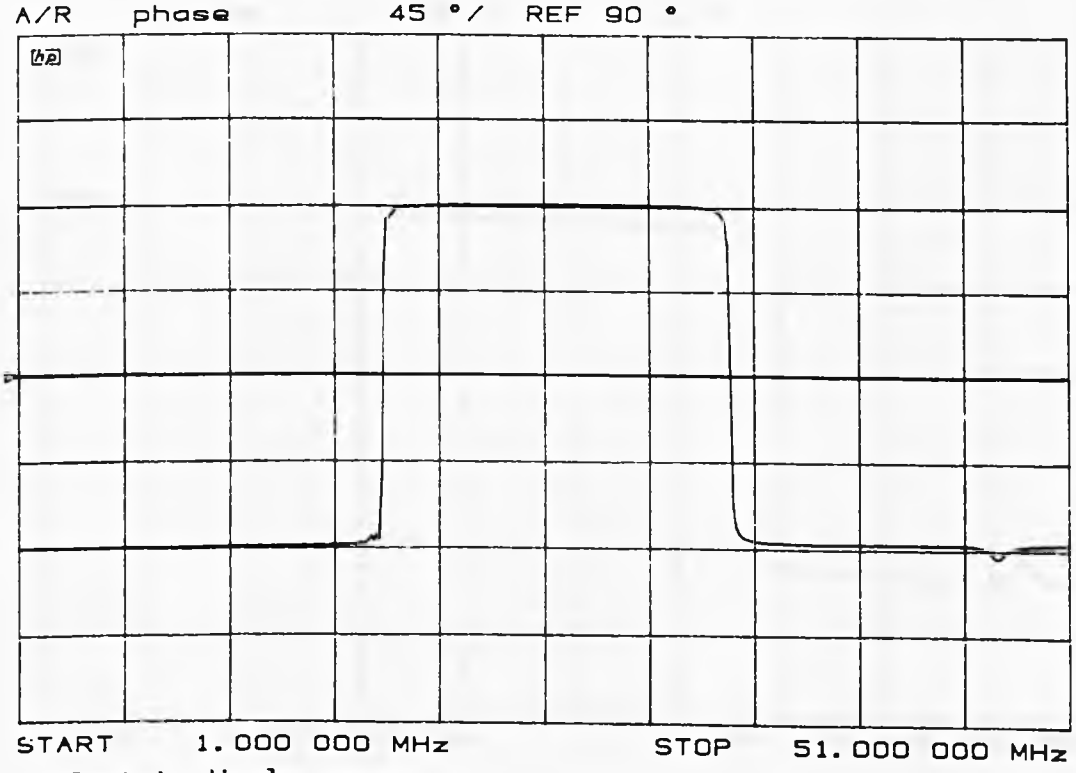

a)electric dipole source

Fig. 2.1.4 Measured frequency response (source .1m from front of bench)

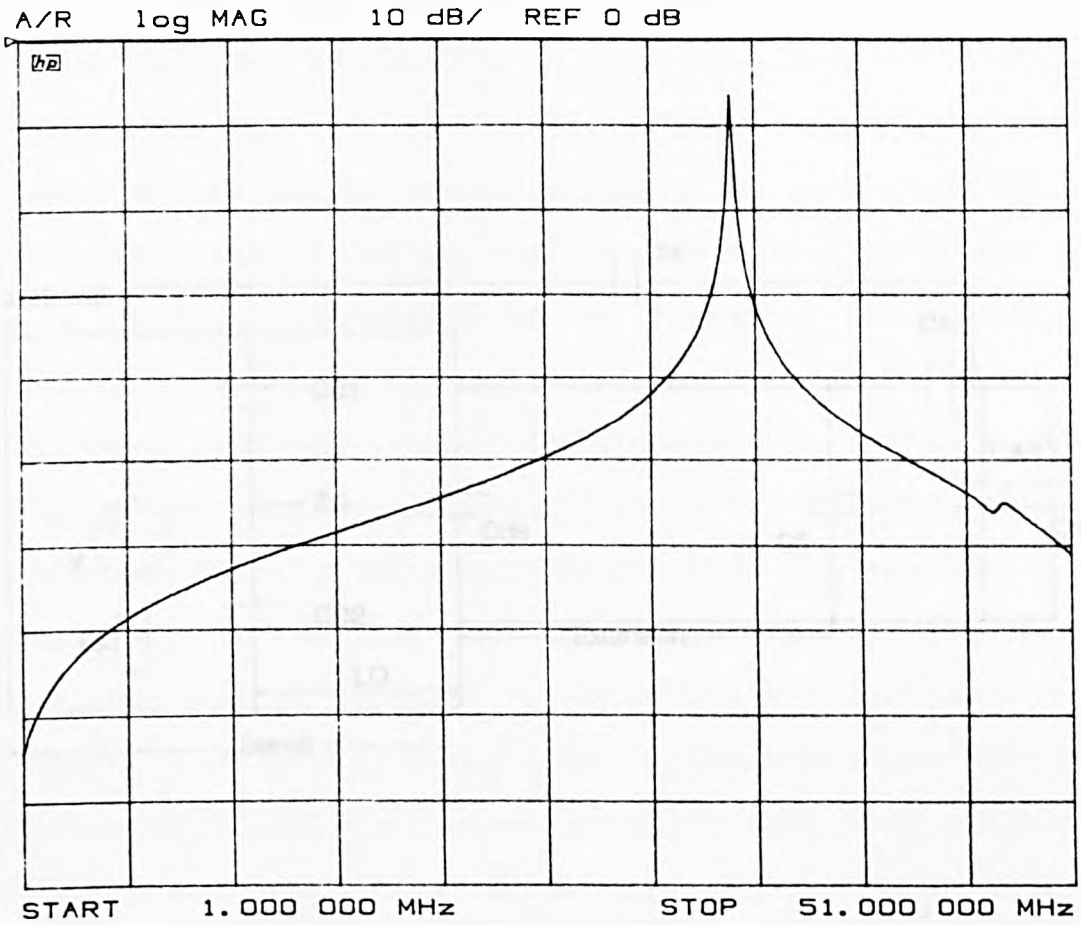

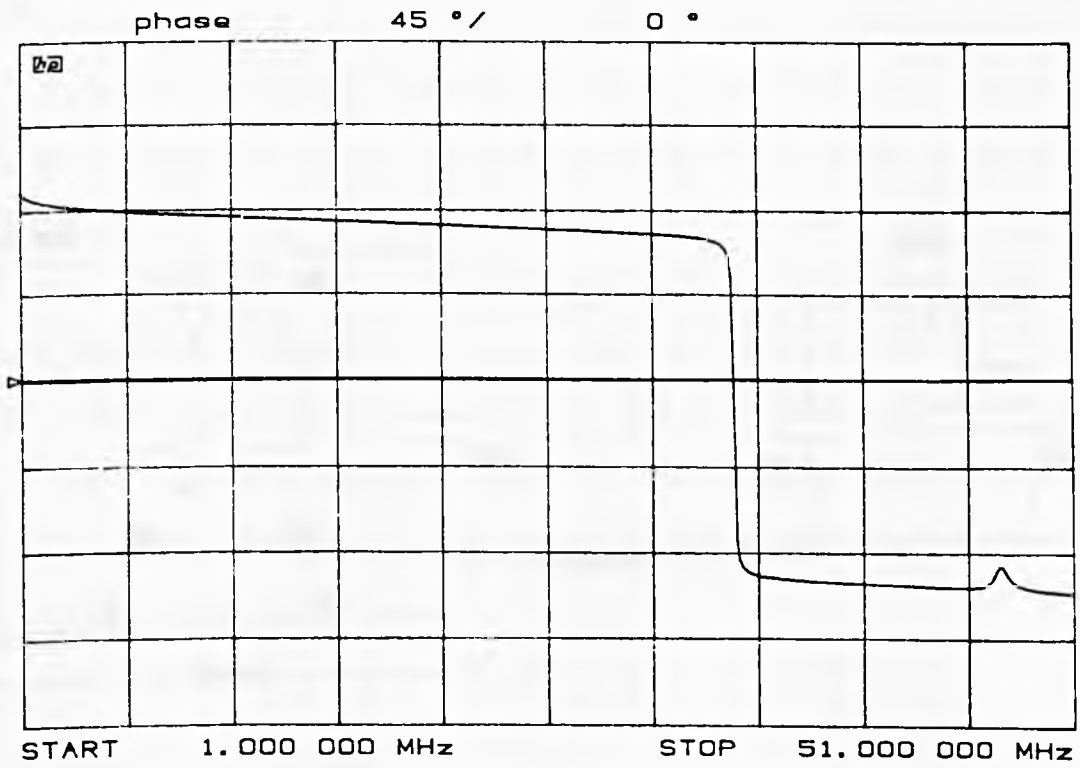

b)magnetic dipole source

Fig. 2.1.4 Measured frequency response (source .1m from front of bench)

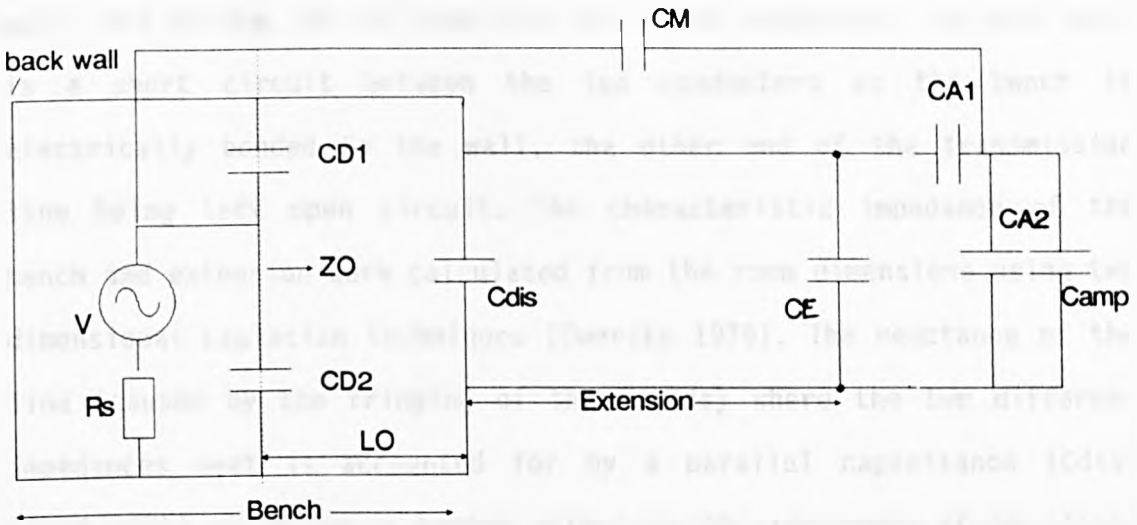

a)electric dipole source

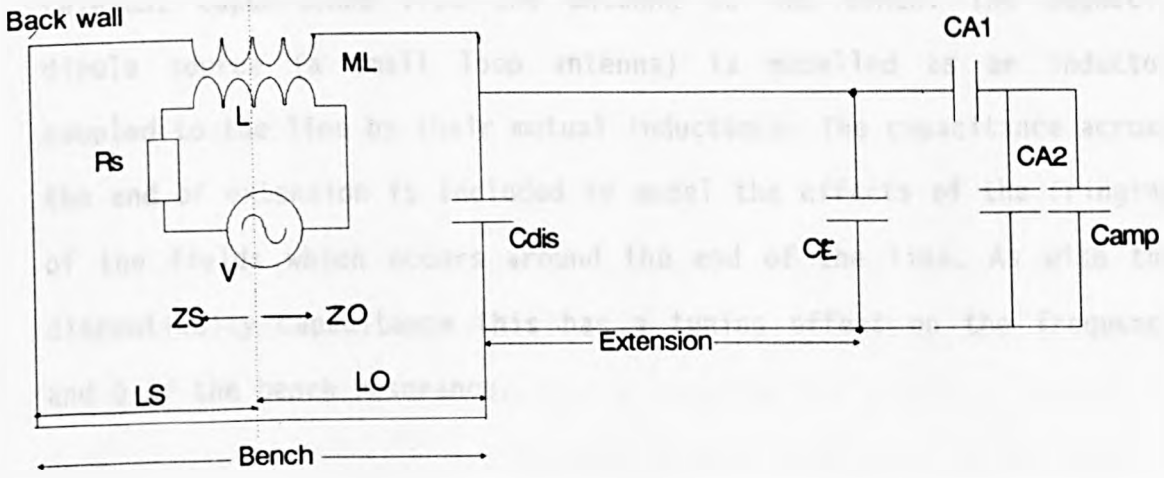

b)magnetic dipole source

Fig. 2.1.5 Improved models to describe energy transfer mechanisms

The improved models (Fig. 2.1.5) are based on a coaxial transmission line with the conducting bench and extension which support the EUT and the sensing antenna as the inner conductor. The walls and ceiling of the room form the outer conductor. The back wall is a short circuit between the two conductors as the bench is electrically bonded to the wall, the other end of the transmission line being left open circuit. The characteristic impedance of the bench and extension were calculated from the room dimensions using two dimensional Laplacian techniques [Dworsky 1979]. The reactance of the line (caused by the fringing of the fields) where the two different impedances meet is accounted for by a parallel capacitance (Cdis) [Saad 1971] which has a tuning effect on the resonance of the line. The sources and active rod antenna are electrically small and over the frequency range of interest they can be modelled as lumped elements. The sensing antenna is modelled as a pair of capacitances to the outer and inner conductors as is the electric dipole source used for the measurements. The input capacitance of the amplifier for the sensing antenna (measured on the network analyser) is in parallel with the relevant capacitance from the antenna to the bench. The magnetic dipole source (a small loop antenna) is modelled as an inductor coupled to the line by their mutual inductance. The capacitance across the end of extension is included to model the effects of the fringing of the fields which occurs around the end of the line. As with the discontinuity capacitance this has a tuning effect on the frequency and Q of the bench resonance.

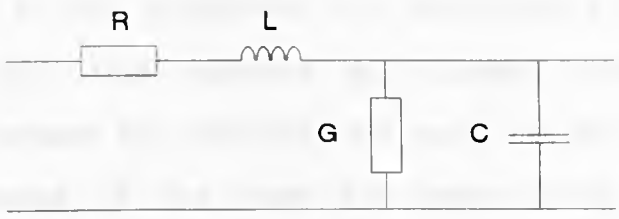

Fig. 2.1.6 Model of TEM transmission line

If the transmission line is assumed to be lossless the characteristic impedance (Z_0) and the propagation constant (γ) are given by the following equations:-

$$Z_0 = \sqrt{\frac{(R + j\omega L)}{(G + j\omega C)}} \qquad 2.1$$

$$\gamma = \sqrt{(R + j\omega L)(G + j\omega C)} \qquad 2.2$$

where R=0 and G=0.

With the electric source the dominant mode of operation in the lower frequencies of the range (below the null in Fig. 2.1.4) is the evanescent waveguide mode which is modelled as a direct capacitive link between the source and sensing antenna. The null in the response occurs when the signals via this and the TEM mode are of equal amplitude and opposite phase. This mutual capacitance does not exist between the sensing antenna and the magnetic source due to the electrostatic shield.

The values of the capacitances of the antennas were arrived at by measuring the capacitance of each antenna over a ground plane and on the conducting bench in the room at 5KHz, assuming them to be constant up to 50MHz as the dimensions are electrically small. The mutual capacitance was also measured as standard expressions for the capacitance between two parallel rods could not be used. This was due to the presence of the room and bench which alter the field distribution between the two since the separation between them is large compared to the distance to the bench and walls. The difference in the length of the two rods is also of the same order as the separation so that even in free space the fringing of the fields would still be significant. The inductance of the loop antenna was measured and the mutual inductance between the loop and the transmission line was calculated to get approximate figures which were then adjusted by trial and error to get the correct coupling levels.

The discontinuity capacitance and fringing capacitance across the end of the extension were not measured or calculated but were adjusted until the resonant frequency of the prediction was correct and had the correct Q. The discontinuity capacitance could be calculated using similar techniques to that used to calculate the impedance of the bench and extension [Dworsky 1979].

The output voltages for the circuits were calculated on a DEC 10 computer in Fortran using standard chain parameter techniques (Appendix A). The programs are included in Appendix B.

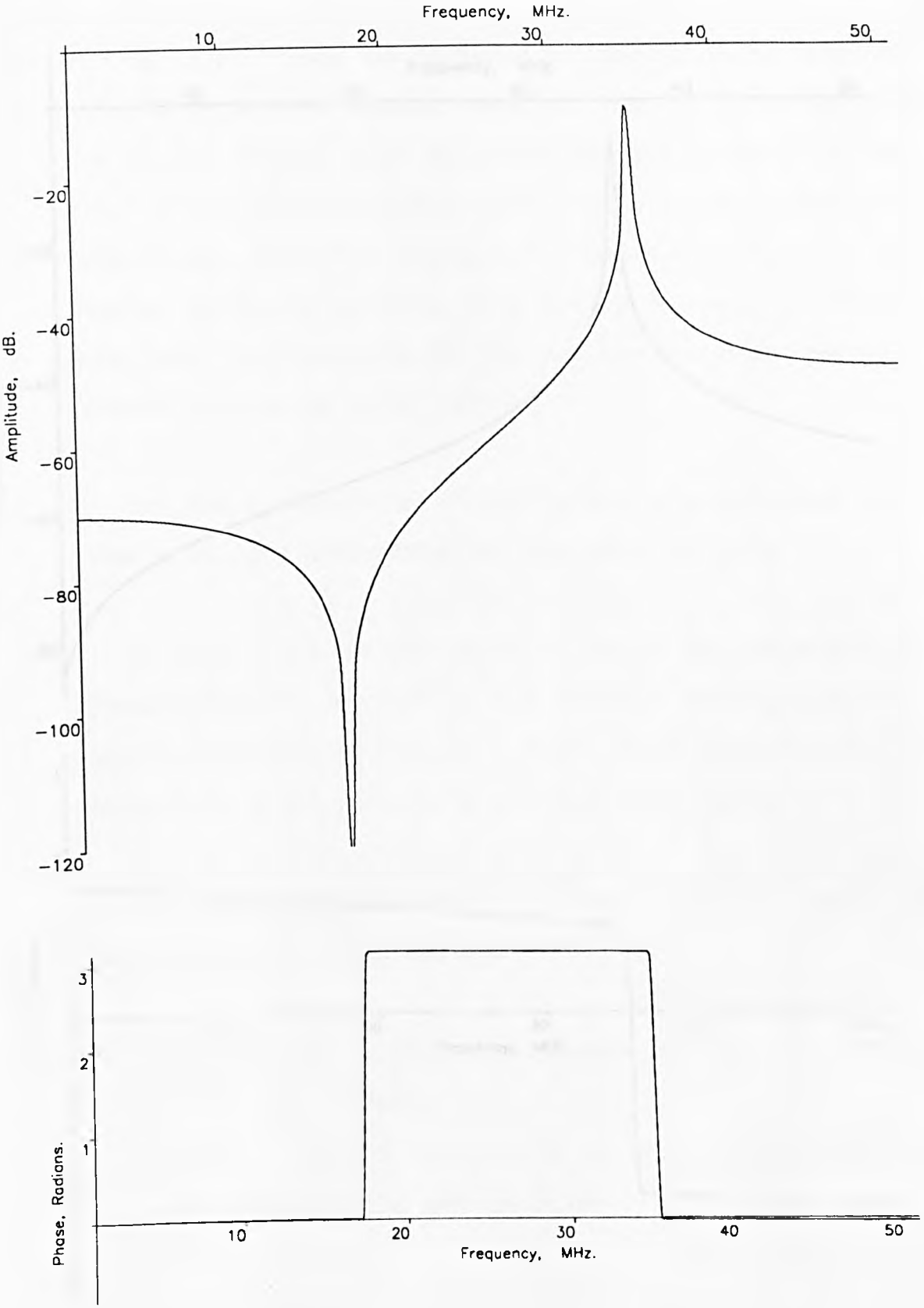

a)electric dipole source

Fig. 2.1.7 Predicted frequency response

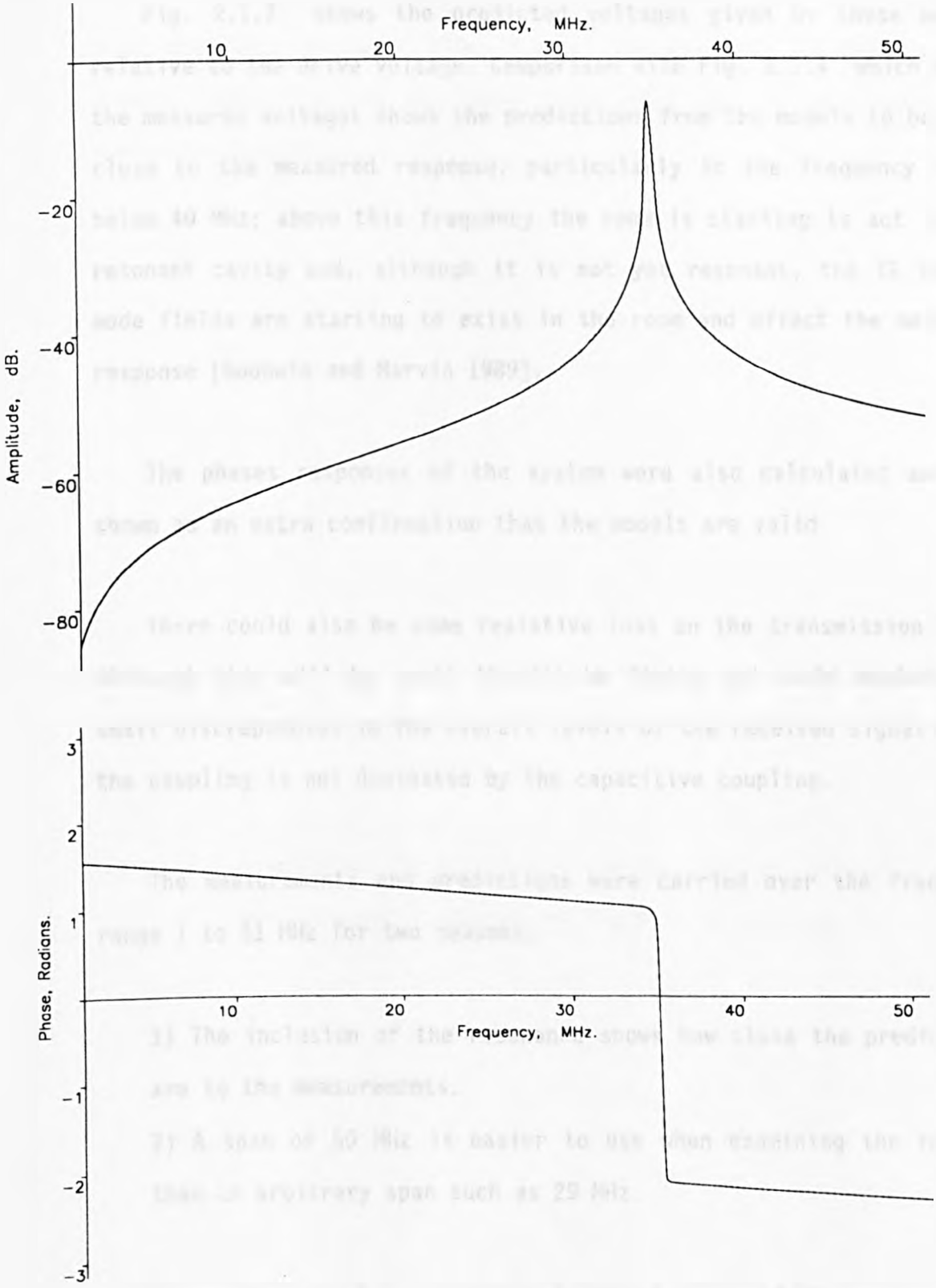

b)magnetic dipole source

Fig. 2.1.7 Predicted frequency response

Fig. 2.1.7 shows the predicted voltages given by these models relative to the drive voltage. Comparison with Fig. 2.1.4 which shows the measured voltages shows the predictions from the models to be very close to the measured response, particularly in the frequency range below 40 MHz; above this frequency the room is starting to act like a resonant cavity and, although it is not yet resonant, the TE and TM mode fields are starting to exist in the room and effect the measured response [Goodwin and Marvin 1989].

The phases responses of the system were also calculated and are shown as an extra confirmation that the models are valid.

There could also be some resistive loss on the transmission line. Although this will be small it will be finite and could explain the small discrepancies in the overall levels of the received signal where the coupling is not dominated by the capacitive coupling.

The measurements and predictions were carried over the frequency range 1 to 51 MHz for two reasons:-

1) The inclusion of the resonance shows how close the predictions are to the measurements.
2) A span of 50 MHz is easier to use when examining the results than an arbitrary span such as 29 MHz.

It can be seen by examination of the models and the measurements that the coupling between the source and sensing antennas for an electric dipole source is dominated by the direct capacitive coupling for frequencies below 5 MHz. For these frequencies the length of the transmission lines is minimal and has little effect and the circuit

can be reduced to a simple capacitive divider network which gives a flat frequency response (Fig. 2.1.8). The coupling of the magnetic dipole source is low at these frequencies due to the nature of inductive coupling.

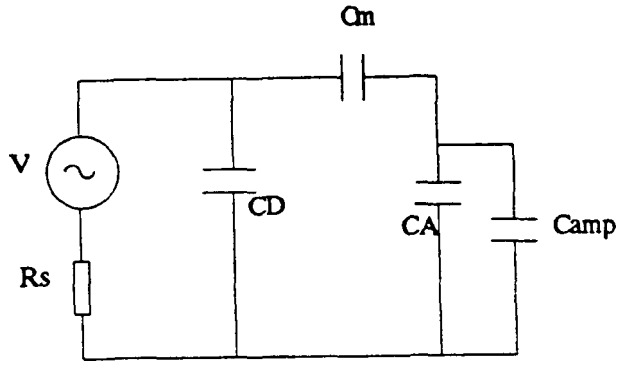

$CA = CA1 + CA2$
$C_D = C_{D1} + C_{D2}$

Fig. 2.1.8 Simplified circuit to describe the coupling between the electric dipole source and the sensing antenna.

2.2 Distinguishing Between Electric and Magnetic Dipole Sources

If a piece of electronic equipment fails to pass an emissions test it is then necessary for the manufacturer to reduce the emissions by whatever means possible. Assuming that the emissions are from the box and not from any connecting cables, the techniques that can be used will depend upon the type of source dipole present. At these frequencies it is difficult to screen a low impedance source (i.e. a magnetic dipole) and it may be necessary to redesign the layout of the circuitry or at least some components. For this reason it would be useful for the manufacturer of the equipment to know the type of source present or, if both types are present, the relative amplitudes of each.

It was suggested [Marvin 1984] that a simple test which distinguishes between the two types of source is to move the source back along the bench towards the back wall and examine the effect on the measured voltage. Fig. 2.2.1 shows the change in measured voltage as this is done for steps of 0.2m from 0.9m from the back wall to 0.1m from the back wall. It can be seen from this figure that with the electric dipole source the voltage drops by about 25dB at the lower end of the frequency range and about 15 dB at the top end of the range with the area around the nulls being subject to various changes as the frequency of the nulls also changes. With a magnetic dipole source the voltage varies by about 5dB; this is not in a constant direction but starts by falling by about 5dB when the source is 0.3m from the back wall and then rising again by about 2dB when the source is 0.1m from the back wall for the frequencies below the resonance. Above the resonance it shows a rise which increases steadily with frequency. Away from the nulls in the response for the electric dipole

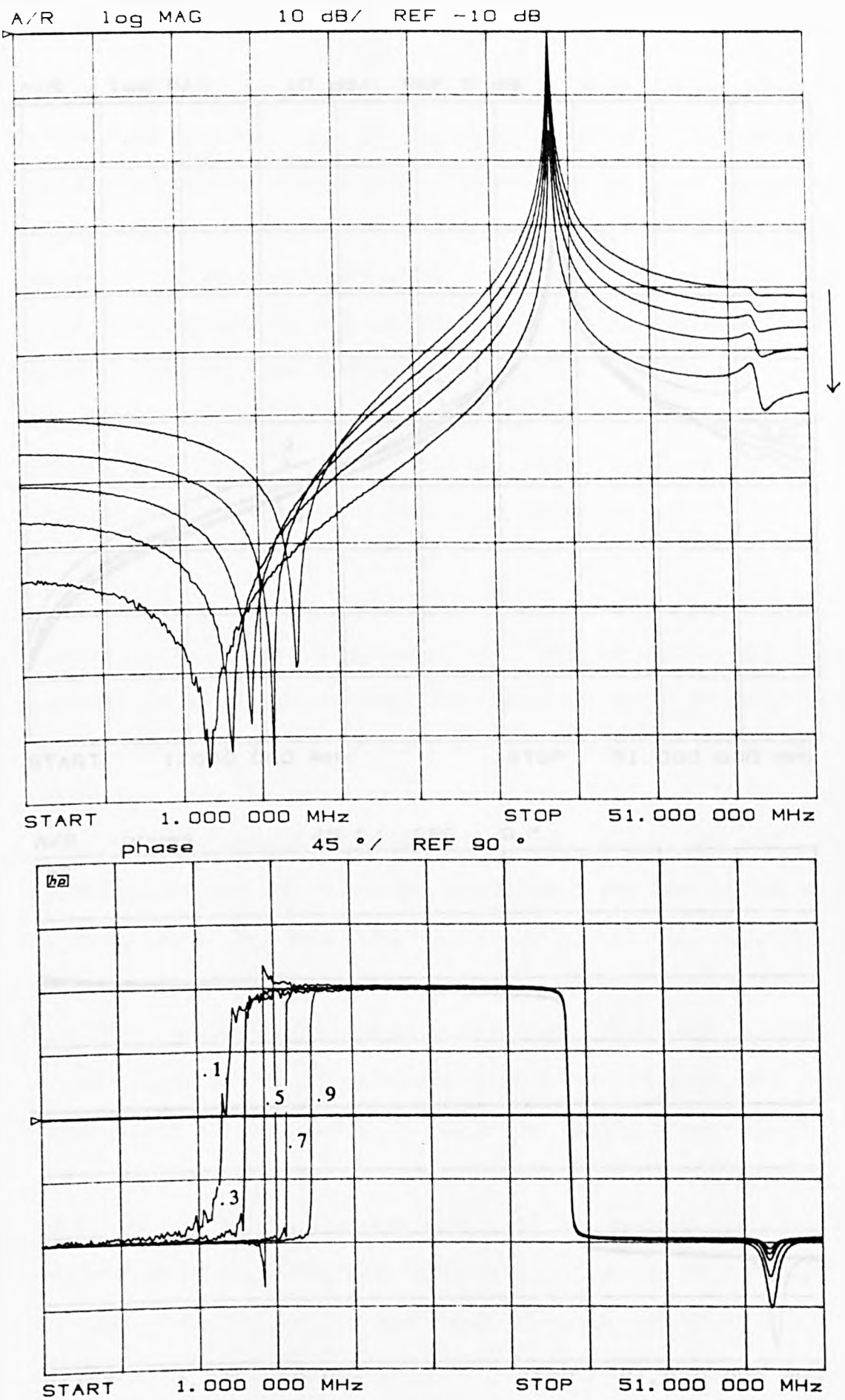

a)electric dipole source

Fig. 2.2.1 Measured voltage as source is moved back along bench

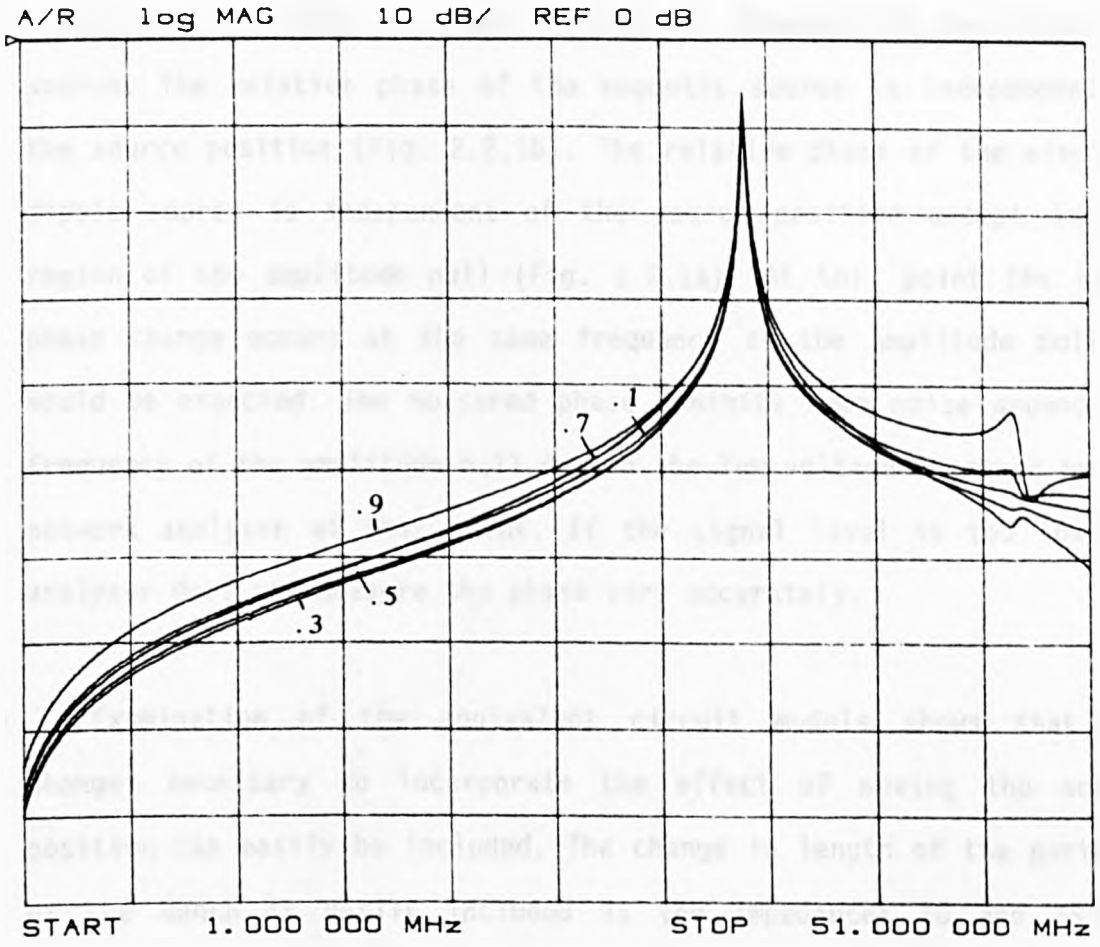

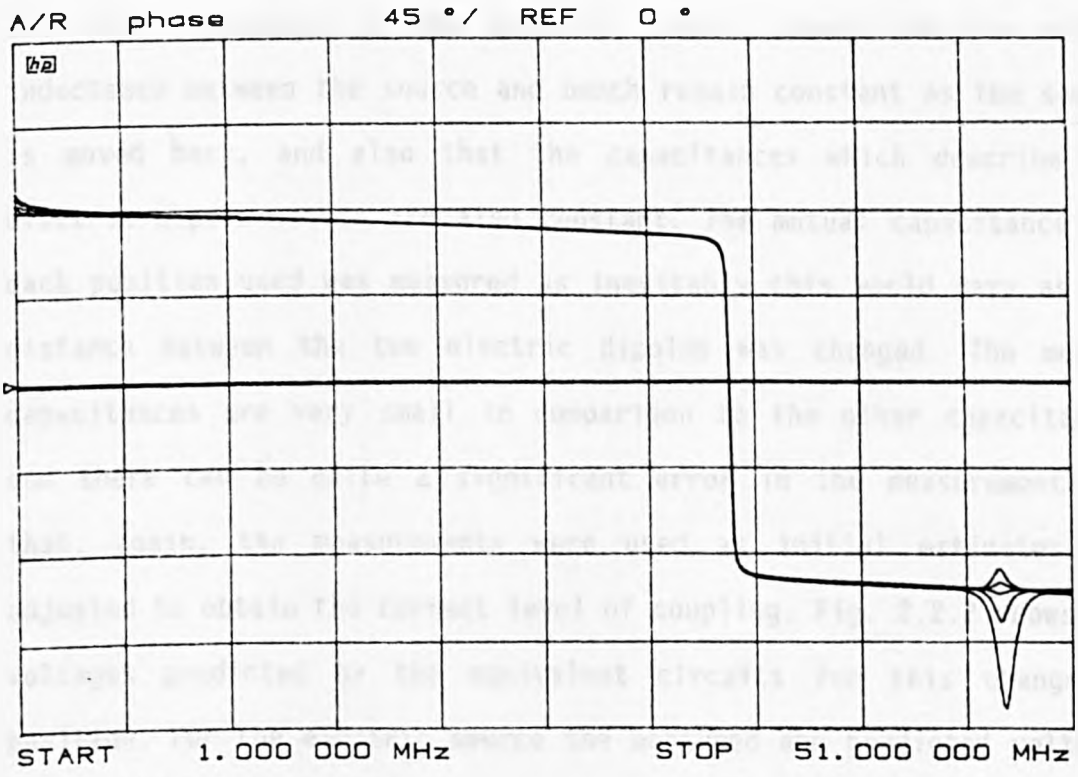

b)magnetic dipole source

Fig. 2.2.1 Measured voltage as source is moved back along bench

source this provides a clear distinction between the two types of source. The relative phase of the magnetic source is independent of the source position (Fig. 2.2.1b). The relative phase of the electric dipole source is independent of the source position except in the region of the amplitude null (Fig. 2.2.1a). At this point the rapid phase change occurs at the same frequency as the amplitude null as would be expected. The measured phase exhibits some noise around the frequency of the amplitude null due to the low voltage received by the network analyser at this point. If the signal level is too low the analyser does not measure the phase very accurately.

Examination of the equivalent circuit models shows that the changes necessary to incorporate the effect of moving the source position can easily be included. The change in length of the portions of the bench is easily included as the impedances ZO and ZS are calculated using the length of the bench (Appendix A). It is assumed that the inductance of the magnetic dipole source and the mutual inductance between the source and bench remain constant as the source is moved back, and also that the capacitances which describe the electric dipole source are also constant. The mutual capacitance for each position used was measured as inevitably this would vary as the distance between the two electric dipoles was changed. The mutual capacitances are very small in comparison to the other capacitances and there can be quite a significant error in the measurements so that, again, the measurements were used as initial estimates and adjusted to obtain the correct level of coupling. Fig. 2.2.2 shows the voltages predicted by the equivalent circuits for this change in position. For the electric source the measured and predicted voltages have a good agreement. The voltage predicted by the magnetic equivalent circuit shows a steady rise as the source is moved back

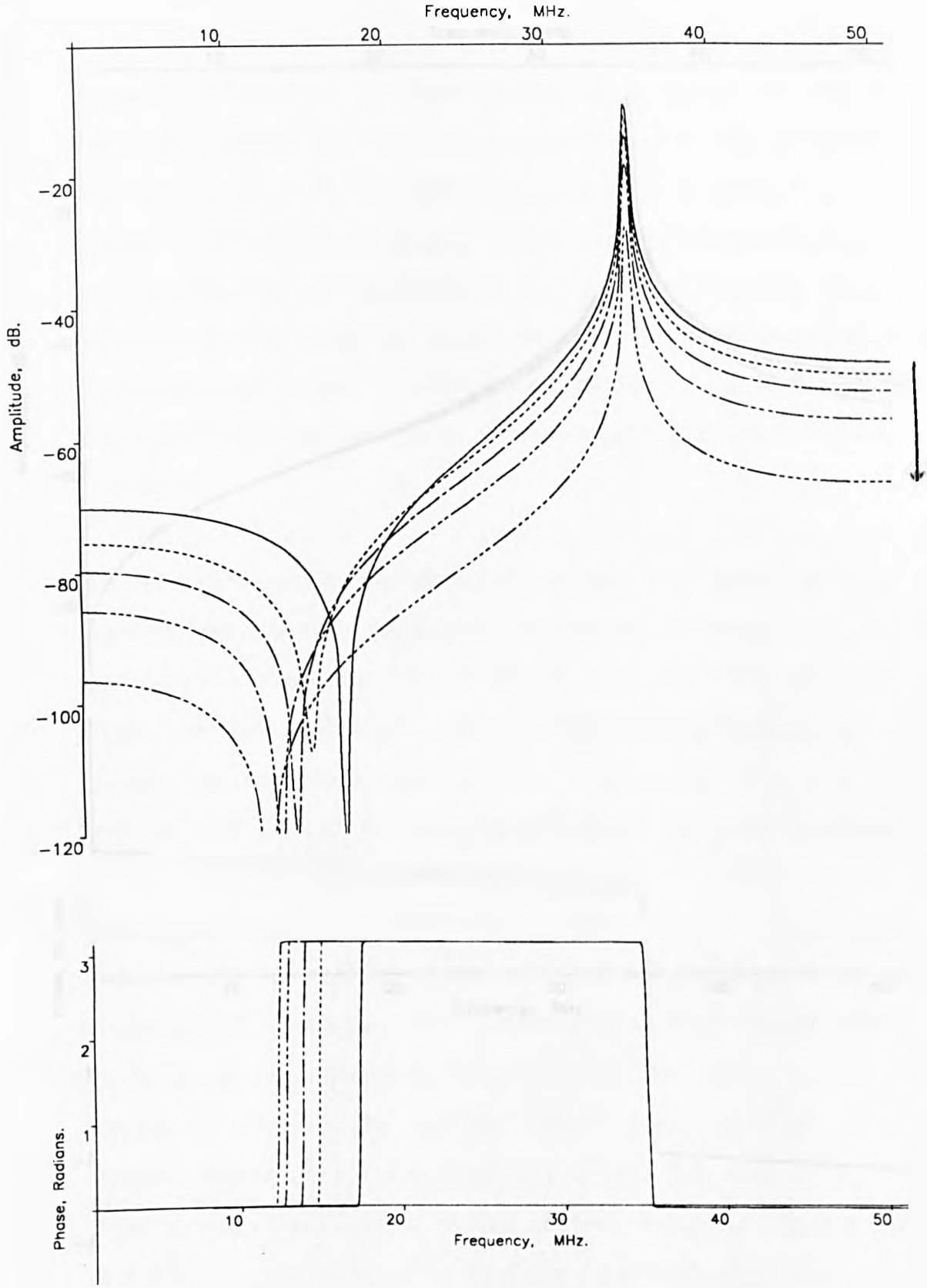

a)electric dipole source

Fig. 2.2.2 Predicted change in measured voltage as source is moved back

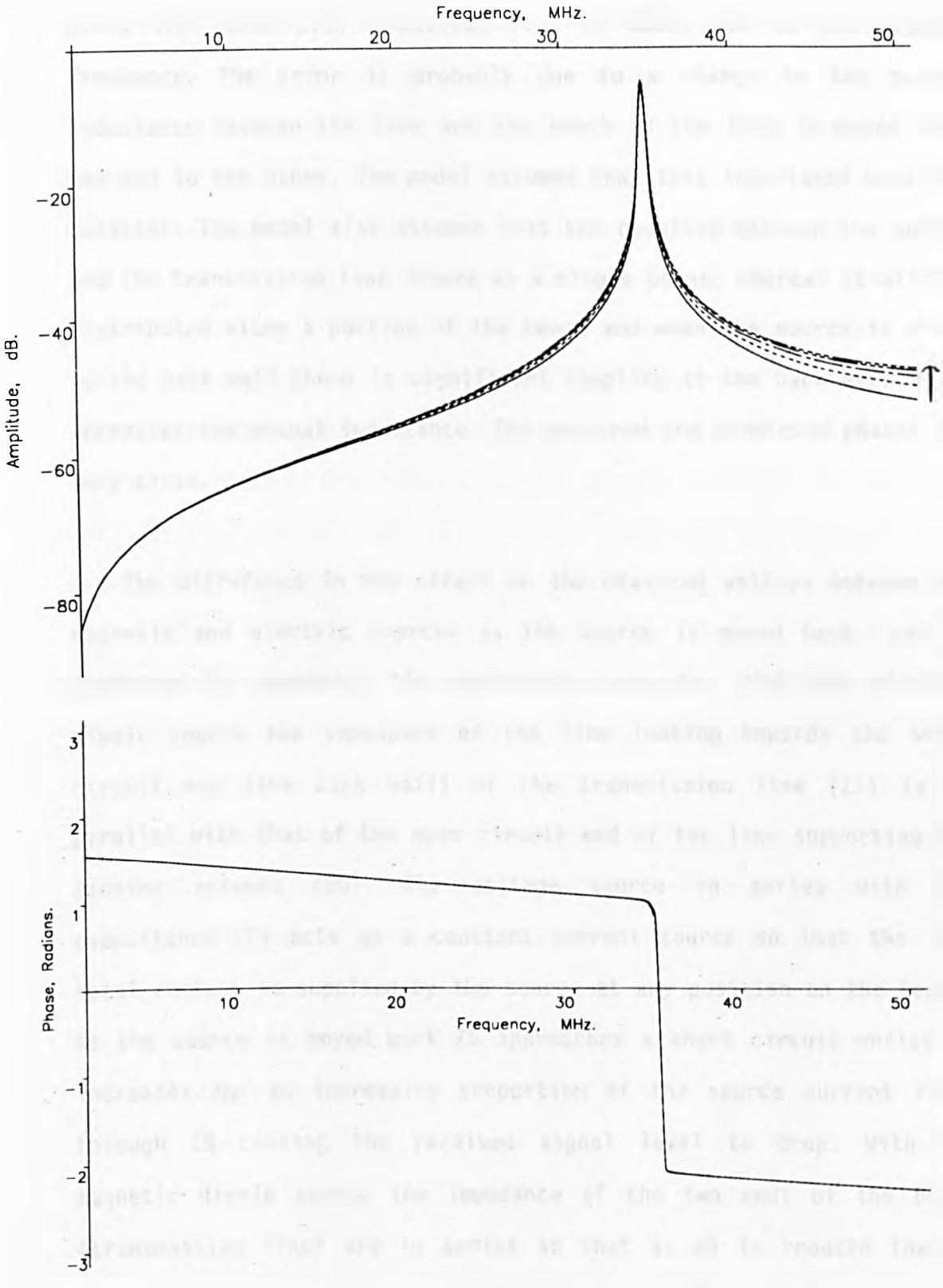

b)magnetic dipole source

Fig. 2.2.2 Predicted change in measured voltage as source is moved back

along the bench with a maximum rise of about 5dB at the highest frequency. The error is probably due to a change in the mutual inductance between the loop and the bench as the loop is moved from one end to the other. The model assumed that this inductance would be constant. The model also assumes that the coupling between the source and the transmission line occurs at a single point, whereas it will be distributed along a portion of the bench and when the source is close to the back wall there is significant coupling to the back wall which increases the mutual inductance. The measured and predicted phases are very close.

The difference in the effect on the measured voltage between the magnetic and electric sources as the source is moved back can be explained by examining the equivalent circuits. With the electric dipole source the impedance of the line looking towards the short circuit end (the back wall) of the transmission line (ZS) is in parallel with that of the open circuit end of the line supporting the sensing antenna (ZO). The voltage source in series with the capacitance CD1 acts as a constant current source so that the same total current is supplied by the source at any position on the bench. As the source is moved back ZS approaches a short circuit whilst ZO increases and an increasing proportion of the source current flows through ZS causing the received signal level to drop. With the magnetic dipole source the impedance of the two ends of the bench (transmission line) are in series so that as ZS is reduced towards zero ZO increases. This means that the current flowing in the circuit does not change significantly and the effect on the received signal is very small.

The difference in the changes of the voltages can be used to distinguish between the two dipole sources where the change is straight forward. In the vicinity of the nulls this is not the case because at different frequencies the change in the measured voltage can be very different. With this simple test it could be possible to give relative amplitudes for the two sources when they are both present (see Chapter 4) except in the frequencies around the nulls. The nulls cover a fair proportion of the range under consideration which makes this property difficult to use over a large portion of the frequency range. If the response can be changed to remove the nulls in the electric dipole case, this simple technique can then be used across the whole frequency range of interest. It would also be easier to calibrate out the variation in a smoother frequency response. In the vicinity of the null (which is very deep) the standard set-up is relatively insensitive and a source which radiates badly at these frequencies will not be easily detected. This means that it could be necessary to set the level of permissible voltage levels for the whole frequency range much lower than need be, otherwise the levels of emissions in this area could be greater than is desired. This is likely to cause a whole system to be over engineered just to pass in the rest of the frequency range with a consequent increase in the development and construction costs.

2.3 Orientation of the Source

As the sources can be described by a set of orthogonal dipoles it would be most useful to be able to measure each dipole independently. This would mean that the fields which would be generated by a device in a particular environment, where the device was to be used, could be calculated to determine before-hand whether they were likely to be a problem (e.g. in the hold of a ship which could be acting as a resonant cavity so that only particular frequencies would be a problem). With a TEM line where propagation occurs in only one direction this is possible since only the dipole with the correct orientation to propagate in the line will couple to that line. The dipoles which are perpendicular to the preferred orientation will not couple to the line. With the bench and extension coupling should only occur for dipole elements with the orientations shown in Fig. 2.3.1 .

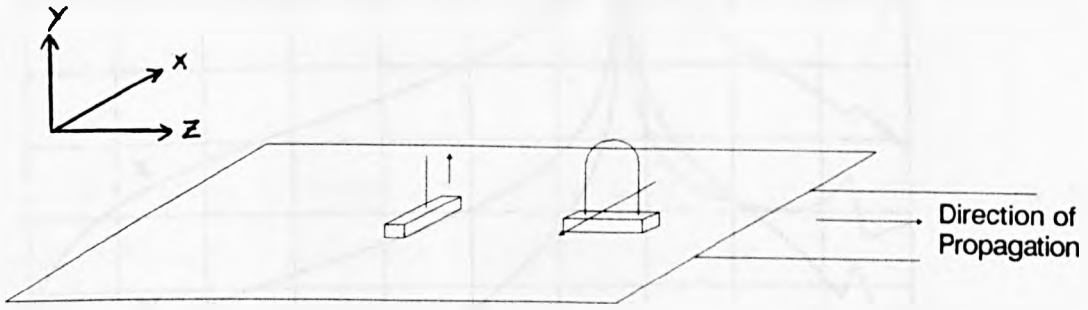

Fig. 2.3.1 Orientation of dipoles for coupling with tx line to occur

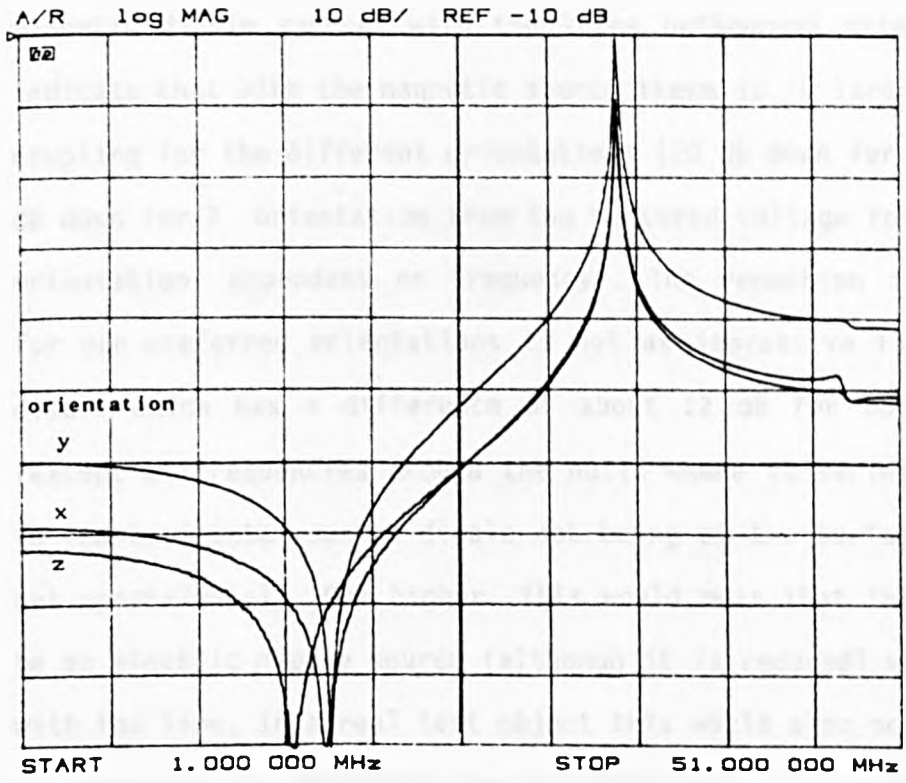

a)electric dipole source

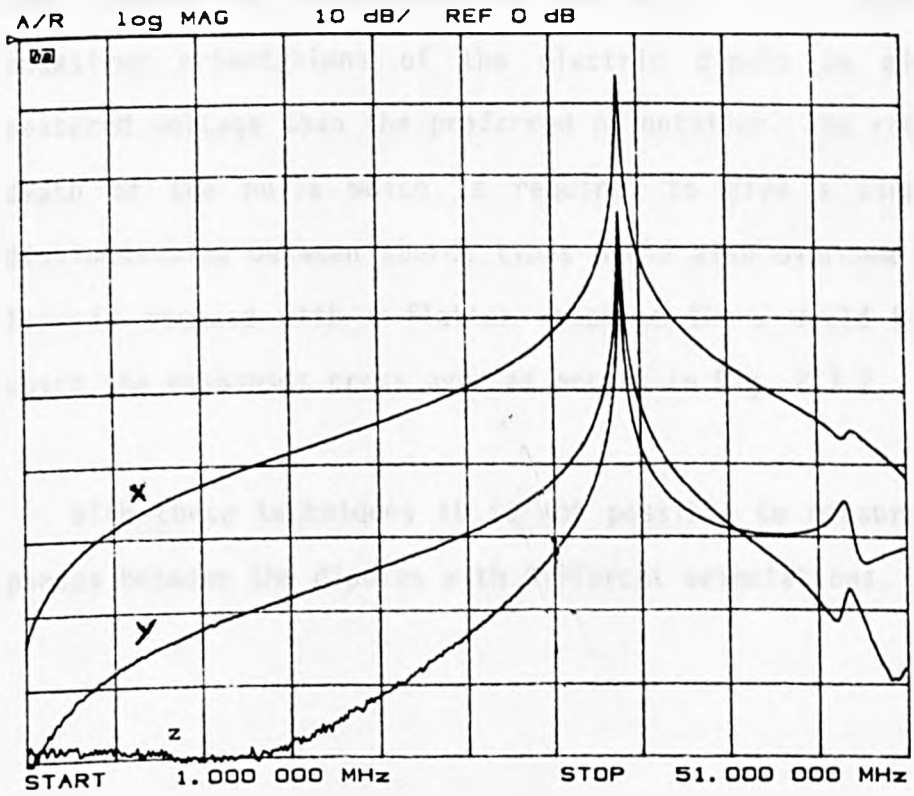

b)magnetic dipole source

Fig. 2.3.2 Measured voltage for three orientations of source

Fig. 2.3.2 shows the measured voltage for the electric and magnetic dipole sources with the three orthogonal orientations. They indicate that with the magnetic source there is a large change in the coupling for the different orientations (20 dB down for X and 30 to 40 dB down for Z orientation from the measured voltage for the preferred orientation, dependent on frequency). The reduction in the coupling for non-preferred orientations is not as impressive for the electric dipole which has a difference of about 12 dB for both orientations (except at frequencies around the nulls where it varies). This is due to the horizontal source dipole not being at the surface of the bench but approximately 20mm higher. This would mean that there would still be an electric dipole source (although it is reduced) which can couple with the line. In a real test object this would also occur so it would be necessary to determine the orientation of the maximum moment for each frequency and then see how much lower the other two orientations are. Around the frequencies of the nulls it is possible for the undesired orientations of the electric dipole to give a greater measured voltage than the preferred orientation. The reduction in the depth of the nulls which is required to give a simple method of distinguishing between source types would also overcome this problem. This is because with a flatter response there would be no point at which the responses cross over as occurs in Fig. 2.3.2.

With these techniques it is not possible to measure the relative phases between the dipoles with different orientations.

3. USING THE CIRCUITS TO INVESTIGATE CHANGES TO THE ROOM

3.1 Introduction

One of the aims of the research described in this thesis is to adapt the screened room test set-ups to obtain a flat or slowly changing frequency response which would have two major advantages:-

1) The test set-up could be more easily calibrated, enabling the measured voltage to be related to the moment of the dipole source.
2) The type of source could be distinguished across the whole range of frequencies of interest; the measurement difficulties around the nulls in the response would be removed.

In addition to these practical advantages there would be no frequency at which the test set-up was particularly insensitive which could allow emission limits to be relaxed. This would then reduce the need to over engineer equipment at some frequencies so that it could pass tests at others, with a consequent saving in cost to the manufacturer and hence the customer. Likewise, it would reduce the opposite (possibly worse) effect of high level emissions being hidden in the deep null.

The models described in Chapter 2 were used to predict the effect of various changes to the test set-up. This chapter considers the effect of loading the bench (transmission line) in various ways :-

1) Adding loss to the bench with resistive cloth
2) Loading the end of the bench capacitively
3) Loading the end of the bench resistively.

Further changes are considered in Chapter 4.

3.2 Adding Loss to the Transmission Line

The results shown in Chapter 2 assume that the transmission line formed by the bench and walls of the screened room is lossless and show a very close agreement between the measured and predicted voltages. Suitable terms can be included in the transmission line equations, which are used in the models, to enable prediction of the effect of introducing loss onto the transmission line. Loss was added to the bench using resistive cloth; a number of possible arrangements were investigated. The cloth was either draped from the bench so that it hung loose (Figs. 3.2.1 and 3.2.2) or was connected between the bench and the wall (Fig. 3.2.3). Cloth was clamped to the bench and walls by means of aluminium strips bolted onto the bench and walls (Fig. 3.2.3). It was held onto the extension by means of large bulldog clips (Fig. 3.2.4) which were found to give an adequate connection between the metal of the bench and the resistive cloth.

Fig. 3.2.1 Draping the bench and extension with conductive cloth

Fig. 3.2.2 Cloth draped from bench

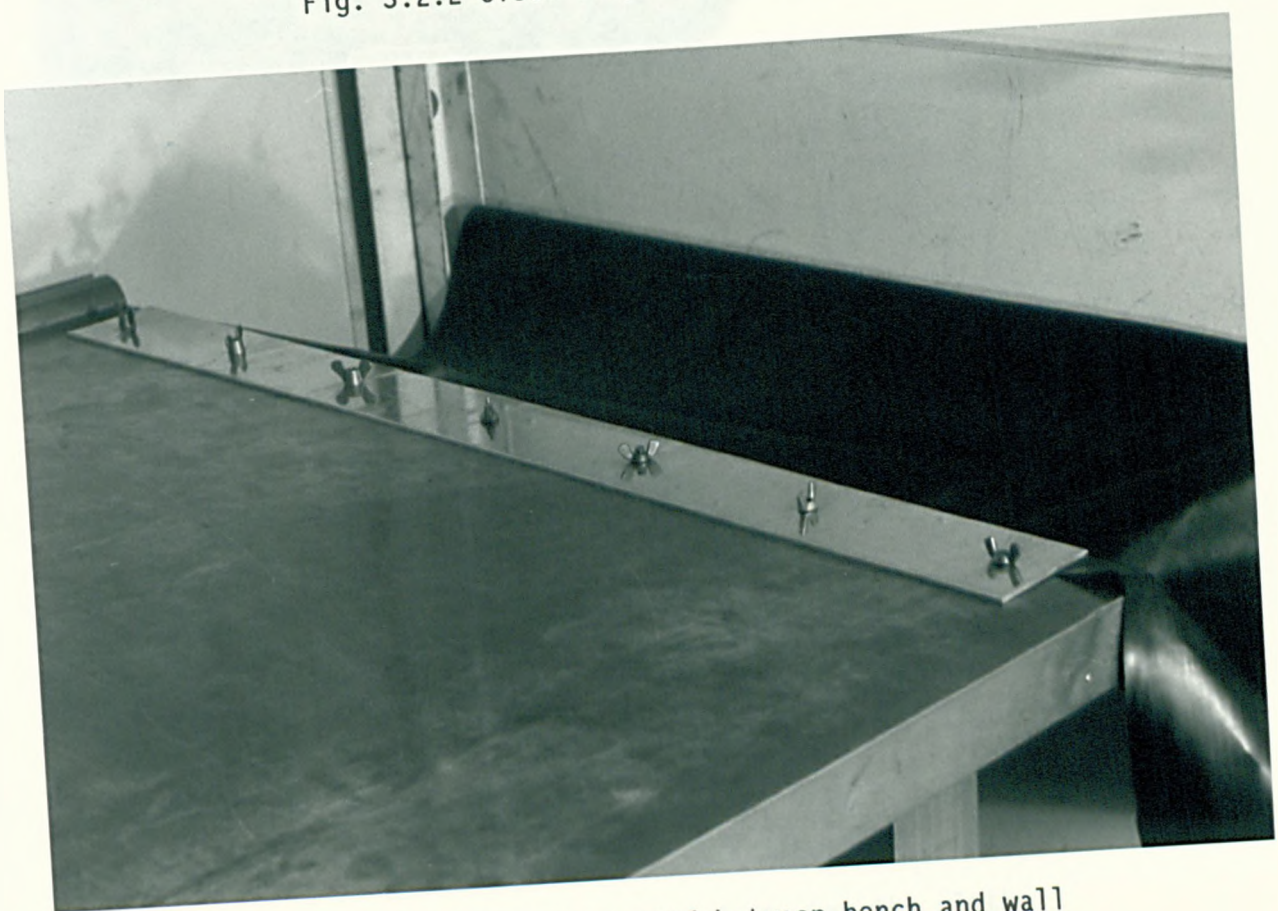

Fig. 3.2.3 Cloth connected between bench and wall

Bulldog clips used to fasten cloth to extension

Fig. 3.2.4 Method of fastening the cloth

The dimensions of the test bench and extension in the room did not easily enable the extension to be bonded to the wall with resistive cloth which is 1 × 0.5 m. It was also considered to be impractical to connect the cloth between the extension and the walls as it would be difficult to position the EUT without removing the cloth every time. This would increase the likelihood of damage to the cloth and a consequent degradation of performance as well as increasing the time taken to carry out each test. With the cloth bonded to the walls and bench the loss is purely resistive whilst with the cloth draped from the bench and not in direct contact with the walls it appears as a resistance in series with a capacitance. On the extension only the latter is possible. The general transmission line model including this loss is shown in Fig. 3.2.5 and Equations 3.1 to 3.4. When the cloth is connected to the bench and walls there is also a distributed capacitive element in parallel with the resistive element but the resistive term will dominate and the capacitance can be ignored for a close approximation.

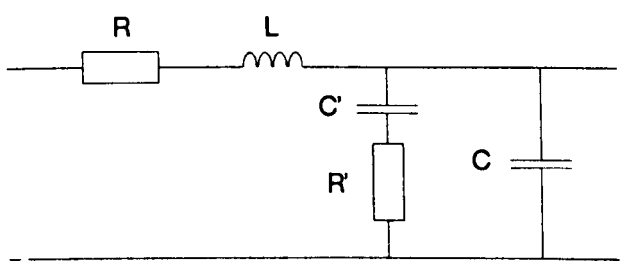

Fig.3.2.5 General transmission line model with loss added

$$ZO = \sqrt{\frac{R + j\omega L}{G + j\omega C}} \qquad 3.1$$

$$\gamma = \sqrt{(R + j\omega L)(G + j\omega C)} \qquad 3.2$$

$$R = 0 \qquad 3.3$$

$$G = \frac{1}{R' + \frac{1}{j\omega C'}} \qquad 3.4$$

R' is the resistance per unit length of the cloth from the bench towards the wall and C' is the capacitance per unit length from the cloth to the wall.

The conductive fabric available for these experiments had resistances of 60Ω or 200Ω per square. It was therefore only possible to verify predictions made using loads which could be constructed using these values of cloth resistance. The capacitance from the cloth to the outer conductor had to be estimated from the dimensions of the test set-up.

Figs. 3.2.1 to 3.2.4 show the various positions of the draping used to add loss to the line. The drapes were hung along both sides of the bench and/or extension to keep the line symmetrical.

Several set-ups were modelled:-

1) loss on the extension only

   66Ω/m +15pF, 20Ω/m + 15pF

2) loss on the bench only

   66Ω/m + 30pF, 20Ω/m + 30pF, 66Ω/m, 20Ω/m

3) loss on bench and extension

66Ω/m + 30pF with 20Ω/m + 15pF

20Ω/m + 30pF with 66Ω/m + 15pF

66Ω/m with 20Ω/m + 15pF

20Ω/m with 66Ω/m + 15pF

The 66Ω and 20Ω were derived from the resistances and dimensions of the resistive cloth used.

Some of the predicted and measured results are shown in Figs. 3.2.6 to 3.2.15. The effect of draping the cloth on the line without connecting it to the walls is quite small. It gives a small reduction in the Q of the resonance and null but not enough to be useful. However, with the cloth bonded to the walls the effect is much greater and a large degree of damping can be achieved when using the lower impedance cloth (i.e. having more loss on the line).

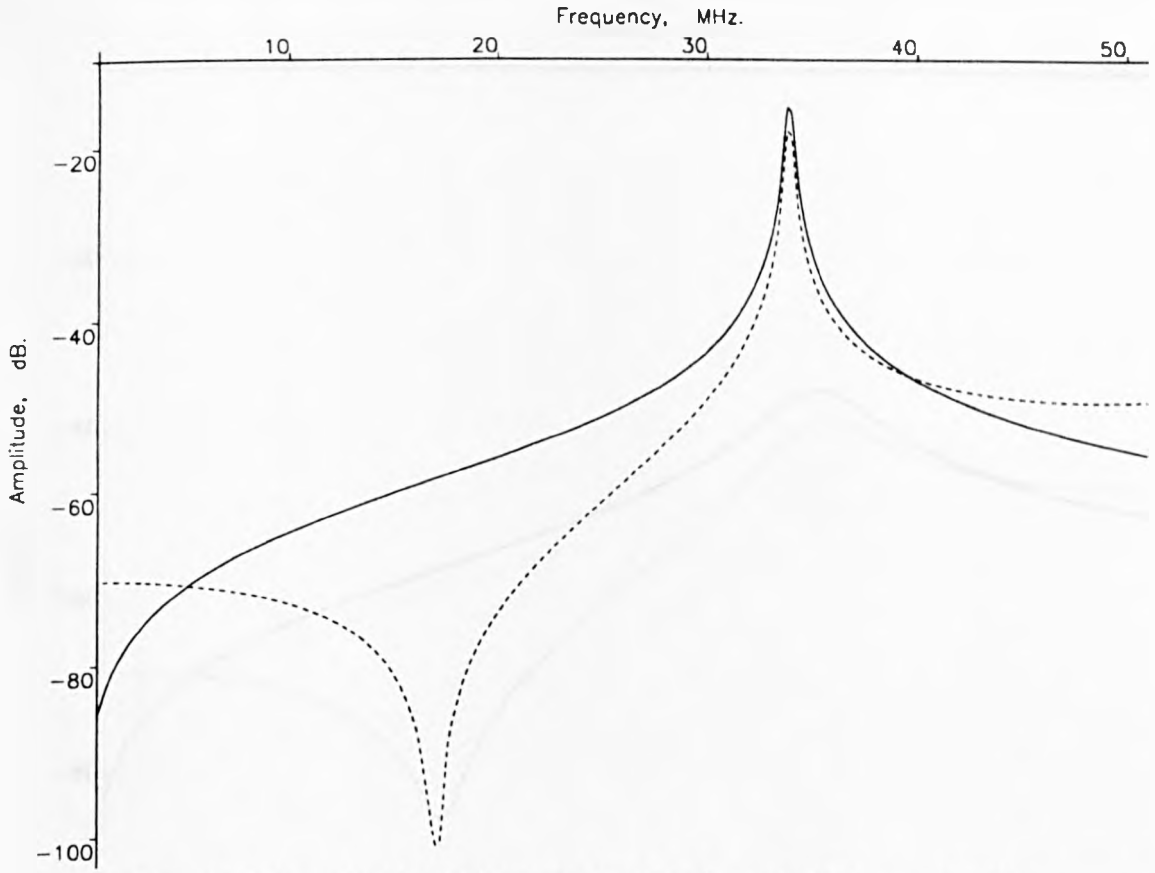

Fig. 3.2.6 Predicted response 66Ω/m + 30pF/m on bench

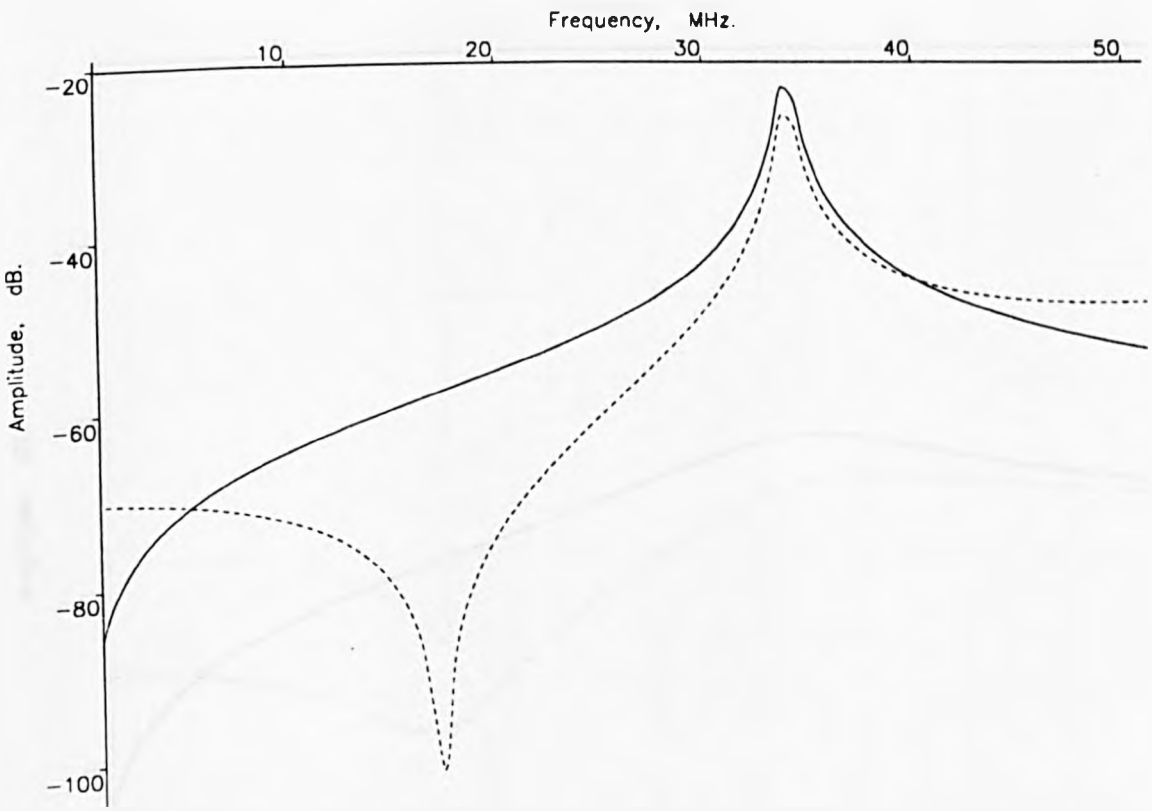

Fig. 3.2.7 Predicted response 66Ω/m on bench

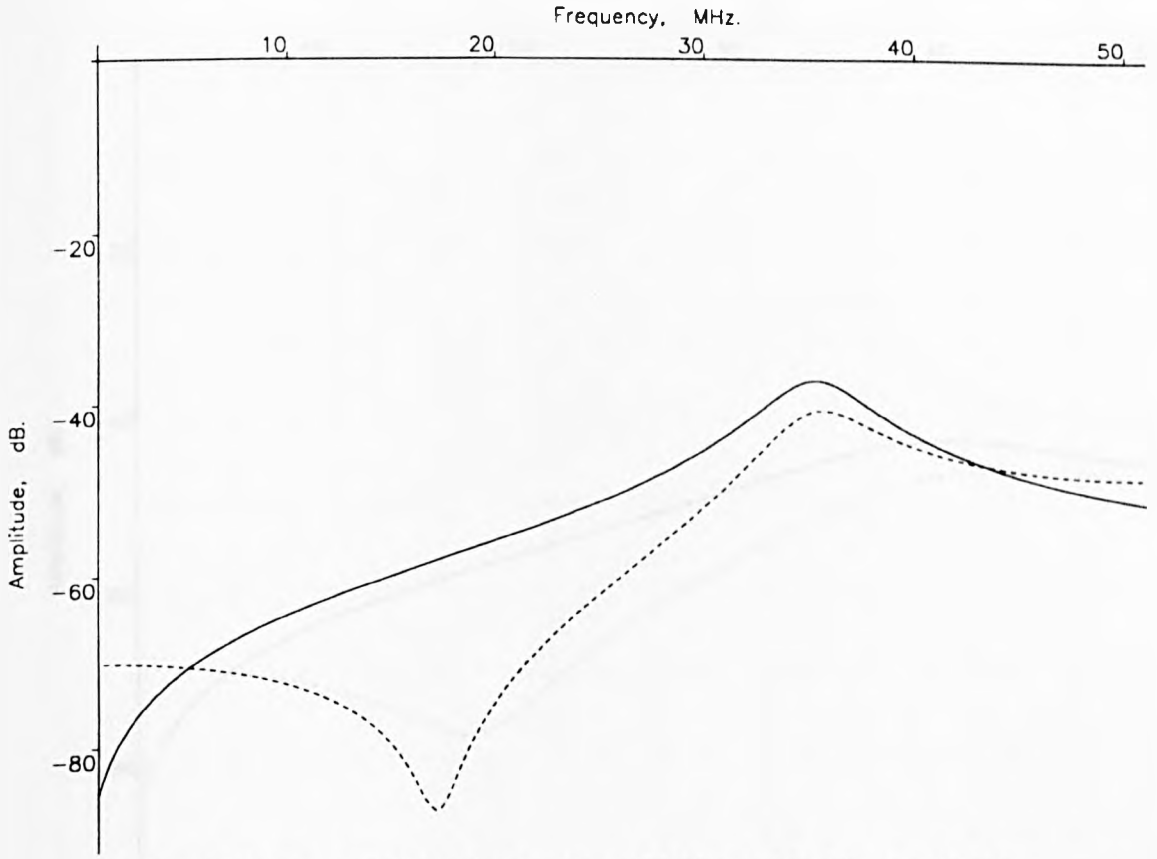

Fig. 3.2.8 Predicted response 20Ω/m + 30pF/m on bench

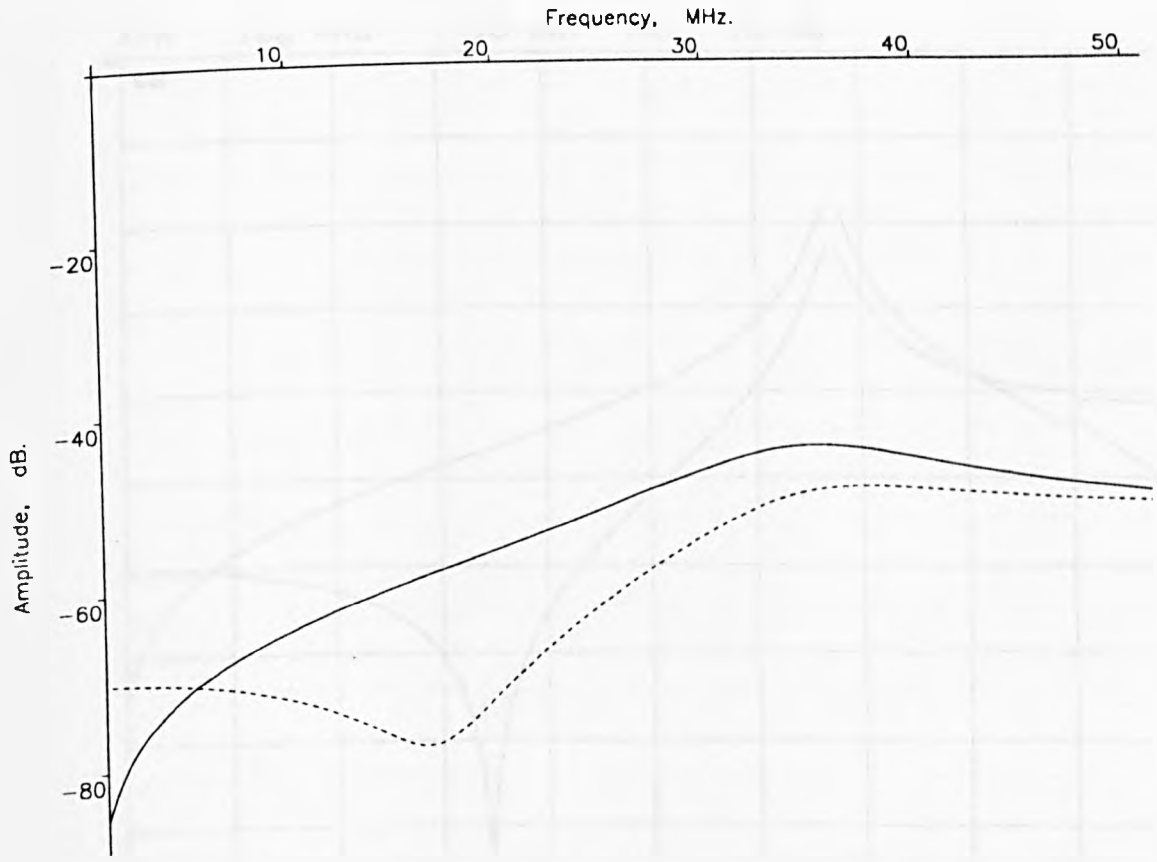

Fig. 3.2.9 Predicted response 20Ω/m on bench

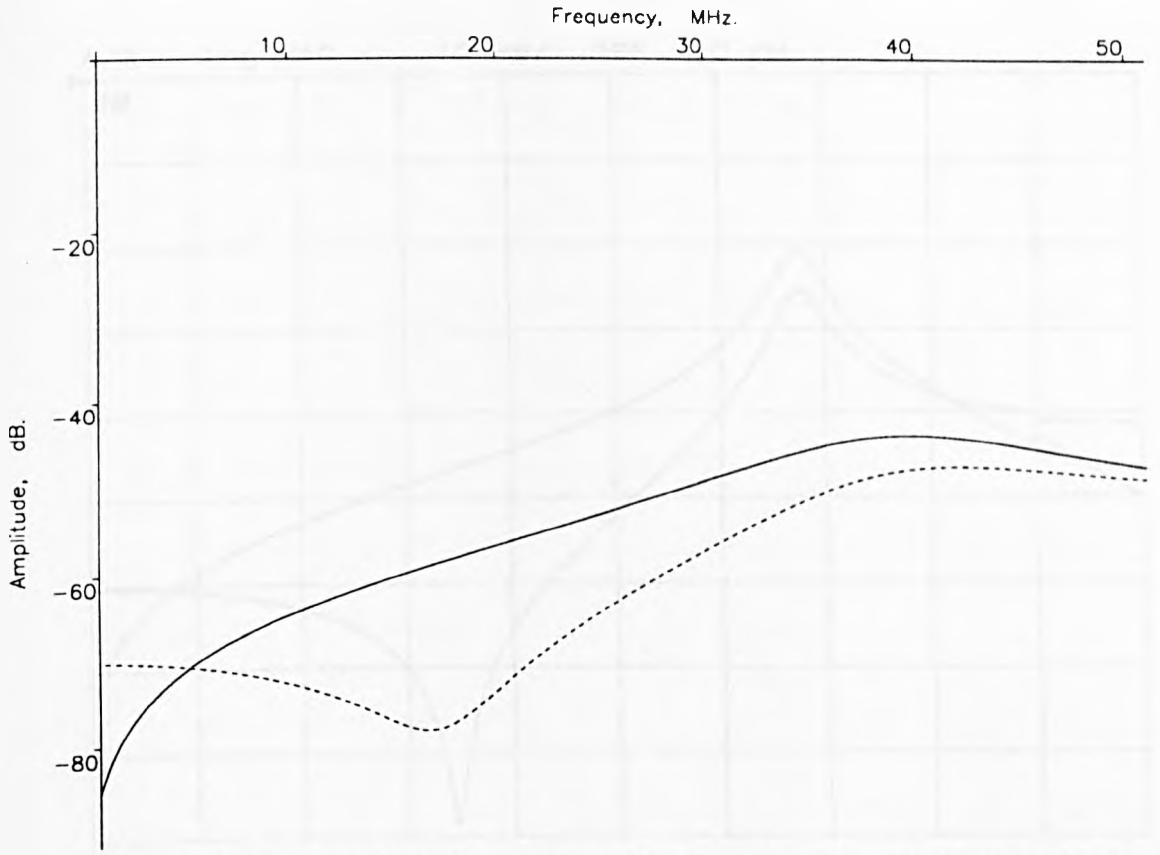

Fig. 3.2.10 Predicted response 20Ω/m on bench and 66Ω/m + 15pF on extension

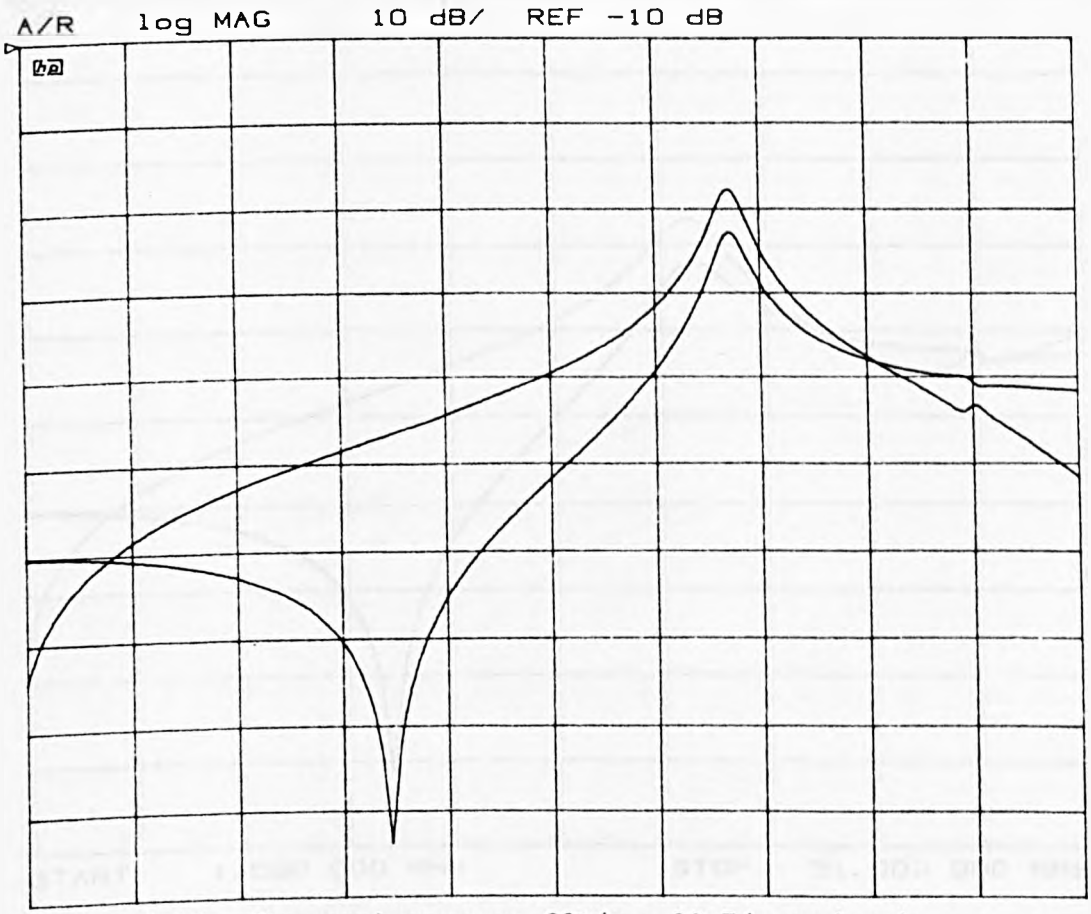

Fig. 3.2.11 Measured response 66Ω/m + 30pF/m on bench

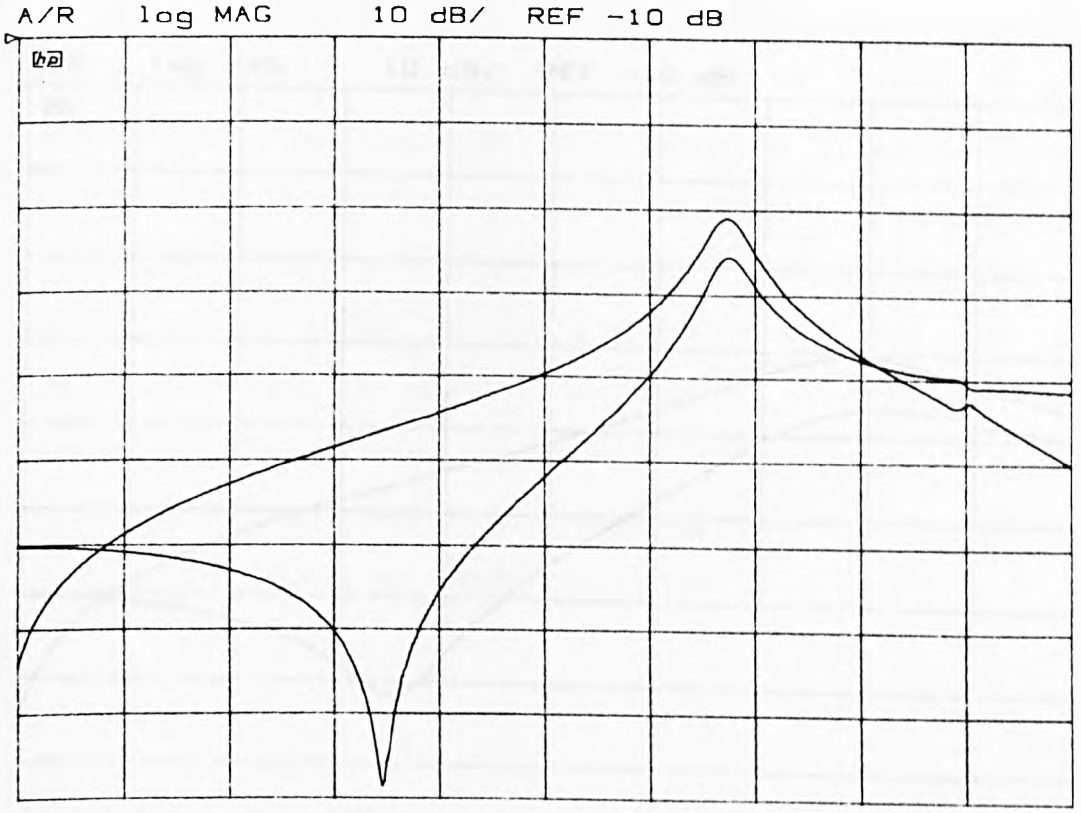

Fig. 3.2.12 Measured response 66Ω/m on bench

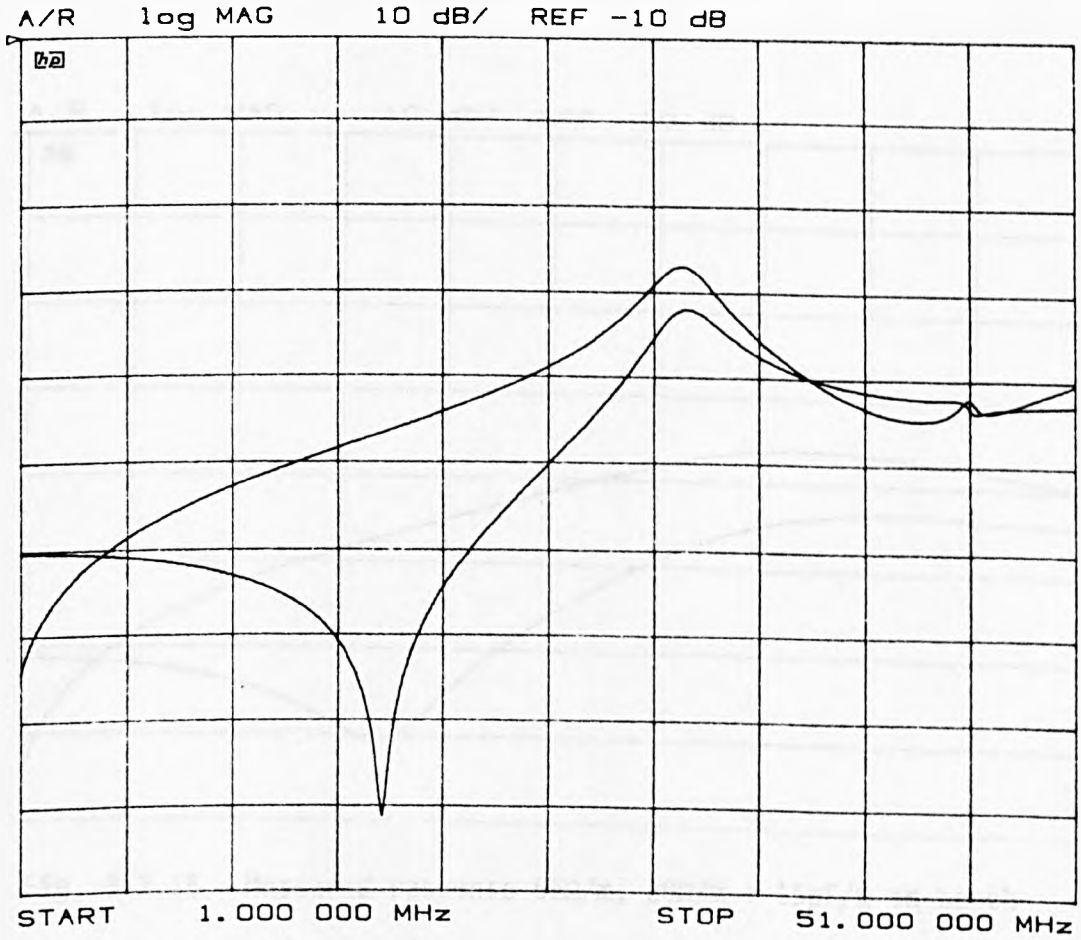

Fig. 3.2.13 Measured response 20Ω/m + 30pF/m on bench

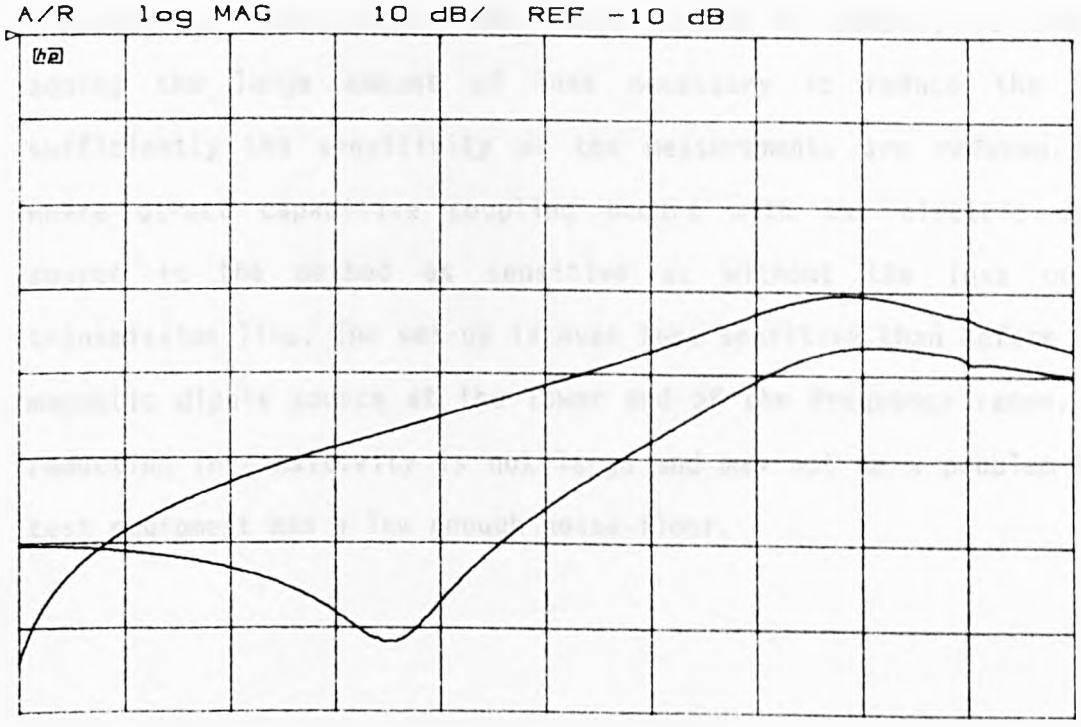

Fig. 3.2.14 Measured response 20Ω/m on bench

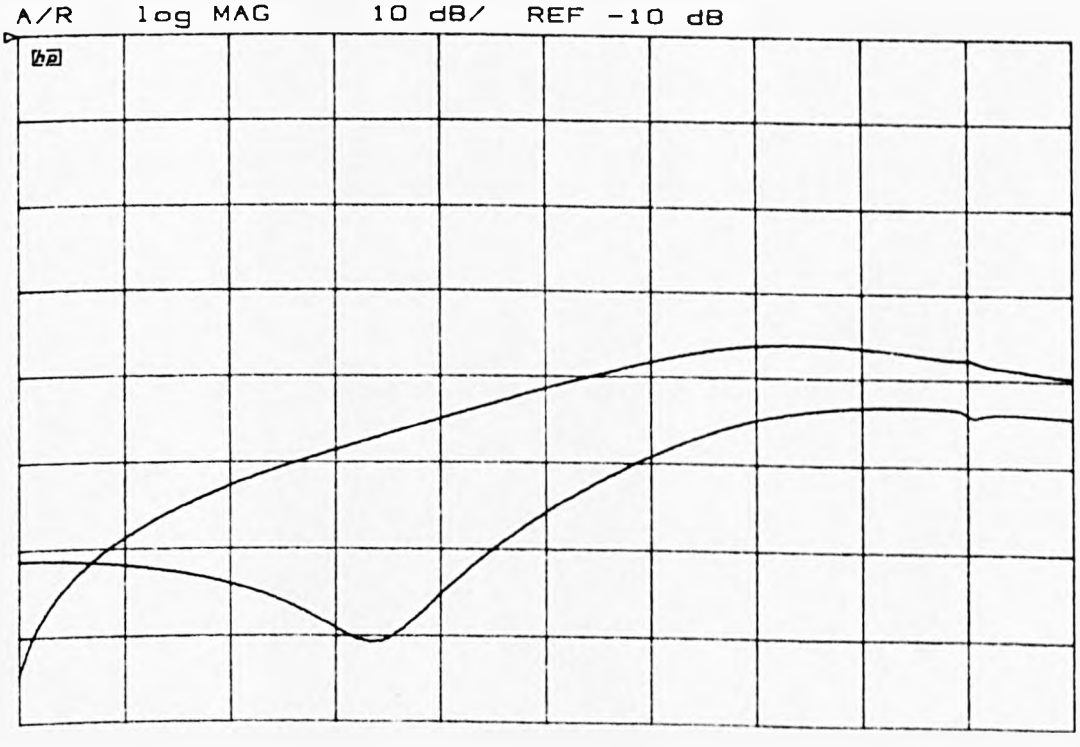

Fig. 3.2.15 Measured response 66Ω/m, 20Ω/m + 15pF/m on bench and extension

Apart from the practical difficulties of connecting the cloth, a disadvantage which occurs with this method of damping is that by adding the large amount of loss necessary to reduce the nulls sufficiently the sensitivity of the measurements are reduced. Only where direct capacitive coupling occurs with the electric dipole source is the method as sensitive as without the loss on the transmission line. The set-up is even less sensitive than before for a magnetic dipole source at the lower end of the frequency range. This reduction in sensitivity is not large and may not be a problem where test equipment has a low enough noise floor.

3.3 Loading The End of The Transmission Line

It is possible to change the input characteristics of the transmission line by altering the load on the end of the line [Dworsky 1979]. A load can be included in the model, as shown in Fig. 3.3.1, and the characteristics of the load can be varied to find a useful response. This was carried out for both resistive and capacitive loads.

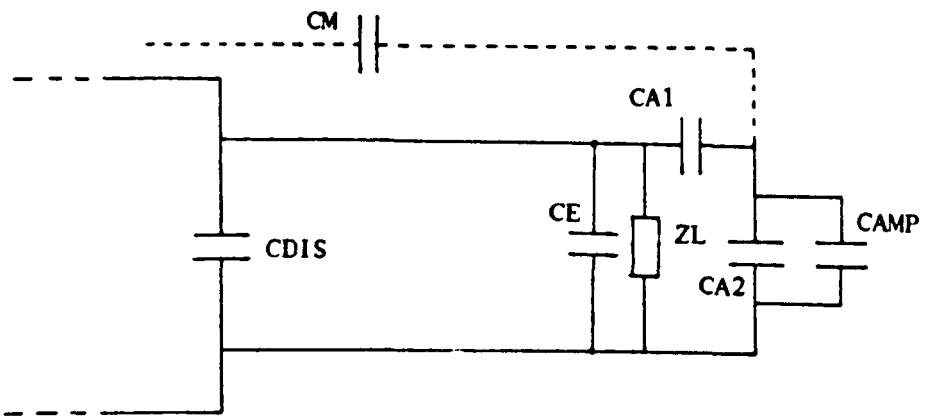

Fig.3.3.1 Model showing load on end of extension

3.3.1 Capacitively loading the end of the transmission line

Figs. 3.3.2 to 3.3.6 show the predicted effect of including various values of capacitance on the end of the line. They do not damp the resonance but tune it across a range of frequencies (the same with the null in the electric response). If a large variable capacitor could be constructed across the end of the bench a method of measurement similar to the stirred mode techniques used at higher frequencies could be used. However, this would not be a simple method of carrying out the measurements. It would require control of the variable capacitor and averaging would be needed for the results; the resulting values would still not have a flat frequency response as the peak and null change in height (or depth) as they are tuned across. It would also be much slower than a method where the instantaneous measured amplitude could be directly converted to a dipole moment. The capacitor would also need to be quite bulky as any connecting cables would need to be as short as possible to keep any inductance in the cable to an insignificant amount. For these reasons this particular technique was not pursued any further.

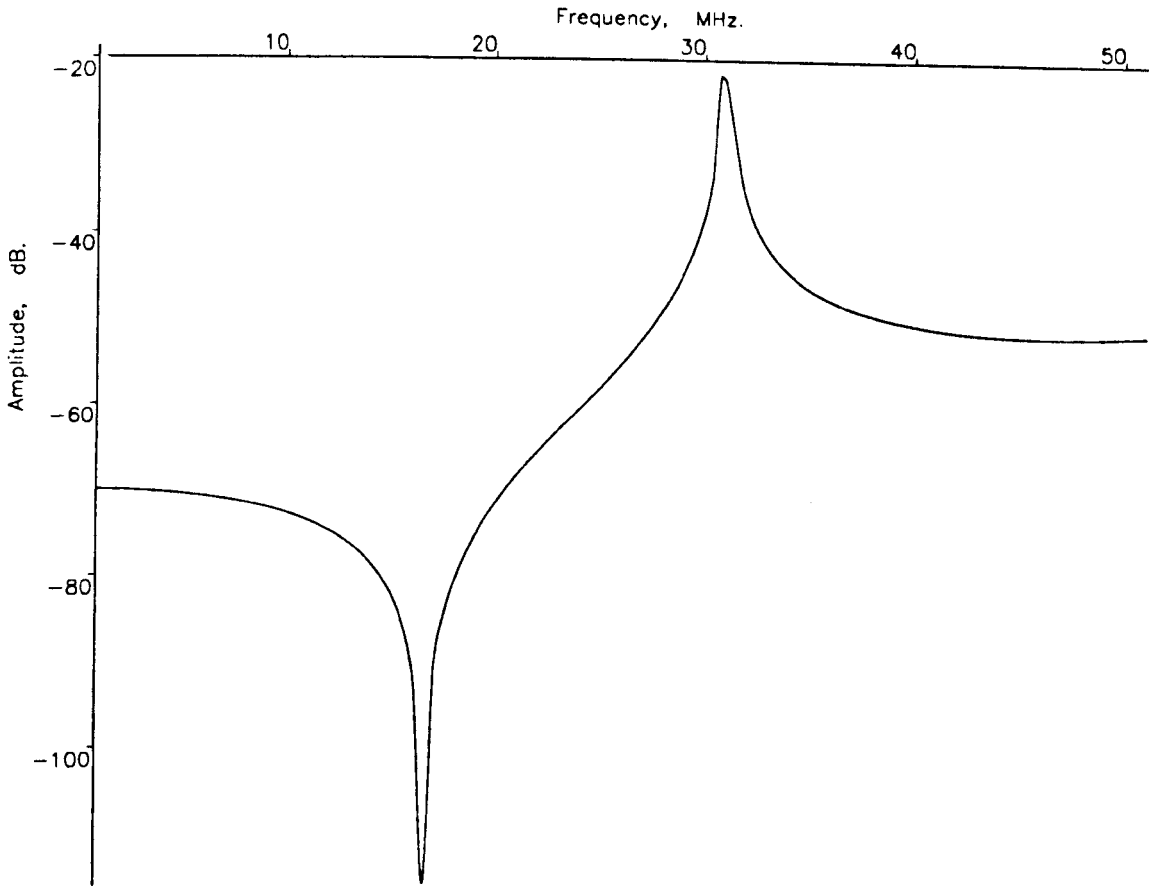

a) electric dipole source

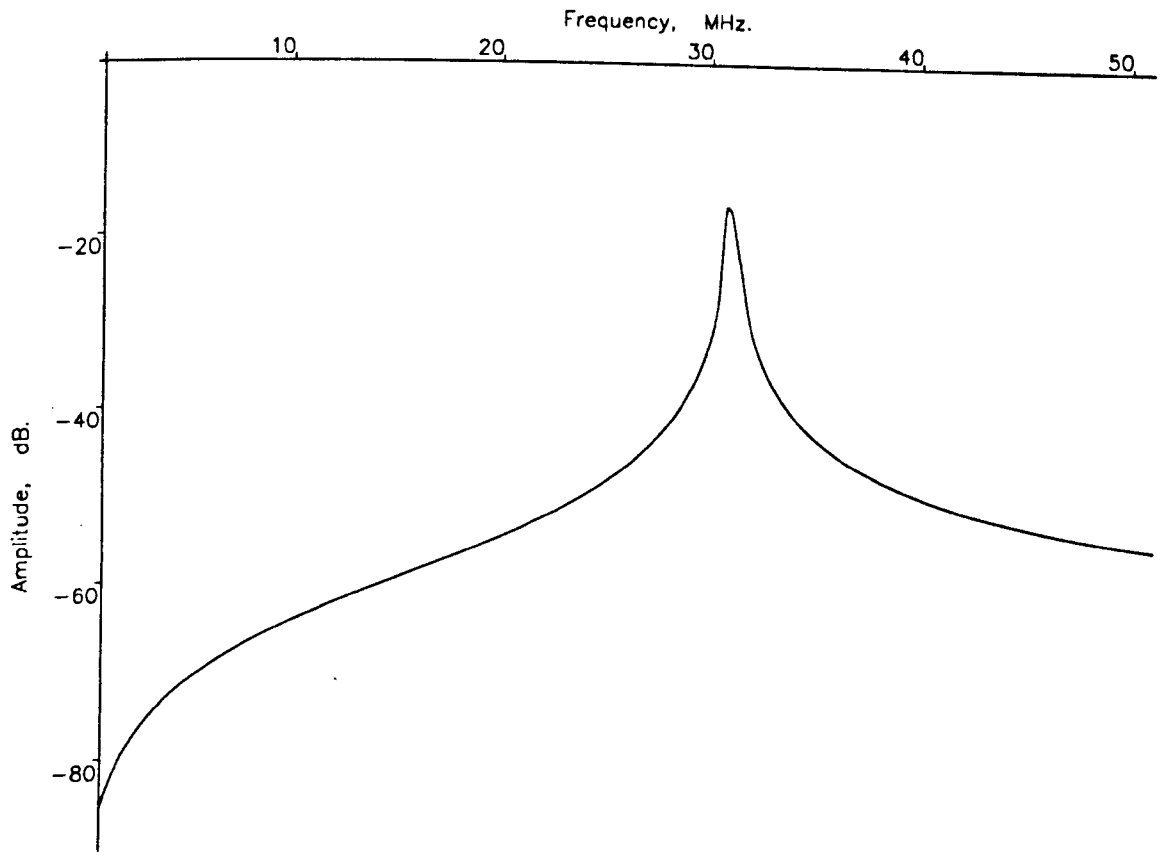

b) magnetic dipole source

Fig. 3.3.2 Predicted effects of 10 pF capacitive load

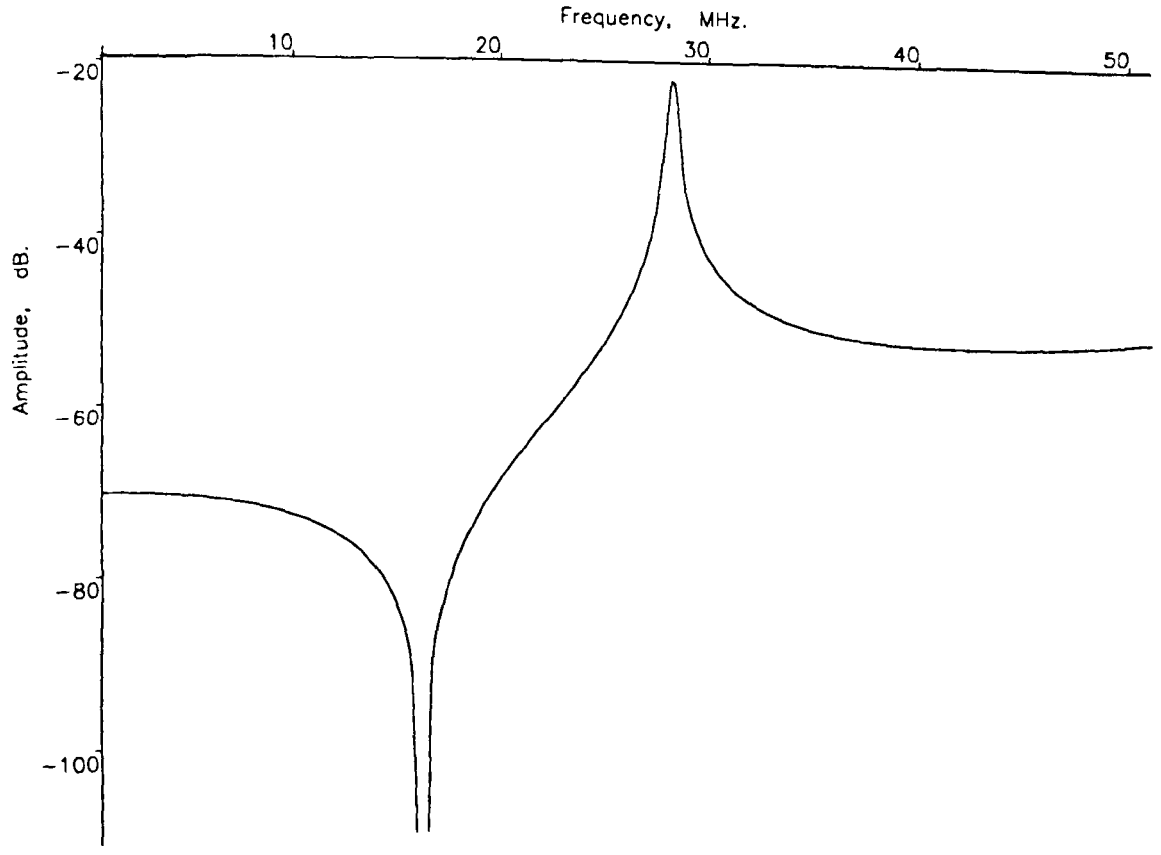

a) electric dipole source

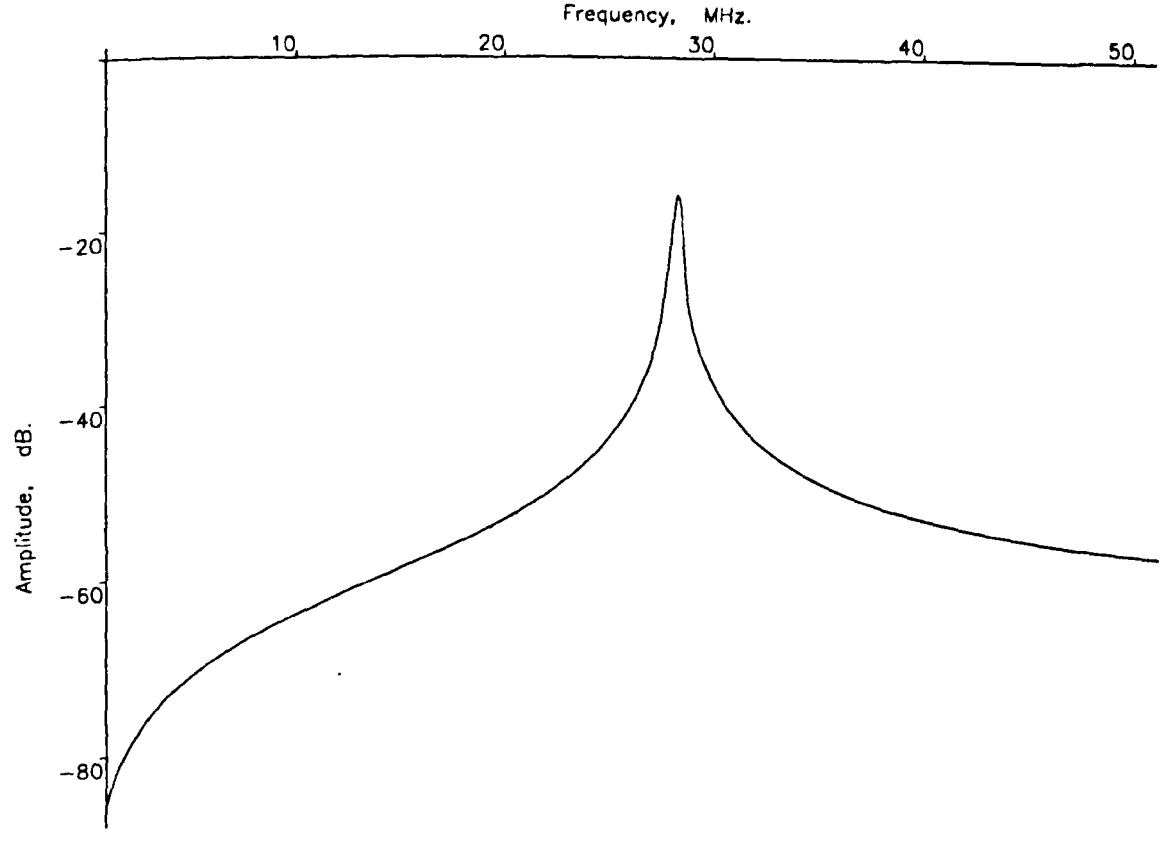

b) magnetic dipole source

Fig. 3.3.3 Predicted effects of 20 pF capacitive load

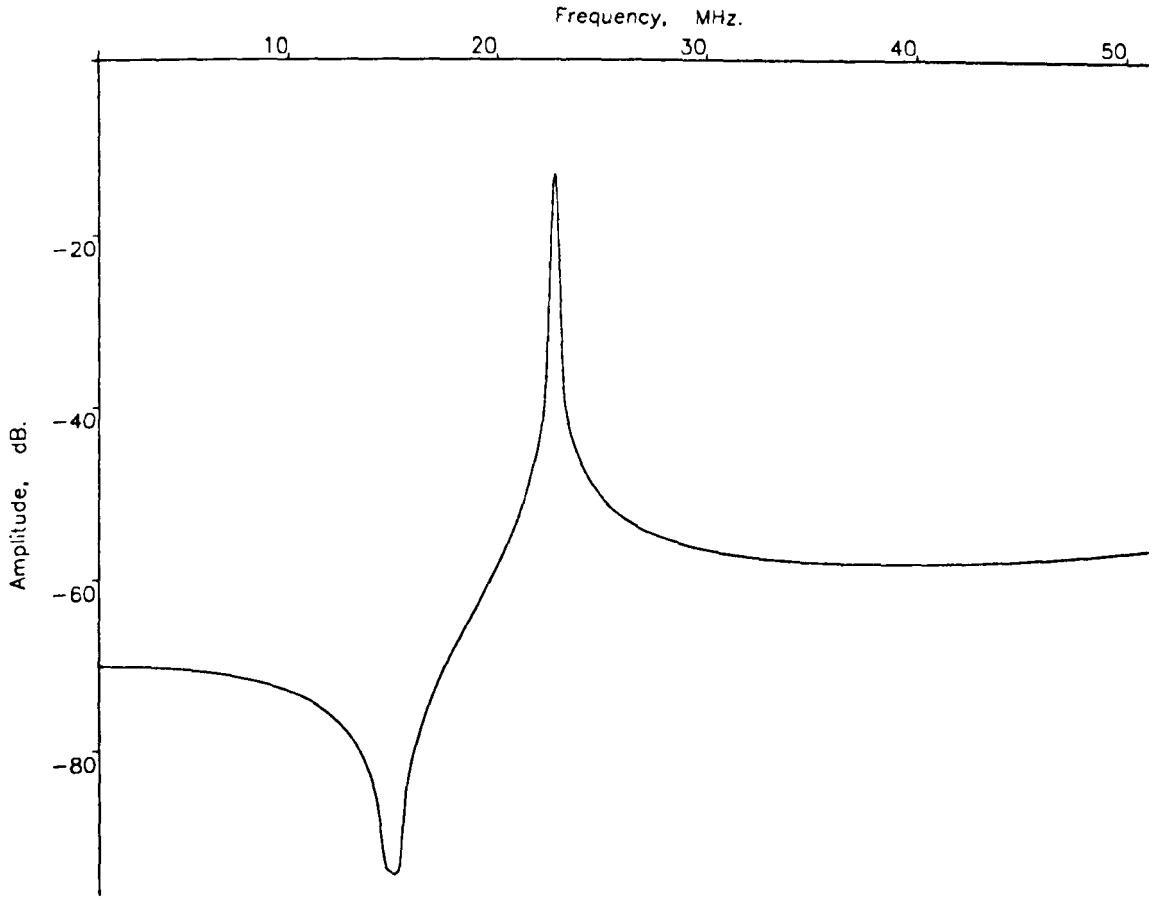

a) electric dipole source

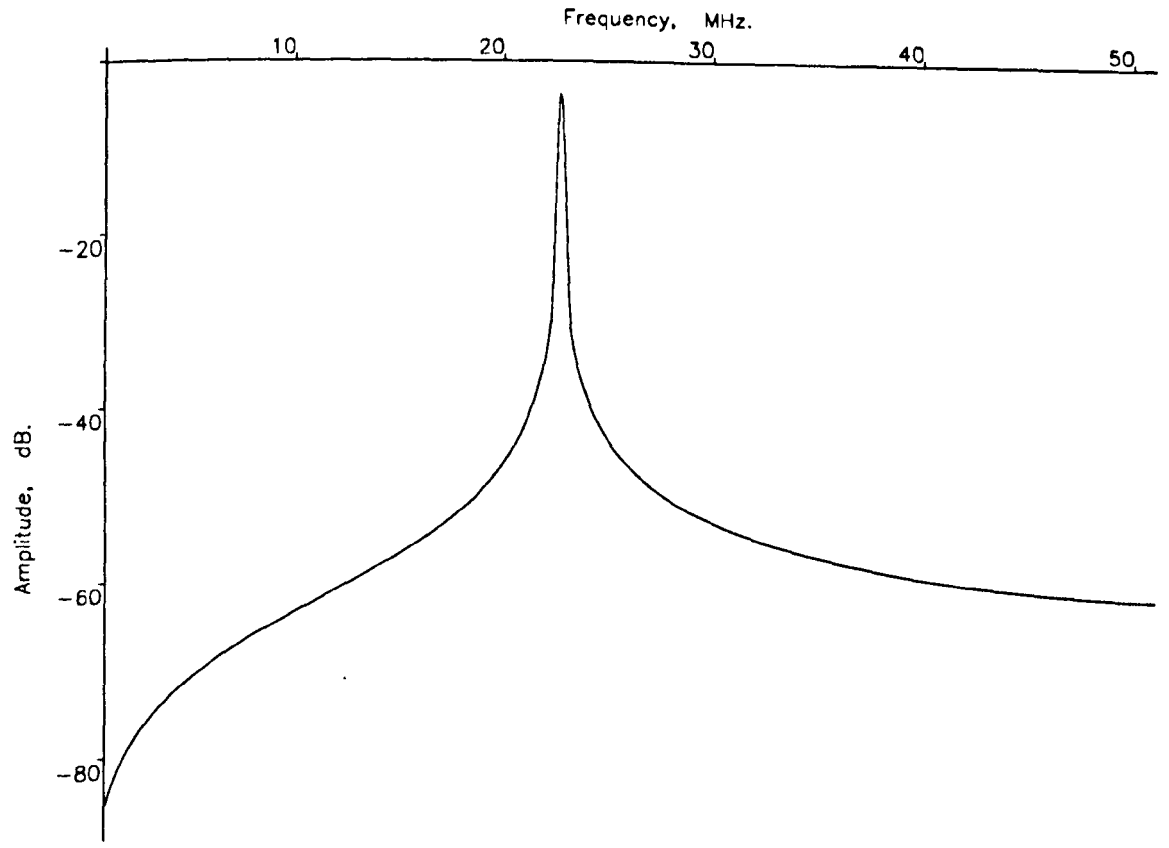

b) magnetic dipole source

Fig. 3.3.4 Predicted effects of 50 pF capacitive load

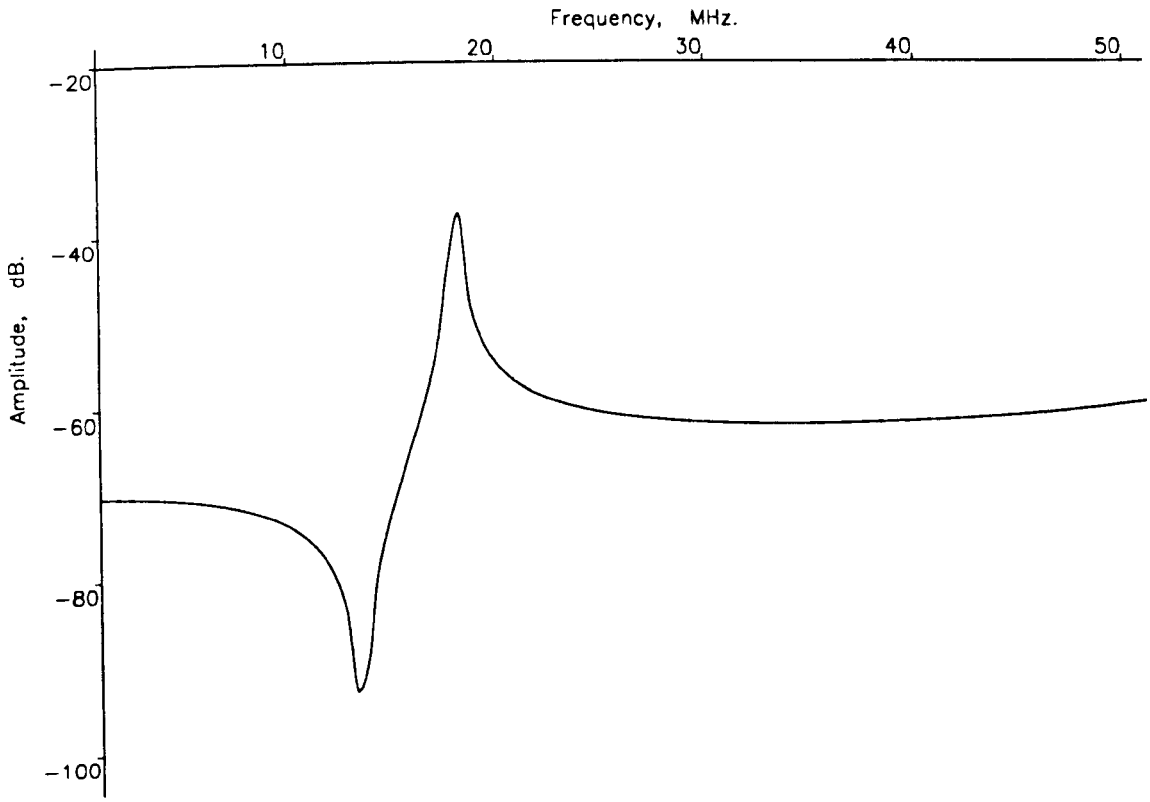

a) electric dipole source

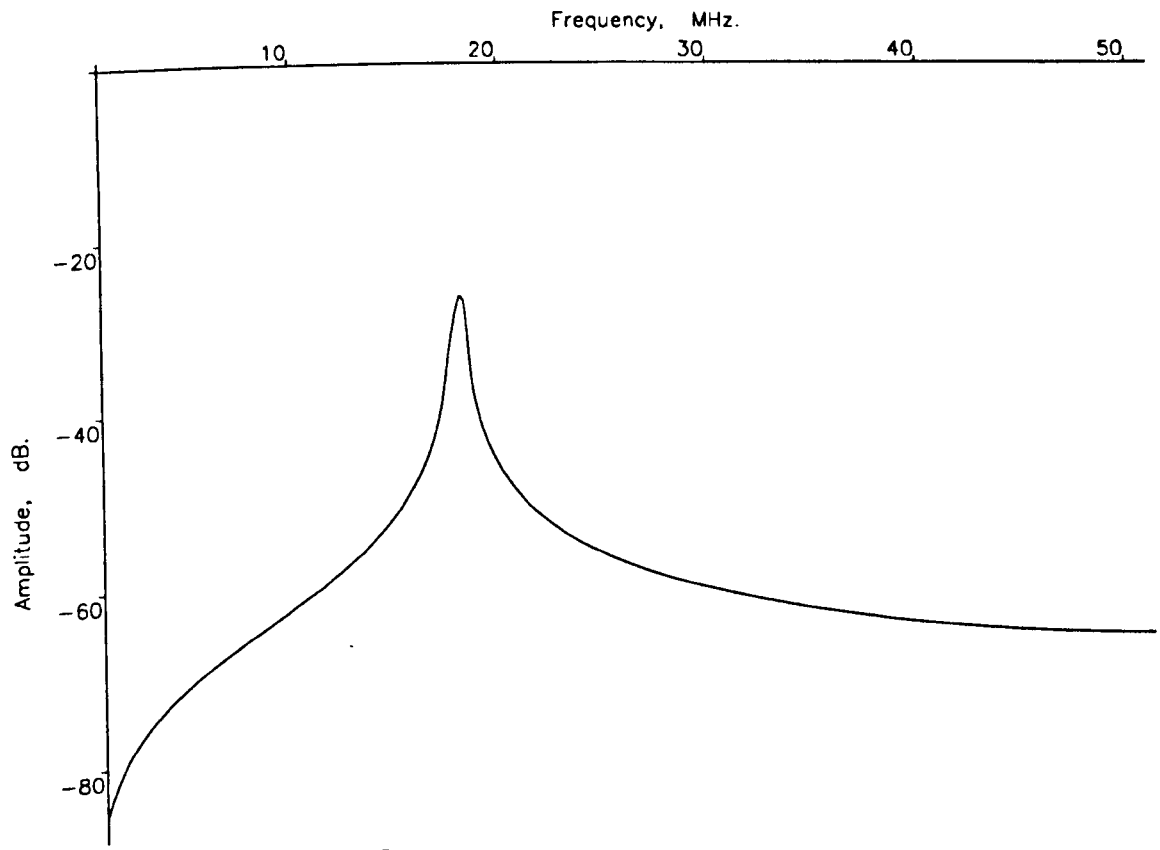

b) magnetic dipole source

Fig. 3.3.5 Predicted effects of 100 pF capacitive load

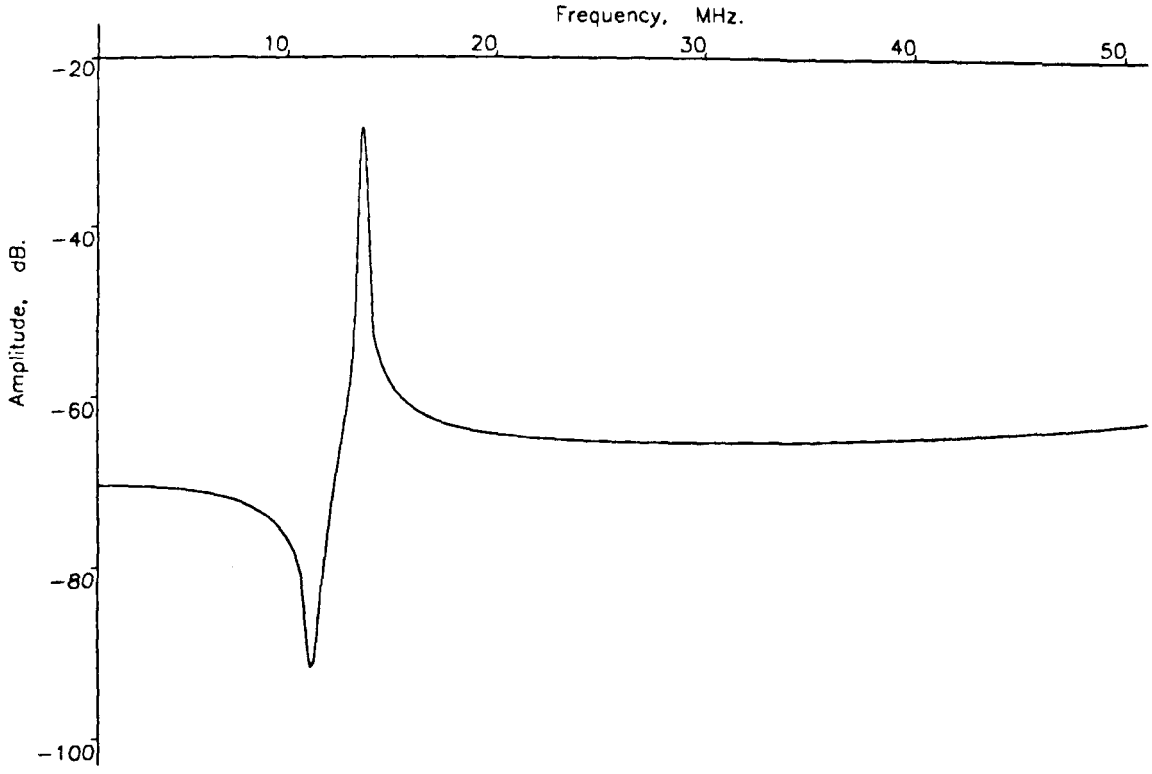

a) electric dipole source

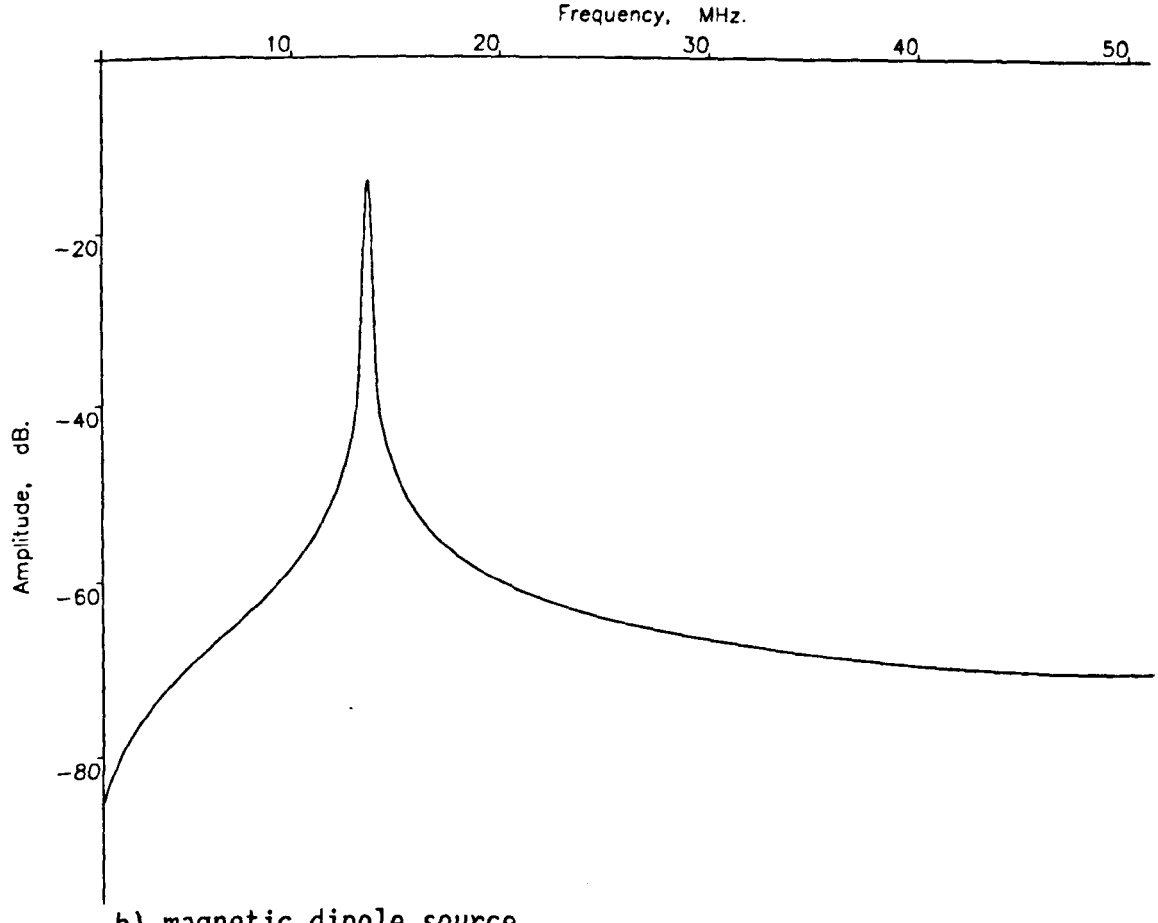

b) magnetic dipole source

Fig. 3.3.6 Predicted effects of 200 pF capacitive load

3.3.2 Resistively loading the end of the transmission line

A uniform open circuit transmission line with a length l will have a series of resonances which are a function of its length. The resonances can be removed by terminating the line in its characteristic impedance. However, the equivalent circuits do not consist of one uniform line and will have a different impedance at different frequencies so that the best load (i.e the load which gives the flattest response) will not necessarily be the 120Ω of the extension. The equivalent circuits were used to predict the effect of different values of resistance on the end of the extension and to find the value which gave the flattest response over the frequency band of interest. The effect of placing a resistive load at the end of each section of line (i.e. at the end of the bench and the end of the extension) was not investigated due to the difficulty in placing a load at the end of the bench.

Figs. 3.3.7 to 3.3.10 show the predictions for various different values of resistance. A value of 10Ω gives a good predicted response with a totally flat response for the electric source up to about 40MHz. The magnetic response is not flat but does have a smoothly varying response which could be calibrated out. The flat response for the electric dipole source occurs because the capacitive coupling between the two electric antennas is dominant over most of the frequency range. This dominance is due to the reduction in the signal conducted down the bench as the resonance is reduced and shifted in frequency.

A practical load can be constructed out of carbon loaded foam (multilayer microwave absorber AN79) and/or conductive sheeting; a

load made out of a string of resistors or including a metal sheet cannot be used due to the inductance which would be present at these frequencies and would destroy the loading effect of the resistors by increasing the impedance (it was investigated).

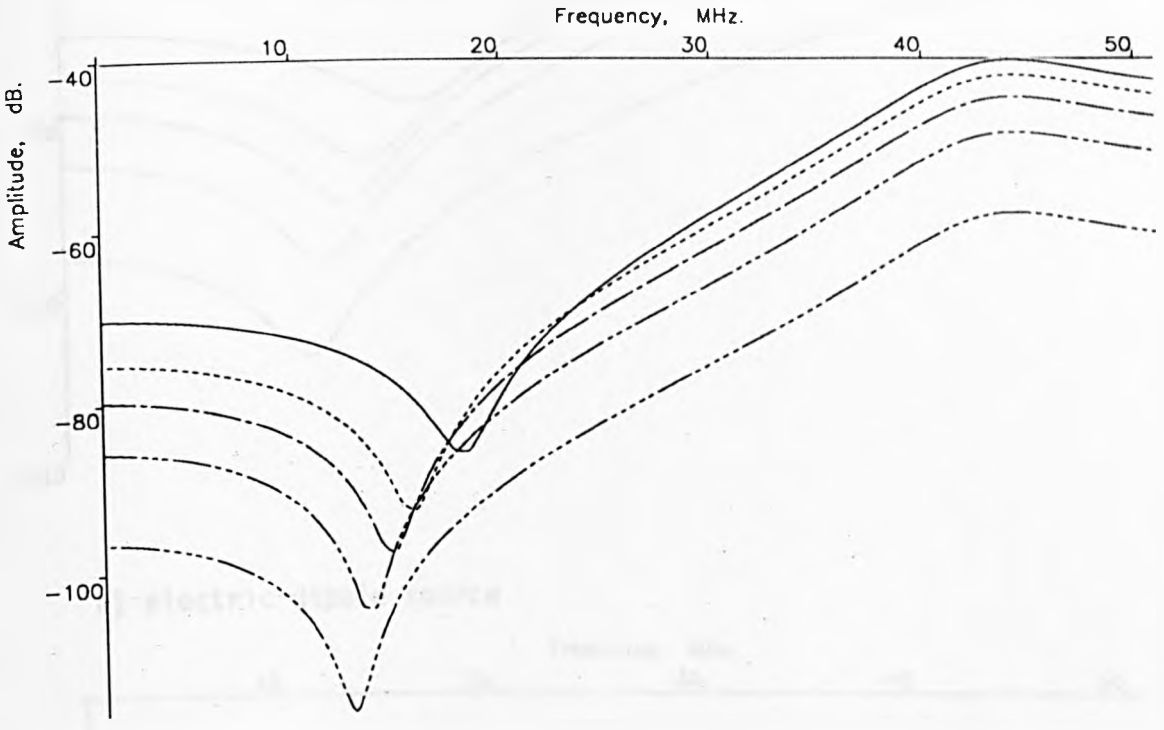

a) electric dipole source

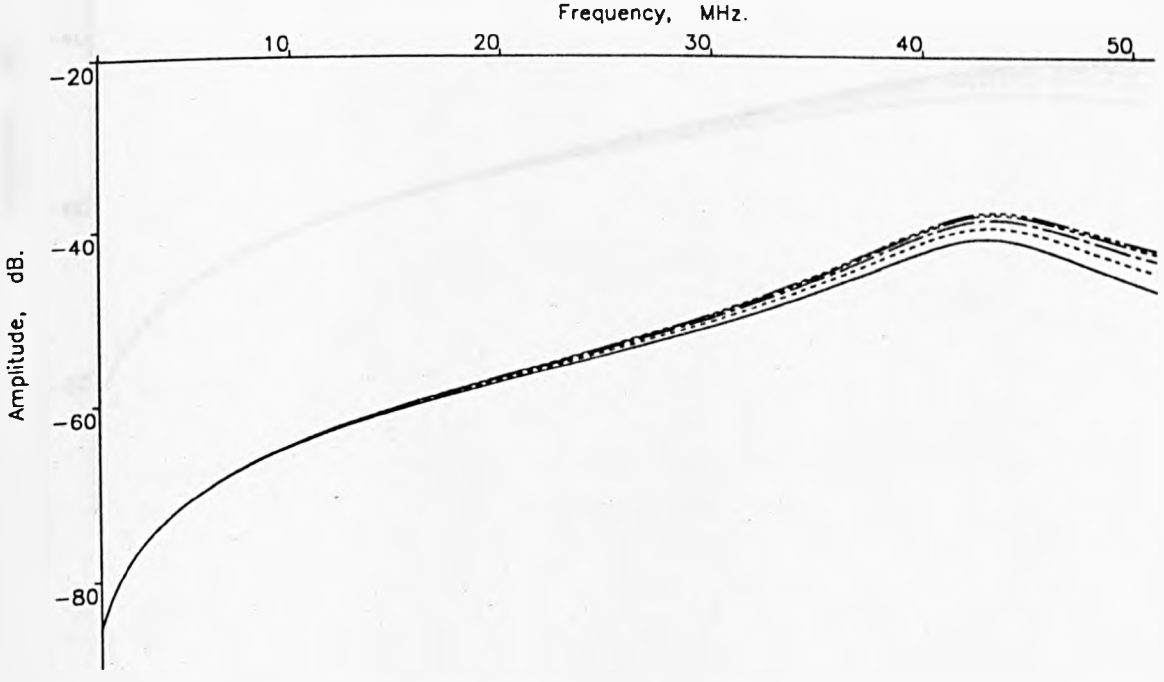

b) magnetic dipole source

Fig. 3.3.7 Predictions for loading 500 Ω resistance

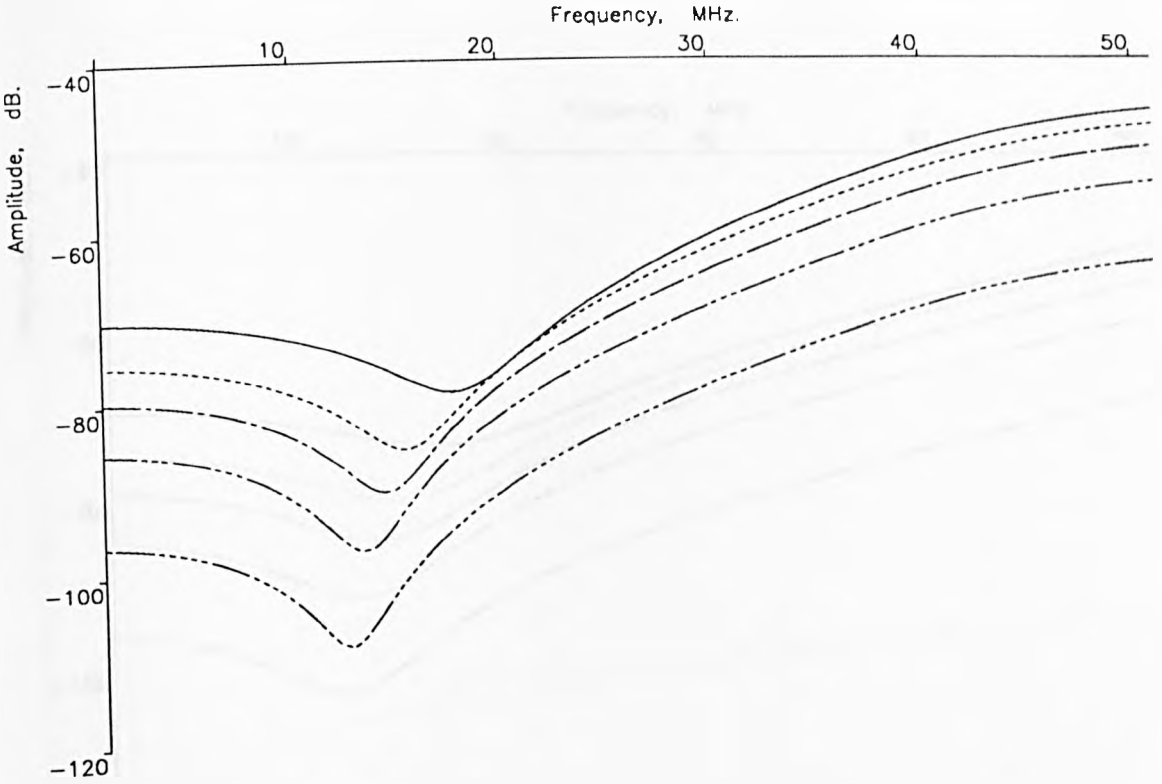

a) electric dipole source

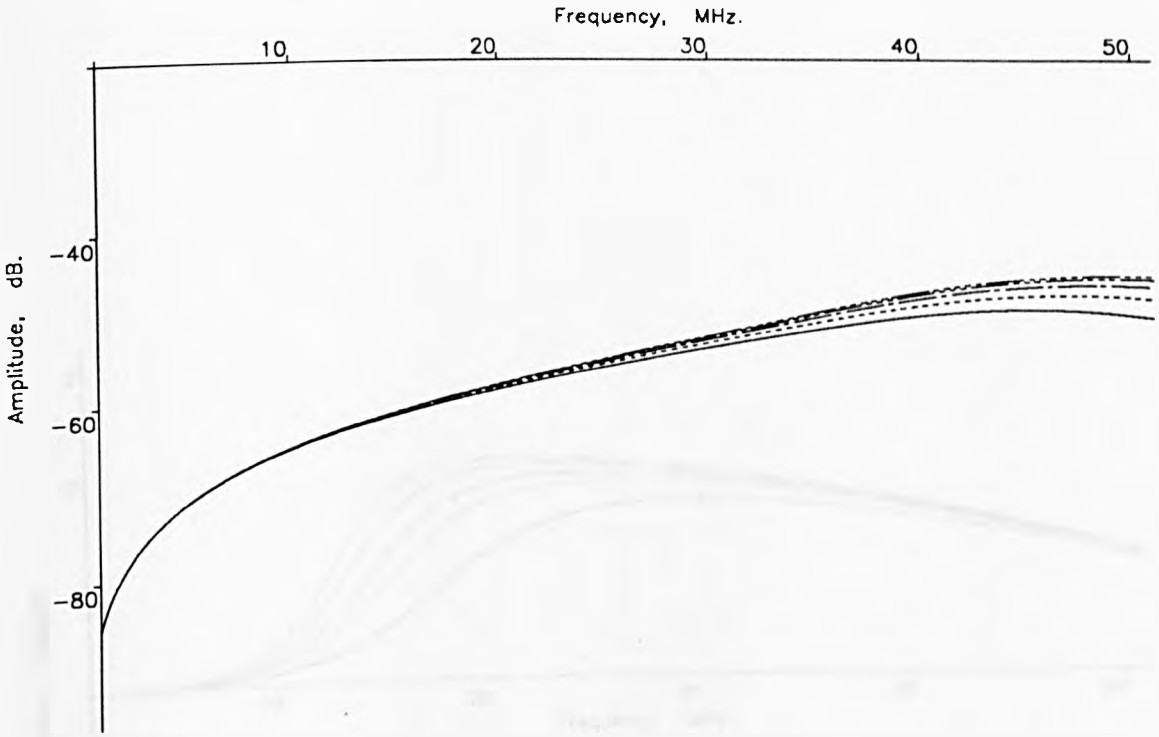

b) magnetic dipole source

Fig. 3.3.8 Predictions for loading 200 Ω resistance

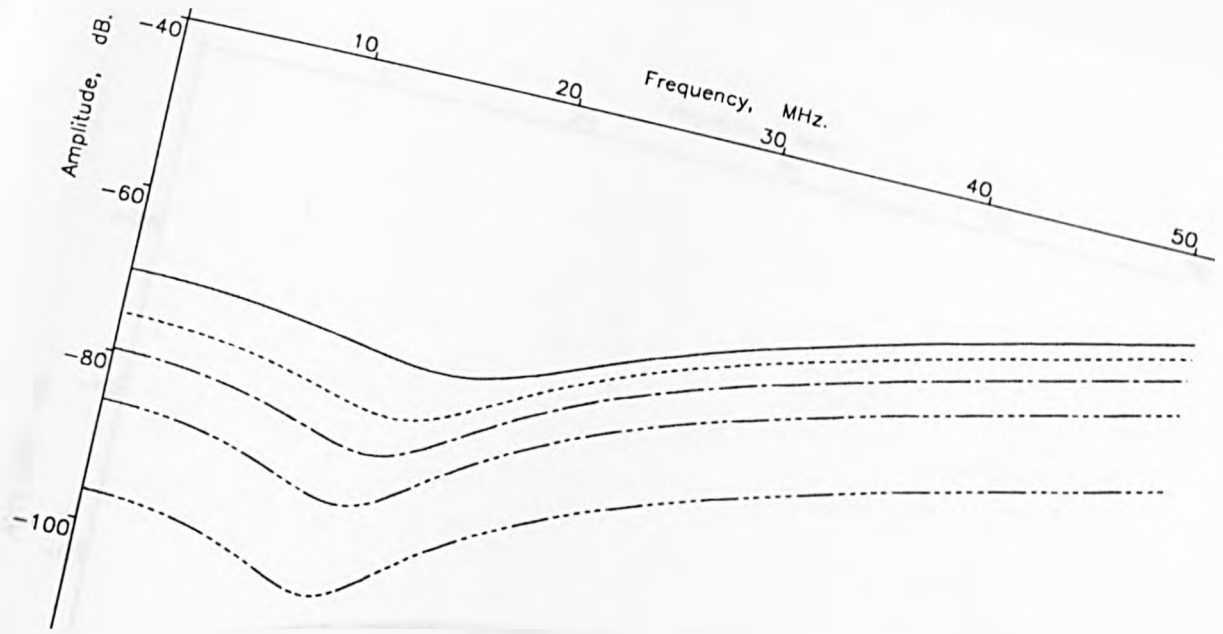

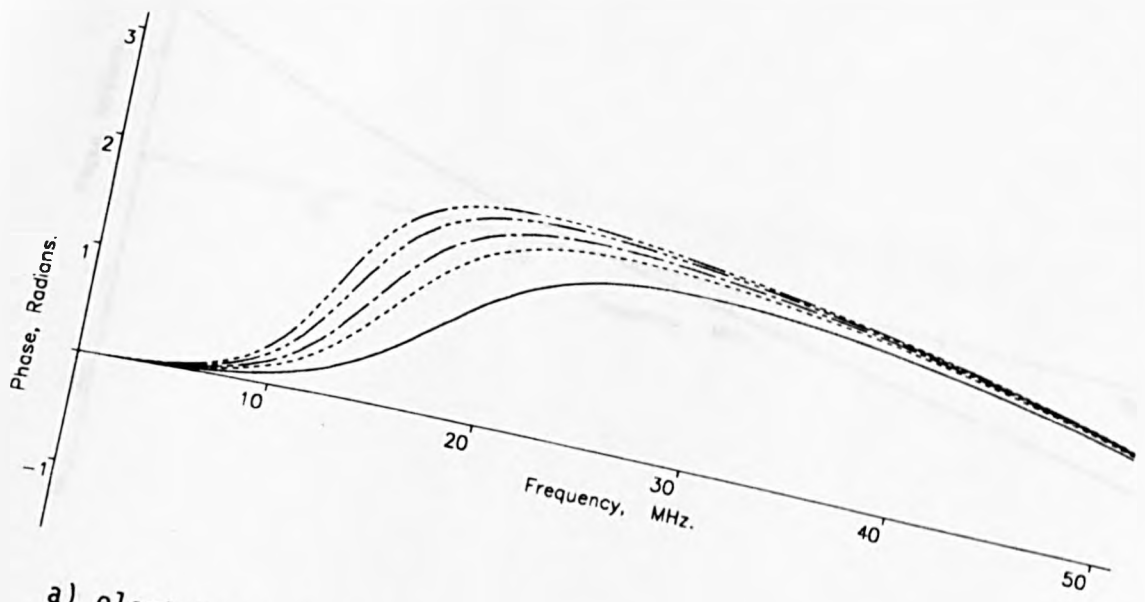

a) electric dipole source

Fig. 3.3.9 Predictions for loading 50 Ω resistance

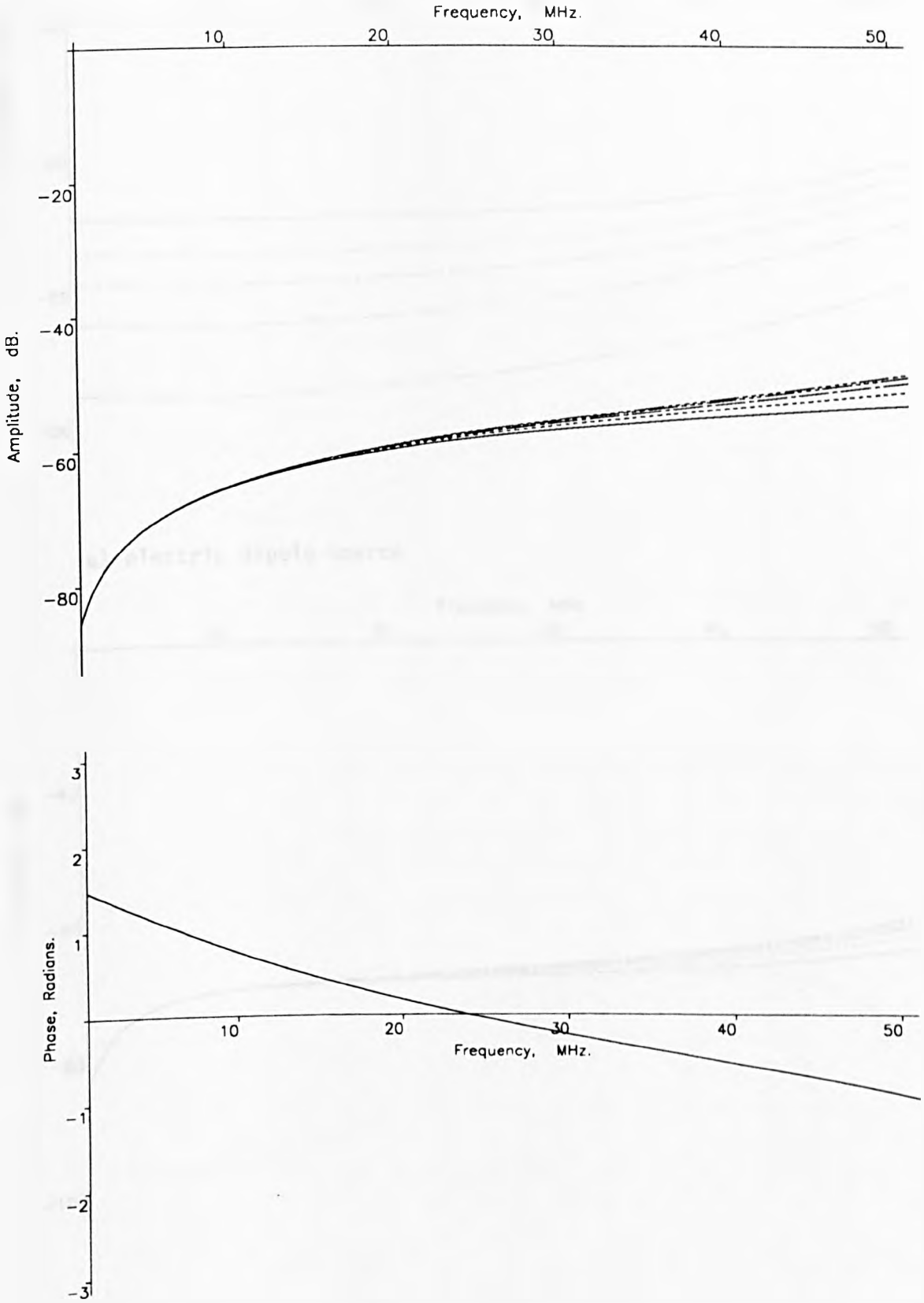

b) magnetic dipole source

Fig. 3.3.9 Predictions for loading 50 Ω resistance

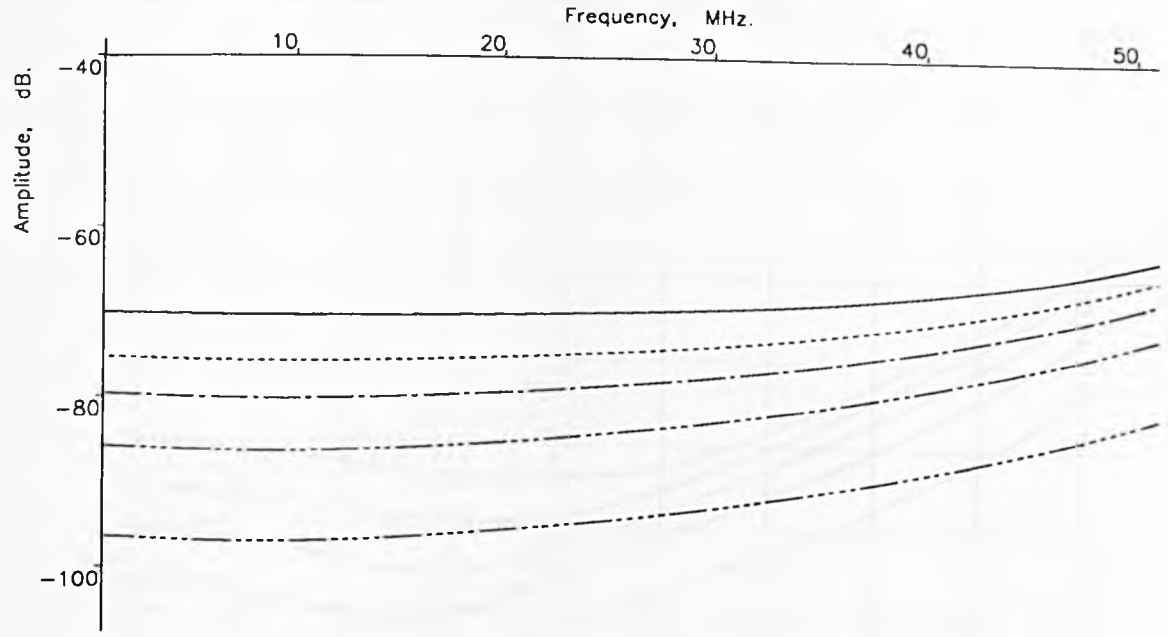

a) electric dipole source

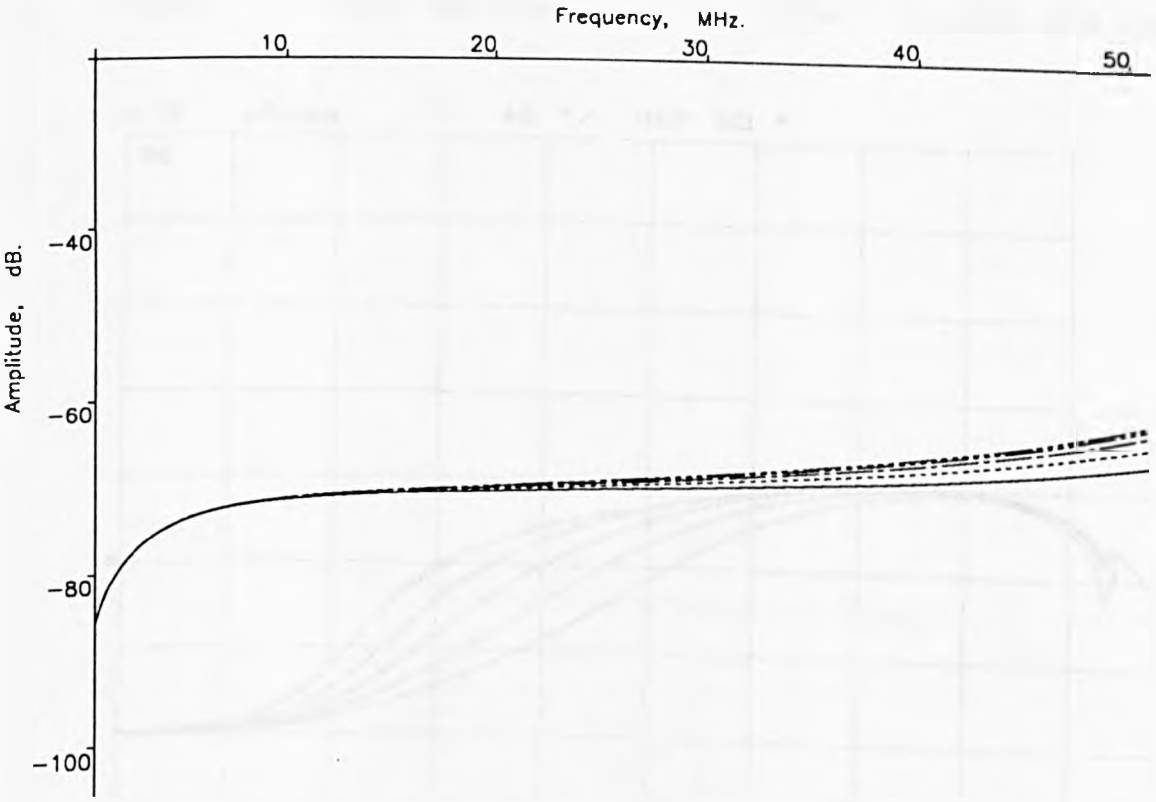

b) magnetic dipole source

Fig. 3.3.10 Predictions for loading 10 Ω resistance

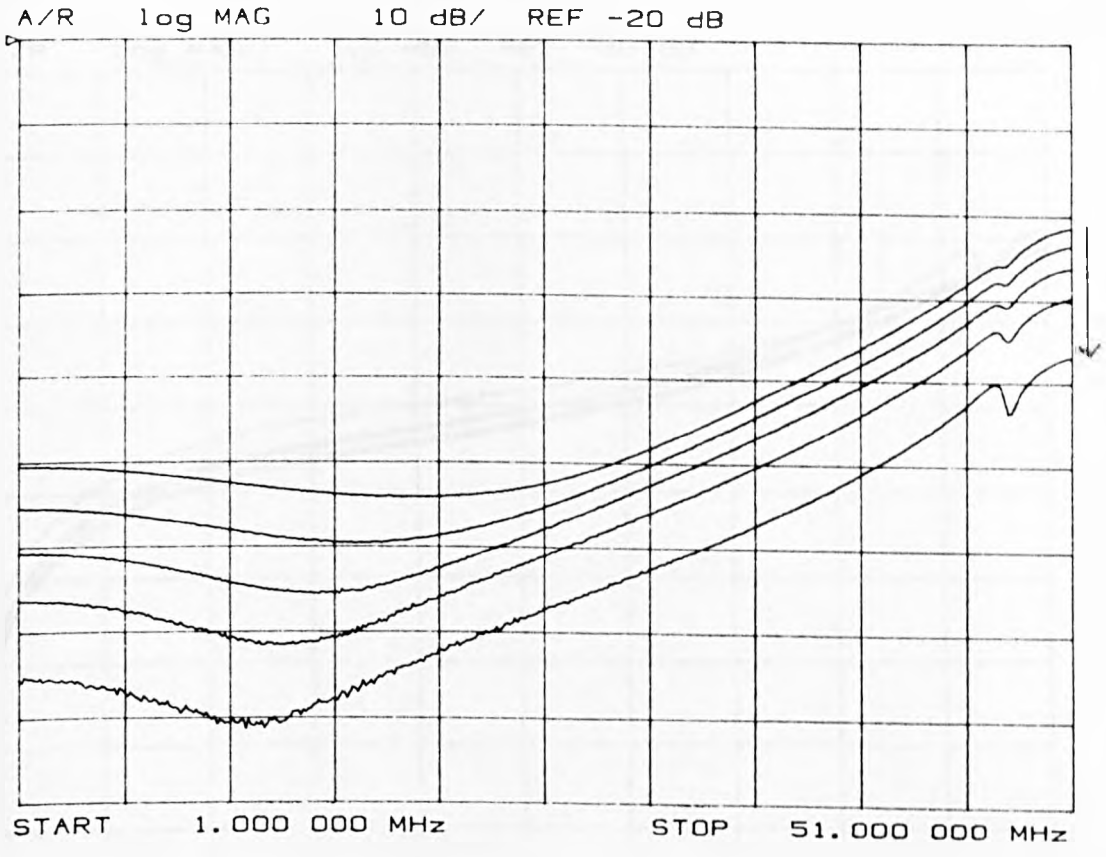

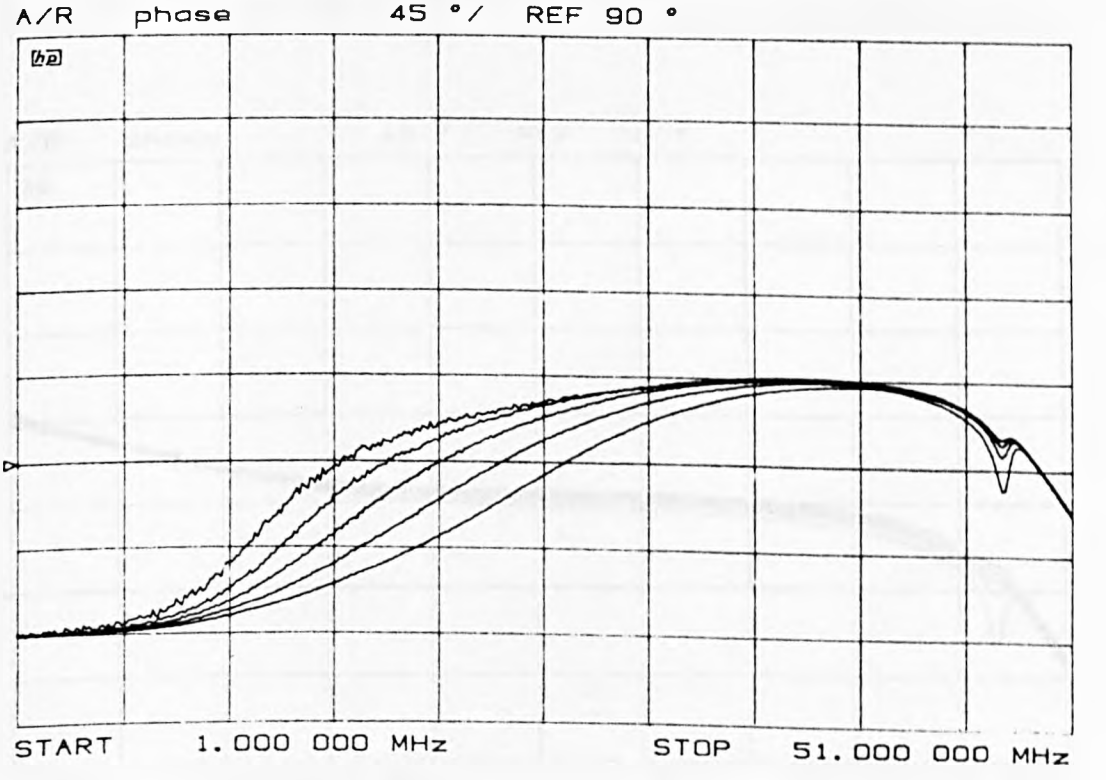

a)electric dipole source

Fig. 3.3.11 Measured response for most effective practical load (50Ω)

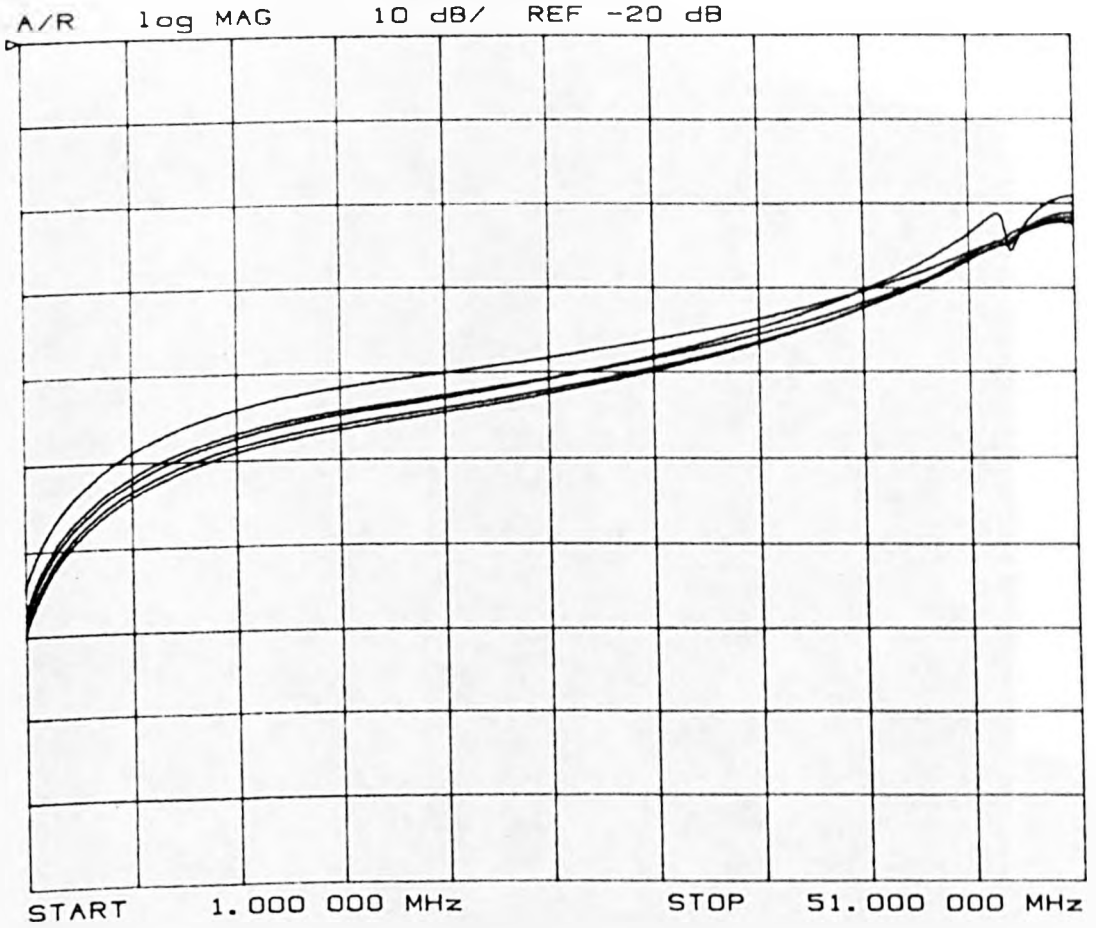

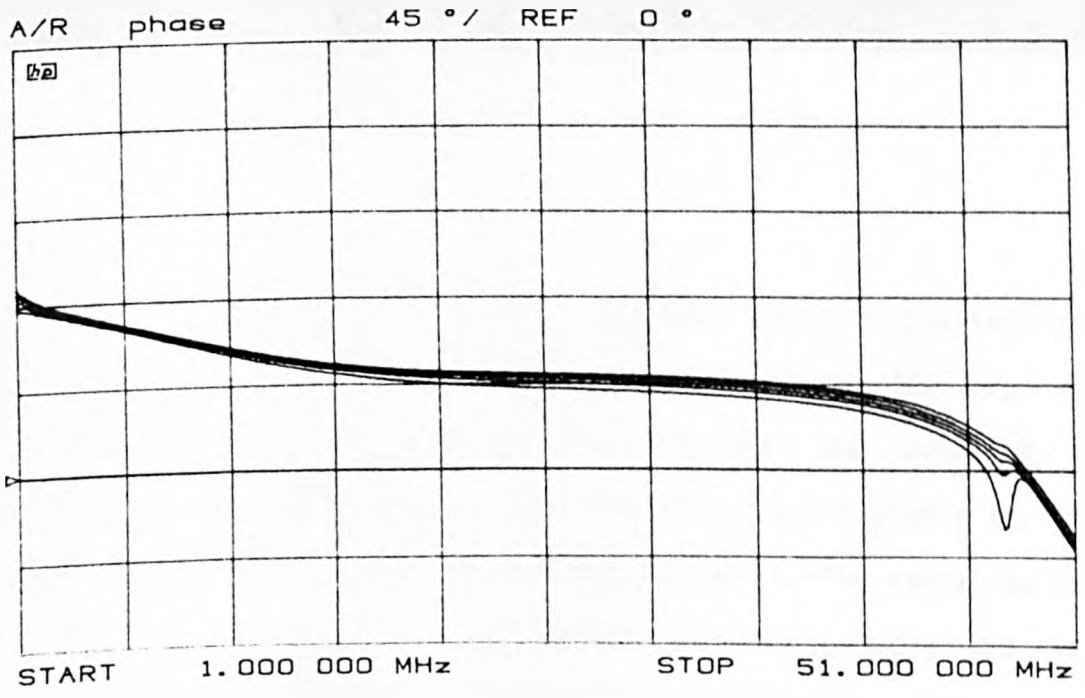

b)magnetic dipole source

Fig. 3.3.11 Measured response for most effective practical load (50Ω)

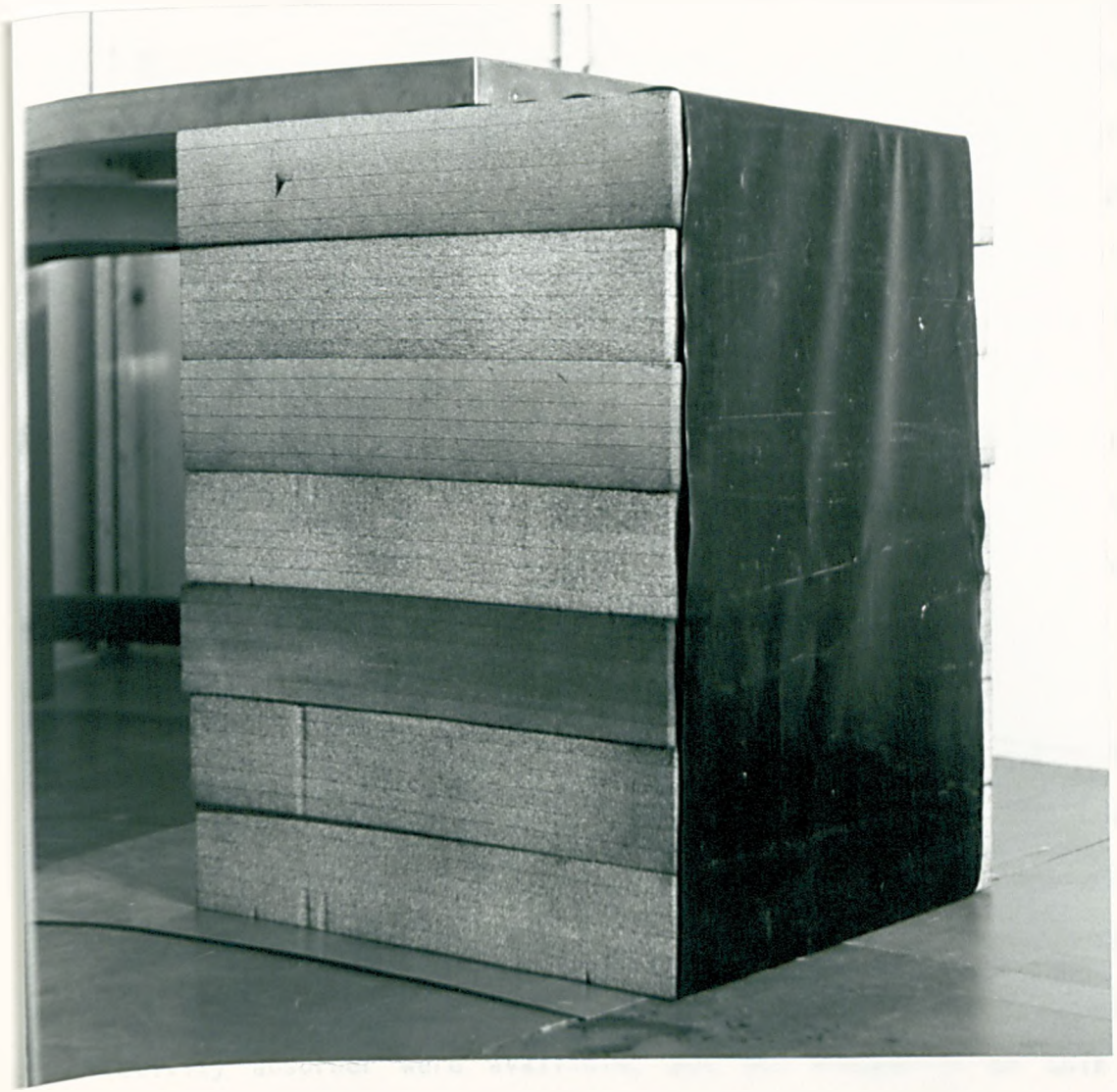

Fig. 3.3.12 Most effective practical load

The most effective practical load which could be constructed gave a response (Fig. 3.3.11) similar to that of the 50Ω load of the predicted frequency response (Fig. 3.3.9). The response has a variation of about 5dB up to 30MHz for the electric dipole source with a steady change for the magnetic dipole source. The variation between the practical load and the predictions is probably due to the positioning of the load which was not placed right at the end of the extension but partly underneath. To be fully correct this portion of the extension should include some loss in the model. The load was

connected from the end of the bench to a ground plane on the floor which was bonded to the outside skin of the room through the wooden floor. The best practical load was constructed of a pile of 7 blocks of RAM supporting the end of the bench with 2 sheets each of 60Ω per square and 200Ω per square conductive plastic wrapped around the pile (Fig. 3.3.12). Higher impedance loads were constructed from varying numbers of blocks connected to the bench with varying values of conductive sheeting. The equivalent resistance of the loads could not be measured due to the high DC surface resistance caused by the painted surface of the blocks of RAM (the manufacturers also could not supply a value for the bulk conductivity of the blocks).

The resistive loads were constructed out of multilayer carbon loaded absorber which contains some layers which have a very small loading of carbon, and hence a relatively high resistance. It would be possible to build a lower impedance load out of more heavily loaded blocks of foam with a constant loading. A few blocks of single resistivity absorber were available, but not enough to be able to construct a full load.

From modelling the response, as well as trying out the loading mechanisms, it became apparent that it is more effective to load the end of the bench than to add loss to the line. Loading the end of the transmission line (bench extension) is also more easily carried out.

3.4 Distinguishing Between Sources

3.4.1 With lossy bench

The effect of adding loss to the line is to reduce the Q of the resonance and also (with the electric source) that of the null. With enough loss (e.g 20Ω/m to the wall on the bench Figs. 3.2.14 and 3.2.15) the Q is reduced sufficiently for the responses, of an electric dipole source, for the different positions on the bench to stop crossing one another in the vicinity of the nulls (Fig. 3.4.1). This enables the two types of source to be distinguished across the whole frequency range although the difference for the various positions is still not constant over the whole range. There are two fairly distinct regions with the higher frequencies not having as great a change as the lower ones. It is therefore possible, although not very easy, to give relative amplitudes for the two sources (Chapter 2.2). If too much loss is included on the line to flatten the response still further by reducing the signal along the TEM line the test will become insensitive for the magnetic source where there is no direct coupling to counterbalance the loss.

3.4.2 Capacitively loaded bench

With the capacitive load the Q of the resonances and nulls are not reduced significantly although they do vary, only the frequencies of them are changed. This means that a simple measurement can still not be used to distinguish between the two types of source across the whole range. Without a complicated measurement procedure this is still difficult to carry out.

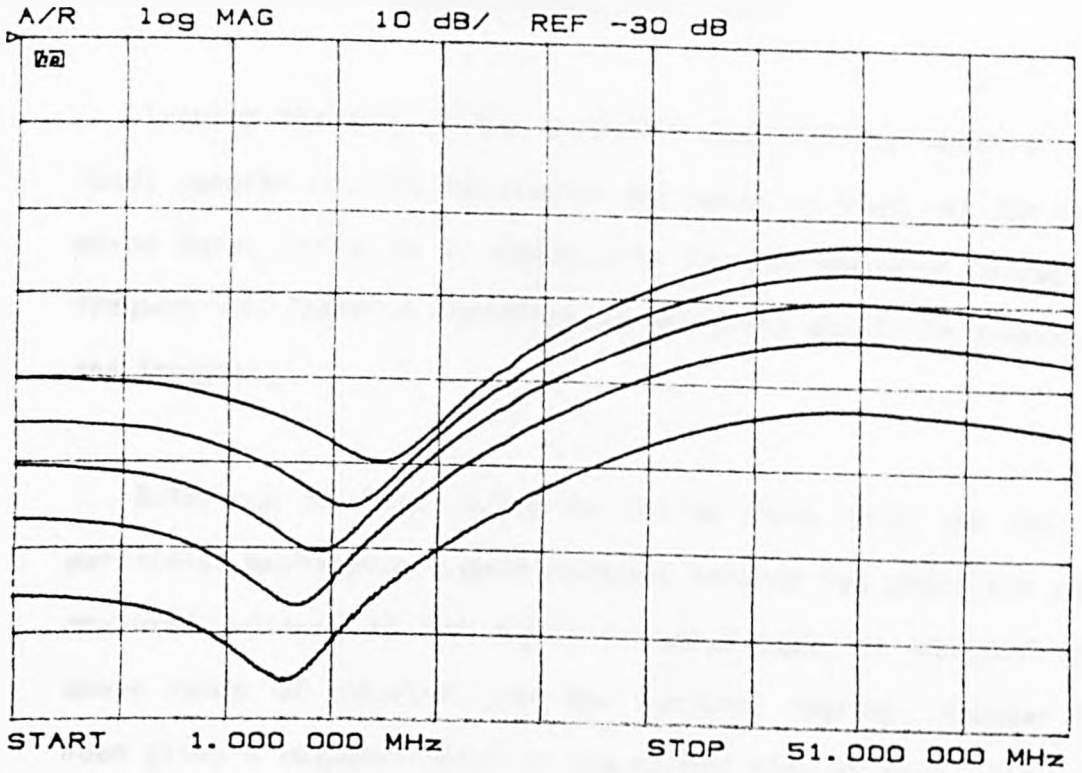

a) electric dipole source

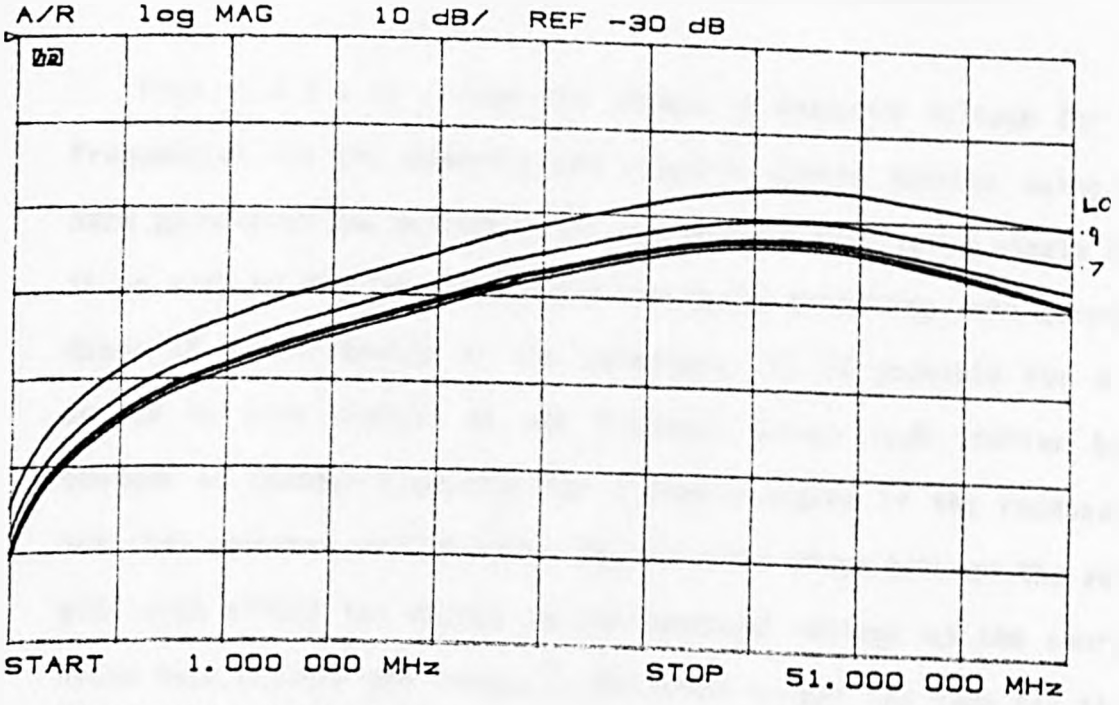

b) magnetic dipole source

Fig. 3.4.1 Measured signal as source is moved back (20Ω/m on bench with 66Ω/m + 30pF/m on extension)

3.4.3 Resistively loaded transmission line

Loading the end of the extension sufficiently (with a resistive load) smooths out the resonances and nulls so that, as the source is moved back, there is a steady drop in the measured voltage at all frequencies. There is therefore no ambiguity about the source type at any frequency.

Reference to Figs. 3.3.6 to 3.3.10 shows that the 10Ω load in particular would give a good response because the predicted change in measured voltage, as the source is moved back, is constant over the whole range of interest (for the electric source). However the 50Ω load gives a response which is reasonably flat in this range and does not have a lot of variation over the frequency range when the source is moved back. Only the top 5MHz has a reduced change and it should not need a large improvement in the load to overcome this.

Figs. 3.4.2 a to c show the change in measured voltage for three frequencies for the magnetic and electric dipole sources being moved back (predicted and measured). It can be seen that for a single source it is easy to distinguish between the types providing some account is taken of the frequency of the emissions. It is possible for a dual source to give changes at one frequency which look similar to the changes at another frequency for a single source if the response has not been smoothed sufficiently. The relative phase between the sources will also effect the change in the measured voltage as the source is moved back because the change in the phase is not the same for the two types of source (Fig. 3.3.3).

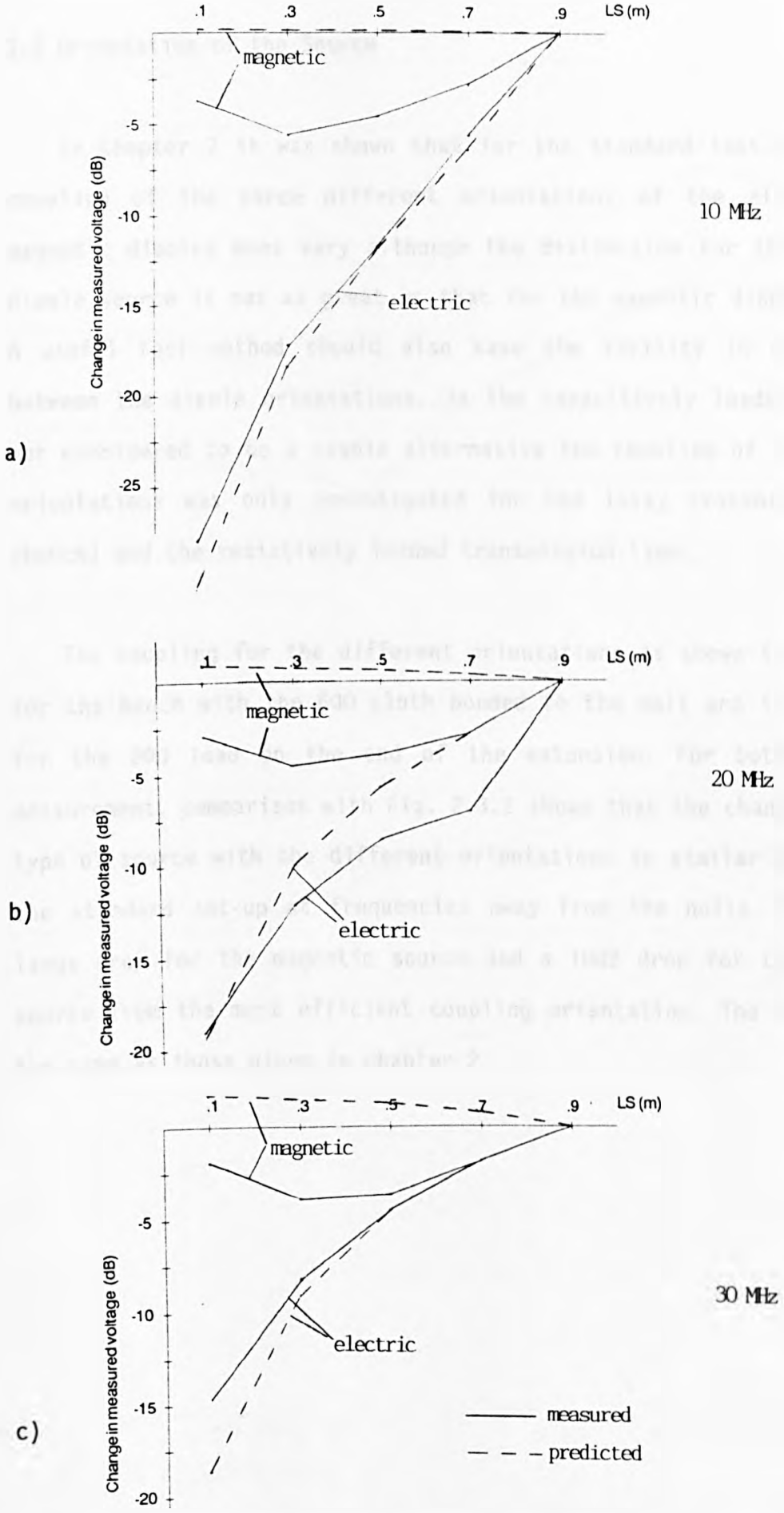

Fig. 3.4.2 Change in measured voltage for three frequencies when source is moved from front of bench

3.5 Orientation of the Source

In Chapter 2 it was shown that for the standard test set-up the coupling of the three different orientations of the electric and magnetic dipoles does vary although the distinction for the electric dipole source is not as great as that for the magnetic dipole source. A useful test method should also have the facility to distinguish between the dipole orientations. As the capacitively loaded case was not considered to be a viable alternative the coupling of the various orientations was only investigated for the lossy transmission line (bench) and the resistively loaded transmission line.

The coupling for the different orientations is shown in Fig.3.5.1 for the bench with the 60Ω cloth bonded to the wall and in Fig.3.5.2 for the 50Ω load on the end of the extension. For both types of measurement, comparison with Fig. 2.3.2 shows that the change for each type of source with the different orientations is similar to that for the standard set-up at frequencies away from the nulls. All have a large drop for the magnetic source and a 10dB drop for the electric source from the most efficient coupling orientation. The reasons are the same as those given in chapter 2.

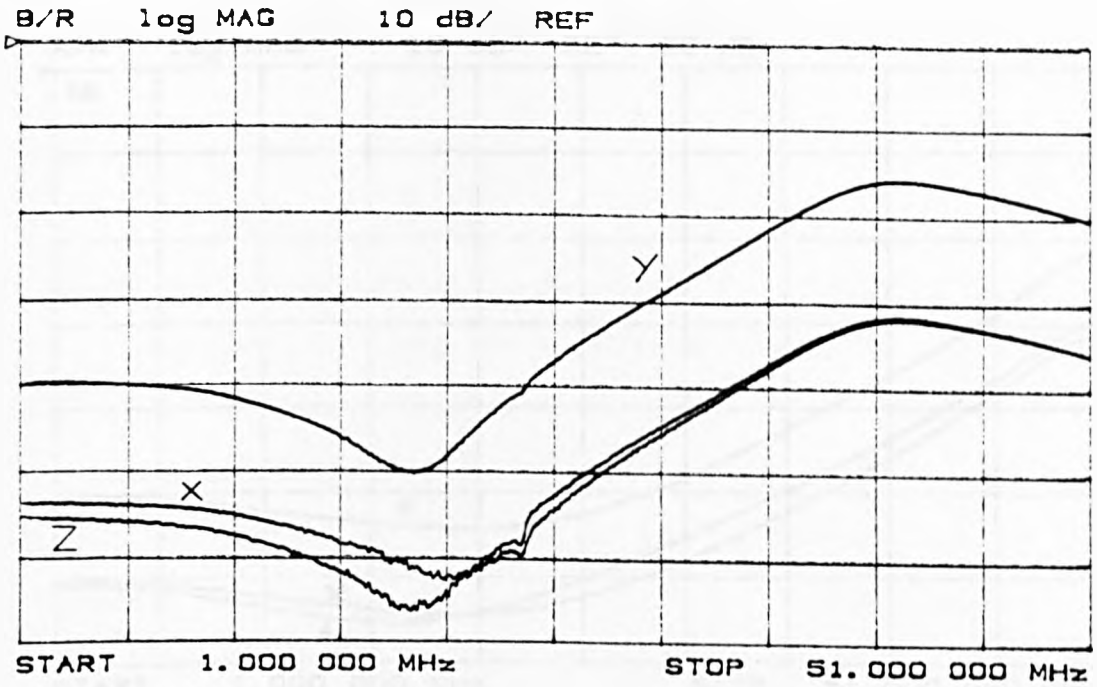

a)electric dipole source

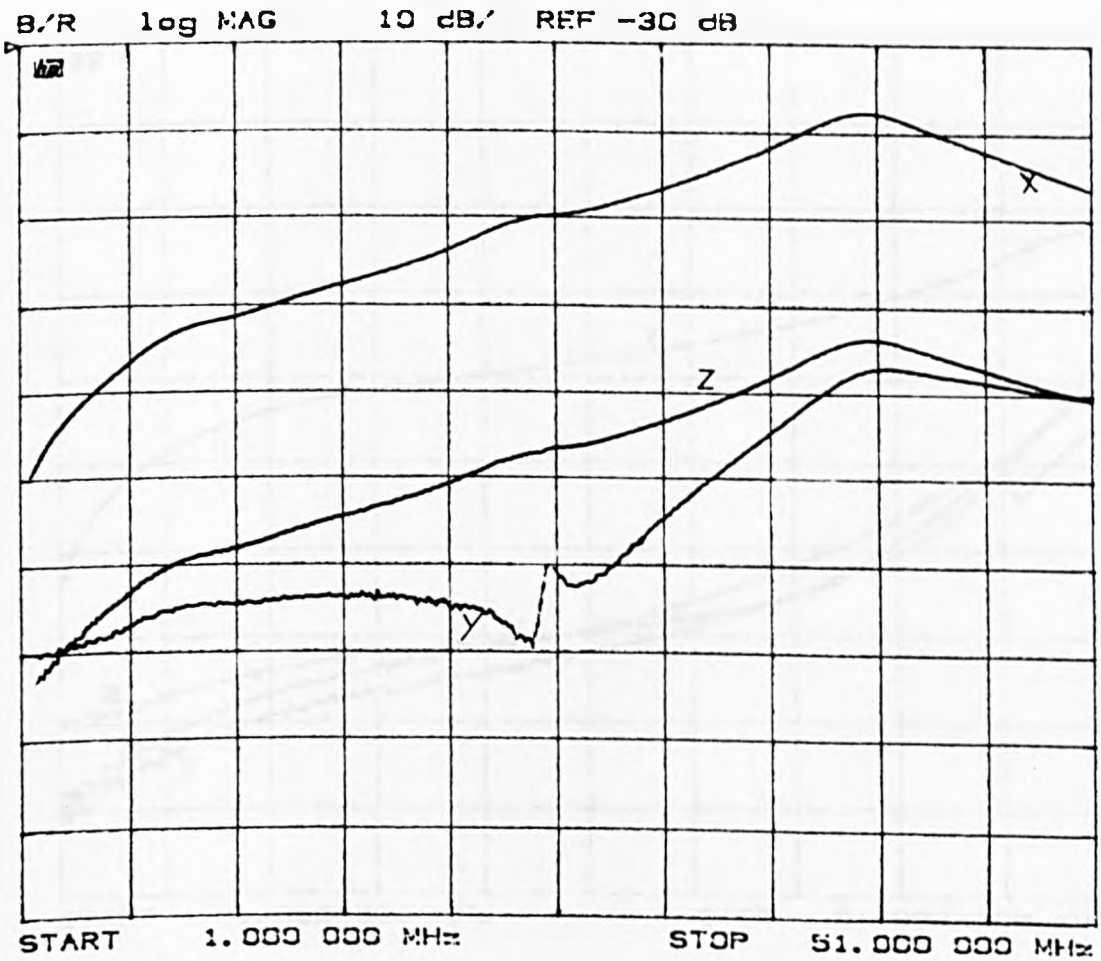

b)magnetic dipole source

Fig. 3.5.1 Change in measured voltage with orientation of source 60Ω/square bonded between bench and wall

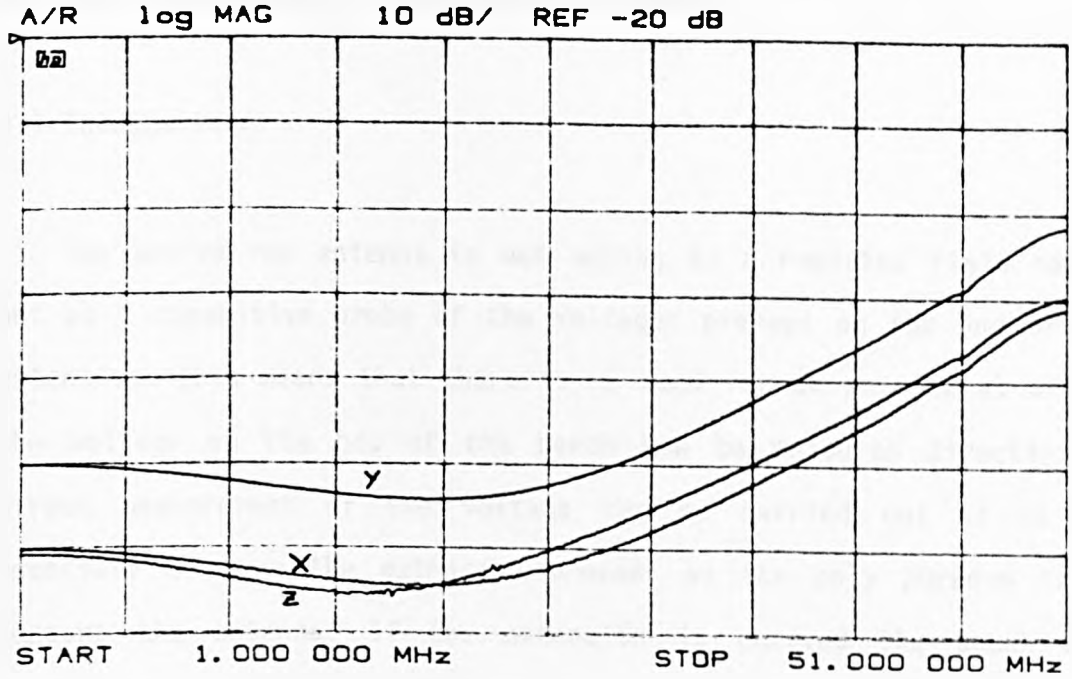

a)electric dipole source

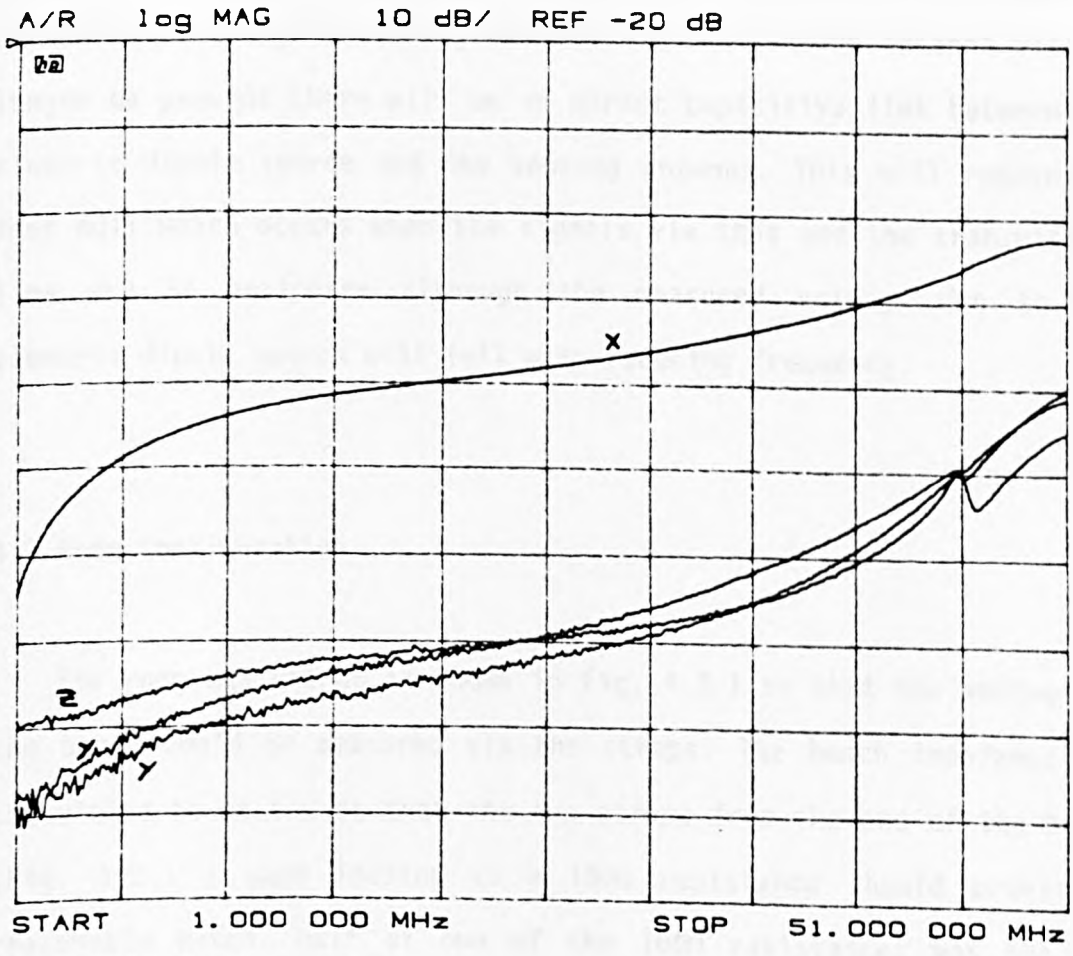

b)magnetic dipole source

Fig. 3.5.2 Change in measured voltage with orientation of source 50Ω load on end of extension

4. DIRECT MEASUREMENT OF VOLTAGE ON THE BENCH

4.1 Introduction

The active rod antenna is not acting as a radiated field sensor but as a capacitive probe of the voltages present on the end of the extension. This means that there is no need for an antenna at all if the voltage on the end of the bench can be measured directly. If direct measurement of the voltage can be carried out it is not necessary to have the extension present as its only purpose is to support the antenna. If the extension is removed the bench will resonate at a higher frequency (approximately ×2), but this resonance can be removed by including a matching load on the end of the bench as part of the voltage measuring network. As the sensing antenna will no longer be present there will be no direct capacitive link between the electric dipole source and the sensing antenna. This will remove the deep null which occurs when the signals via this and the transmission line are in antiphase although the measured voltage due to the electric dipole source will fall with reducing frequency.

4.2 Room Configuration

The room was set up as shown in Fig. 4.2.1 so that the voltage on the bench could be measured via the straps. The bench impedance was calculated to be 56Ω so that the two straps from the end of the bench (Fig. 4.2.1) each leading to a 100Ω resistance should provide a reasonable match. Half of one of the 100Ω resistances was the 50Ω input impedance of the network analyser (Fig. 4.2.2). Two straps were used to keep the system as symmetrical as possible. Ideally the load

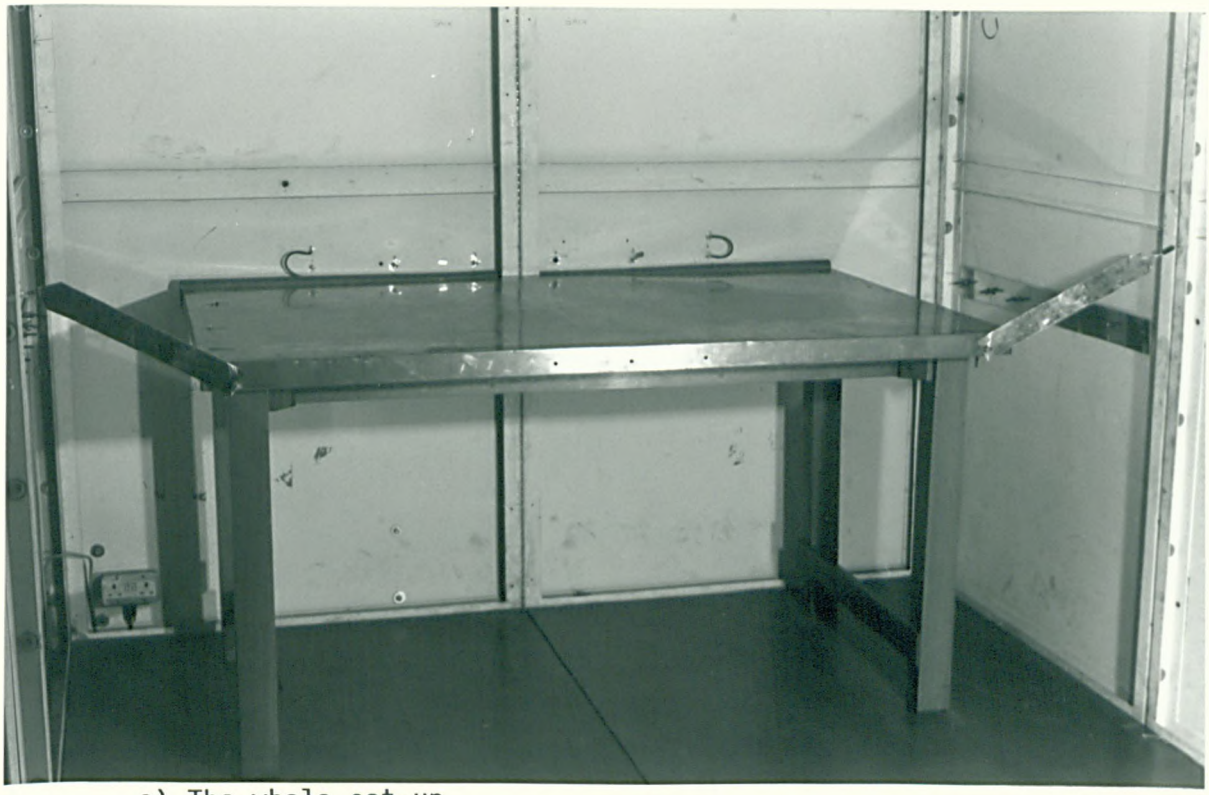

a) The whole set-up

b) Detail of the straps construction

Fig. 4.2.1 Straps to the end of the bench

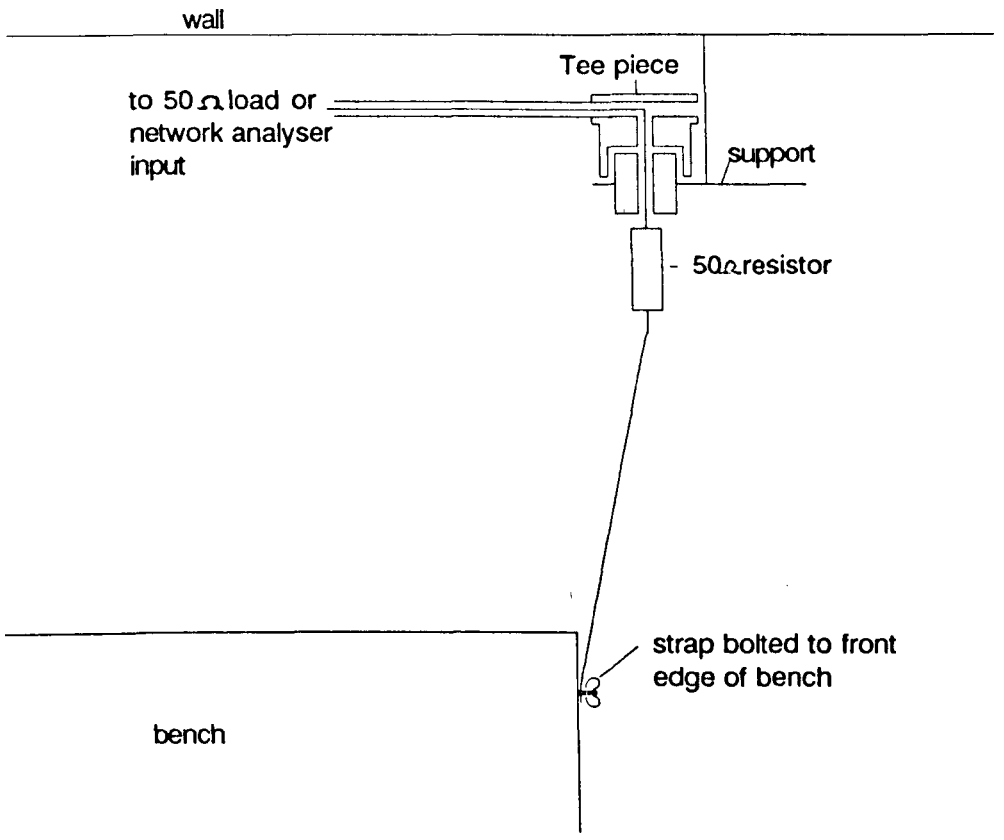

Fig. 4.2.2 Construction of the straps

should be spread across the whole of the end of the bench to minimise discontinuities. This is difficult to construct as it would need to be shaped to connect with the cable to the measurement receiver so the two broad straps were used. The straps were broad to ensure that the impedance (particularly the inductance) of the connections was as low as possible to avoid adding extra impedance into the system. The straps were also as short as possible so that they were electrically short and their length could be ignored as the apparent impedance of the straps would not change with frequency. If the straps were long enough to become a significant part of a wavelength in length at any frequency the input impedance would change rapidly with frequency as the load on the end of the straps is unlikely to match the impedance of the straps.

This test set-up was modelled by removing the transmission line forming the extension and the discontinuity capacitance as well as the antenna capacitances and the mutual capacitance between the antenna and electric dipole source to give the equivalent circuits shown in Fig. 4.2.3. The matching load was added across the end of the bench and the voltage across the load calculated using the same techniques as for the earlier model. The program is shown in Appendix C. The model shows the bench terminated with 50Ω and the program calculates half the voltage across this impedance to give the prediction of the measured voltage.

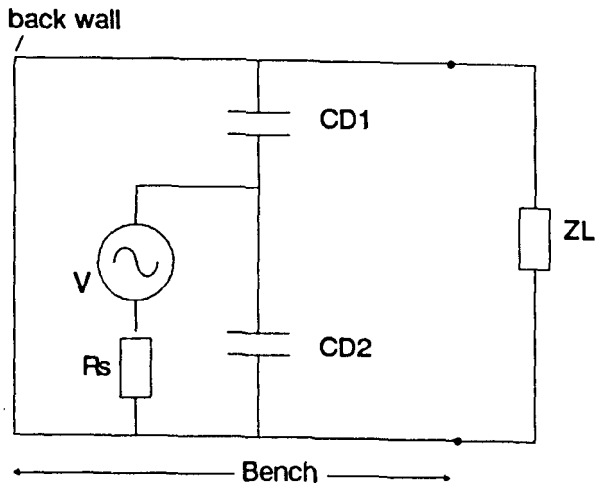

a)electric dipole source

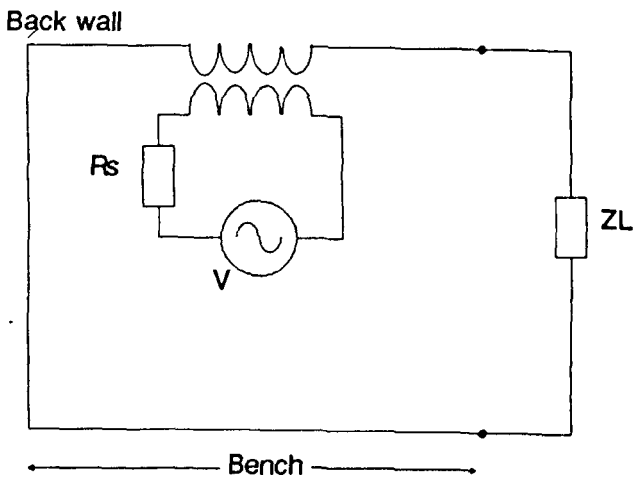

b)magnetic dipole source

Fig. 4.2.3 Equivalent circuits for the terminated bench

4.3 Measured and Predicted Results

The frequency response calculated is shown in Fig. 4.3.1 and the measured response is shown in Fig. 4.3.2. Comparison of the two sets of graphs shows that again the predictions are very close to the actual response although they do start to fall off at the very top end of the frequency range. This fall off is probably due to two mechanisms:-

1) the inductance present in the straps from the bench to the wall which will increase the impedance of the loads.
2) the length of the straps is becoming longer with respect to the wavelength at higher frequencies and this will start to effect the impedance seen by the bench.

The predicted and measured phases are also included and confirm the closeness of the prediction to the measured results. The measured voltage for both the electric and magnetic dipole sources rises steadily with frequency. The change with frequency is greater for the electric dipole source than for the magnetic source. As the frequency is reduced the portion of the transmission line towards the back wall is reduced in impedance and in the electric dipole case starts to short out the portion of the line which forms part of the voltage measuring circuit. With the magnetic source the two portions of the transmission line are in series so that the reduction in the impedance of one section has a smaller effect on the output voltage. As there is no measuring antenna present there is no capacitive divider network to give the flat response at the lower frequencies with the electric dipole source which causes the measured voltage to carry on falling with reducing frequency. This means that this technique is less

sensitive than the standard test set-up for the electric dipole source, particularly at frequencies below about 5 MHz.

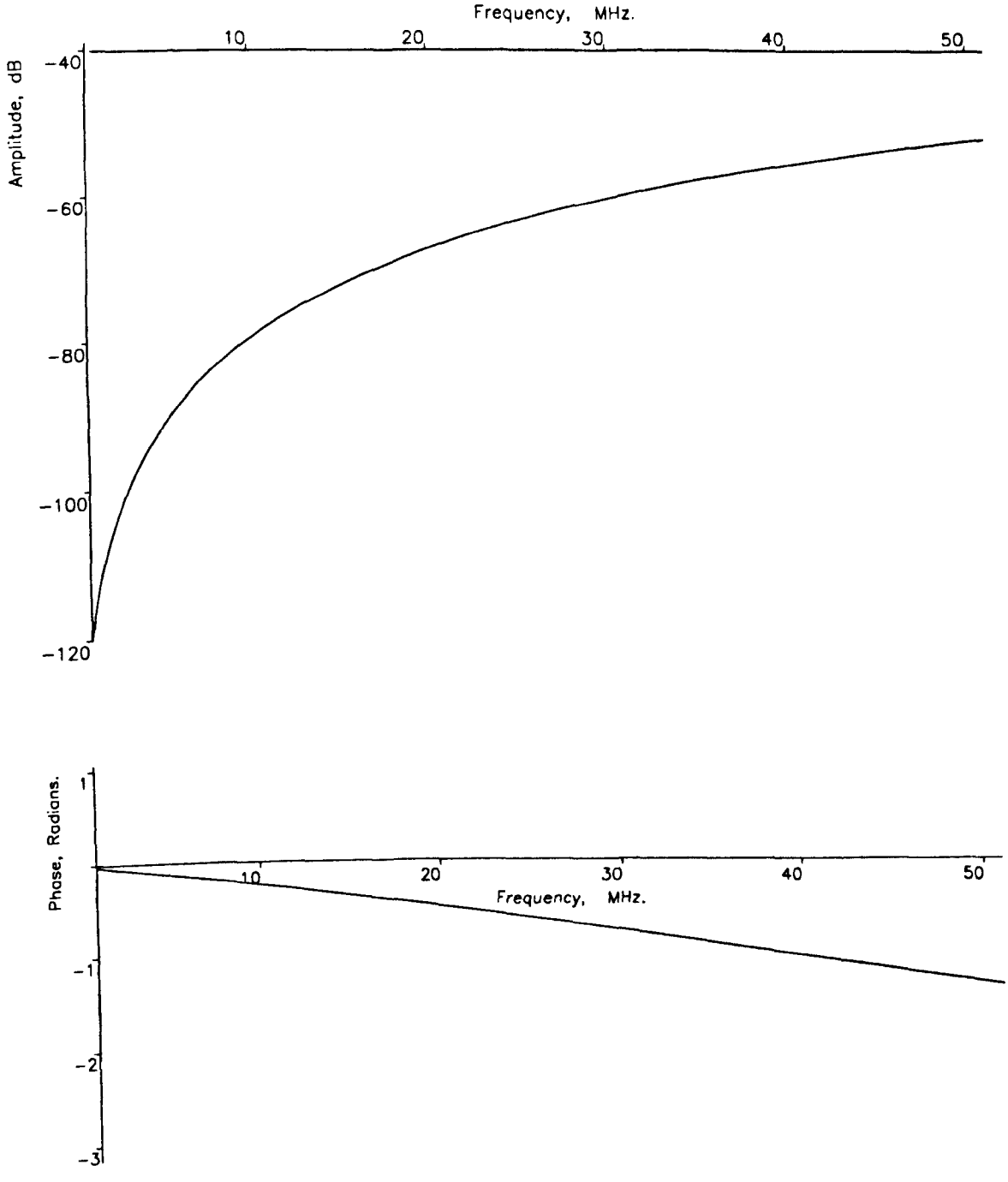

a)electric dipole source

Fig. 4.3.1 Predicted response for bench terminated with straps

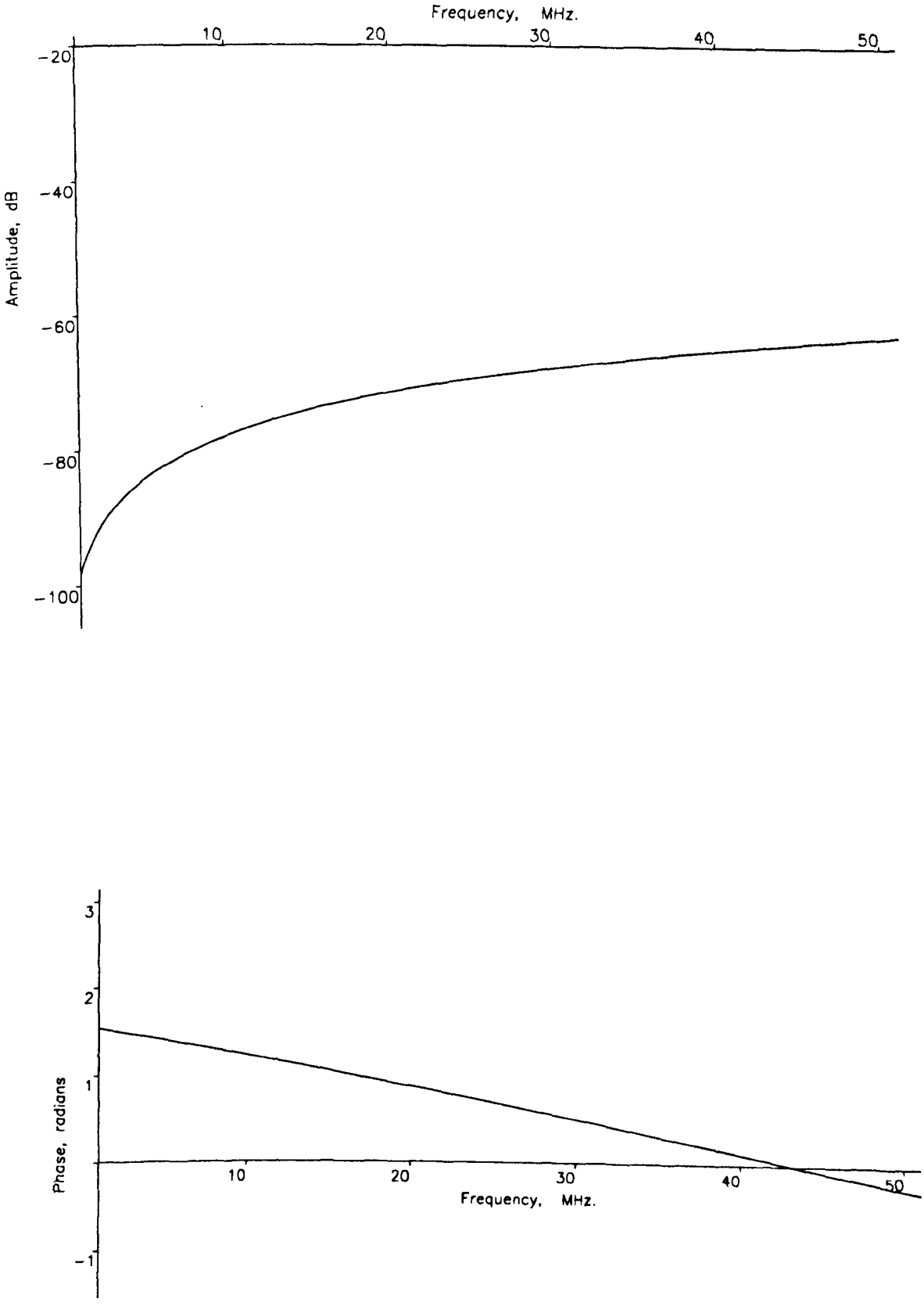

b)magnetic dipole source

Fig. 4.3.1 Predicted response for bench terminated with straps

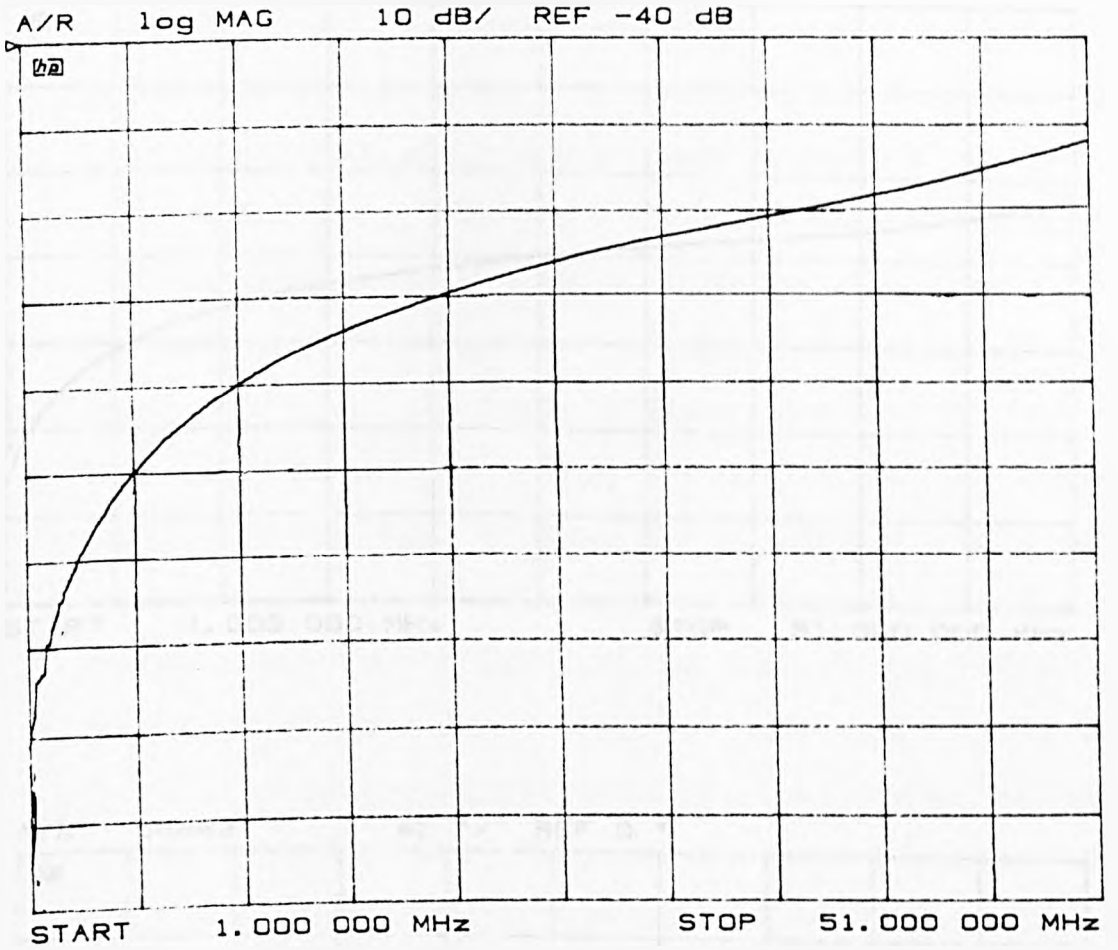

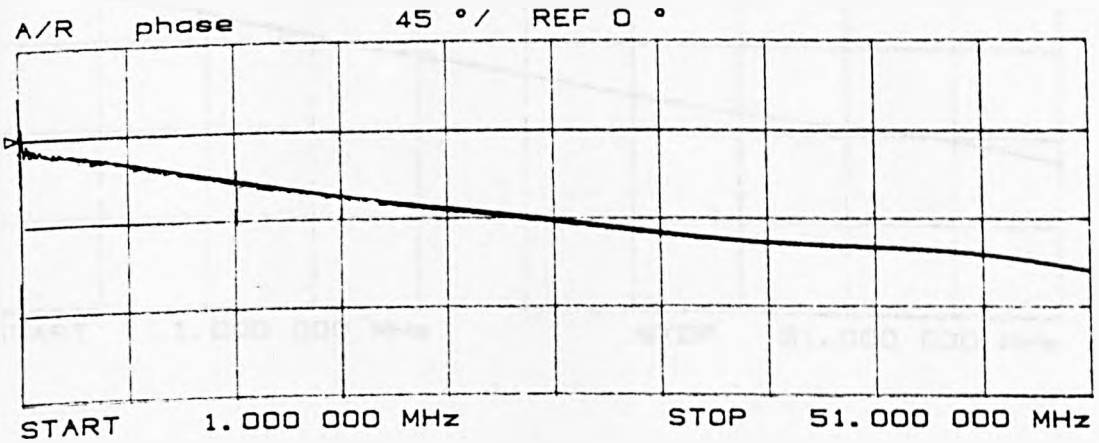

a)electric dipole source

Fig. 4.3.2 Measured response for bench terminated with straps

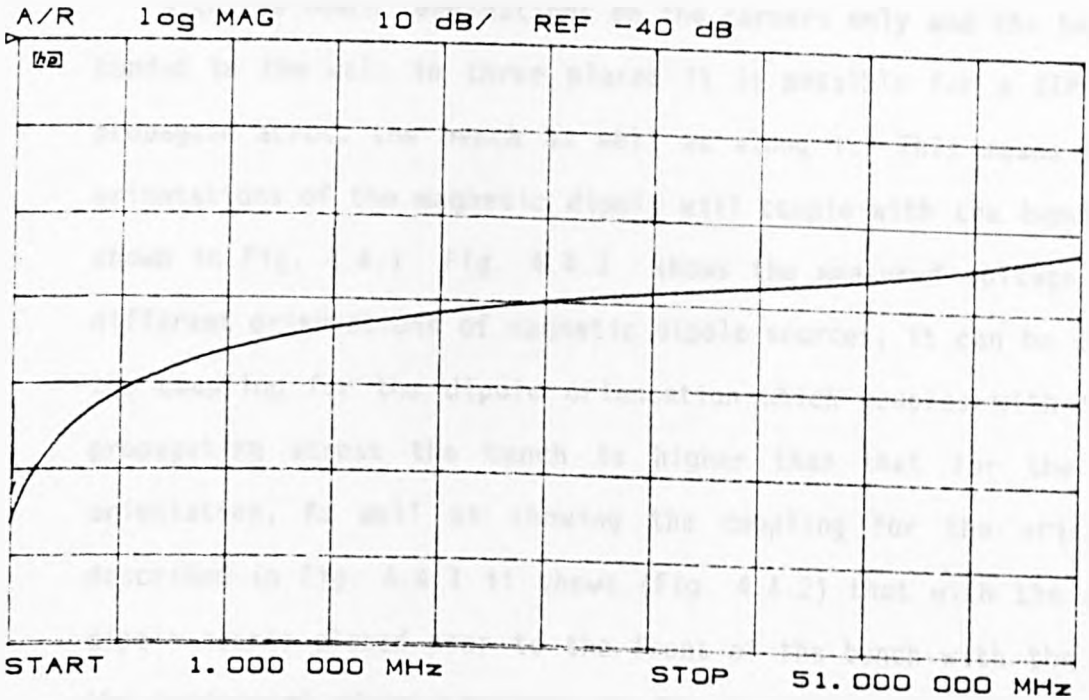

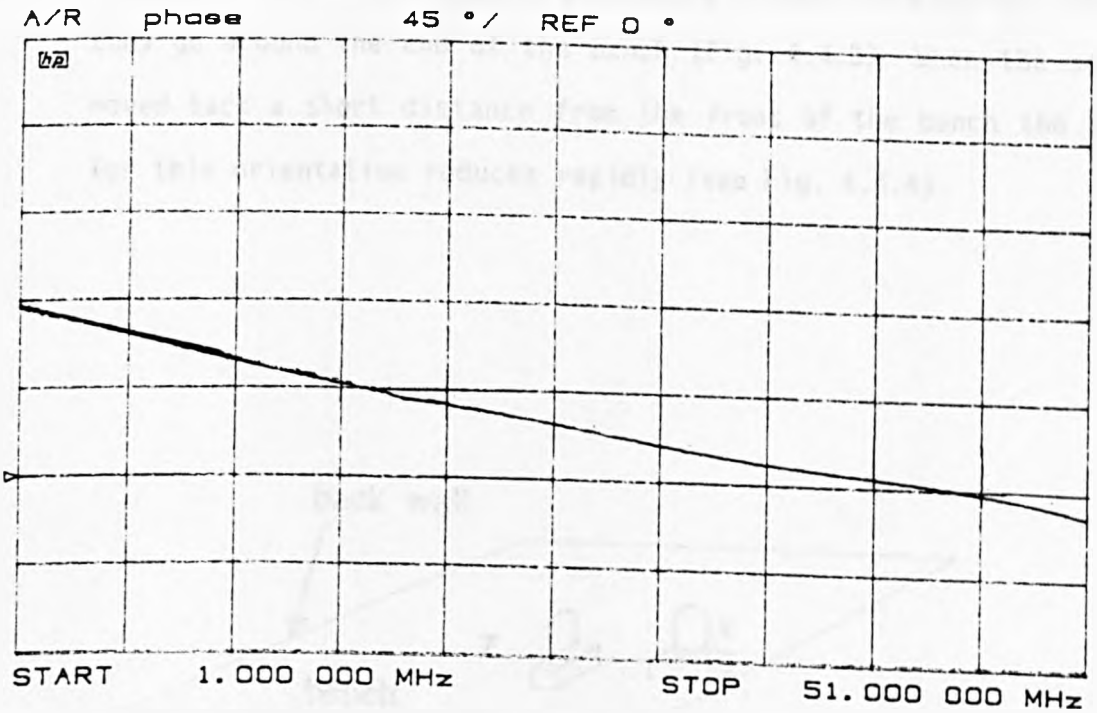

b)magnetic dipole source

Fig. 4.3.2 Measured response for bench terminated with straps

4.4 The Effect of Orientation of the Source

With the bench terminations on the corners only and the bench only bonded to the wall in three places it is possible for a TEM wave to propagate across the bench as well as along it. This means that two orientations of the magnetic dipole will couple with the bench, as is shown in Fig. 4.4.1. Fig. 4.4.2 shows the measured voltage for the different orientations of magnetic dipole sources, it can be seen that the coupling for the dipole orientation which couples with the wave propagating across the bench is higher than that for the desired orientation. As well as showing the coupling for the orientations described in Fig. 4.4.1 it shows (Fig. 4.4.2) that with the magnetic dipole source placed near to the front of the bench with the loop in the horizontal plane coupling to the bench is higher than for the desired orientation. This is believed to be caused by the magnetic fields of the wave propagating across the bench cutting the loop where they go around the end of the bench (Fig. 4.4.3). When the source is moved back a short distance from the front of the bench the coupling for this orientation reduces rapidly (see Fig. 4.4.4).

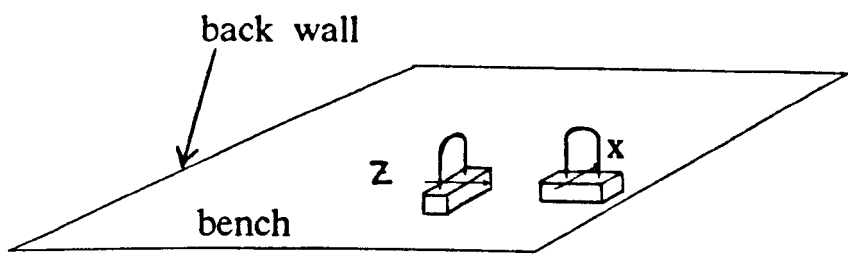

Fig. 4.4.1 Orientations of magnetic dipole which will couple with the bench

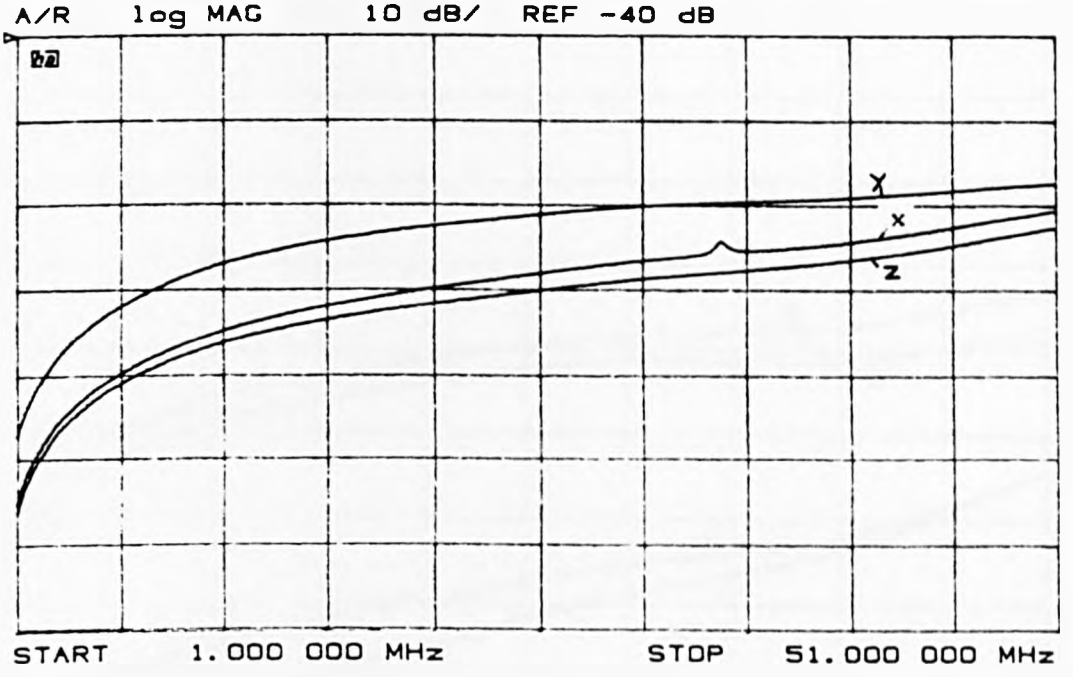

Fig. 4.4.2 Measured response for different orientations of magnetic dipole source

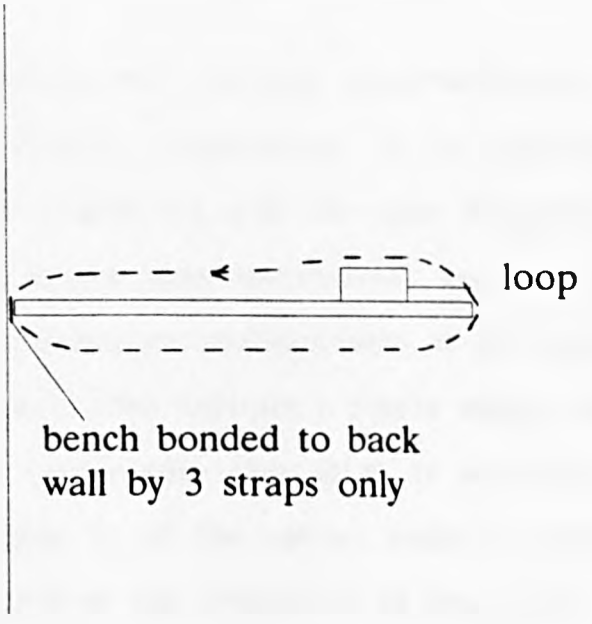

Fig. 4.4.3 Magnetic field cutting horizontal loop at front of bench

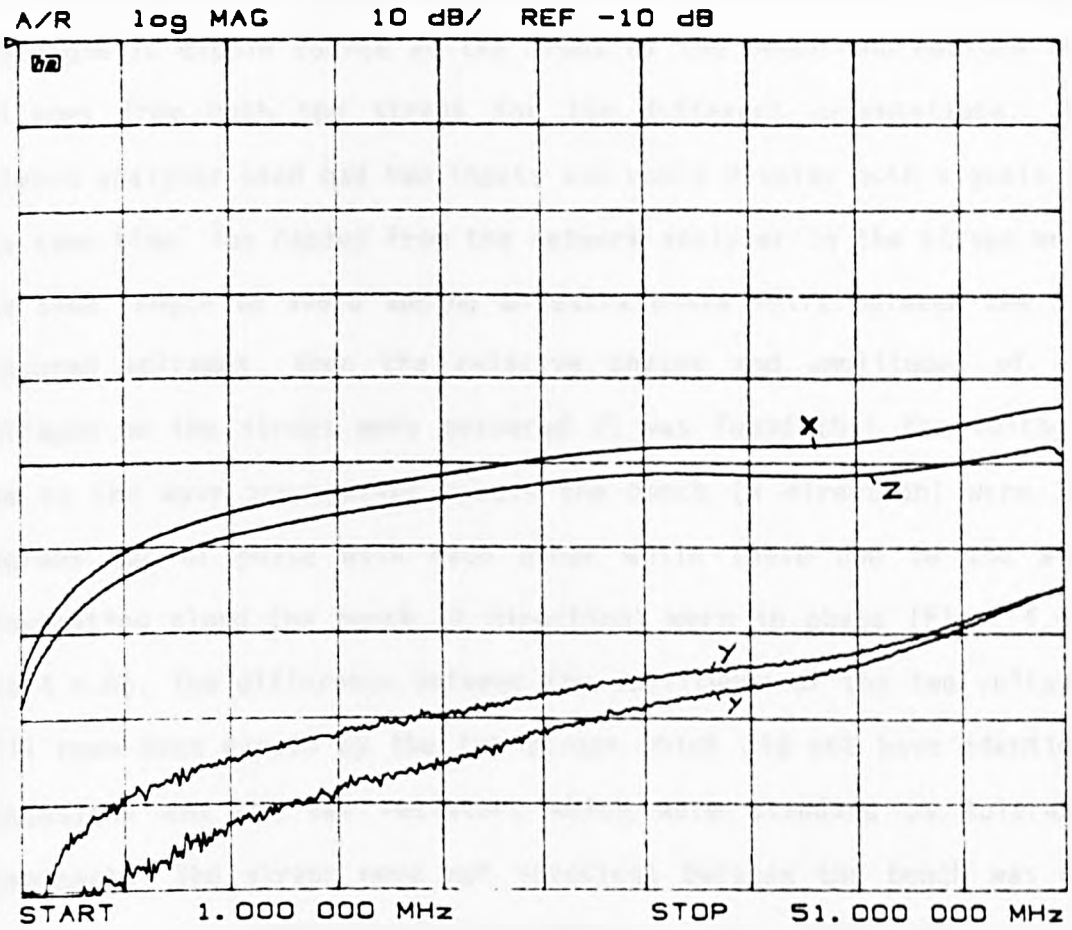

Fig. 4.4.4 Reduction in coupling when horizontal loop is moved back from front of bench

This extra coupling will prevent discrimination between magnetic dipoles with different orientations. It is possible for a pair of magnetic dipoles (radiating with the same frequency) with different orientations to excite both longitudinal and transverse waves which interfere destructively or constructively at the point of measurement. The measurement will then indicate a dipole moment which may be either much smaller or larger than that which is actually present. Even if the measured signal is of the correct order of magnitude it will be difficult to determine the orientation of the dipole.

The easiest way of demonstrating this extra coupling is to place the magnetic dipole source at the front of the bench and measure the voltages from both the straps for the different orientations. The network analyser used had two inputs and could display both signals at the same time. The cables from the network analyser to the straps were the same length to avoid adding an extra phase shift between the two measured voltages. When the relative phases and amplitudes of the voltages on the straps were measured it was found that the voltages due to the wave propagating across the bench (x direction) were 180 degrees out of phase with each other while those due to the wave propagating along the bench (z direction) were in phase (Figs. 4.4.5 and 4.4.6). The difference between the amplitudes of the two voltages will have been caused by the two straps which did not have identical dimensions and the two resistors which were standard 5% tolerance components. The straps were not identical because the bench was not quite central in the room but was offset by a few centimetres and the straps were made as short as possible.

If the straps and loads are arranged so that for a single source the voltages measured at each corner have identical amplitudes, in phase for the desired wave and anti-phase for the unwanted wave, the voltages can be summed to give a measure of the voltage due to the wave propagating in the required direction only. For this to work correctly the cables of the two paths must be matched closely to ensure that no extra phase difference between the two signals is added.

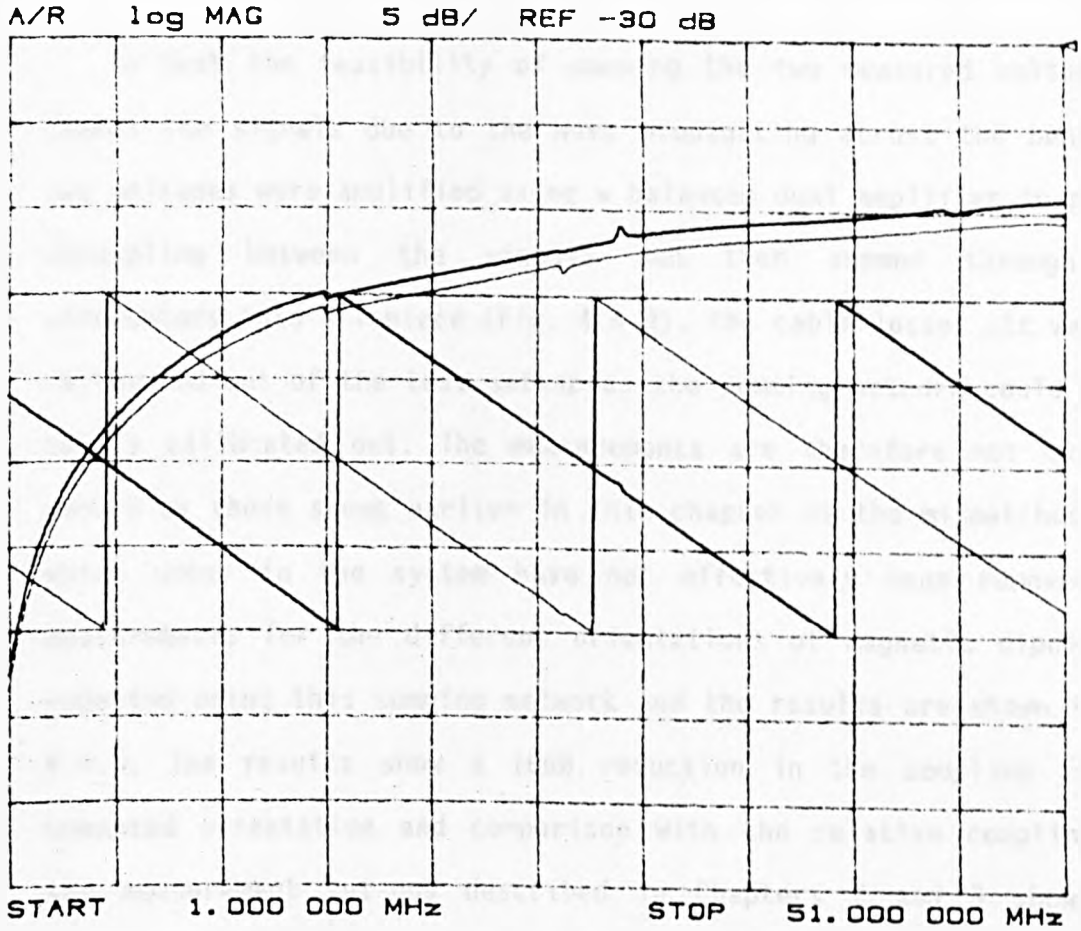

Fig. 4.4.5 Voltages on two straps for wave propagating across the bench

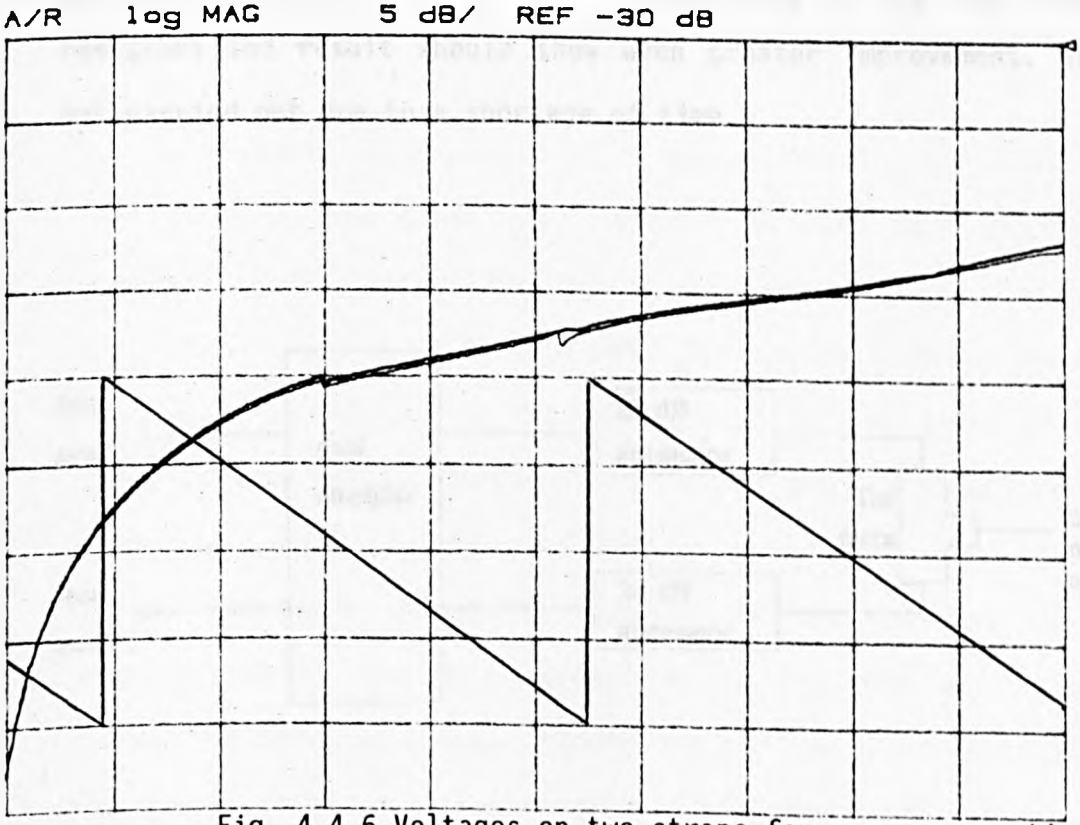

Fig. 4.4.6 Voltages on two straps for wave propagating along the bench

To test the feasibility of summing the two measured voltages to cancel the signals due to the wave propagating across the bench the two voltages were amplified using a balanced dual amplifier to provide decoupling between the signals and then summed through 20dB attenuators into a T-piece (Fig. 4.4.8). The cable losses etc were not calibrated out of the test set-up as the summing network could not be easily calibrated out. The measurements are therefore not quite as smooth as those shown earlier in this chapter as the mismatches, etc, which occur in the system have not effectively been removed. The measurements for the different orientations of magnetic dipole were repeated using this summing network and the results are shown in Fig. 4.4.8. The results show a 10dB reduction in the coupling for the unwanted orientation and comparison with the relative couplings for the measurement set-ups described in Chapters 2 and 3 shows that similar results are obtained. This is without the amplitudes being perfectly matched so with careful matching of the two straps and resistors the result should show even greater improvement. This was not carried out due to a shortage of time.

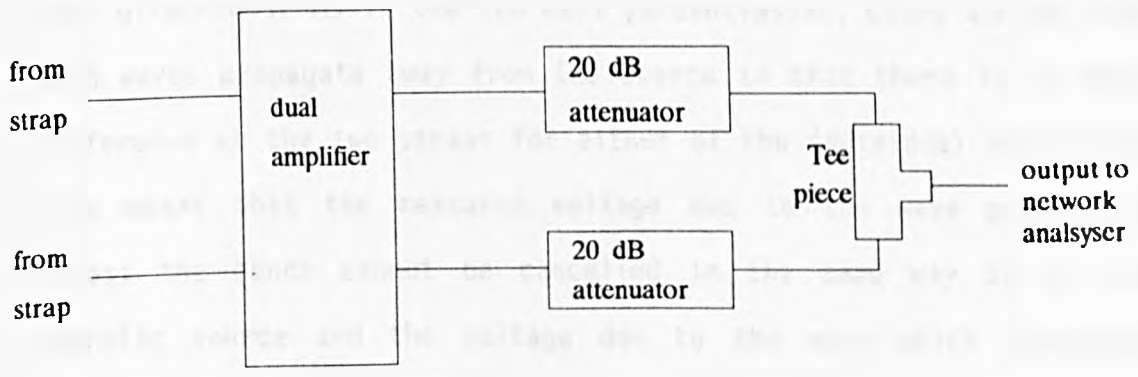

Fig. 4.4.7 Summing network

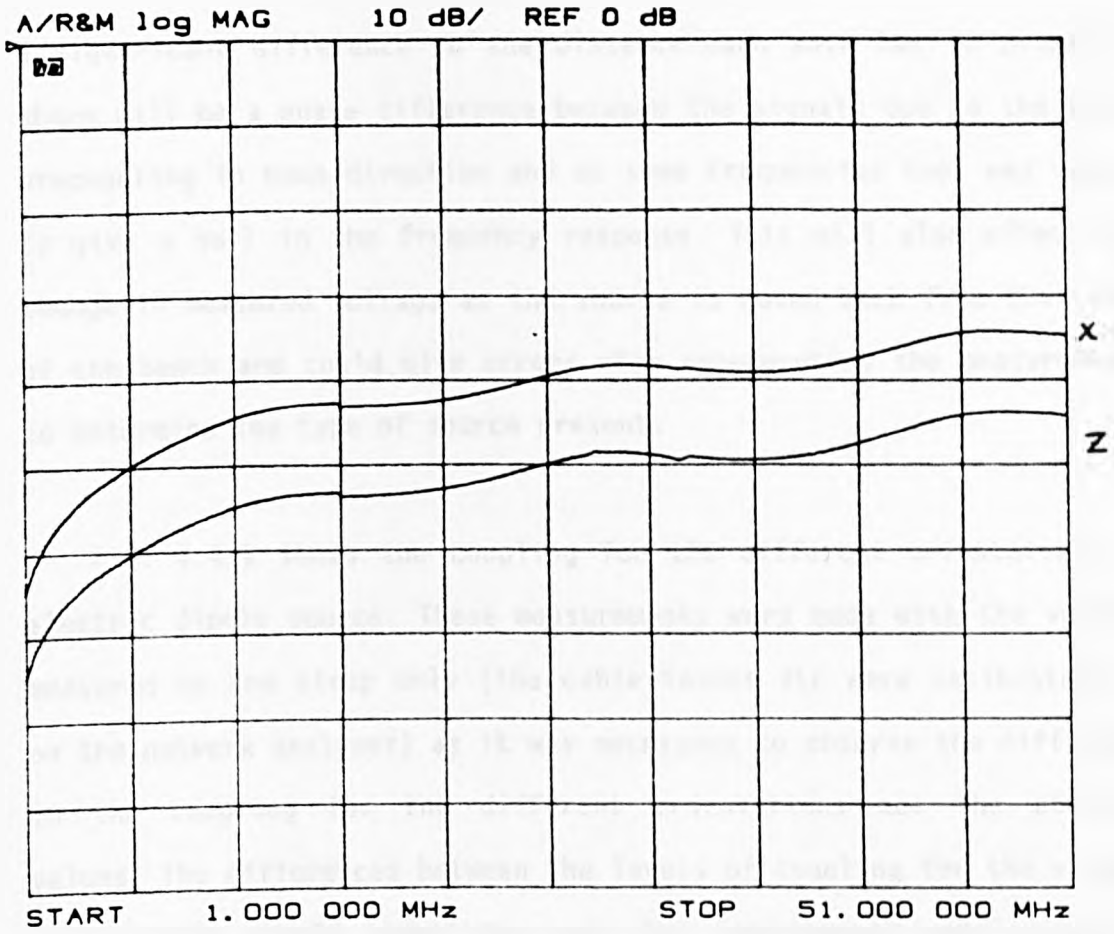

Fig. 4.4.8 Measurements for different orientations of magnetic dipole source with the voltages from the two straps summed

An electric dipole will also induce waves propagating in both directions on the bench (Fig. 4.4.2). In this case a single (the desired) orientation of the dipole will induce waves propagating in both directions. As in the TEM cell [Sreenivasiah, Chang and Ma 1981] both waves propagate away from the source so that there is no phase difference at the two straps for either of the individual directions. This means that the measured voltage due to the wave propagating across the bench cannot be cancelled in the same way as for the magnetic source and the voltage due to the wave which propagates across the bench will always be present. If the phase shift of each of the propagating waves is the same or small the error will be constant and can be accounted for during room calibration. However, if there is

a significant difference in the distance each wave has to propagate there will be a phase difference between the signals due to the waves propagating in each direction and at some frequencies they may cancel to give a null in the frequency response. This will also effect the change in measured voltage as the source is moved back from the front of the bench and could give errors when interpreting the measurements to determine the type of source present.

Fig. 4.4.9 shows the coupling for the different orientations of electric dipole source. These measurements were made with the voltage measured on one strap only (the cable losses etc were calibrated out on the network analyser) as it was necessary to observe the difference in the coupling for the different orientations not the absolute values. The differences between the levels of coupling for the various orientations should remain the same for measurements made on one or two straps as the voltages on each strap should be the same. The change in coupling for the different orientations of electric dipole source can be seen to be similar to those obtained for the test set-ups discussed in Chapters 2 and 3. For all set-ups the orientation of the electric dipole source is not as easily determined as that of the magnetic dipole source. Even with a horizontal dipole there will exist an electric potential between the dipole and the bench which will induce a voltage onto the transmission lines.

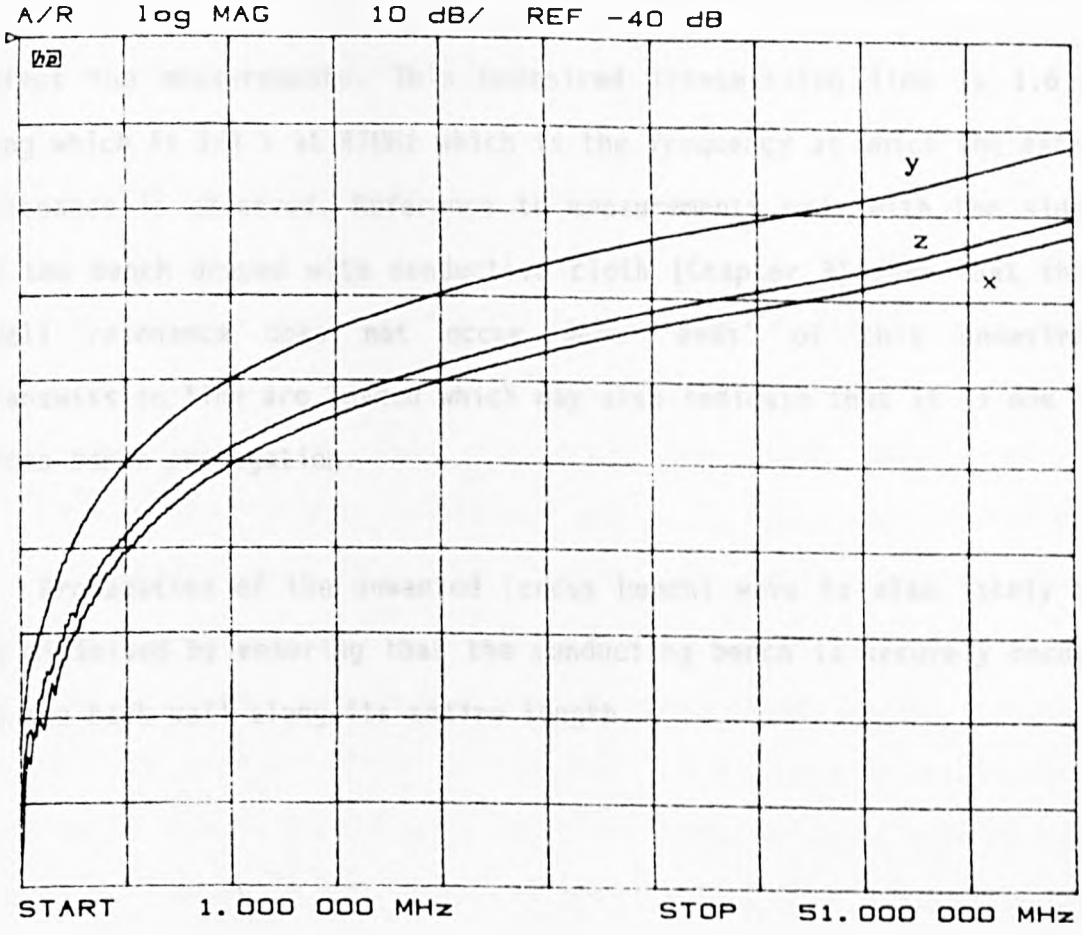

Fig. 4.4.9 Measured voltages for different orientations of electric dipole source

The coupling of the electric and magnetic dipoles with waves which propagate across the bench instead of along it may explain the small resonance which occurs in the measurements made with the bench extension in place. Any wave which does propagate across the bench in such a manner will be subject to reflections from the positions at which the transmission line impedance changes due to a change in its dimensions (i.e from both edges of the extension). This and the length of the extension compared to its width mean that such a wave will not readily reach the antenna at the end of the extension and will normally be of a much lower amplitude than the wave propagating in the desired direction. However, as the dimensions of the transmission lines are different in the two orientations, at the resonant frequency of the undesired path the received voltage may be great enough to

affect the measurements. This undesired transmission line is 1.6 m long which is 1/4 λ at 47MHz which is the frequency at which the extra resonance is observed. Reference to measurements made with the sides of the bench draped with conductive cloth (Chapter 3) show that this small resonance does not occur when 'ends' of this undesired transmission line are loaded which may also indicate that it is due to cross bench propagation.

Propagation of the unwanted (cross bench) wave is also likely to be minimised by ensuring that the conducting bench is securely bonded to the back wall along its entire length.

4.5 Distinguishing Between Sources

4.5.1 With a single source type present

The predictions (Fig. 4.5.1) indicate that as the electric source is moved towards the back wall the drop in the voltage on the bench will be similar to that previously seen with the measurement techniques described in Chapters 2 and 3. In this case the change in the measured voltage is constant across the whole frequency range. The predictions for the magnetic source (Fig. 4.5.1 b) indicate a rise in the measured amplitude across the frequency range as the source is moved back from the front of the bench. The change in amplitude is predicted to rise from about 0 dB at the bottom of the frequency range to about 5 dB at 50 MHz. Practical measurements (Fig. 4.5.2) show that the signal does rise as the source is moved back towards the wall but that it rises by about 20 dB across the frequency range. Although the theory and practice are not as close as could be desired this does give a very unambiguous test for distinguishing between single source types. The difference between the model and practical measurements is probably due to the modelling of the coupling between the source and the bench, and the assumption that this coupling does not change as the source is moved. It is unlikely to be due to the impedance of the straps as this would affect the measurements for the electric dipole source as well as the measurements for all positions of the magnetic dipole source.

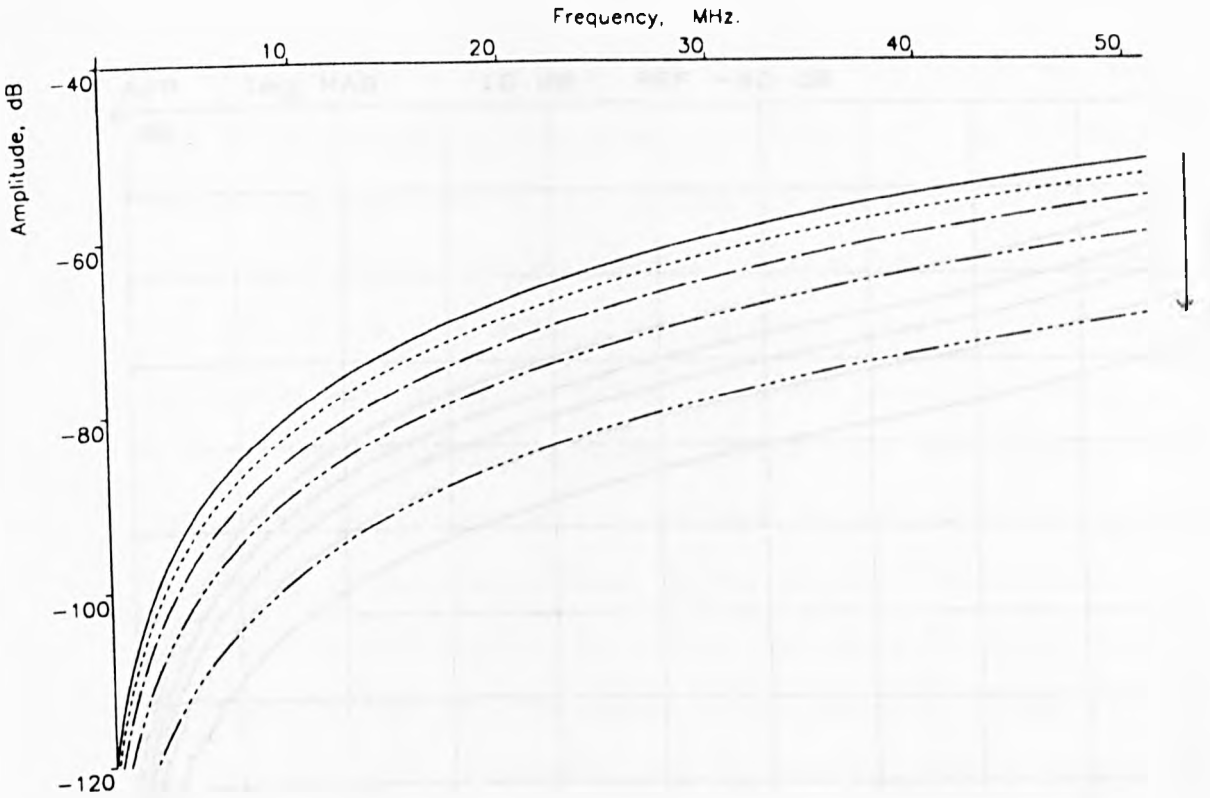

a)electric dipole source

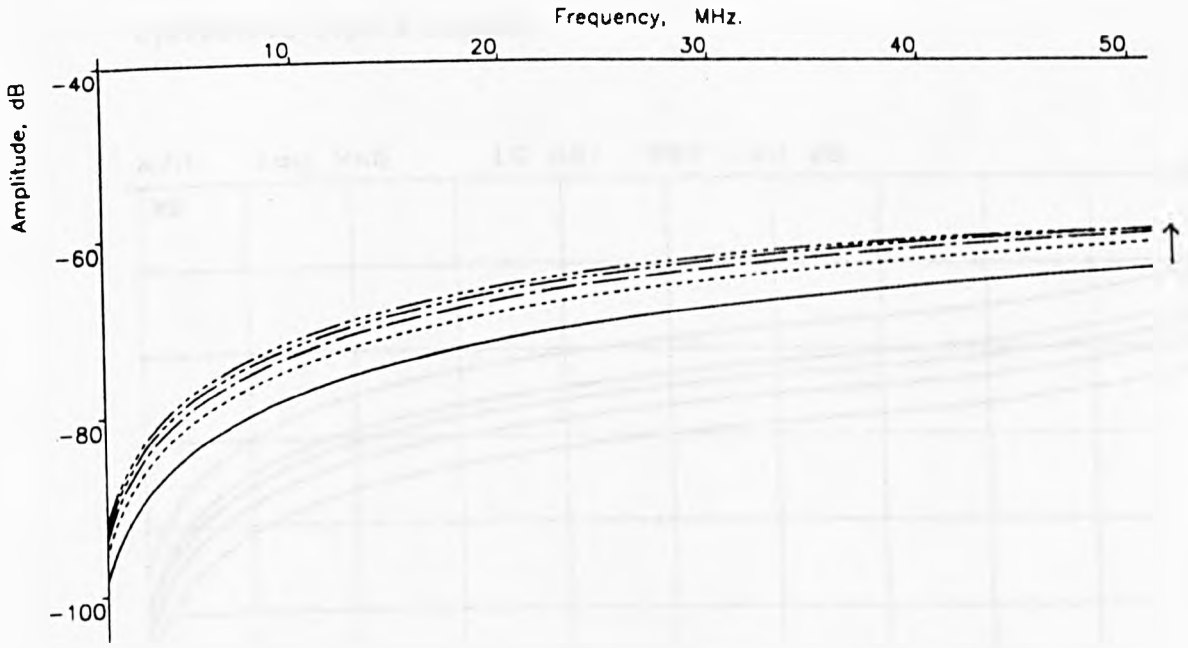

b)magnetic dipole source

Fig. 4.5.1 Predicted voltages as source is moved back from front of bench

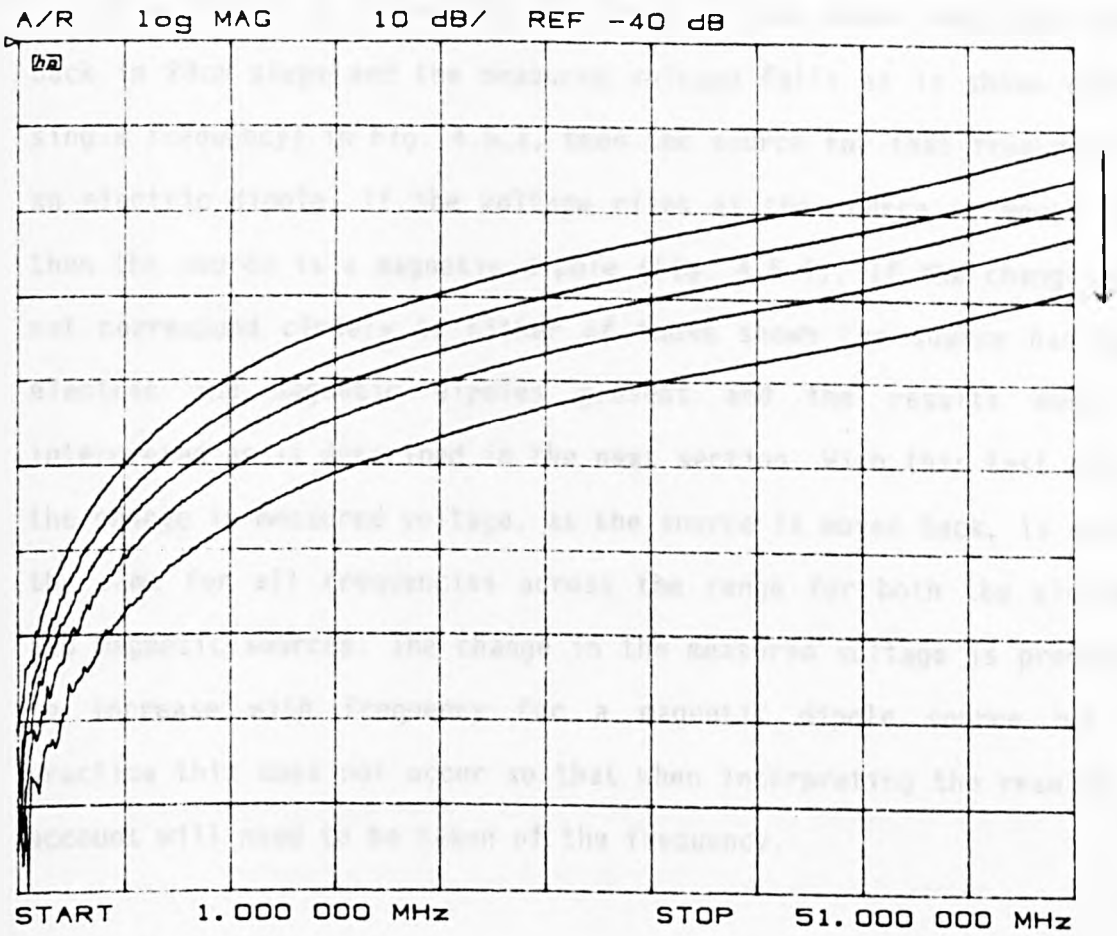

a)electric dipole source

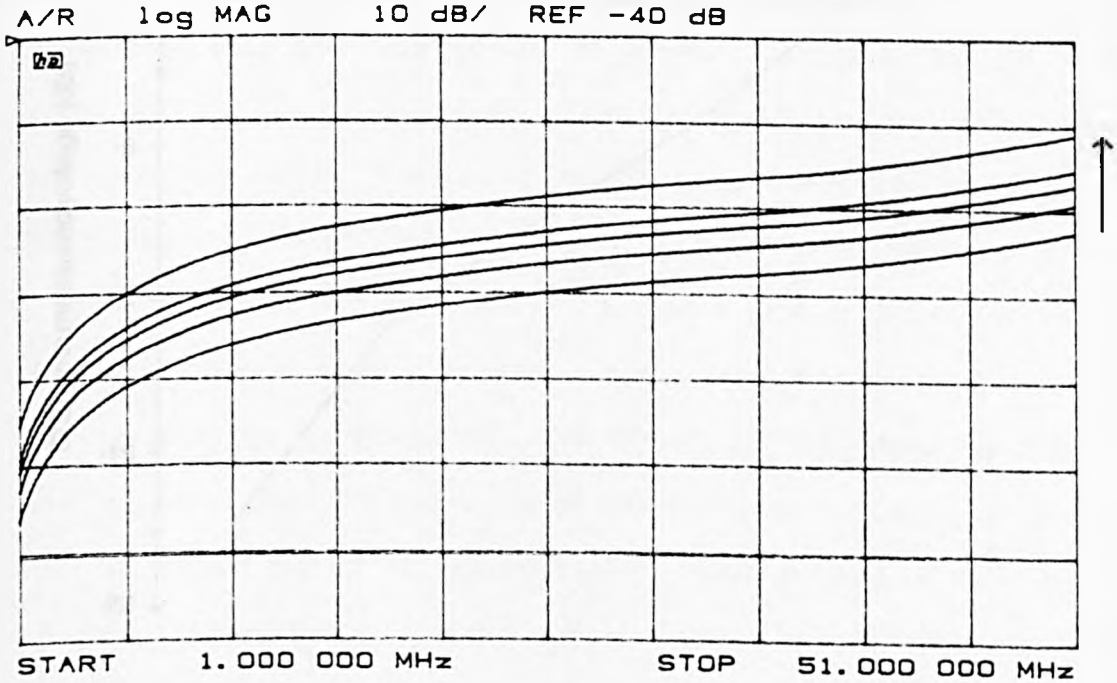

b)magnetic dipole source

Fig. 4.5.2 Measured voltage as source is moved back

If a source is placed at the front of the bench and then moved back in 20cm steps and the measured voltage falls as is shown (for a single frequency) in Fig. 4.5.3, then the source for that frequency is an electric dipole. If the voltage rises as the source is moved back then the source is a magnetic dipole (Fig. 4.5.4). If the change does not correspond closely to either of those shown the source has both electric and magnetic dipoles present and the results must be interpreted as is described in the next section. With this test set-up the change in measured voltage, as the source is moved back, is nearly the same for all frequencies across the range for both the electric and magnetic sources. The change in the measured voltage is predicted to increase with frequency for a magnetic dipole source but in practice this does not occur so that when interpreting the results no account will need to be taken of the frequency.

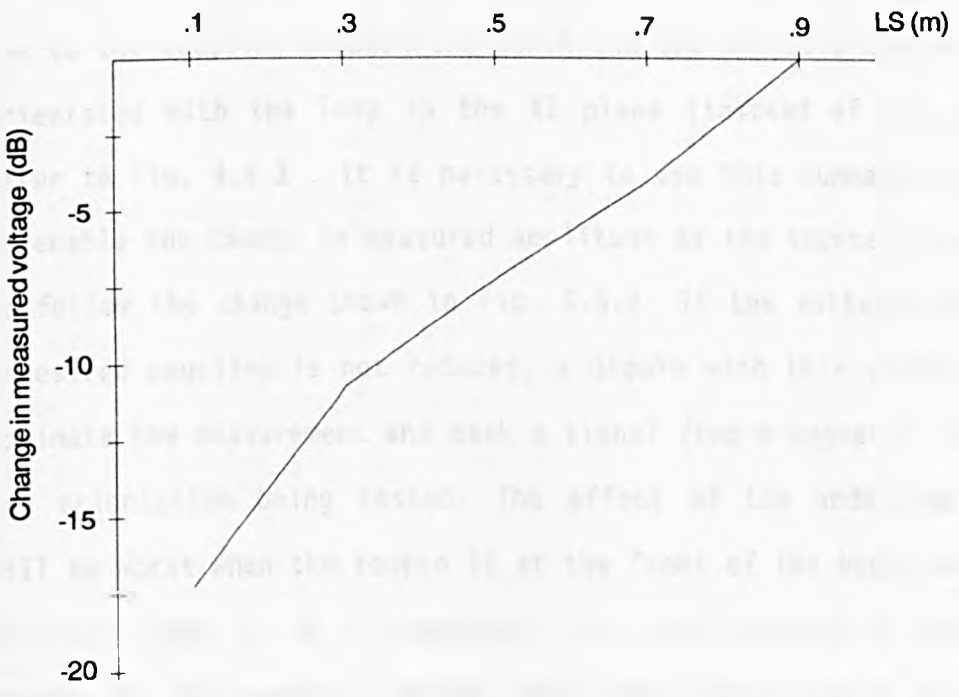

Fig. 4.5.3 Change in measured voltage for an electric dipole source moved back from the front of the bench

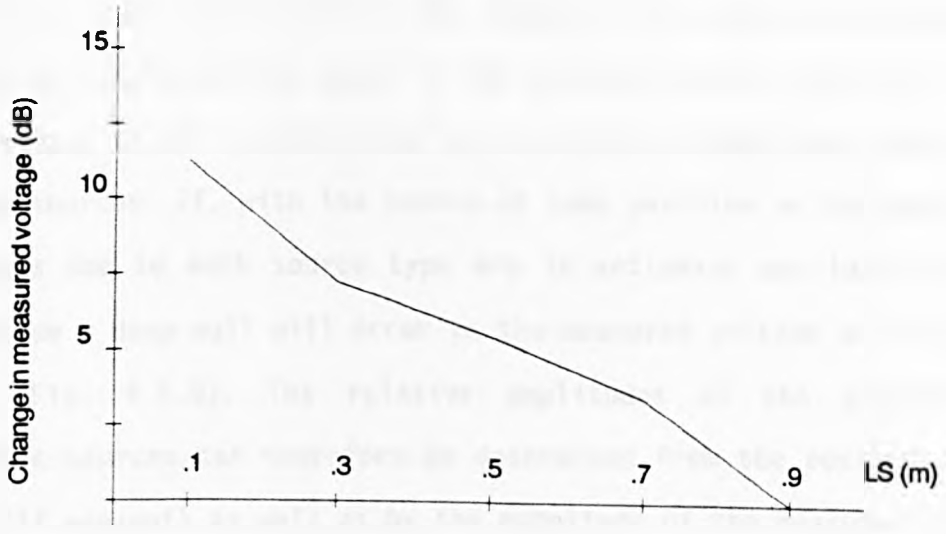

Fig. 4.5.4 Change in measured voltage for a magnetic dipole source moved back from the front of the bench

Section 4.4 describes a method of reducing the measured voltage due to the coupling between the bench and the magnetic dipole which is orientated with the loop in the XZ plane (instead of the XY plane) refer to Fig. 4.4.3 . It is necessary to use this summation technique to enable the change in measured amplitude as the source is moved back to follow the change shown in Fig. 4.5.2. If the voltage due to this undesired coupling is not reduced, a dipole with this orientation may dominate the measurement and mask a signal from a magnetic dipole with the orientation being tested. The effect of the undesired coupling will be worst when the source is at the front of the bench so that the desired signal is at its weakest. This will produce a more complex change, as the source is moved, which may follow one of the patterns described below for a dual source and would then give results which are likely to be interpreted incorrectly.

4.5.2 With both source types present

With a dual source present the change in the measured voltage will not be as simple as that shown in the previous section but will change in a manner which is determined by the relative amplitudes and phases of the sources. If, with the source at some position on the bench, the voltages due to each source type are in antiphase and have the same amplitude a deep null will occur in the measured voltage at that point (e.g. Fig. 4.5.5). The relative amplitudes of the electric and magnetic sources can therefore be determined from the position of the null (if present) as well as by the magnitude of the measured voltages with the source at the front and the back of the bench. If the null occurs at the front of the bench the shape of the response must be used to determine the relative amplitudes. The relative amplitudes of the sources change very rapidly as they are moved back and this means that over only a small portion of the bench the rate of change in the measured amplitude will not correspond to that of either source. From the examples given in Figs. 4.5.5 to 4.5.7, which are predicted responses, it can be seen that on either side of the cross over point the change can be matched to that of one or other of the sources and the relative amplitudes given whether there is a null present or not. For measured responses the difference between the changes for the two types of source is even greater ensuring that it will be even easier to distinguish between the source types.

The best way of following the above arguments is to examine some examples. These are given in Figs. 4.5.5 to 4.5.7.

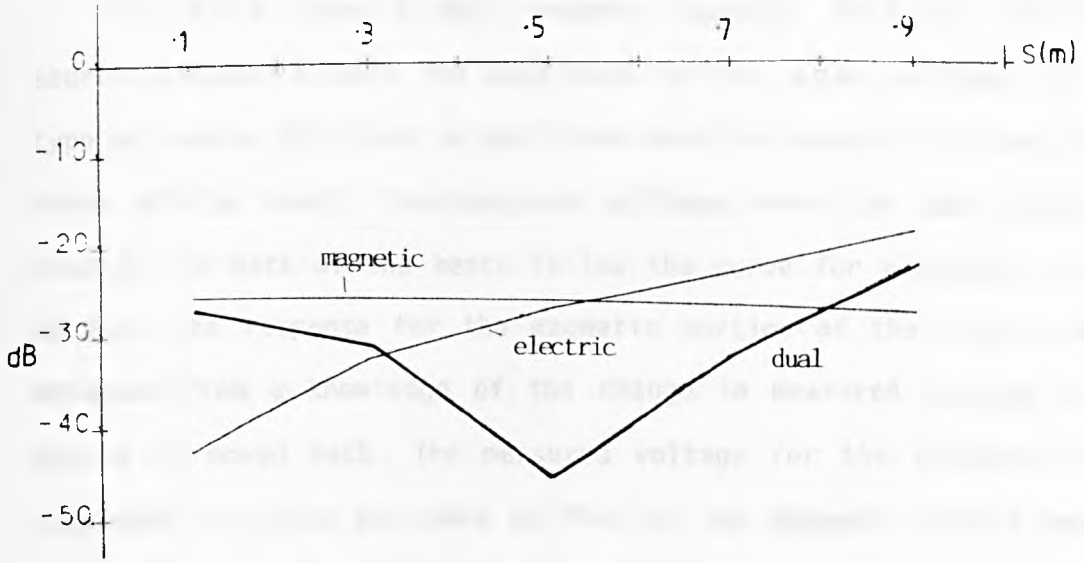

Fig. 4.5.5 Change for a dual source

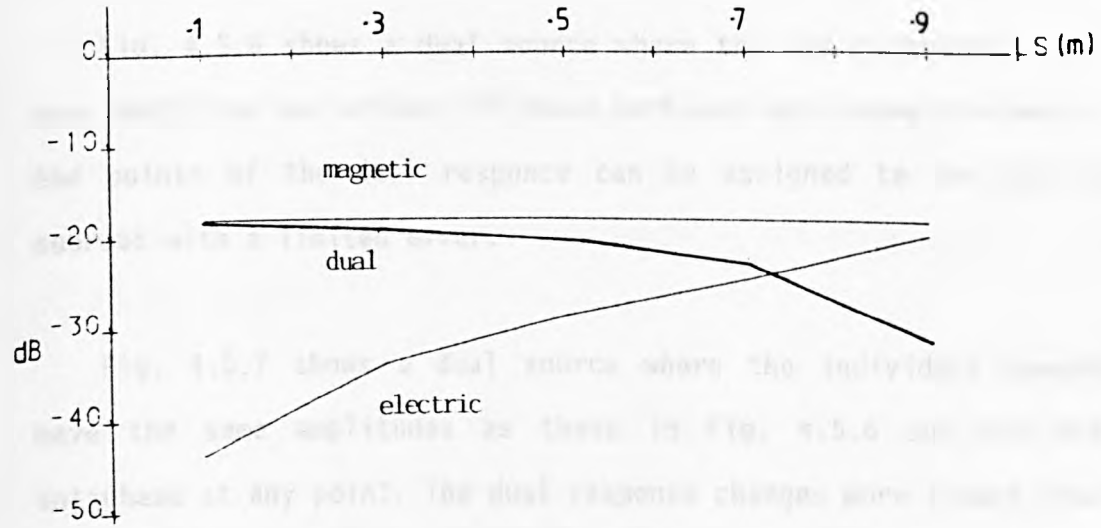

Fig. 4.5.6 Change for a different dual source

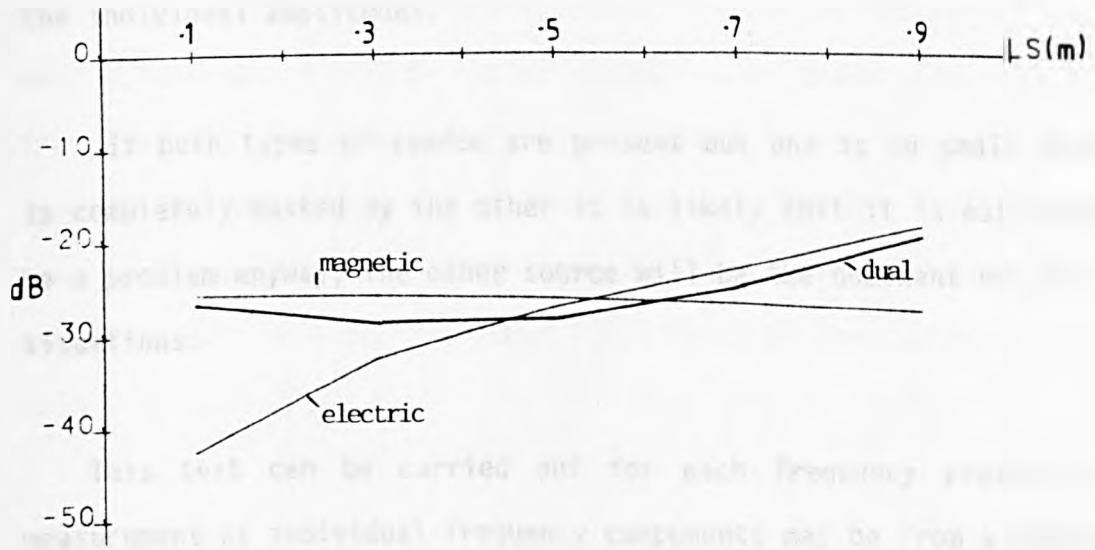

Fig. 4.5.7 Change for a third dual source

Fig. 4.5.5 shows a dual response together with the individual source components where the amplitudes of the output voltage for each type of source are close in amplitude when the source is placed at the front of the bench. The measured voltages when the dual source is towards the back of the bench follow the curve for a magnetic source so that the response for the magnetic portion of the source can be obtained from a knowledge of the change in measured voltage as the source is moved back. The measured voltage for the electric dipole component can then be taken as that of the magnetic source and the corresponding dipole moment assigned.

Fig. 4.5.6 shows a dual source where the two components have the same amplitude but are out of phase part way back along the bench. The end points of the dual response can be assigned to the individual sources with a limited error.

Fig. 4.5.7 shows a dual source where the individual components have the same amplitudes as those in Fig. 4.5.6 but are not in antiphase at any point. The dual response changes more slowly from one response to the other but again the end points can be used to assign the individual amplitudes.

If both types of source are present but one is so small that it is completely masked by the other it is likely that it is not going to be a problem anyway, the other source will be the dominant one in most situations.

This test can be carried out for each frequency present in a measurement as individual frequency components may be from a different source within the equipment under test.

4.5.3 Construction of the dual source

The dual source used for these tests was constructed from the two sources which were used individually. Both sources were fastened onto a base which held them approximately 10cm apart (Fig. 4.5.8). Each dipole was driven from a separate signal generator. The generators were phase locked with the actual phase between the two drive signals being adjustable. The cable runs between the signal generators and source dipoles were made of identical lengths so that the phase difference in the dipole drive signals could be measured at the generators rather than at the dipoles. The cables to the sources were terminated in 50Ω preventing standing waves so that the signal amplitudes at the signal generators should be the same as those at the dipoles. Ignoring cable losses (which are small and identical for both sources) the amplitude and relative phase of the drive signal for each dipole was known.

By setting up the dual source this way the signal generators could be set for particular relative amplitudes and the relative phases then adjusted to test the theory. The relative phases could be set to any desired phase once the basic difference between the two generators had been determined. Although the generators were locked onto each other the phase difference was different for each frequency and had to be adjusted if the frequency of operation was changed. The change of phase and amplitude for each type of source was predicted to be constant over the frequency range but a range of frequencies had to be tested to confirm it.

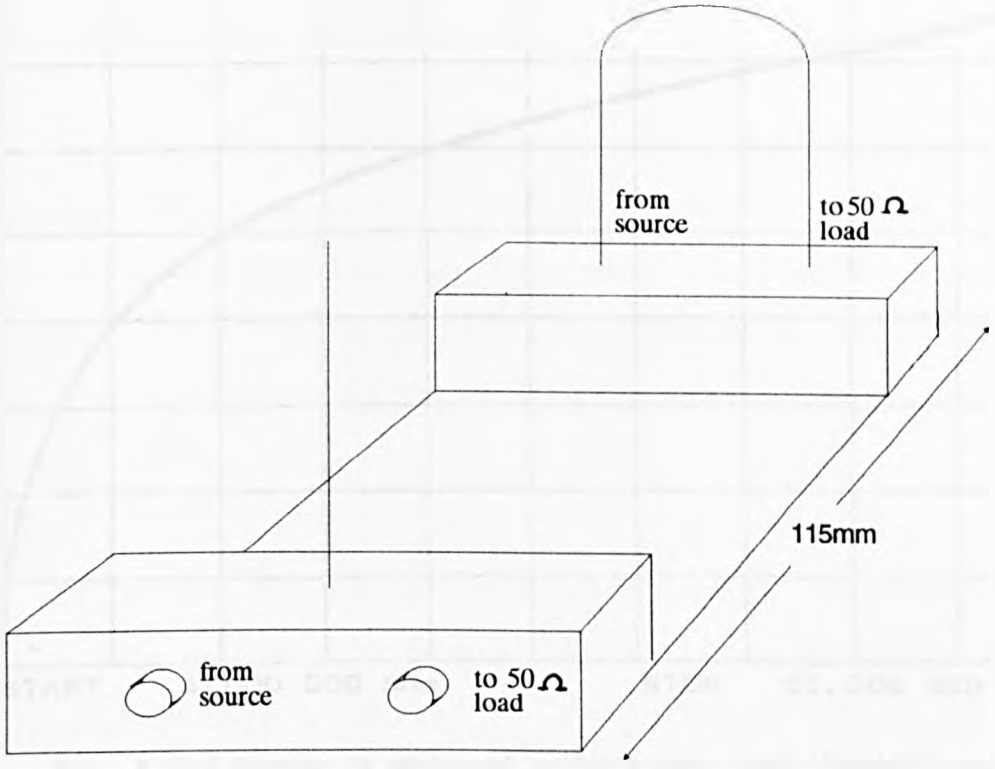

Fig. 4.5.8 Construction of dual source

Before constructing the dual source in this manner the effect of the proximity of each source upon the other was determined. The measured voltages in the tests with and without the second dipole in place was compared for the standard test set-up. The second dipole in each case was loaded to simulate the effect of the source impedance but was not connected to the first dipole or the signal generator. The change in the measured voltage in each case was found to be less than 1dB (Fig. 4.5.9) which is within the bounds of the repeatability of the measurements. The effect of moving the source 5 cm to one side of the centre line was also investigated and found to be minimal.

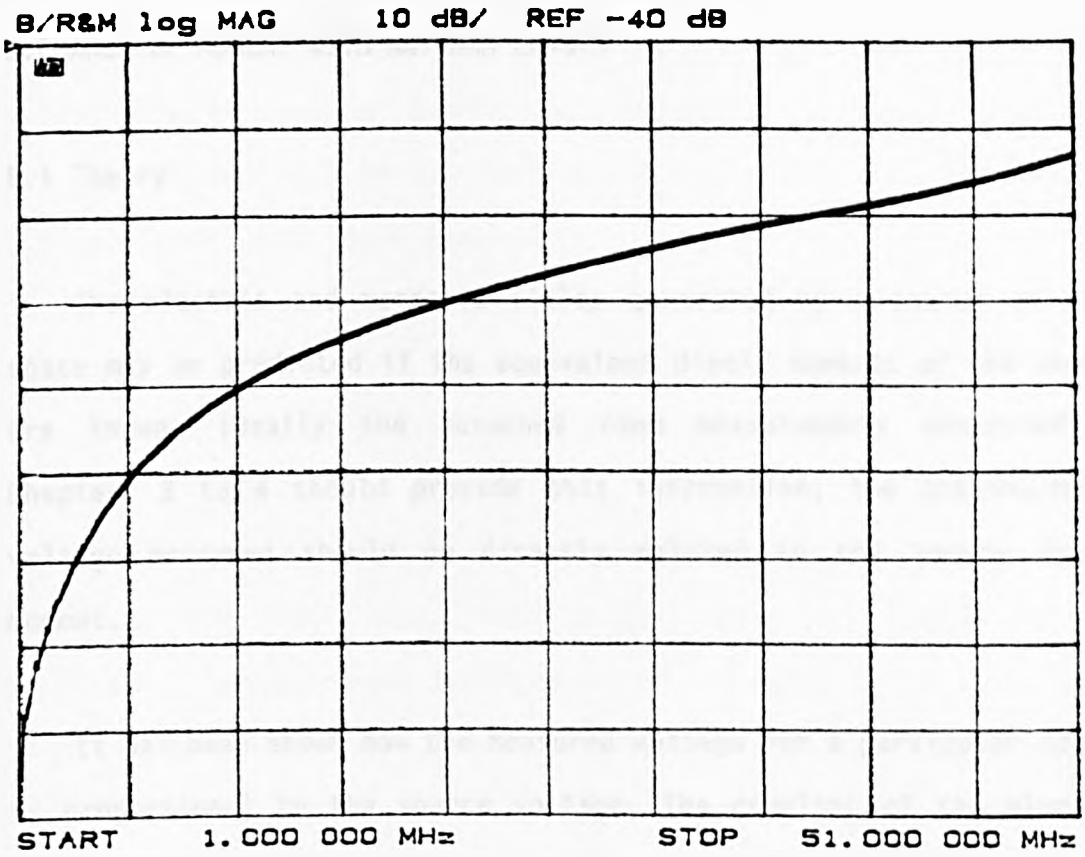

Fig. 4.5.9 Change in measured voltage when 2nd (loaded) source is moved close to first

4.6 Conclusions

It has been shown that it is possible to measure the voltage from the end of the bench to obtain the moment of the individual dipoles which make up a radiating source. By summing the voltages from the two corners of the bench it is possible to separate the individual dipole orientations. The change in measured voltage as the source is moved back gives a clear indication of the source type present and can be used to give relative amplitudes of the two sources. This can be carried out for each frequency present as it cannot be guaranteed that all the frequencies radiated by a piece of equipment are from the same source within it.

5.CHANGE OF MOMENT WITH ANTENNA LENGTH

5.1 Theory

The electric and magnetic fields generated by a source in free space may be predicted if the equivalent dipole moments of the source are known. Ideally the screened room measurements described in Chapters 2 to 4 should provide this information; the antenna/bench voltage measured should be directly related to the source dipole moment.

It has been shown how the measured voltage for a particular source is proportional to the source voltage. The coupling of the electric and magnetic dipole sources is also dependent (in terms of the equivalent circuits) on the capacitances, inductances etc which depend onthe physical dimensions of the source. For example, the capacitances which describe the coupling of the electric dipole source to the system are dependent on the length of the electric dipole source.

For a given drive voltage the moment of the source will be dependent on its dimensions. As the measured voltage is also dependent on the dimensions of the source it may or may not be related to the source dipole moment.

In this chapter a theoretical analysis of the effect of the length of an electric dipole on its moment is given and the results of a practical investigation of the relationship of the source length and the measured voltage is presented. The change in moment and the change in measured voltage are compared to determine whether the size of the electric dipole source affects the accuracy of the results. The moment

of a magnetic dipole source is also described but the relationship between the measured voltage and the moment for different moments is not investigated due to the difficulty in constructing the magnetic dipole sources with known dimensions.

5.1.1 Electric monopole over a ground plane

The moment of an elemental electric dipole is defined as the length of the dipole multiplied by the current (assuming that the current is constant over the length). For a short electric monopole ($L < \lambda/10$) where the current is assumed to have a triangular distribution the moment (M_e) is given by equation 5.1.

$$M_e = I \times L/2 \qquad \text{(Amps metres)} \qquad 5.1$$

where I is the input current and L is the length of the rod.

The drive voltage is known for the experimental source but the current is not. However, the input capacitance of the test sources can be measured using the network analyser and can also be calculated. The relationship between the source voltage and the input current is given by equation 5.2:

$$I = \frac{V}{R_r + jX} \qquad 5.2$$

where R_r is the radiation resistance of the monopole and X is the input reactance.

The radiation resistance for a small monopole is assumed to be negligeable [Jordan and Balmain 1968, p 544] so that the moment is given by equation 5.3:

$$M_e = \frac{V \times L}{2 \times |X|} \qquad 5.3$$

Since the previous voltages measured and calculated for the screened room have all been given in dB with respect to the input voltage of the source antenna its moment is given in the same form below (equation 5.4):

$$M\ (\text{dBAm}) = V\ (\text{dBV}) + 20 \log \left[\frac{L}{2 \times |X|}\right] \qquad 5.4$$

As the results are all given as measured voltage with respect to the drive voltage these are compared with the second term in the right hand side of equation 5.4 which is hence forward called the 'gain' for lack of any other term. The variation should be the same in the calculated term as in the measured voltage for a particular change in the length of the source. If the two terms also have the same frequency dependence then it will be possible to determine the relationship between the measured voltage and the moment of the antenna and simple to calibrate a room using a known source.

There are several techniques available for calculating the input reactance of a monopole, one method given in Jordan and Balmain, 1968, pages 545 to 547. This technique gives an equation for the input reactance of a monopole above a ground plane and is given as equation 5.5. It assumes a sinusoidal current variation on the monopole. Where the monopole is short this will approximate to the triangular distribution assumed for equation 5.1.

$$X = \frac{-15}{\sin^2\beta l}\left\{ \sin(2\beta L)\left[-U + \ln\left[\frac{L}{\beta a^2}\right] + 2Ci(2\beta L) - Ci(4\beta L) \right]\right.$$

$$\left. -\cos(2\beta L)\left[2Si(2\beta L) - Si(4\beta L) \right] - 2Si(2\beta L) \right\} \qquad 5.5$$

where U = 0.5772... (EULERS CONSTANT)

AND $$Si\ (x) = \int_0^x \frac{\sin x}{x}\, dx \qquad 5.6$$

$$Ci\ (x) = -\int_x^\infty \frac{\cos x}{x}\, dx \qquad 5.7$$

$$\beta = \frac{2\pi}{\lambda} \qquad 5.8$$

a = radius of antenna

L = length of antenna

The input capacitance was calculated for monopole lengths of 0.2, 0.1 and 0.05m with a diameter of 2.5mm. The calculated input capacitances were then used to determine the second term on the RHS of equation 5.4 for frequencies from 5 to 50MHz for each dipole length. The results are shown in table 5.1 (C and X) and in Fig.5.1.1 (the 'gain').

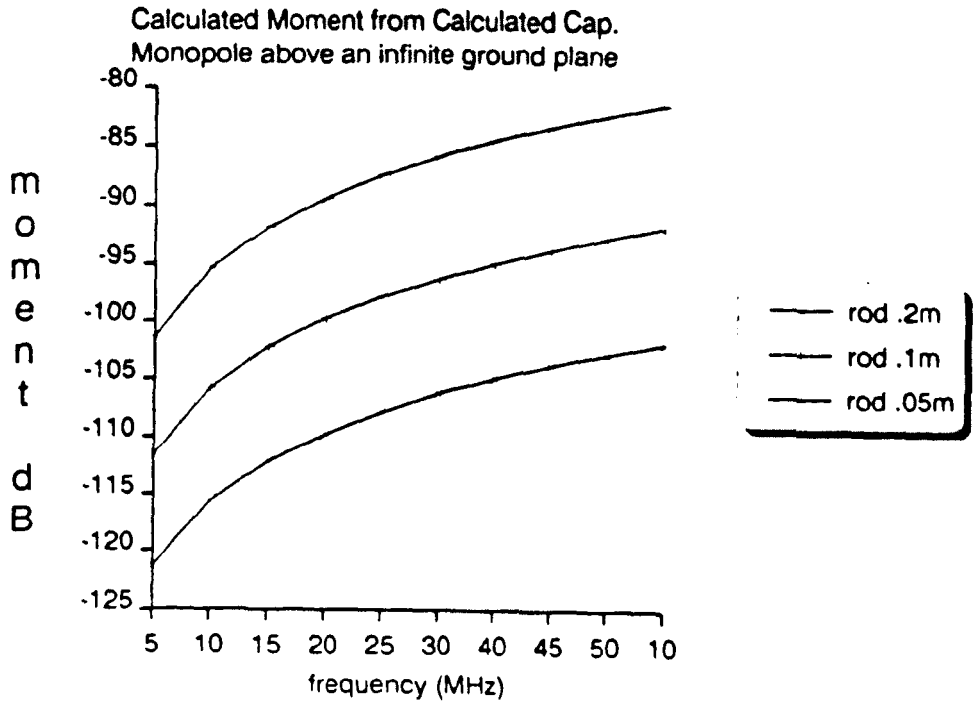

Fig. 5.1.1 The 'gain' derived from the calculated input capacitance

The input capacitance can also be measured on the network analyser by comparing the reflected and incident waves with a directional coupler and hence X can be calculated. The coaxial connector at the base of the source (Fig. 2.1.1a) cannot be calibrated out of the measured values, but its capacitance was measured and removed from the total values measured and the resulting values for the input capacitance are shown in table 5.1. From this the second term on the RHS of equation 5.4 can be calculated. The measured values of C and X for antenna heights of .2, .1 and .05 m are also shown in Table 5.1 and the calculated 'gain' is shown in Fig.5.1.2.

Frequency MHz	Calculated Capacitance (pF)	Calculated moment 'gain (dB)	Measured Capacitance (pF)	Measured moment 'gain' (dB)
length 0.2m				
5	2.72	-101.4	3.6	-98.9
10	2.74	-95.30	3.6	-92.9
15	2.72	-91.83	3.6	-89.4
20	2.72	-89.33	3.6	-86.9
25	2.72	-87.37	3.6	-85.0
30	2.72	-85.80	3.6	-83.4
35	2.72	-84.47	3.6	-82.0
40	2.71	-83.33	3.7	-80.6
45	2.71	-82.31	3.7	-79.6
50	2.70	-81.42	3.7	-78.7
length 0.1m				
5	1.67	-111.6	2.4	-108.5
10	1.64	-105.8	2.3	-102.8
15	1.65	-102.2	2.3	-99.3
20	1.65	-99.69	2.3	-96.8
25	1.65	-97.77	2.4	-94.5
30	1.64	-96.23	2.4	-92.9
35	1.64	-94.86	2.4	-91.6
40	1.64	-93.73	2.4	-90.4
45	1.64	-92.69	2.4	-89.4
50	1.64	-91.78	2.4	-88.5
length 0.05m				
5	1.09	-121.3	1.7	-117.5
10	1.06	-115.6	1.6	-112.0
15	1.04	-112.2	1.6	-108.5
20	1.03	-109.8	1.6	-106.0
25	1.03	-107.9	1.6	-104.0
30	1.03	-106.2	1.6	-102.5
35	1.04	-104.9	1.6	-101.1
40	1.04	-103.7	1.6	-100.0
45	1.04	-102.7	1.6	-98.9
50	1.04	-101.8	1.6	-98.0

Table 5.1 Calculated and measured capacitance and moment 'gain for the various source lengths

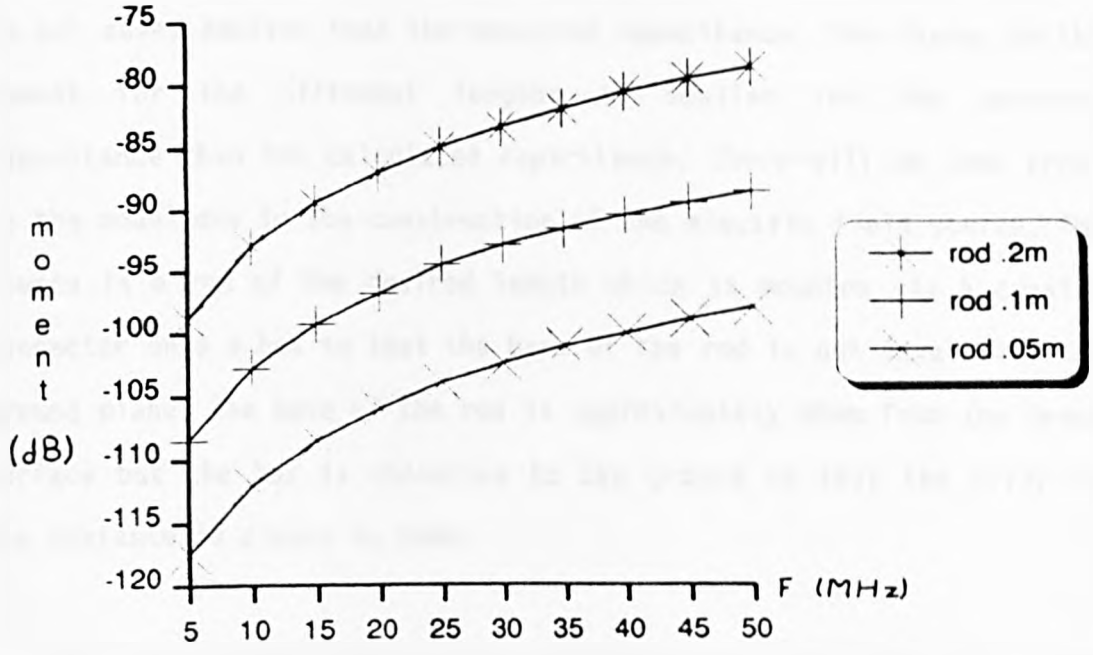

Fig. 5.1.2 The 'gain' derived from the measured input capacitance

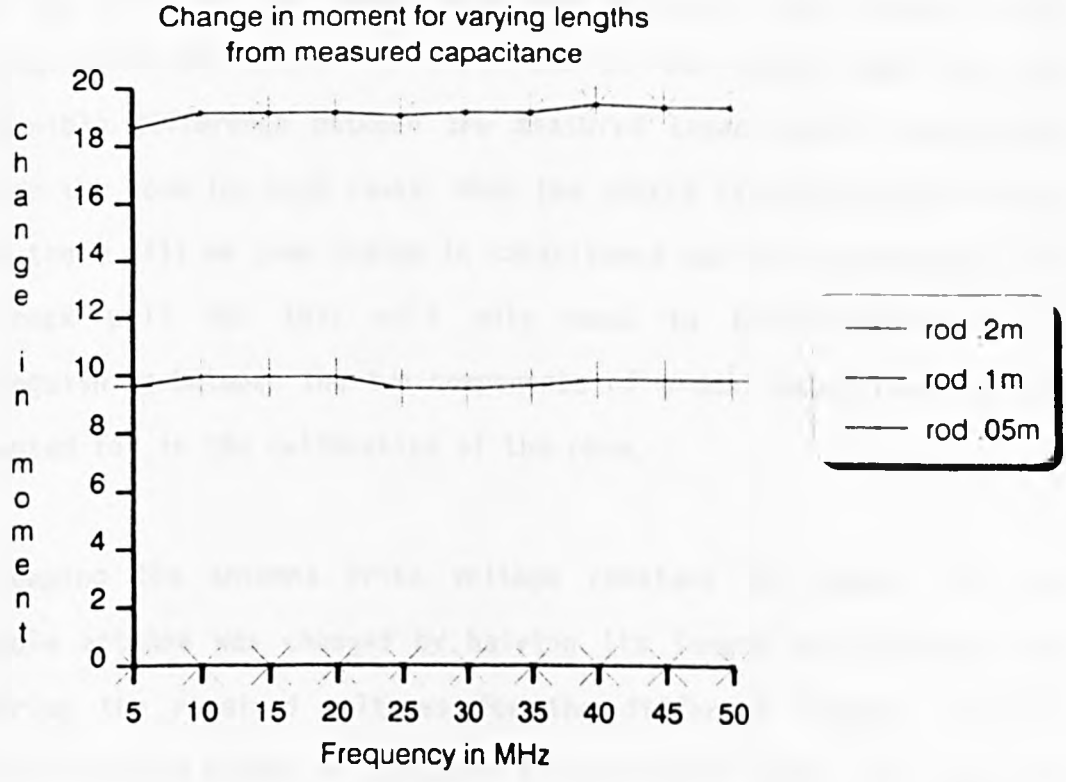

Fig. 5.1.3 The change in the 'gain' for the different lengths (from measured capacitance, 5cm source is reference)

Examination of Table 5.1 shows that the calculated capacitance is in all cases smaller than the measured capacitance. The change in the moment for the different lengths is smaller for the measured capacitance than the calculated capacitance. There will be some error in the model due to the construction of the electric field source. The source is a rod of the desired length which is mounted via a coaxial connector onto a box so that the base of the rod is not level with the ground plane. The base of the rod is approximately 60mm from the bench surface but the box is connected to the ground so that the error in the distance is closer to 20mm.

The input capacitances of the antennas were also measured inside the screened room to determine whether there would be any significant change in the moment of the source when it was enclosed by the room. This was carried out with the source at the specified position 10cm from the front of the bench with the extension both present and missing. With the source at the front of the bench there was no discernible difference between the measured capacitances inside and outside the room for both cases. When the source is at the back of the bench there will be some change in capacitance due to the proximity of the back wall but this will only need to be considered when distinguishing between the two components of a dual source and can be accounted for in the calibration of the room.

Keeping the antenna drive voltage constant the moment of the monopole antenna was changed by halving its length successively and comparing the received voltages for the different lengths. It was assumed that the change in impedance of the dipole across the range of frequencies and lengths would be negligible when compared to the 50Ω load on the line and therefore that the drive voltage would remain

constant for all the changes. This was carried out with the standard test setup, with the end of the extension loaded and with the direct measurement from the end of the bench.

The results for the various test setups considered are discussed in sections 5.2 to 5.4.

5.1.2 Magnetic dipole

The moment of a magnetic loop is given by:-

$$M_m = \pi a^2 I \quad Am^2 \qquad 5.9$$

where I is the current flowing through the loop and πa^2 is the area of the loop

$$I = \frac{V}{R + jX} \qquad 5.10$$

where V is the voltage driving the loop
R is the impedance of the load and source
X is the reactance of the loop

As with the electric dipole the moment can be expressed as:

$$M\ (dBAm^2) = V\ (dBV) + 20 \log \frac{\pi a^2}{\sqrt{R^2 + X^2}} \qquad 5.11$$

For the loop which has been used as the test source the 'gain' term from equation 5.11 is plotted in Fig.5.1.3. The value of inductance which has been used is 140nH. Fig. 5.1.3a shows the 'gain' as defined above. Fig. 5.1.3b shows the 'gain' multiplied by ω as the coupling of the magnetic dipole source to the transmission line (bench) is dependent on the operating frequency.

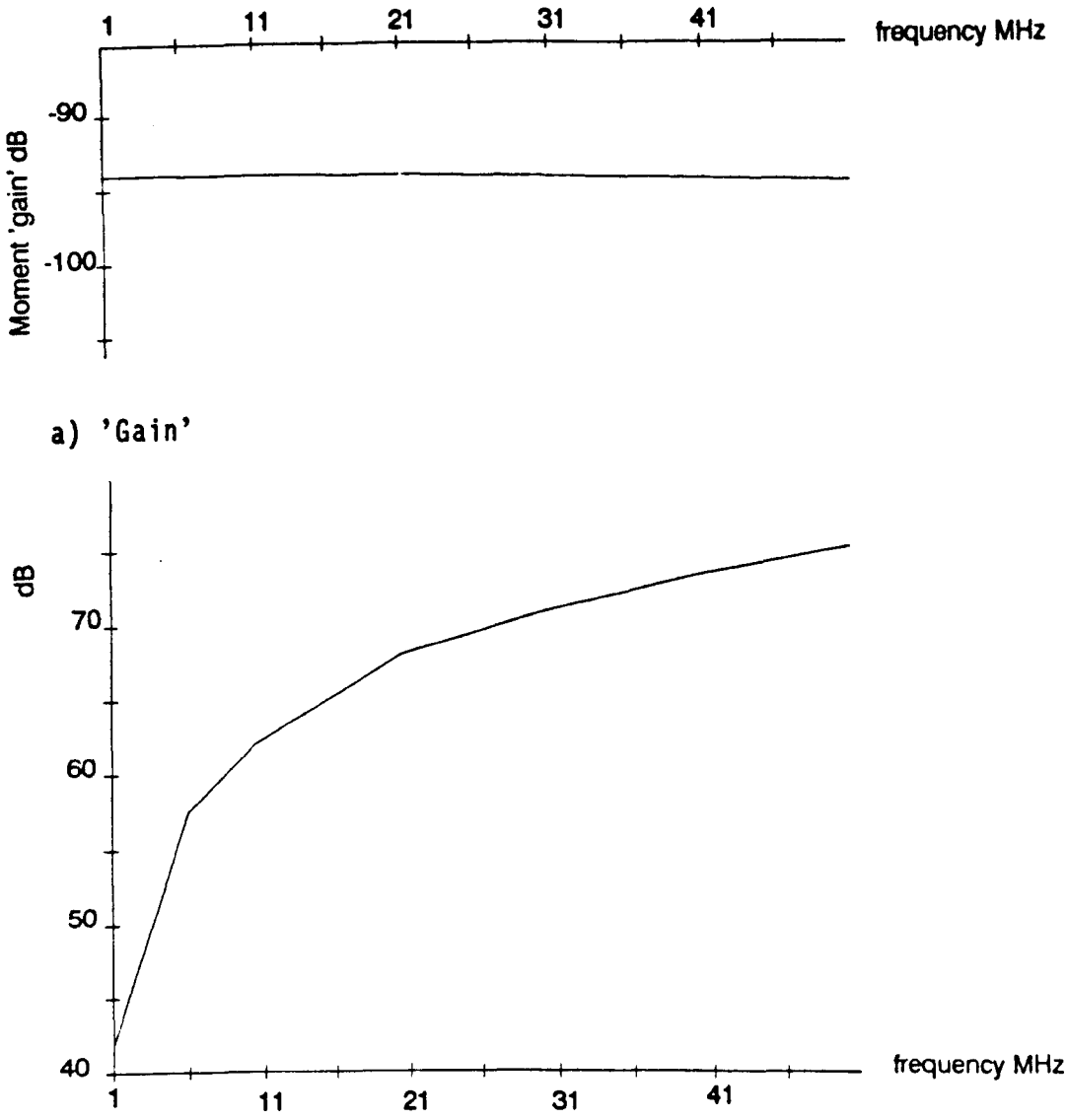

Fig. 5.1.4 The 'gain' for the magnetic dipole used for the measurements

Due to the difficulty in constructing magnetic dipole sources of known moment, measurements were not carried out on the effect of a change in moment on the measured voltage for the various test setups. If the plot of 'gain' + 20 log ω is compared with the measured voltage, for the loaded bench and the direct measurement, the change in measured voltage with frequency can be seen to be similar. The frequency dependence of the measurement setup must be accounted for during the room calibration.

5.2 Standard Test Setup

Fig. 5.2.1 shows the change in measured voltage for the same changes in electric dipole length as were used when the input capacitance was measured directly and used to calculate the moment. The measured change in the received voltage for the electric dipole source is smaller than that predicted from both the calculated and measured input capacitances. If reference is made to the equivalent circuits (Fig. 2.1.5) there are three capacitances from the dipole source; the capacitance to the infinite ground plane is approximately the capacitance to the bench in the model but there are also the capacitances to the measuring antenna and the rest of the room. These capacitances will also change. Fig. 5.2.1 shows that the change in the measured voltage is slightly different on either side of the null in the frequency response (refer to Fig. 2.1.4). This can be explained due to the different coupling mechanisms which exist. Below the null the response is dominated by the direct capacitive coupling to the sensing antenna while above it the measurement is dominated by the coupling to the transmision line formed by the bench and the room walls. Due to the different spacings the relevant capacitances will change differently with variations in the antenna lengths.

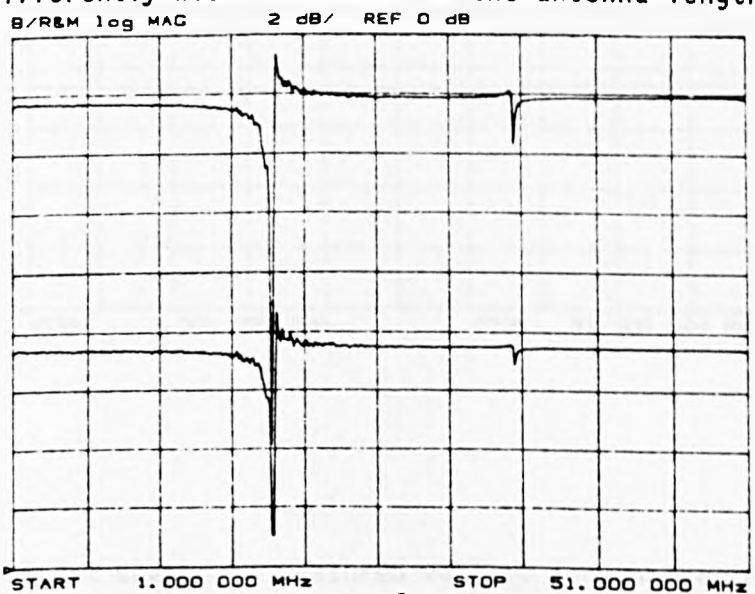

Fig. 5.2.1 Change in measured voltage for the 'standard test setup'

5.3 With End of Transmission Line Loaded

The measurements for this were carried out with the bench loaded with the 50Ω (equivalent) load. The results for this case are shown in Fig. 5.3.1. The changes are very similar to those for the standard test setup as they are subject to the same influences by the room. The change in the measured voltage is the same for frequencies which are below the null (for the standard setup) and is also close for the higher frequencies. The change between the two regions is gradual, rather than abrupt as occurs with the standard measurement setup, due to the gradual change between the coupling mechanisms which occurs with this method.

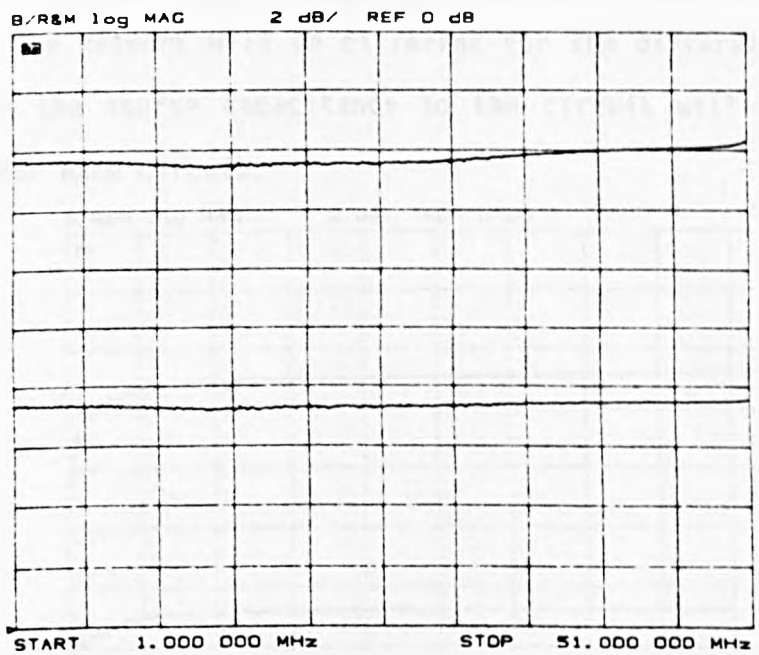

Fig. 5.3.1 Change in measured voltage for change in source length (50Ω load on end of bench)

5.4 Direct Measurement

The results for this setup are shown in Fig. 5.4.1. Above 5MHz the change is again similar to that measured for the standard test setup. Due to the lack of direct coupling between the source and sensing antenna this technique is less sensitive at the lower frequencies, particularly with the smallest source. As the smallest source was used to 'calibrate' the network analyser (ie. was set as the 0dB reference) inaccuracies and noise which occur due to the lack of sensitivity appear in the traces for the longer two sources below 5MHz.

The change in the measured voltage is slightly lower (.5dB) than for the standard setup. This can be explained by comparing the equivalent circuits. The impedance of the bench and extension with the antenna will be different to that for the bench only which is terminated by 50Ω. As the ratios of impedance between the different parts of the network will be different for the different circuits the change in the source capacitance to the circuit will give different results for each circuit.

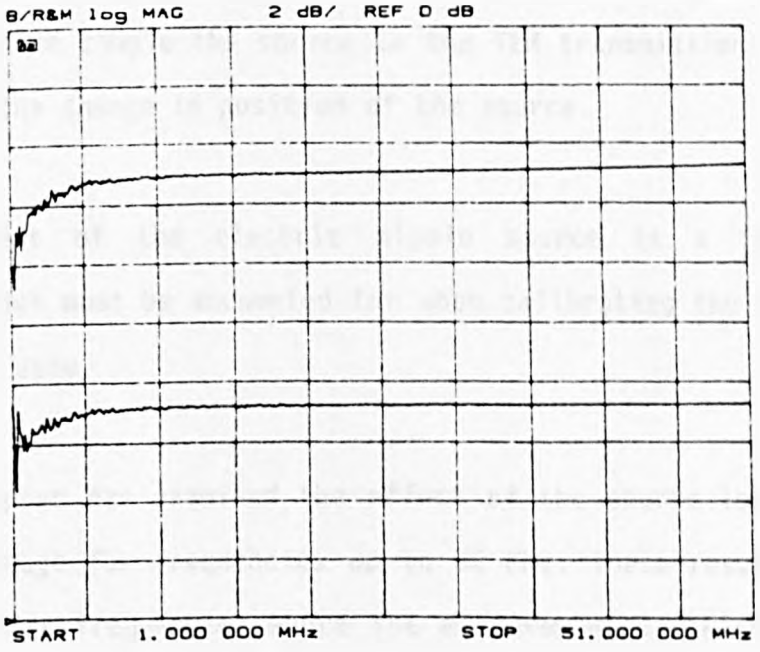

Fig. 5.4.1 Change in measured voltage with length of source (direct measurement from bench)

5.5 Conclusions

The change in measured voltage with change in electric dipole source length is not the same as that predicted from equation 5.4 using the change in the measured input capacitance of the source. Over the range of lengths investigated the change in the measured voltage is just under 4dB less than the change in the moment calculated from the measured input capacitance for all the test setups investigated. If the EUT is resticted in size (eg less than 200mm high) and the measurement method is calibrated with a source which is in the middle of the range of sizes which can be tested the errors in the measurement will be limited to a value (+/-2dB) which is far less than the errors presently experienced due to the resonances and nulls which occur in the frequency response of the system.

This investigation has only examined the effect of the length of the source on the measured voltage. It has not examined the effect of raising a given source above the level of the bench. This would also effect the accuracy of the results as the capacitances and the mutual inductance which couple the source to the TEM transmission line would change with the change in position of the source.

The moment of the electric dipole source is a function of frequency which must be accounted for when calibrating the measurement set up to be used.

This chapter has examined the effect of the source length on the measured voltage for frequencies up to 30 MHz. These results may not hold for higher frequencies where the measurement techniques will be different.

This chapter completes the section on the work carried out at frequencies up to 30 MHz. The next chapter introduces the methods carried out for frequencies in the range 30 to 200 MHz. The rest of this thesis is concerned with improving the repeatability of measurements carried out in this higher frequency range.

6 THEORY OF FIELDS IN A RESONANT CAVITY

6.1 The Field Patterns

A waveguide is a device capable of guiding electromagnetic waves and can take several forms. The type under consideration is a conducting pipe with a rectangular cross section. When the wavelength of an electromagnetic wave is less than twice the larger dimension of the cross section of the waveguide the wave will propagate down the guide. The fields within the guide are given by Equations 6.1 to 6.6. These are for the transverse electric (TE) modes propagating in the Z direction.

$$E_x = -\frac{Cn\pi}{b} \cos\frac{m\pi x}{a} \sin\frac{n\pi y}{b} e^{j(\omega t - Bz)} \qquad 6.1$$

$$E_y = -\frac{Cm\pi}{a} \sin\frac{m\pi x}{a} \cos\frac{n\pi y}{b} e^{j(\omega t - Bz)} \qquad 6.2$$

$$E_z = 0 \qquad 6.3$$

$$H_x = \frac{Cm\pi B}{\omega\mu a} \sin\frac{m\pi x}{a} \cos\frac{n\pi y}{b} e^{j(\omega t - Bz)} \qquad 6.4$$

$$H_y = \frac{Cn\pi B}{\omega\mu b} \cos\frac{m\pi x}{a} \sin\frac{n\pi y}{b} e^{j(\omega t - Bz)} \qquad 6.5$$

$$H_z = \frac{C\pi}{j\omega\mu}\left[\left[\frac{m}{a}\right]^2 + \left[\frac{n}{b}\right]^2\right] \cos\frac{m\pi x}{a} \cos\frac{n\pi y}{b} e^{j(\omega t - Bz)} \qquad 6.6$$

where $B = \sqrt{\omega^2\mu\epsilon - k}$ and $k = \sqrt{\left[\frac{m\pi}{a}\right]^2 + \left[\frac{n\pi}{b}\right]^2}$

a and b are the dimensions of the guide cross section
and m and n are positive integers. One of these integers can be zero for the TE modes but not both.

Fig. 6.1.1 shows the directions x, y and z and the dimensions a, b and d.

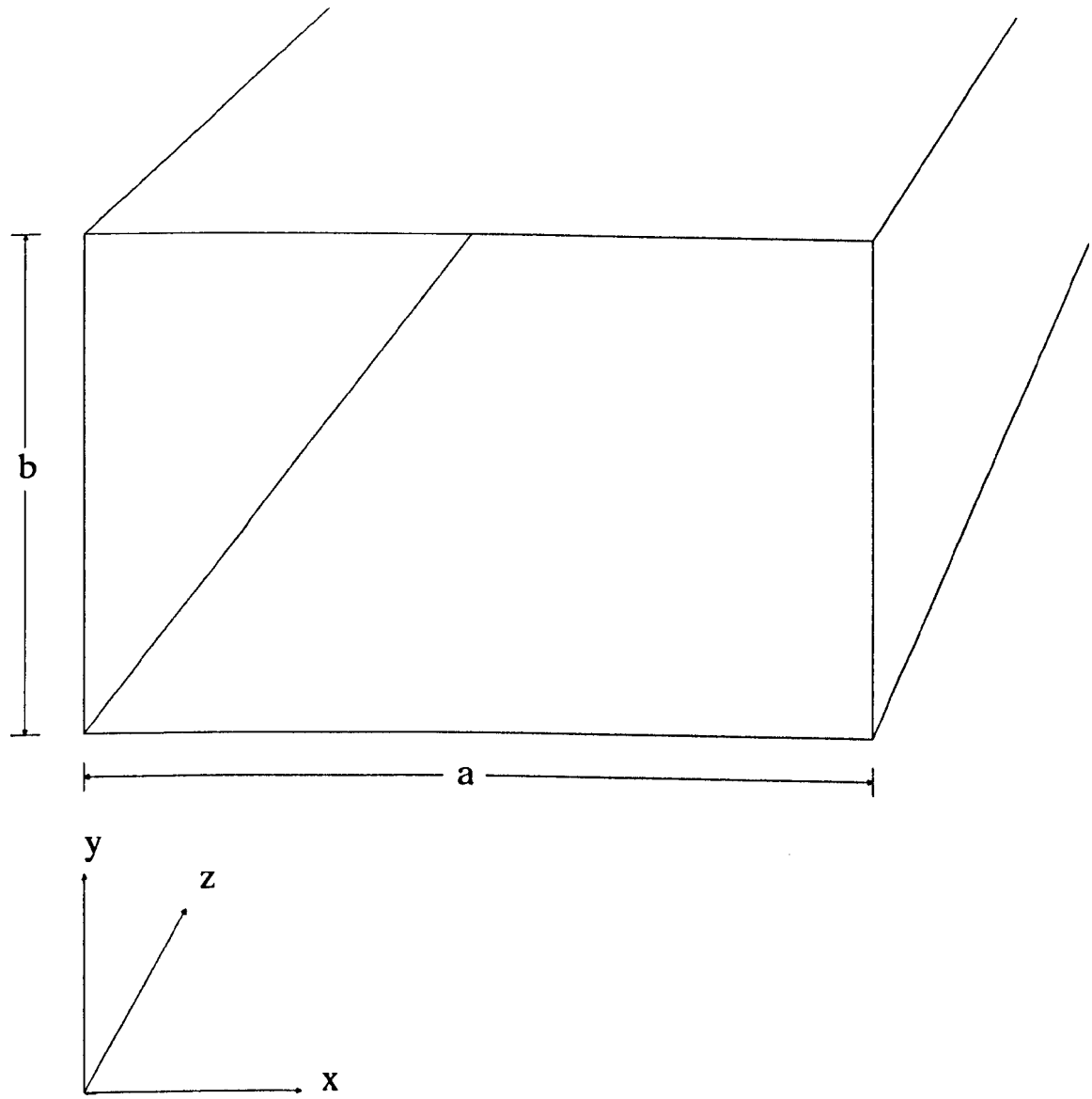

Fig. 6.1.1 Showing the dimentions of a waveguide and the orientations for x, y and z

The Equations 6.1 to 6.6 show the expressions for the field for modes called transverse electric, TE, (with no component of electric field in the direction of propagation). A similar set exist for modes with no component of magnetic field in the direction of propagation (transverse magnetic, TM). The first transverse magnetic mode which can propagate is the $TM_{1,1}$ mode (i.e neither m or n can be zero) which means that the lowest propagating mode is the $TE_{0,1}$ or $TE_{1,0}$ depending on the dimensions of the waveguide [Ramo, Whinnery and Van Duzer 1965].

There exists a frequency (the cut-off frequency) for each mode below which any wave induced into the guide will be attenuated and will not propagate. Equation 6.7 shows the relationship between the mode numbers, the electrical properties of the material in the guide and the cut-off frequency.

$$f_c = \frac{1}{2\pi\sqrt{\epsilon\mu}} \sqrt{\left[\frac{m}{a}\right]^2 + \left[\frac{n}{b}\right]^2} \qquad 6.7$$

where m,n,a and b have the same meanings as before.

At frequencies below cut off the impedance of the guide is reactive, inductive for TE and capacitive for TM. The impedance of the guide is defined as the ratio of the transverse electric fields to the transverse magnetic fields.

The TEM (transverse electromagnetic) mode does not propagate down a waveguide and propagating modes are either transverse electric (TE) with no electric field in the direction of propagation or transverse magnetic (TM) with no magnetic field in the direction of propagation. The lowest frequency which will propagate will always be $TE_{0,1}$, higher modes will exist as a mixture of the two types which are said to be

degenerate if their cut-off frequencies are the same. It is possible for different modes to operate with the same frequency as well as the normal TE and TM with the same mode numbers; these are also said to be degenerate (e.g TE_{12} and TE_{21} for a guide with square cross section).

If the waveguide is terminated with a perfect conductor the wave will be totally reflected. If it is so terminated at both ends a wave induced into the cavity will be reflected backwards and forwards and a standing wave pattern will be set up. Solution of Maxwell's equations for the totally bounded box (where electric fields tangential to the walls are constrained to be zero and perpendicular magnetic fields are zero) gives the following results for the field distribution within the cavity for the equivalent TE (equations 6.8 to 6.13) and TM (equations 6.14 to 6.19) modes from the waveguide. These equations apply at resonant frequencies (i.e. $n \times \lambda_g / 2$ is d , λ_g is the guide wavelength).

$$E_x = \frac{n\pi}{b} \cos \frac{m\pi x}{a} \sin \frac{n\pi y}{b} \sin \frac{p\pi z}{d} \qquad 6.8$$

$$E_y = -\frac{m\pi}{a} \sin \frac{m\pi x}{a} \cos \frac{n\pi y}{b} \sin \frac{m\pi z}{d} \qquad 6.9$$

$$E_z = 0 \qquad 6.10$$

$$H_x = -\frac{mp\pi^2}{j\omega\mu ad} \sin \frac{m\pi x}{a} \cos \frac{n\pi y}{b} \cos \frac{p\pi z}{d} \qquad 6.11$$

$$H_y = -\frac{np\pi^2}{j\omega\mu bd} \cos \frac{m\pi x}{a} \sin \frac{n\pi y}{b} \cos \frac{p\pi z}{d} \qquad 6.12$$

$$H_z = \frac{\pi^2}{j\omega\mu}\left[\left(\frac{m}{a}\right)^2+\left(\frac{n}{b}\right)^2\right] \cos \frac{m\pi x}{a} \cos \frac{n\pi y}{b} \sin \frac{p\pi z}{d} \qquad 6.13$$

Field patterns for TE modes
m, n and p = 0, 1, 2, 3 etc [Ramo, Whinnery and Van Duzer 1965]

$$E_x = -\frac{mp\pi^2}{j\omega\epsilon ad} \cos\frac{m\pi x}{a} \sin\frac{n\pi y}{b} \sin\frac{p\pi z}{d} \qquad 6.14$$

$$E_y = -\frac{np\pi^2}{j\omega\epsilon bd} \sin\frac{m\pi x}{a} \cos\frac{n\pi y}{b} \sin\frac{p\pi z}{d} \qquad 6.15$$

$$E_z = \frac{\pi^2}{j\omega\epsilon}\left[\left[\frac{m}{a}\right]^2+\left[\frac{n}{b}\right]^2\right] \sin\frac{m\pi x}{a} \sin\frac{n\pi y}{b} \cos\frac{p\pi z}{d} \qquad 6.16$$

$$H_x = \frac{n\pi}{b} \sin\frac{m\pi x}{a} \cos\frac{n\pi y}{b} \cos\frac{p\pi z}{d} \qquad 6.17$$

$$H_y = -\frac{m\pi}{a} \cos\frac{m\pi x}{a} \sin\frac{n\pi y}{b} \cos\frac{p\pi z}{d} \qquad 6.18$$

$$H_z = 0 \qquad 6.19$$

Field patterns for TM modes
m, n and p = 1, 2, 3, etc

The fields excited within the cavity depend on the type and orientation of the field source. It is possible for more than one resonant mode to exist at the same frequency. Fig. 6.1.2 shows the orientation of magnetic fields which will be generated by a magnetic loop where the plane of the loop is in the vertical plane perpendicular to the wall the probe is mounted on. The fields which will couple with the loop are shown as dashed lines, those shown as dotted lines will not couple with the loop and hence will not be excited.

The room has a series of high Q resonances at frequencies which are calculated from equation 6.20, signals at other frequencies which may be injected into the cavity are rapidly attenuated [Ramo, Whinnery and Van Duzer 1965].

$$f_{mnp} = \frac{1}{2\sqrt{\epsilon\mu}} \sqrt{\left[\frac{m}{a}\right]^2 + \left[\frac{n}{b}\right]^2 + \left[\frac{p}{d}\right]^2} \qquad 6.20$$

m (x)	n (y)	p (z)	freq MHz	m (x)	n (y)	p (z)	freq MHz
0	1	1	72.1	1	1	4	161.5
0	1	2	92.5	1	2	0	142.7
0	1	3	119.0	1	2	1	146.6
0	1	4	148.4	1	2	2	157.7
0	1	5	179.5	1	2	3	174.5
0	2	1	132.0	1	2	4	195.7
0	2	2	144.2	2	0	1	132.0
0	2	3	162.4	2	0	2	144.2
0	2	4	185.0	2	0	3	162.4
0	3	1	194.4	2	0	4	185.0
1	0	1	72.1	2	1	0	142.7
1	0	2	92.5	2	1	1	146.6
1	0	3	119.0	2	1	2	157.7
1	0	4	148.4	2	1	3	174.5
1	0	5	175.9	2	1	4	195.7
1	1	0	90.3	2	2	0	180.5
1	1	1	96.3	2	2	1	183.6
1	1	2	112.4	2	2	2	192.6
1	1	3	135.0	3	0	1	194.4

Table 6.1 The frequencies of resonant modes in the screened room

Table 6.1 shows the frequencies of the resonances calculated from equation 6.20 for the dimensions of the room under consideration (2.34 × 2.34 × 4.58m). The response of the empty room measured with a small loop antenna and excited by a similar small loop on the back wall (Fig. 6.1.2) is shown in Fig. 6.1.3. Comparison with the calculated resonant frequencies shows that there is good agreement between the equation and practical results. Small differences are due to imperfections in the screened room (e.g. the internal walls are not smooth but have metal supports at intervals which will perturb the fields).

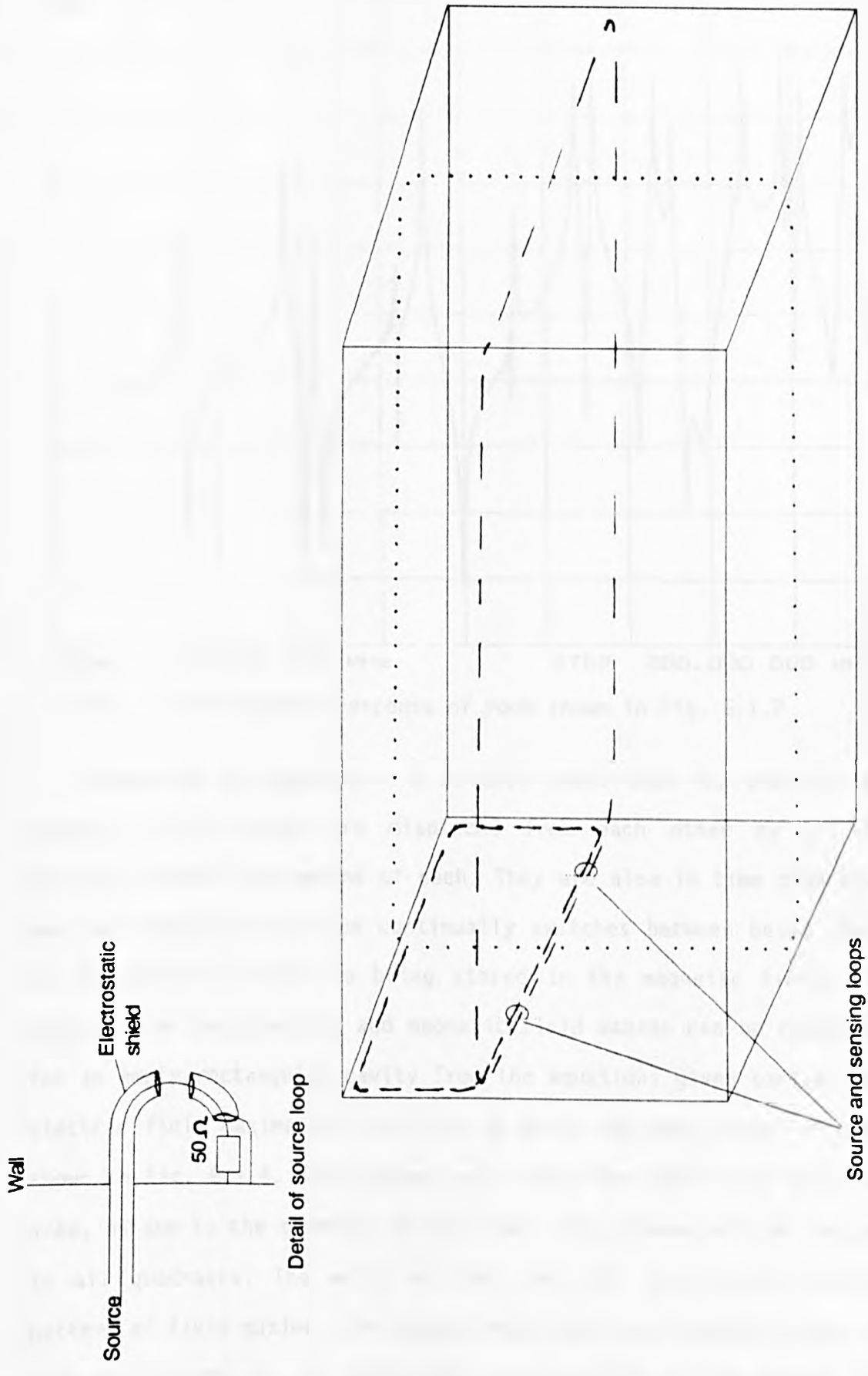

Fig. 6.1.2 Screened room showing magnetic loops etc

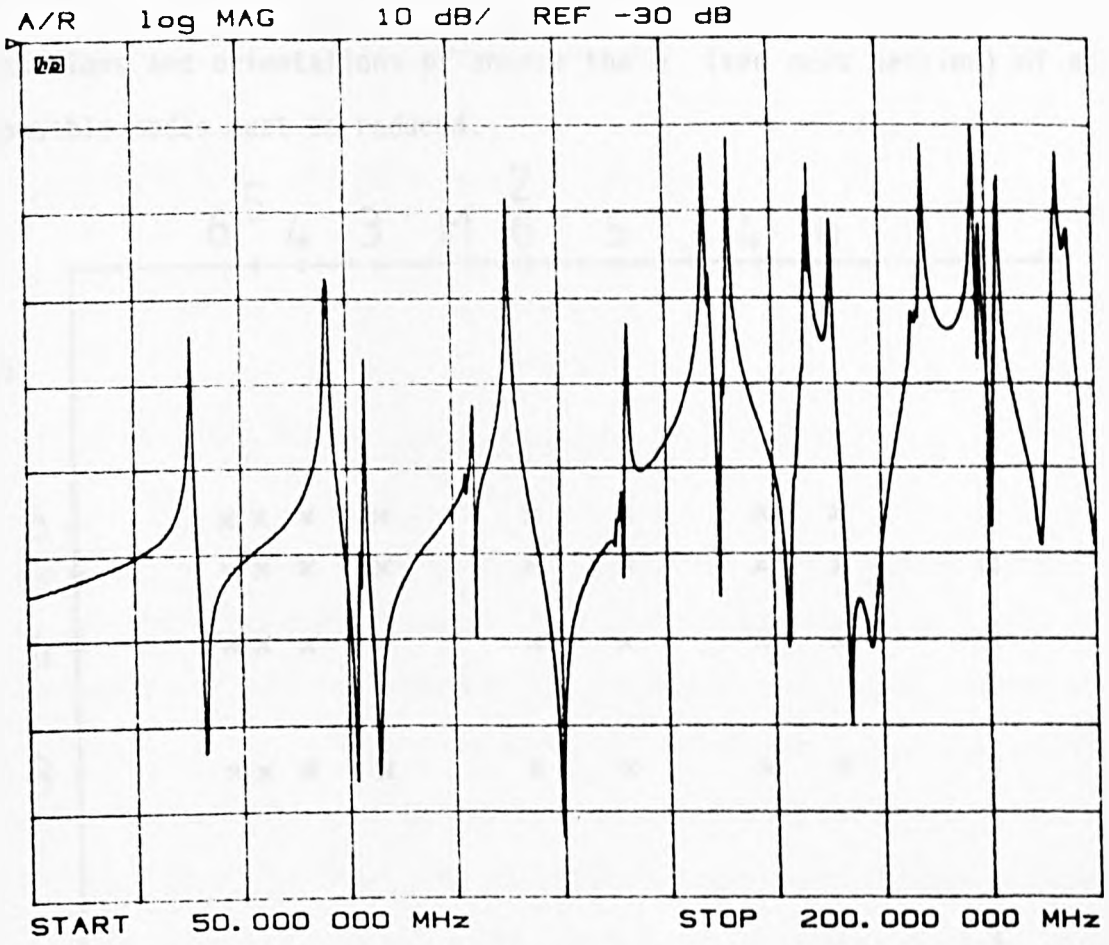

Fig. 6.1.3 Frequency response of room shown in Fig. 6.1.2

Inspection of equations 6.8 to 6.19 shows that the electric and magnetic field maxima are displaced from each other by 1/2 the distance between the maxima of each. They are also in time quadrature and the energy in the room continually switches between being stored in the electric fields to being stored in the magnetic fields. The positions of the electric and magnetic field maxima can be calculated for an empty rectangular cavity from the equations given earlier. The electric field maxima of the first 36 modes for each value of n are shown in Fig. 6.1.4. The diagram only shows one quarter of the floor area, as due to the symmetry of the room, the pattern will be the same in all quadrants. The walls of the room will also have a similar pattern of field maxima. The actual modes which are present at any one time will depend on the orientation and position of the source. This means that to get a smooth frequency response for all possible

positions and orientations of source the Q (see next section) of all possible modes must be reduced.

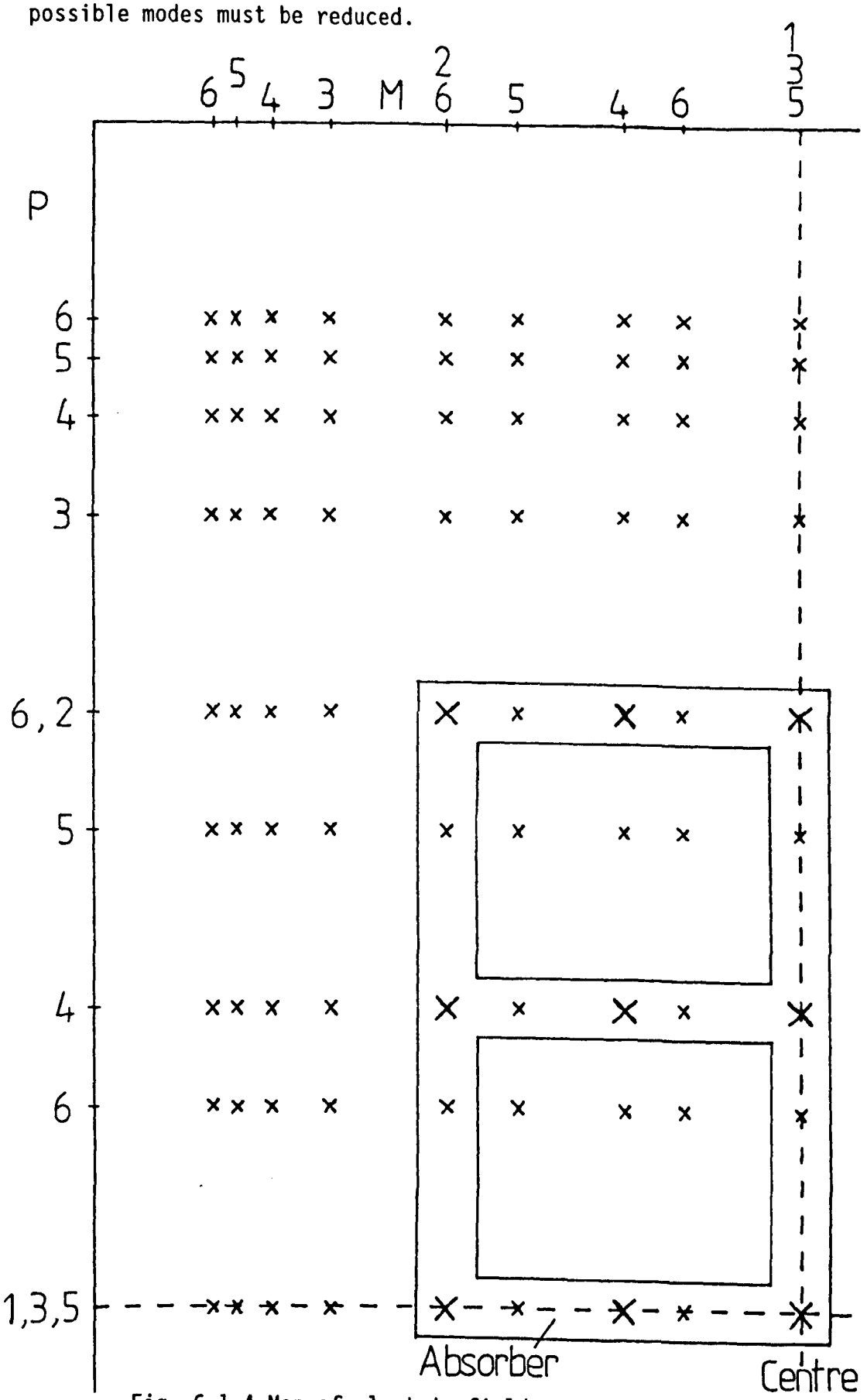

Fig. 6.1.4 Map of electric field maxima for first 36 modes

6.2 Reducing the Q of the Resonances

6.2.1 Definition of Q in a resonant cavity

The Q of the cavity is defined as

$$Q = 2\pi \times \frac{\text{the average power contained in the cavity}}{\text{the power dissipated in one cycle}} \qquad 6.21$$

Therefore to reduce the Q of a resonance (i.e. to dissipate energy) it is necessary to absorb power from the fields at some point. The maximum power will be absorbed by placing a dissipating medium at a field maximum for a mode (i.e electric field absorber at the position of maximum E field or a magnetic absorber at the position of maximum H field). These absorbers need not act as plane wave absorbers because standing wave patterns are being considered, not waves in free space. The technique relies on the standing wave pattern being set up. The easiest absorbing materials to obtain are carbon loaded foams which are used as wave absorbers at higher frequencies (above about 600MHz)and ferrite loaded materials which are also plane wave absorbers at higher frequencies (most effective above 1 GHz).

6.2.2 Dissipation of energy using a dielectric

For a non-perfect dielectric with $\mu_r = 1$ Maxwell's equation is

$$\nabla \times \underline{H} = \sigma \underline{E} + j\omega \underline{E} \qquad 6.22$$

Where σ is the conductivity of the material.

The dielectric dissipates most of the available power when the conductivity is given by equation 6.23 (see Appendix D).

$$\sigma = \omega\epsilon \qquad 6.23$$

At a frequency f maximum power will be dissipated when $\sigma = \omega\epsilon$ ($\omega=2\pi f$) and the field within the dielectric is at a maximum which occurs when it is positioned at an electric field maxima. It is assumed that the addition of the dielectric does not perturb the field patterns so that the maxima are still in the same positions. The energy dissipated will change with ω and with ϵ (see Appendix D) but these parameters are not variable. Energy dissipation will increase with ω until the point where the field does not propagate into the centre of the absorber and hence the dissipation may start to decrease again. This will occur at frequencies higher than are under discussion here due to the relatively low conductivity of the carbon loaded foam.

The dielectric available for this work was the carbon loaded foam used in the lower frequency work but six blocks each consisting of a single conductivity were also available. Therefore six values of σ could be used to test the theory for the single value of ϵ (assuming that ϵ is the same for all the blocks). The values of the bulk conductivity were not known and could not be supplied by the manufacturers.

7 PRACTICAL LOADING OF THE EMPTY ROOM

7.1 Loading Single Modes

The theory described in the last chapter indicates that a small piece of lossy dielectric material placed at the position of one of the E field maxima of a mode will reduce the Q of that resonance by absorbing some of the energy from the fields. For a given permittivity the dielectric will absorb most power from the cavity when $\sigma = \omega\epsilon$ which means that it may be necessary to use different conductivities for the different positions to damp the Q of the resonances enough to obtain a flat or steadily changing frequency response.

Some carbon loaded foam with different conductivities was obtained to test this. A column of the absorber was placed at the position of a maximum of one of the modes, and the fields were monitored to examine the reduction in the Q of the resonance. This was done for six different conductivities as well as for a column of the multilayer absorber used in the lower frequency work. The room was excited using a small magnetic loop on the back wall with its orientation such that the lowest frequency (TE_{101}) was excited. This mode only has a vertical E field without any horizontal E fields (Fig. 7.1.1). The fields were monitored by looking at the surface currents induced in the walls using a similar loop placed about 1m away on the same wall (Fig. 7.1.1). The first mode with its maximum at position 1 in Fig. 7.1.2 is the only mode with that frequency and the effect of the absorber on that mode can be easily seen. Higher order modes have frequencies which are the same for several modes and the effect on one mode cannot be as easily seen. This is due to the dimensions of the room being in the ratio 1:1:2 so that many modes are degenerate.

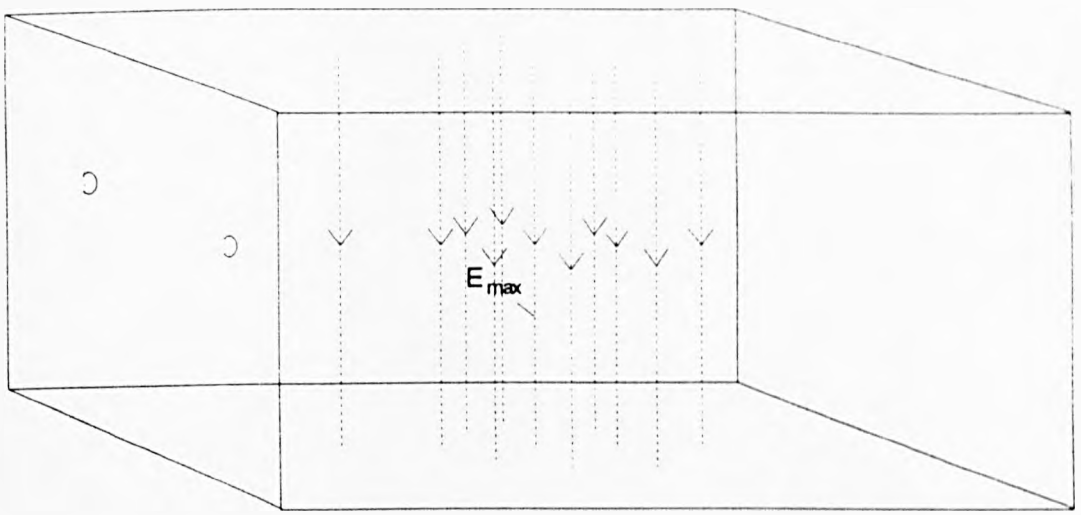

Fig. 7.1.1 The positioning of the source and sensing loops and the E fields generated by the first mode

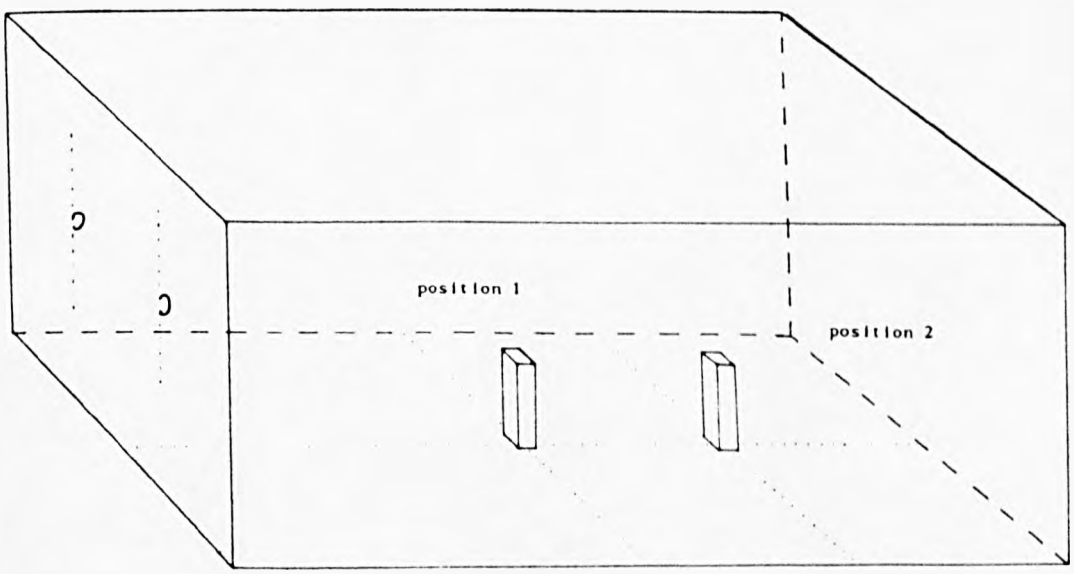

Fig. 7.1.2 The positioning of the absorber columns for the initial measurements

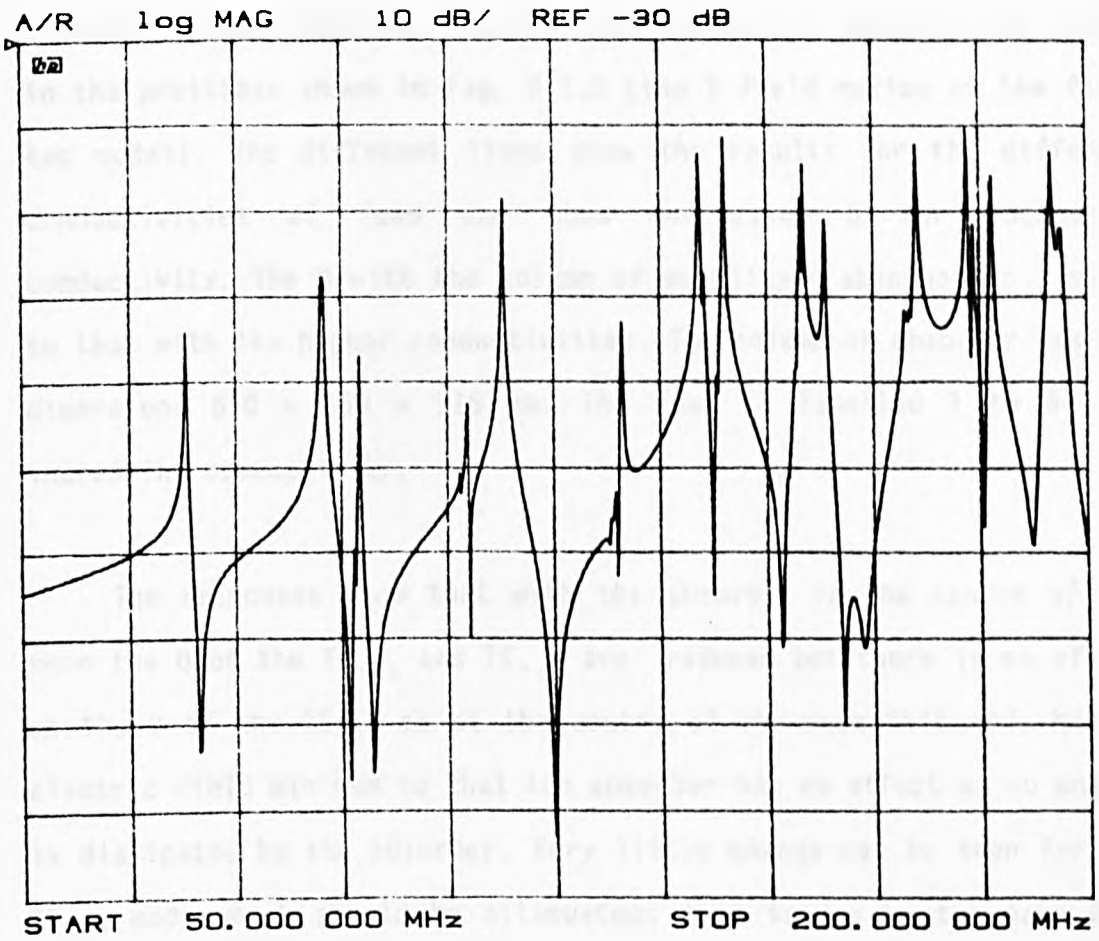

Fig. 7.1.3 Response of empty room with vertical loops

Fig. 7.1.3 shows the voltage measured from the sensing loop as a function of frequency for the totally empty room. The exciting loop is driven with a constant amplitude voltage and is terminated with 50Ω to earth to reduce standing waves on the excited transmission line. However, at these frequencies the impedance of the inductance will be significant and will cause standing waves on the transmission lines which feed it. A power splitter is included in the drive circuit to minimise the effect of the reflections on the measured reference voltage. It is assumed that the exciting loop itself is not resonant at a frequency within the desired range so does not add any extra structure to the measured frequency response.

The first six modes only are shown in Figs. 7.1.4 and 7.1.5 which show the voltage from the loop when the columns of absorber are placed in the positions shown in Fig. 7.1.2 (the E field maxima of the first two modes). The different lines show the results for the different conductivities of foam and show decreasing Q for increasing conductivity. The Q with the column of multilayer absorber is similar to that with the higher conductivities. The column of absorber has the dimensions 610 × 150 × 115 mm. The foam is labelled 1 to 6 with increasing conductivity.

The responses show that with the absorber in the centre of the room the Q of the TE_{101} and TE_{103} are reduced but there is no effect on the Q of the TE_{102} as at the centre of the room this mode has an electric field minimum so that the absorber has no effect as no energy is dissipated by the absorber. Very little change can be seen for the TE_{111} mode which should be attenuated; this is due to the wave with the same mode numbers which is being reflected back and forwards in the other direction (vertically) so that its electric field does not coincide with the absorber and still therefore has a high Q.

With the absorber in the position of the maxima of the TE_{102} and TE_{112} modes (position 2 in Fig. 7.1.2) the Q of these modes are reduced by the increasing conductivities of absorber as with the first modes but the lower modes are also reduced. This is because the first mode (TE_{101}) has an electric field which is not zero at that point so that some of the energy from that mode is absorbed. The reduction in the Q of these resonances is not as great as with the first modes due to the existence of the other sets of fields. Beyond these modes the mode structure becomes to complex to observe the effect.

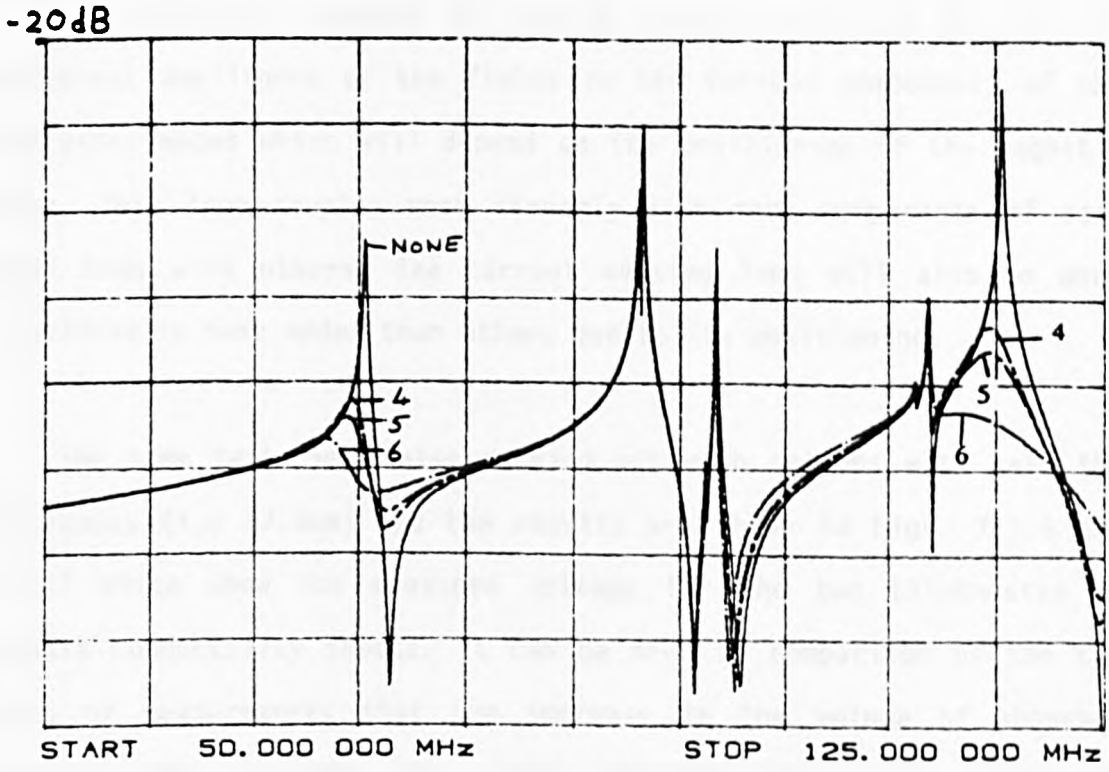

Fig. 7.1.4 First 6 modes with absorber in position 1

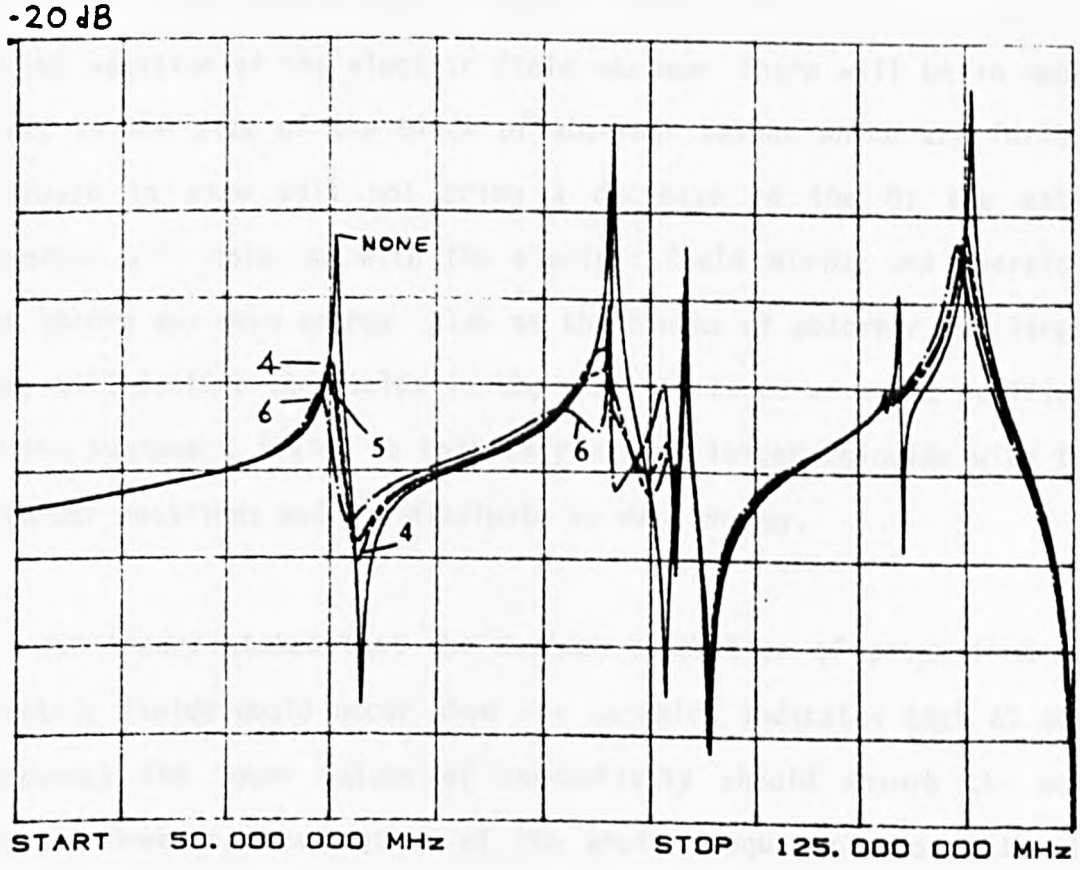

Fig. 7.1.5 First 6 modes with absorber in position 2

The different degrees of masking which occur are due to the different amplitudes of the fields in the various components of the different modes which will depend on the positioning of the magnetic loop. This loop couples more strongly with some components of each mode than with others. The current sensing loop will also be more sensitive to some modes than others due to its positioning.

The same tests were also carried out with columns with half the thickness (i.e 57.5mm) and the results are shown in Figs. 7.1.6 and 7.1.7 which show the measured voltage for the two thicknesses of single conductivity sheets. It can be seen by comparison of the two sets of measurements that the increase in the volume of absorber present does increase the energy absorbed from the system and therefore does reduce the Q. In order to maximise the damping effect it will be necessary to have as large a volume of absorber as possible at the position of the electric field maximum. There will be an upper limit to the size of the block of absorber beyond which any further increase in size will not bring a decrease in the Q; the extra absorber will coincide with the electric field minima and therefore not absorb any more energy. Also as the blocks of absorber get larger they will perturb the fields in the room and hence move the positions of the maximum E fields so that they may no longer coincide with the absorber positions and not dissipate so much energy.

The theory stated that the maximum absorption of power from the electric fields would occur when $\sigma = \epsilon\omega$ which indicates that at some frequency the lower values of conductivity should absorb the most energy. However, examination of the whole frequency range with the columns in position 1 showed that the most conductive foam (no. 6) appeared to give the most damping at all frequencies where a reduction

could be observed. This indicates that for all the range of frequencies under consideration the most conductive foam was the most efficient which would indicate that a more conductive foam might be better, particularly at the higher frequencies.

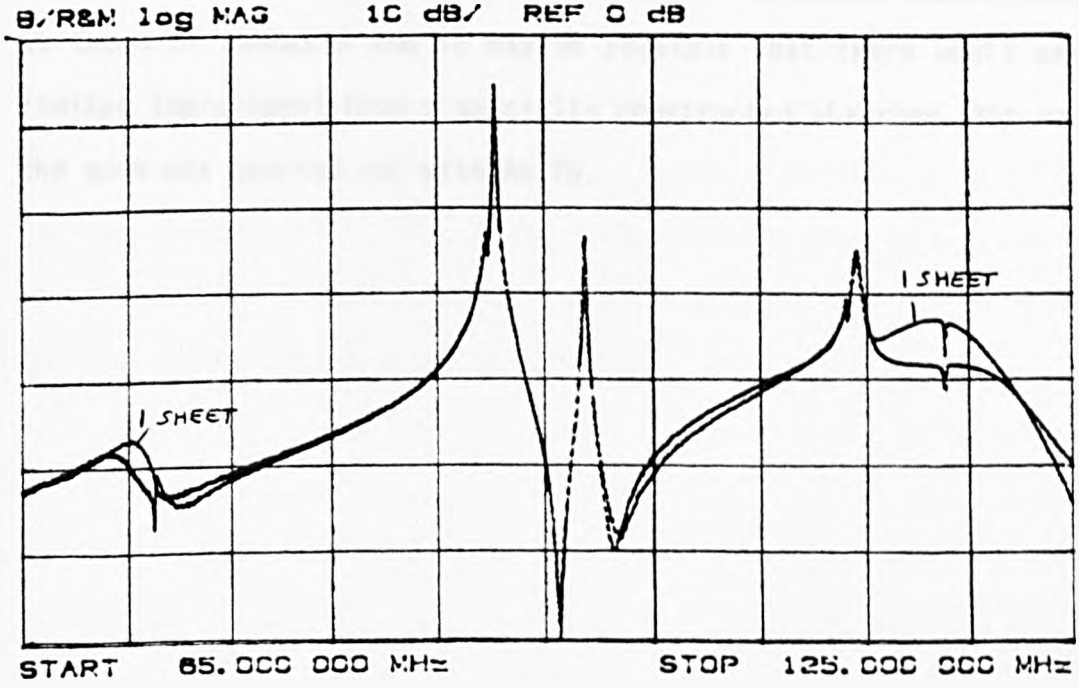

Fig. 7.1.6 Response with two thicknesses of single conductivity foam in pos.1 (no.6)

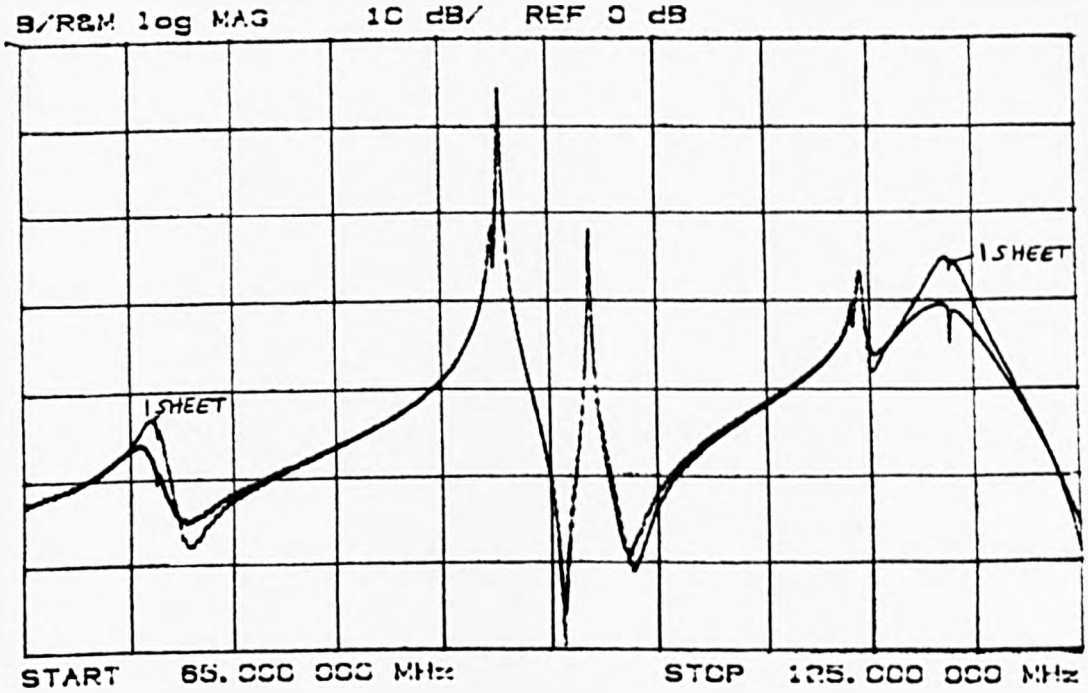

Fig. 7.1.7 Response with two thicknesses of single conductivity foam in pos.1 (no.5)

The most efficient would probably be a multilayer absorber with the lowest conductivity being that of the highest value used for these tests and with one or two layers with a higher conductivity (i.e. higher carbon loading). However, the multilayer absorber (AN 79) gave results in the measurements discussed above which were nearly as good as those of number 6 and it may be possible that there would only be limited improvement from a specially constructed absorber. The rest of the work was carried out with AN 79.

7.2 Full Loading

7.2.1 The full loading on the floor

Examination of the map of the electric field maxima (Fig. 6.1.3) shows that it is possible to cover at least one maximum for each mode by building a box shaped block of absorber as shown in that Figure. For a small room the simple shape is enough to cover frequencies in the range of interest. For larger rooms where higher order modes will fall into this frequency band it is simple to add extra dividing sections to the box shape (Fig. 7.2.1).

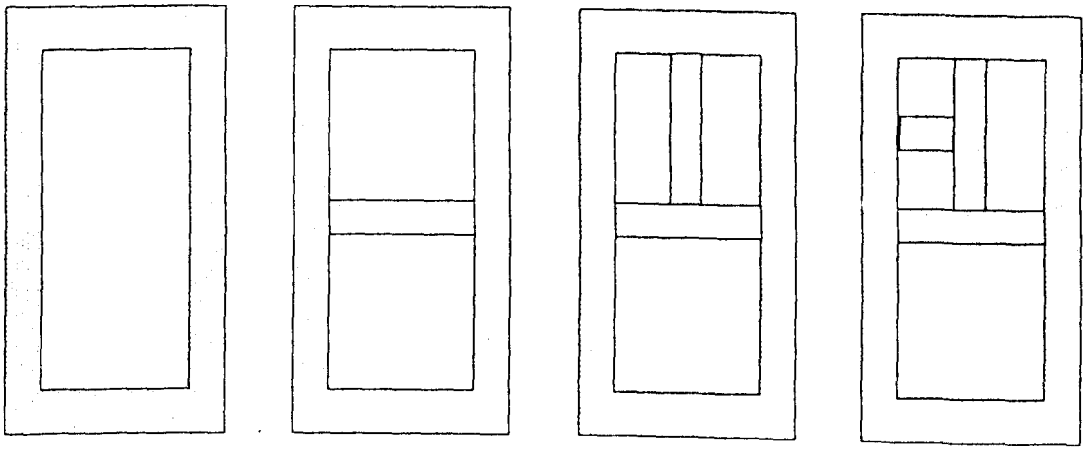

Fig. 7.2.1 Adding subsequent dividing sections to the box shape

The box shape covers one sixteenth of the floor area of the room due to its symmetrical properties, with one corner in the centre of the room and the sides of the box parallel to the walls of the room. This means that it should be possible to construct the shape several times and to get similar results from each set of measurements.

Fig. 7.2.2 shows the frequency response with the room excited and the fields sensed as in the previous section with the full box shaped load placed on the floor in the room as shown in Fig. 7.2.3 . The load is constructed out of the multilayer absorber as there was not enough of the single conductivity types to construct the full load. It shows a great deal of damping when compared to the empty room but is still not particularly flat as there are modes with purely horizontal electric fields which are not absorbed by the load when it is placed on the floor (e.g. TE_{110}). Also as the absorber is no longer small it is perturbing the fields and may not be as effective as it could be as the E field maxima may not coincide with the absorber.

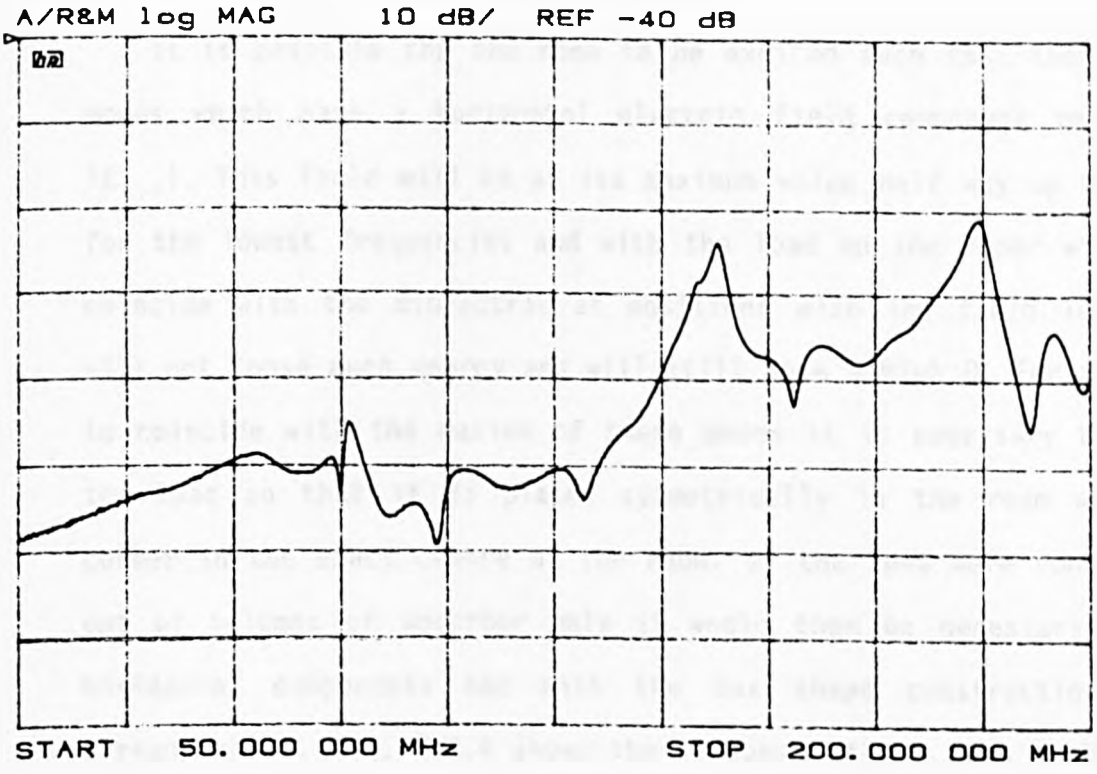

Fig. 7.2.2 Frequency response with box load on floor
(vertical loop excitation)

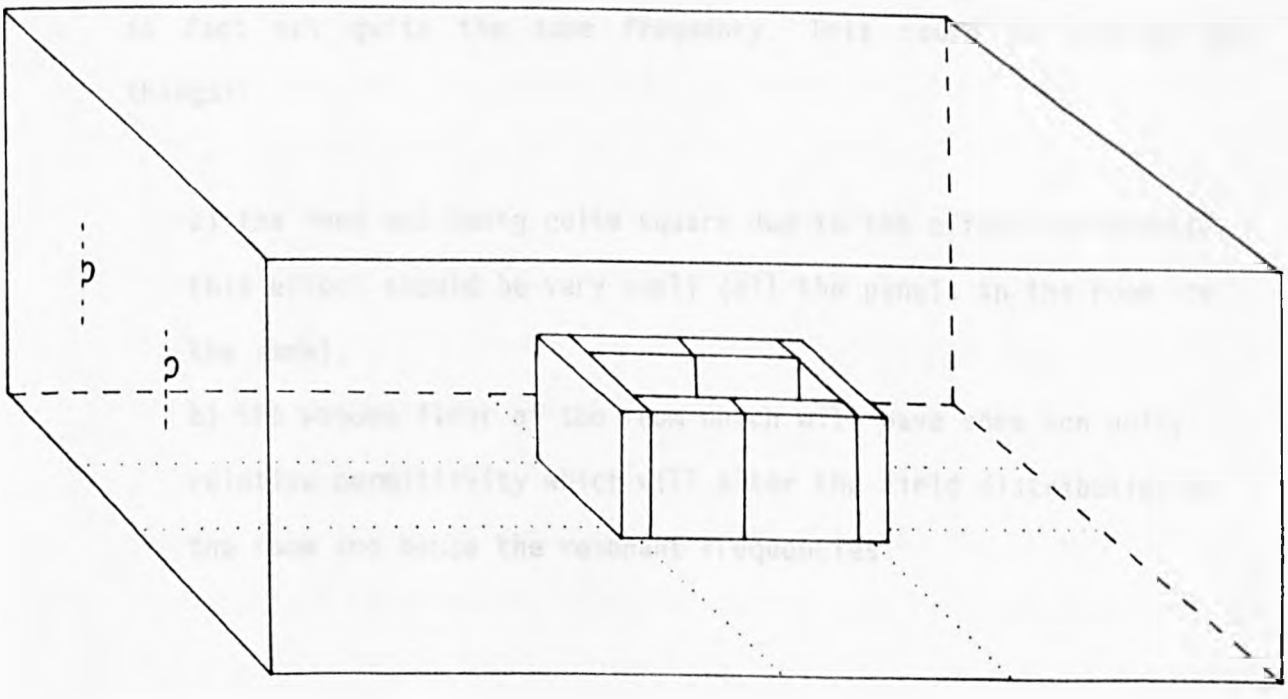

Fig. 7.2.3 Position of box load and source

7.2.2 The full loading raised above the floor

It is possible for the room to be excited such that there exist modes which have a horizontal electric field component only (e.g TE_{110}). This field will be at its maximum value half way up the room for the lowest frequencies and with the load on the floor will only coincide with the dielectric at positions with low field levels so will not loose much energy and will still have a high Q. For the load to coincide with the maxima of these modes it is necessary to raise the load so that it is placed symmetrically in the room with one corner in the exact centre of the room. If the load were constructed out of columns of absorber only it would then be necessary to add horizontal components but with the box shape construction these already exist. Fig. 7.2.4 shows the response of the room excited and sensed with diagonal loops so that all modes can be present. There is no load present. It can be seen that the many of the resonances have very close double peaks. These are the modes which should be degenerate due to the square cross section of the room but which are in fact not quite the same frequency. This could be due to two things:-

a) the room not being quite square due to the effects of gravity this effect should be very small (all the panels in the room are the same).

b) the wooden floor of the room which will have some non unity relative permittivity which will alter the field distribution in the room and hence the resonant frequencies.

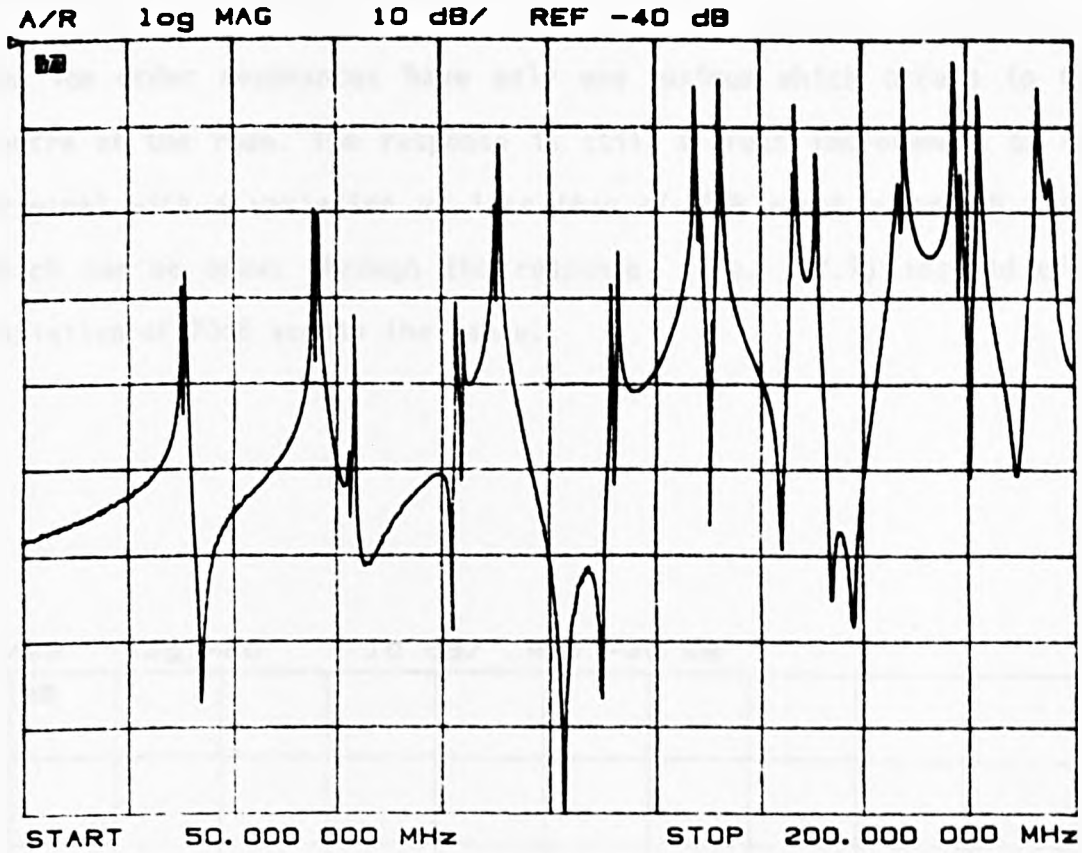

Fig. 7.2.4 Frequency response with diagonal loops (no load)

Fig. 7.2.5 shows the response if the room is excited as before but with the loop at an angle so that it excites all modes including those with purely horizontal and vertical E fields (e.g TE_{110}, TE_{101} and TE_{011}). The load is placed on the floor. The response is flatter than expected at the lower frequencies, probably due to the fact that the horizontal electric fields for the TE_{110} and TE_{011} are not zero where the absorber is so that some of the energy is absorbed from these modes and hence the Q is reduced. There is more variation than the response for the room excited with the vertical loops only. Fig. 7.2.6 shows the response for the same excitation if the load is raised from the floor so that the top of the load is half way up the room's height. Comparison of these last two figures show that the raised load does improve the response slightly. This is due to the perturbation of the fields by the absorber as well as the fact that most of the modes have an electric field maximum which coincides with the lower load; a

few low order resonances have only one maximum which occurs in the centre of the room. The response is still a great improvement on the original with a variation of less than +/-10dB about a smooth curve which can be drawn through the response (Fig. 7.2.7) instead of a variation of 70dB across the range.

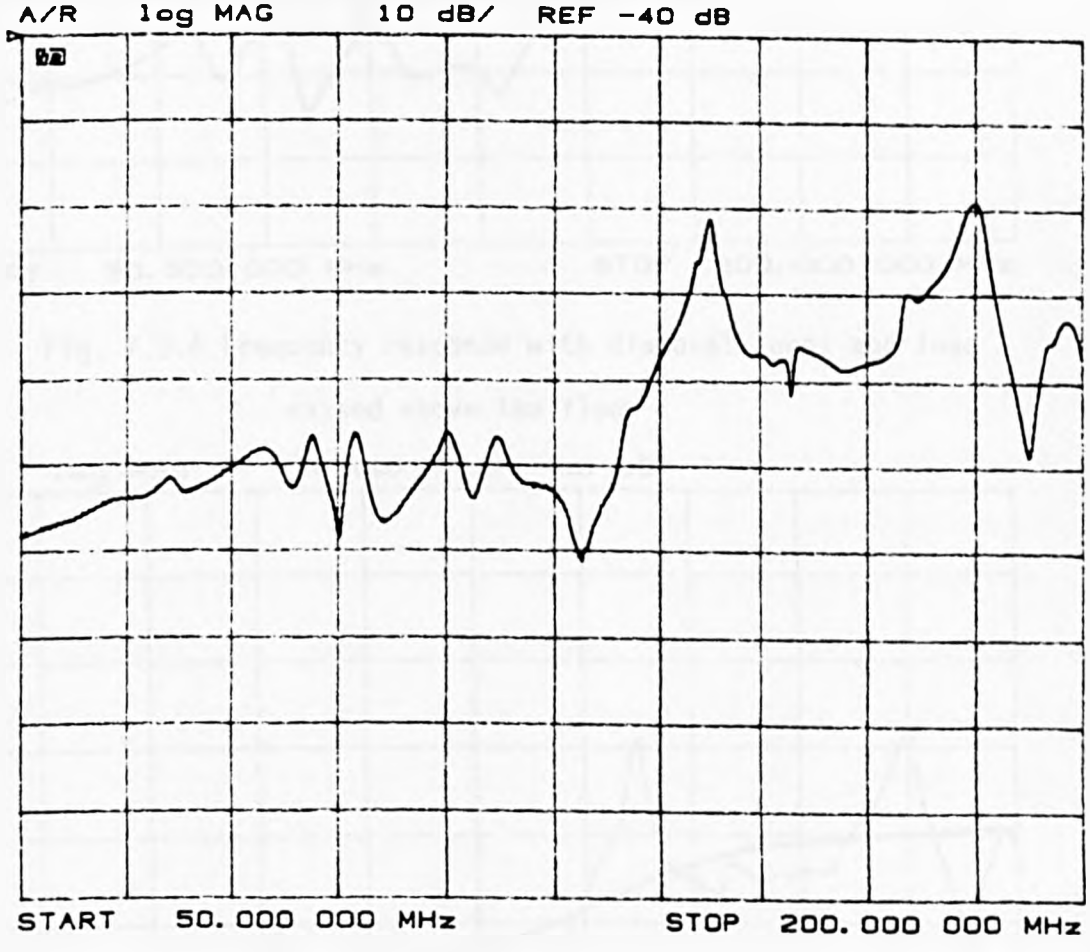

Fig. 7.2.5 Frequency response with diagonal loops, load on floor

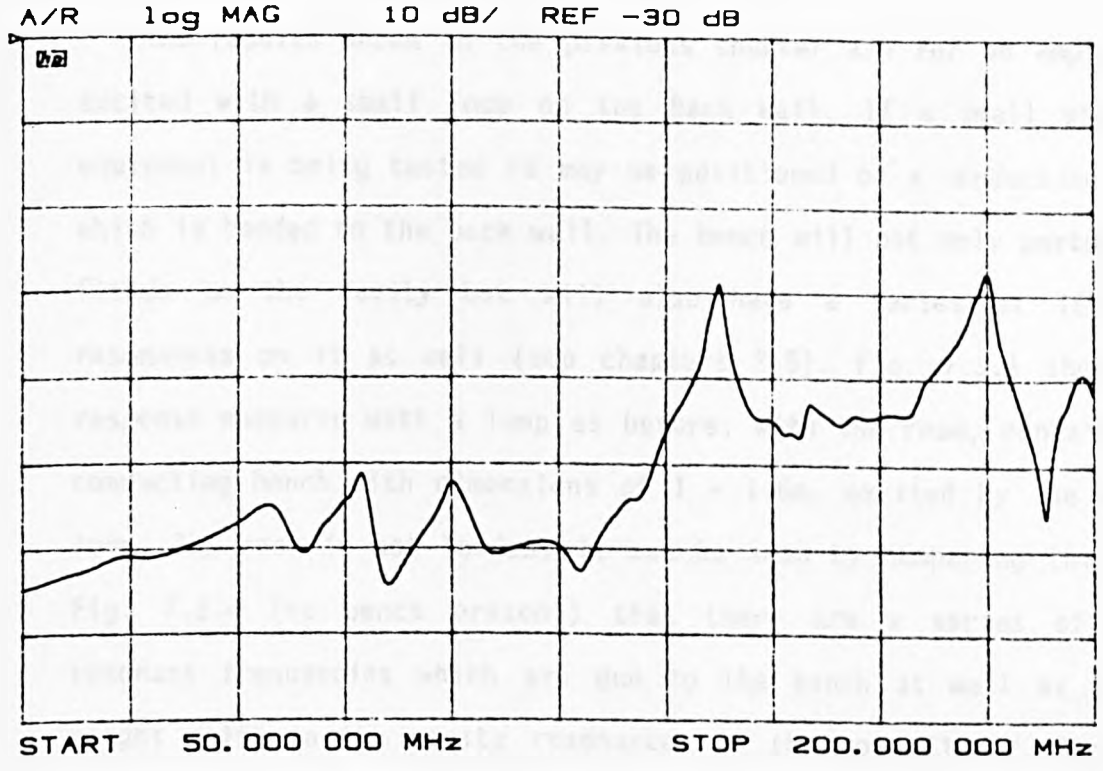

Fig. 7.2.6 Frequency response with diagonal loops and load raised above the floor

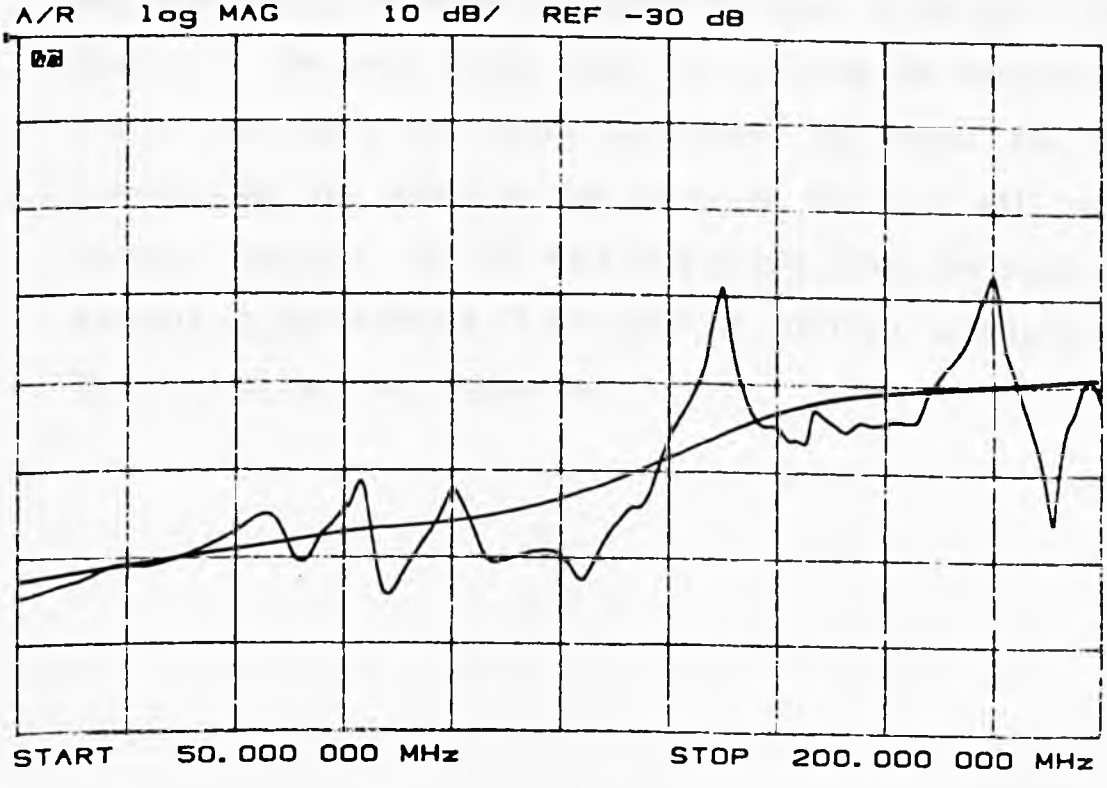

Fig. 7.2.7 A smooth line drawn through the response of Fig. 7.2.6

7.3 The Effect of Adding the Bench

The results shown in the previous chapter are for an empty room excited with a small loop on the back wall. If a small piece of equipment is being tested it may be positioned on a conducting bench which is bonded to the back wall. The bench will not only perturb the fields in the cavity but will also have a series of TEM mode resonances on it as well (see chapters 2-5). Fig. 7.3.1 shows the response measured with a loop as before; with the room, containing a conducting bench with dimensions of 1 × 1.6m, excited by the second loop. The room is not loaded. It can be seen by comparing this with Fig. 7.2.4 (no bench present) that there are a series of extra resonant frequencies which are due to the bench as well as a very slight shift in the cavity resonances of the room itself. The most obvious addition is the resonance at about 50MHz which is due to the 1/4 wave resonance of the TEM mode propagating across the bench (this may occur due to the method of bonding the bench to the wall, refer to Chapter 4). The bench is not quite 1/4 λ wide as the fringing of the fields (and hence the extra capacitance at either end of the transmission line formed by the bench and the room) will tune the resonant frequency. The TEM wave propagating along the bench should resonate at approximately 75 MHz which is difficult to observe due to the first of the room resonances.

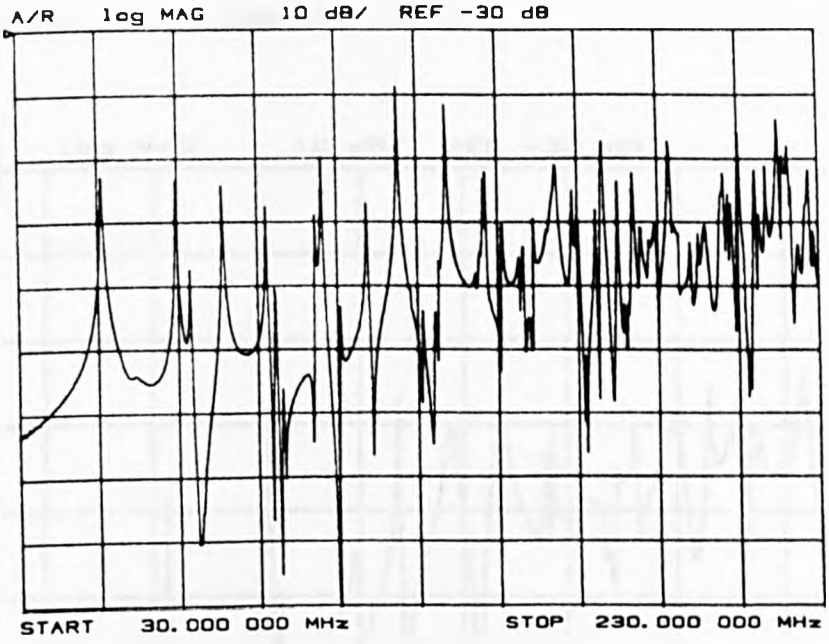

Fig. 7.3.1 Frequency response with the bench present

As was shown with the lower frequency measurements it is possible to reduce the TEM mode resonances by loading the bench. If the sides of the bench are bonded to the walls with the 60Ω/square conductive plastic which was found to be useful at the lower frequencies (Chapter 3) the TEM waves propagating both across and along the bench will cease to be resonant. The waves propagating across the bench will have the line terminated at both ends with a load which is close enough to the line impedance to reduce the resonances and the waves propagating along the bench will have the line made very lossy so that again it is no longer resonant. Fig.7.3.2 shows the results when the bench is bonded to the wall in this manner. The method of bonding the bench to the wall is that used earlier (chapter 3). Comparison with Fig. 7.3.1 shows that loading the bench in this way does reduce the TEM mode resonances and brings the response back to be very close to that of the empty room (particularly at the lower frequencies - Fig. 7.2.4) although there is some slight shift in the frequency of the resonances and some smoothing of the higher frequency resonances. This smoothing will be due to perturbation of the fields by the bench and some energy

dissipation in the conductive plastic.

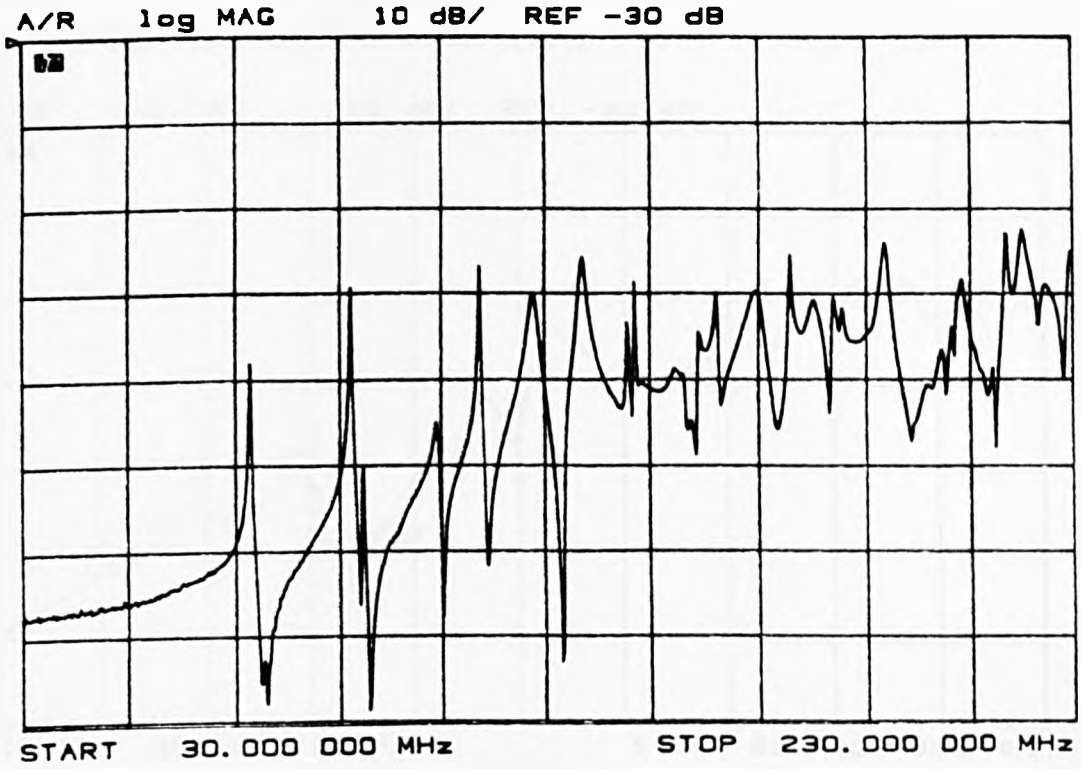

Fig. 7.3.2 Frequency response with bench bonded to wall with 60Ω per square conductive plastic

The addition of the bench will perturb the field distribution in the room particularly at the end of the room where the bench is. Due to the complexity of the problem the field distribution with the bench in place was not calculated, but by putting the box load into the room in the half of the room near the bench and in the half of the room remote from the bench it was possible to investigate the effect of the bench. Figs7.3.3 and 7.3.4 show the response with the room still sensed with the magnetic loop but excited with the small electric dipole source placed at the front of the bench where the EUT would be placed. They show that the fields at the end containing the bench have been disturbed by the bench and the load does not absorb as much energy from the resonances as the response is not quite as smooth as with the absorber remote from the end of the bench. With the load

remote from the bench the load absorbs enough energy from the fields to give quite a flat response over most of the frequency range. (These are with the load raised off the floor).

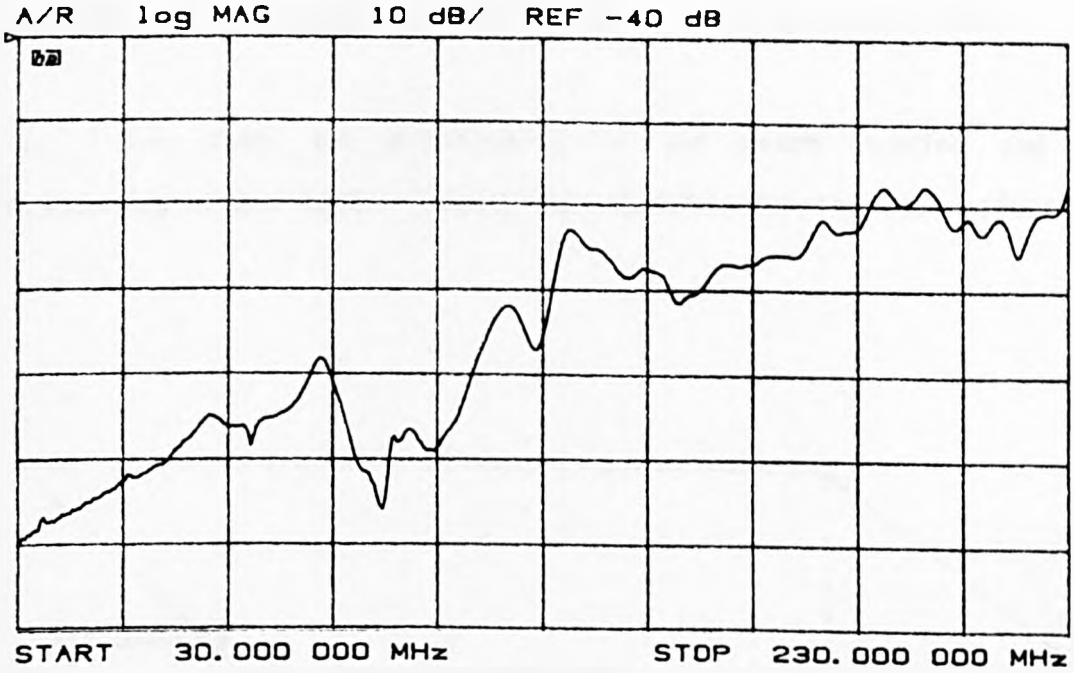

Fig. 7.3.3 Frequency response including the room load remote from the bench (electric dipole source, loop probe)

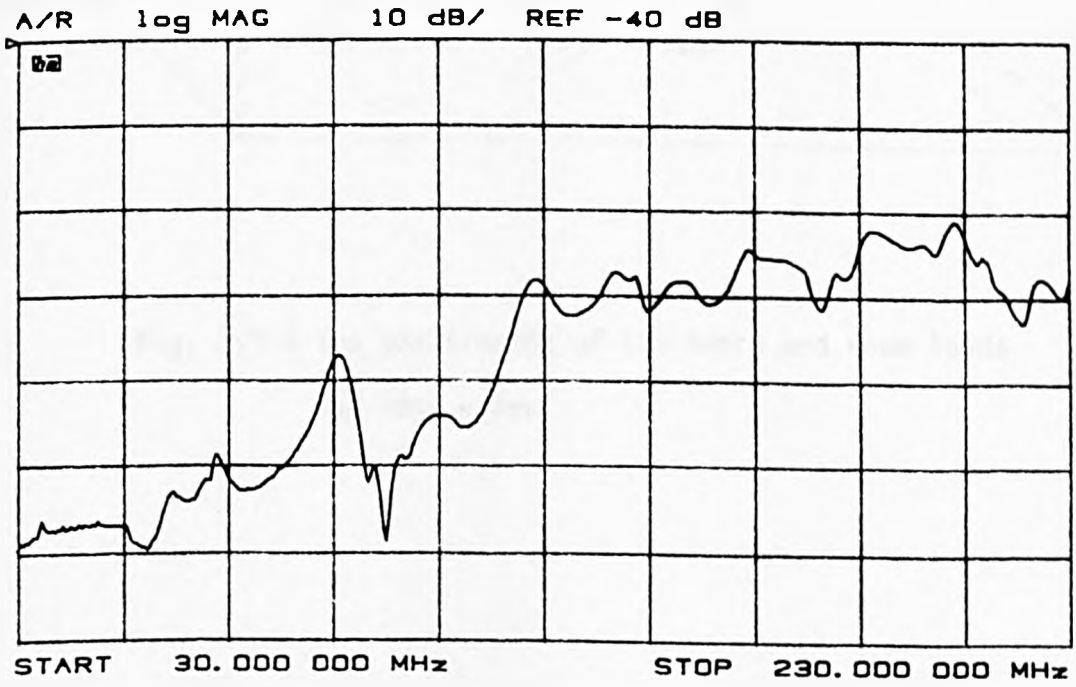

Fig. 7.3.4 Frequency response including the room load near the bench (electric dipole source, loop probe)

The response of the room is still not as flat as is desired but is very good when compared to the original response. It does follow a fairly smooth curve which has no deep nulls and can be more easily accounted for during system calibration if this is carried out.

Fig. 7.3.5 shows the positioning of the bench loading and the positioning of the carbon loaded foam absorber for the best effect.

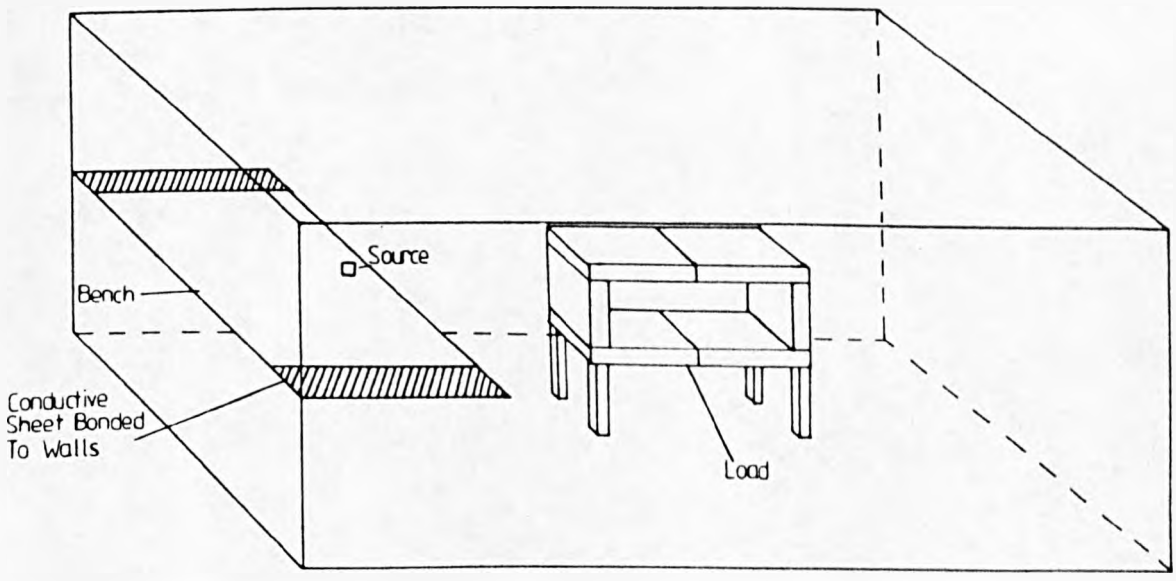

Fig. 7.3.5 The positioning of the bench and room loads for best effect

7.4 The Effect of Including the Biconical Antenna as the Field Transducer

Electromagnetic field measurements in this frequency range are often carried out using a biconical dipole. This type of antenna is not small (approximately 1.2m by .6m) and will also have a perturbing effect on the fields in the room particularly one as small as that used for these experiments. The support for this antenna is usually a tripod which can be made of wood, plastic or metal. The tripod will also scatter the fields if it is made of a conductor which should be avoided as its effect on the measured fields will be unknown. The antenna is placed a specified distance from the source (e.g 1 or 3 m) with the required orientation (vertical or horizontal). In the room which was being used for these measurements the antenna was placed 1m from the source which was 10cm from the front of the bench as before [Def Stan 59/41]. The small electric dipole source used in the previous chapters was used as the source. The antenna was included in the room as the measuring device with the cable taken out straight behind it and round the walls to the connector from the room (Fig. 7.4.1), this ensures that the cable layout is defined and has minimum perturbation of the fields within the room and the layout is also as repeatable as possible.

Figs. 7.4.2 and 7.2.3 show the measurements when the antenna was used with no loading of the room and bench at all and with the full loading in the room (i.e bench and raised box load remote from bench). The antenna does effect the fields in the room and has a slight smoothing effect in the unloaded room which can be seen by comparison with Fig. 7.2.4 which shows the response for the magnetic loops. With the fully loaded room the antenna also has a smoothing effect.

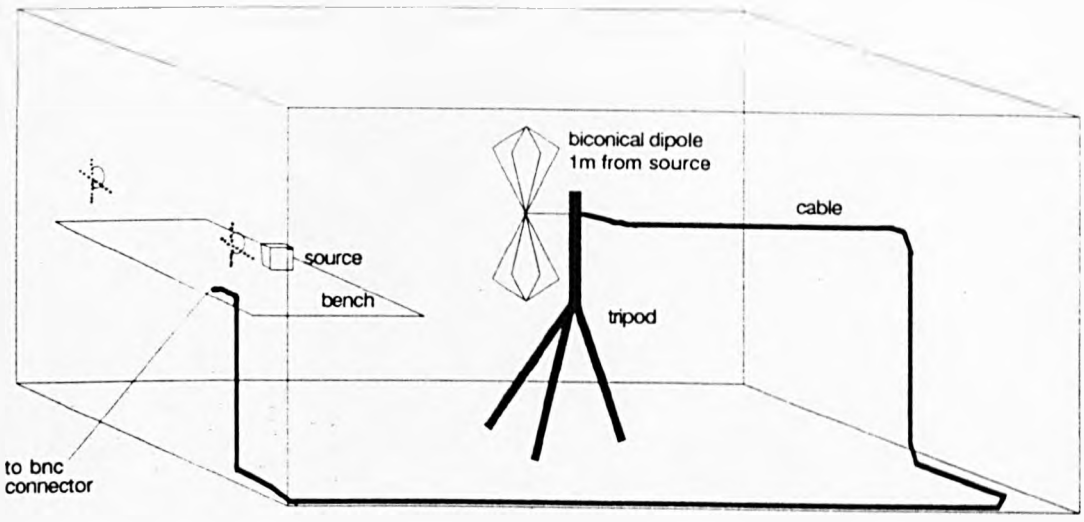

Fig. 7.4.1 Layout of biconical antenna and cable within the room

The antenna has two counteracting effects:-

1) The antenna will scatter the fields incident on it and hence change the amplitude and positions of the E field maxima so that less energy will be dissipated in the absorber.

2)The antenna will absorb some of the energy from the fields and therefore reduce the Q of the resonances.

With the antenna present the room response has improved and now has a variation of less than +/-5db about a smooth curve which can be drawn through the frequency response.

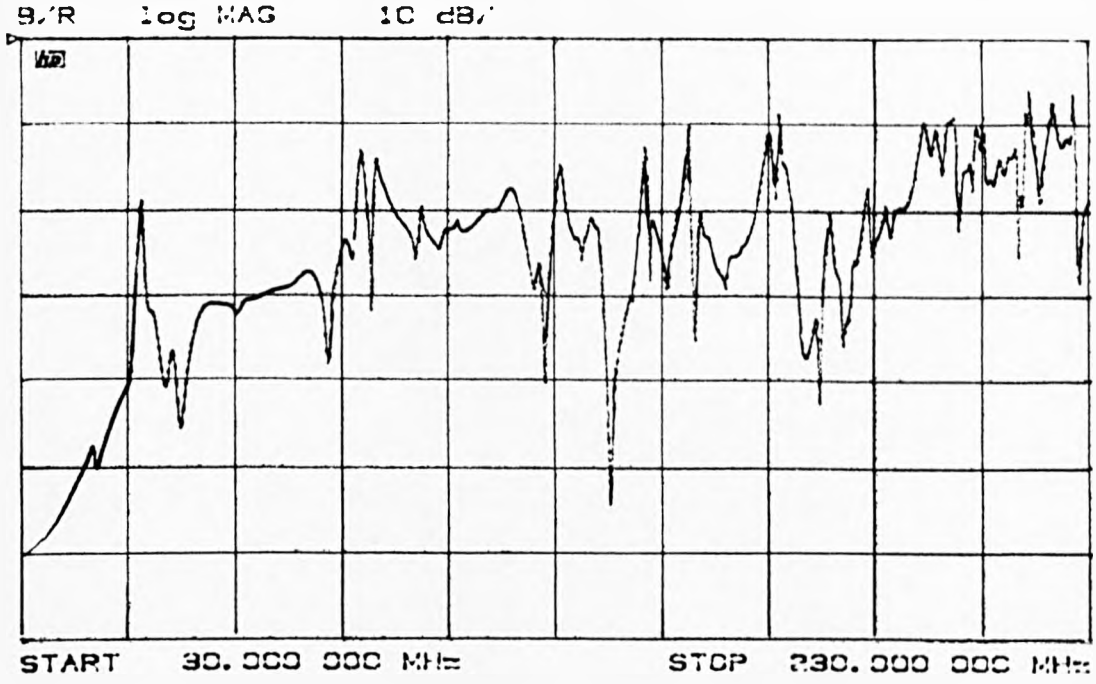

Fig. 7.4.2 Frequency response with biconical antenna, no loading

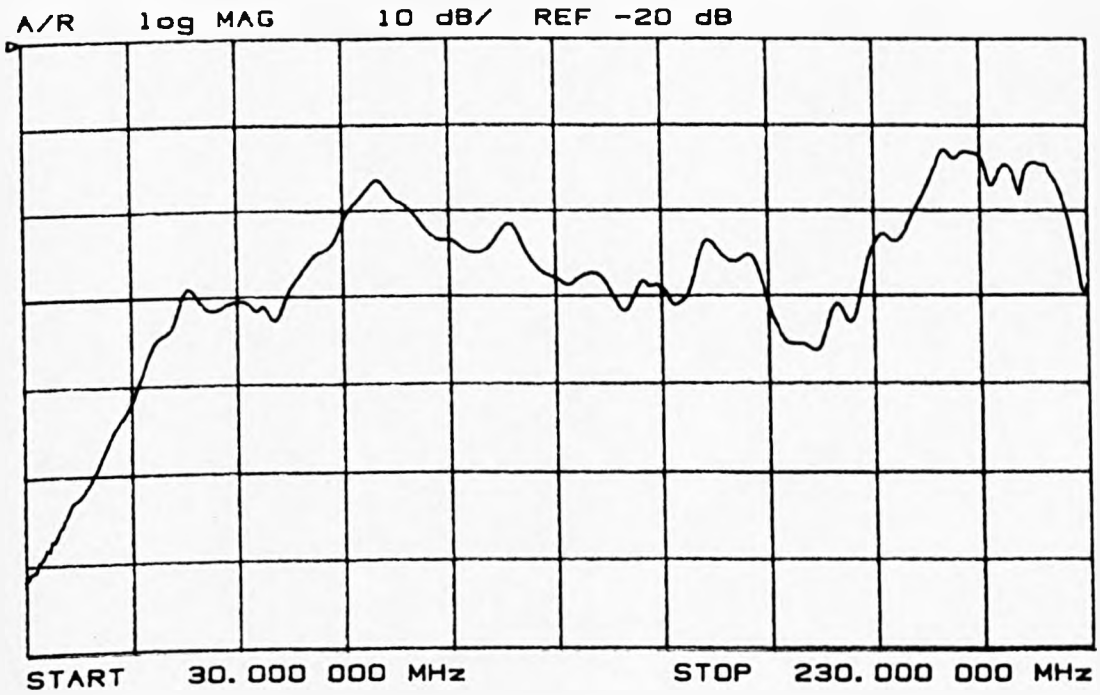

Fig. 7.4.3 Frequency response with biconical antenna, full loading

7.5 The Effect of Variations in the Positioning of the Antenna

In the empty screened room when high Q resonances are present a small change in the position of the sensing antenna may cause a large change in the field sensed by the antenna making it is very difficult to make repeatable measurements. This is a problem if the results are to be compared for different test items or for changes to a single item. Fig. 7.5.1 (a) to (h) shows the variation of the results if the antenna is moved over a 3 × 3 grid of positions just 10cm apart (in the unloaded room). The measurements are shown relative to the response measured with the antenna in the position 1 (refer to Fig. 7.5.3). At the lower frequencies this movement has very little effect but as the frequency is increased the effect gets greater and large errors can occur.

The same measurements were carried out with the bench and raised box loading in the room. One position was missed because the antenna support (tripod) and load could not occupy the same space. The results are shown in Fig. 7.5.2 (a) to (g) and show that there is a great deal less variation than with the unloaded room. The results from position 1 in particular does show some variation from the basic (particularly at the lower frequencies) but this could be partly due to the antenna being too near to the absorber. The variation is still less than that for the unloaded room.

This loading technique would be easier to use in a slightly larger room where the load and the antenna would be further apart. A larger room would probably also reduce the dependence of the measurements on the antenna position still further.

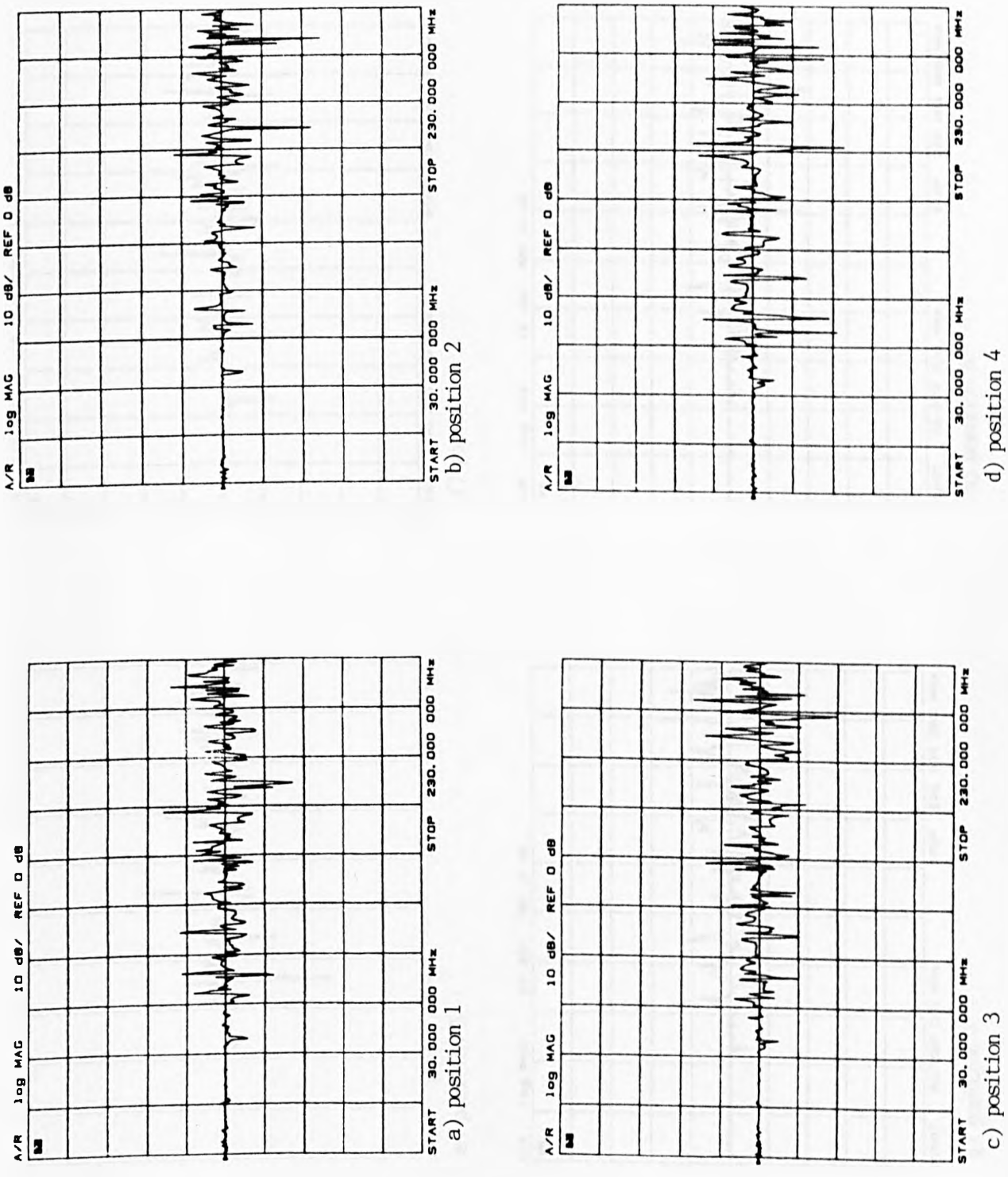

Fig. 7.5.1 Change in measured voltage if antenna is moved over 3 × 3 grid with no loading

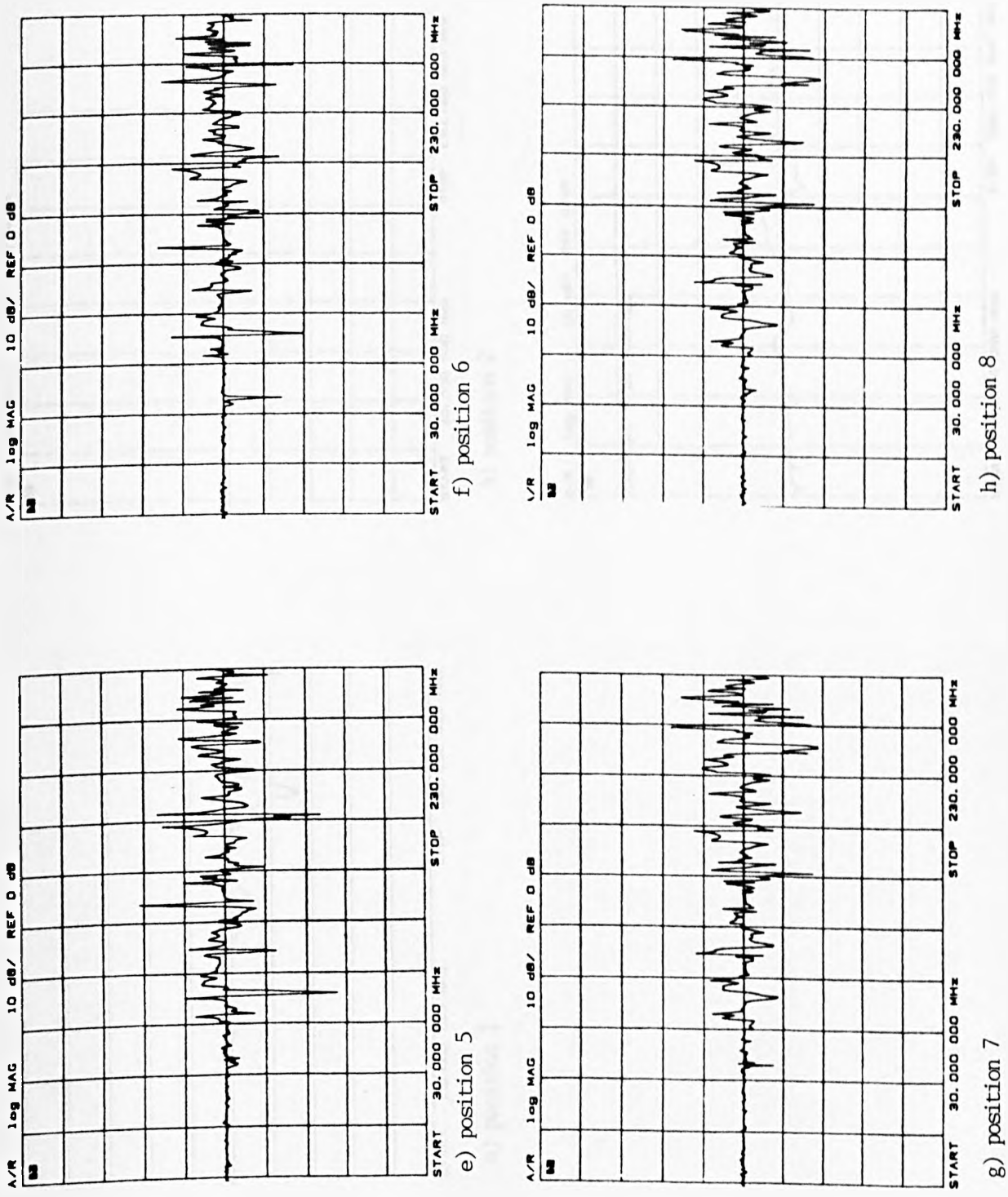

Fig. 7.5.1 Change in measured voltage if antenna is moved over 3 × 3 grid with no loading

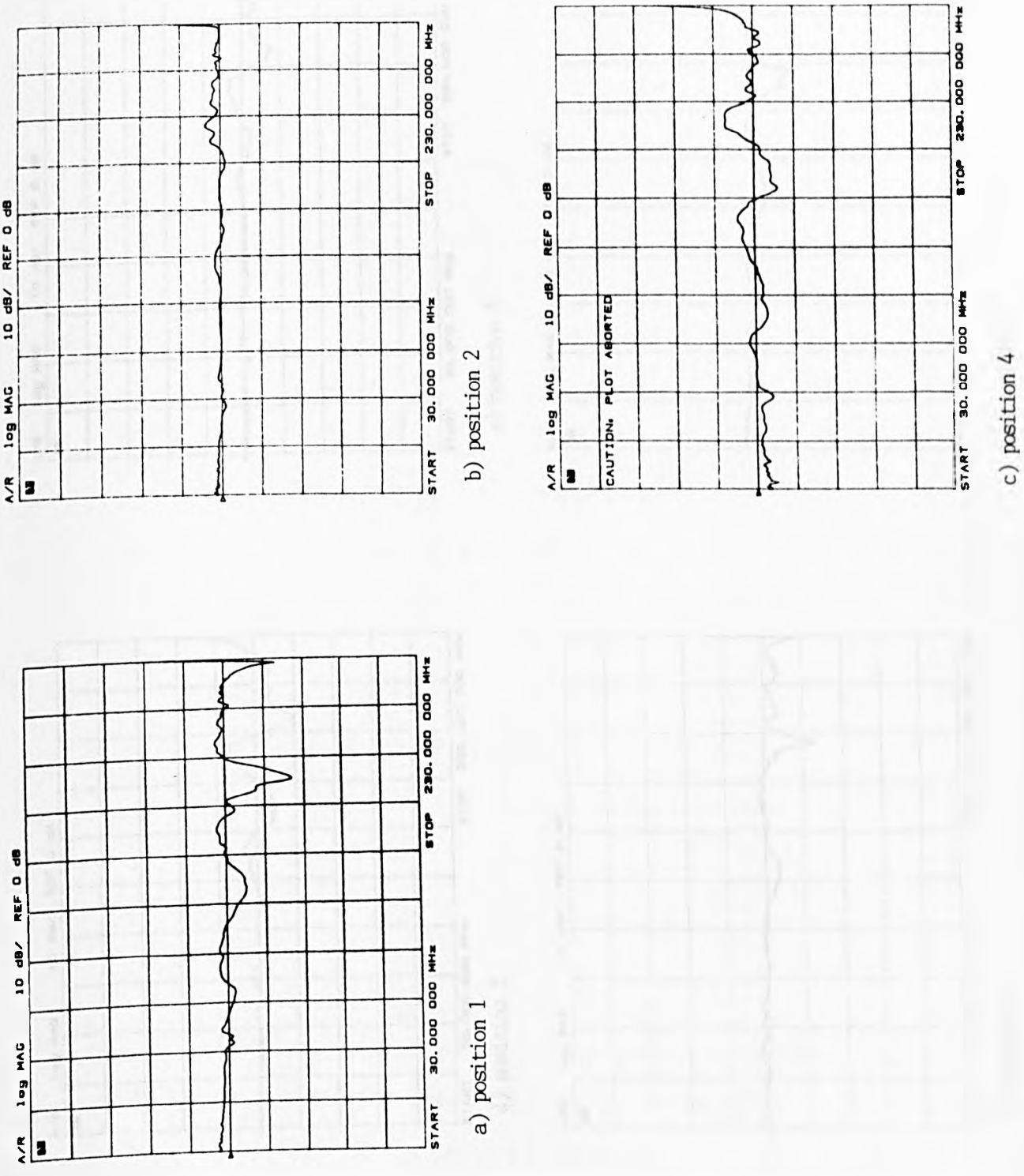

Fig. 7.5.2 Change in measured voltage if antenna is moved over 3 × 3 grid with room loaded

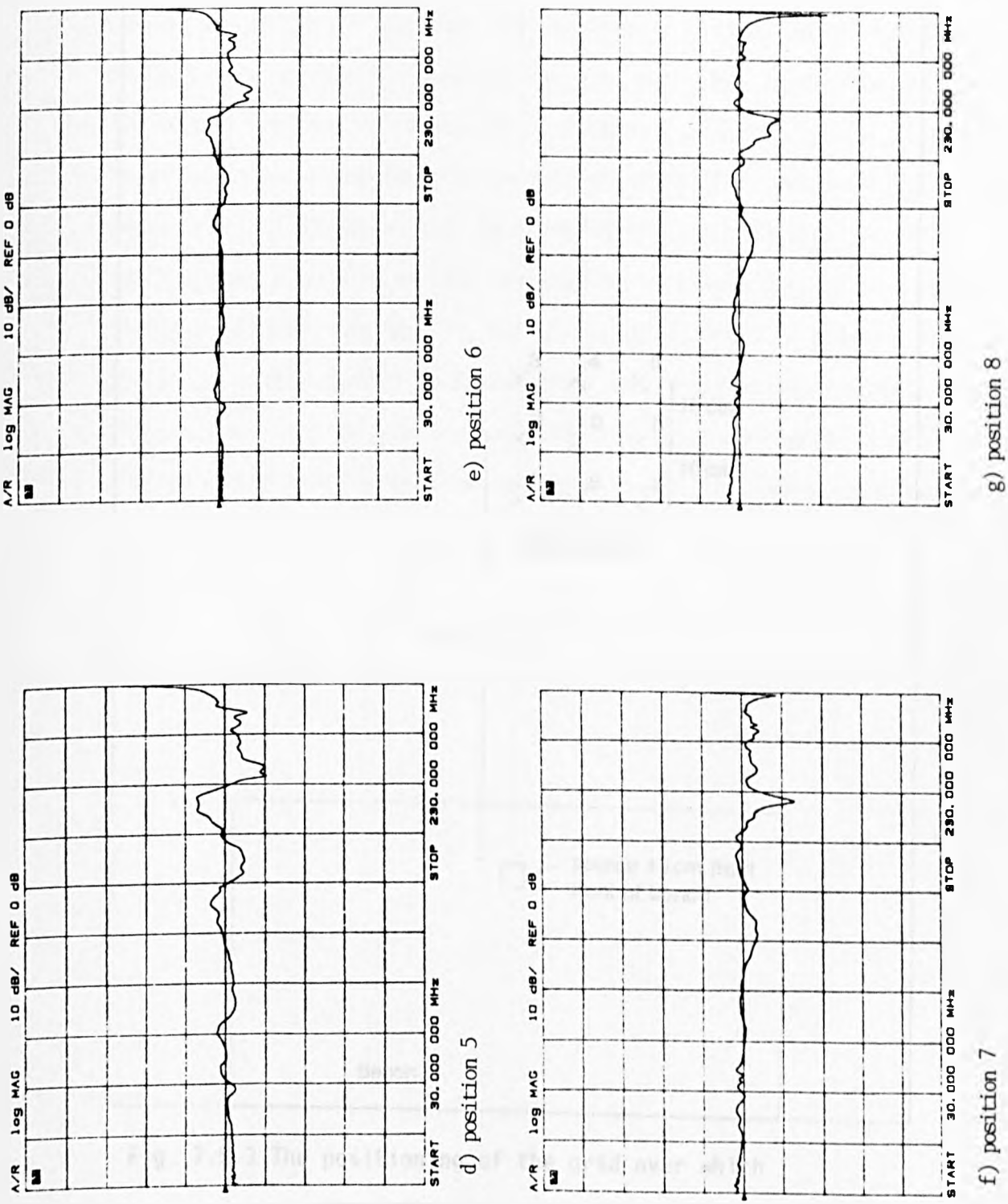

Fig. 7.5.2 Change in measured voltage if antenna is moved over 3 × 3 grid with room loaded

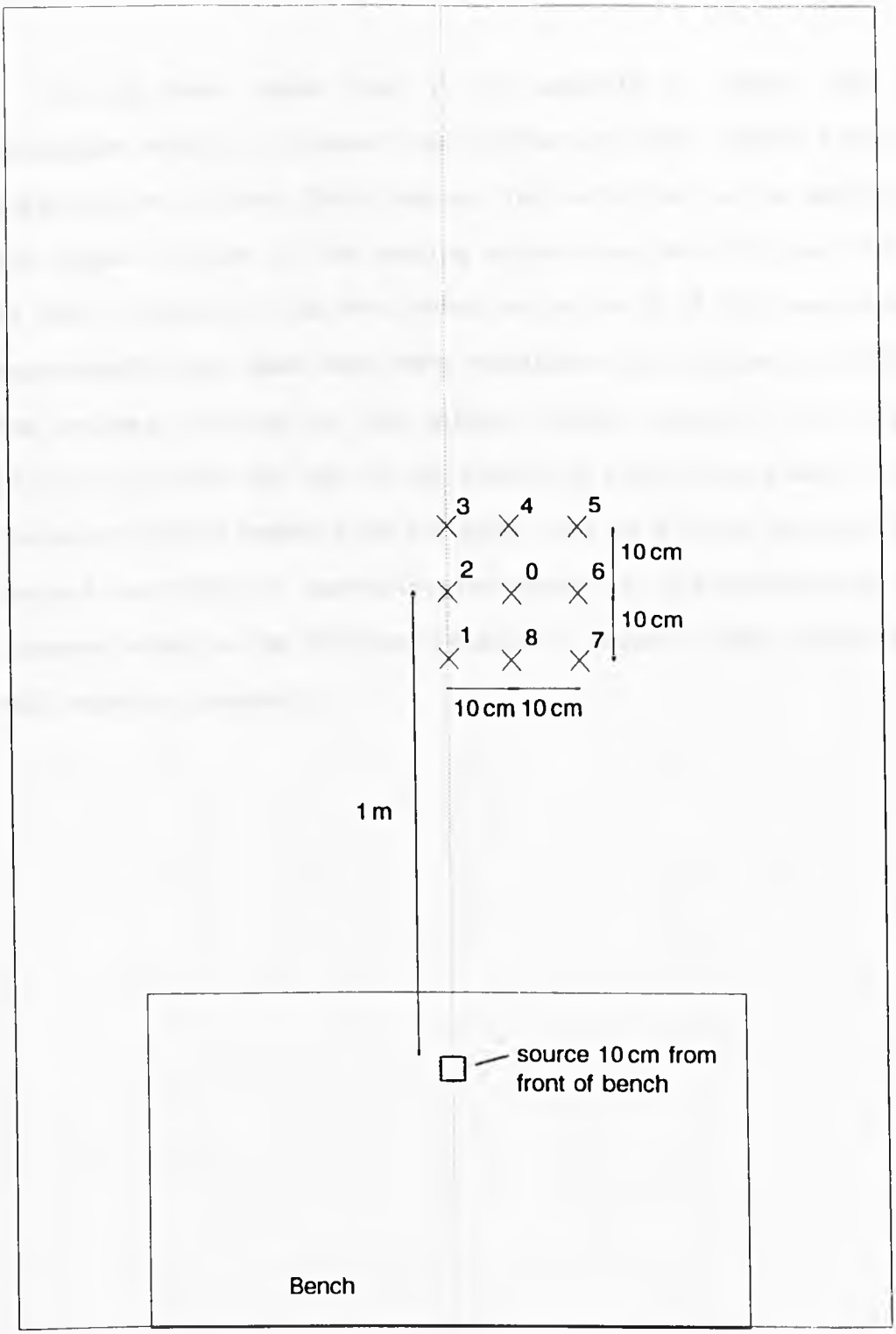

Fig. 7.5.3 The positioning of the grid over which the antenna was moved

7.6 Conclusions

It has been shown that it is possible to reduce the Q of resonances within a screened room by placing carbon loaded material at positions of electric field maxima. The variation in the amplitude of the output voltage of the sensing antenna has been reduced from 50dB to 10dB. In addition to this reduction in the Q of the resonances the measurements have been made more repeatable by reducing the effect of the antenna position on the antenna output voltage. This has been carried out with the use of two sheets of conductive plastic and six blocks of carbon loaded foam and shows that by placing absorber in the correct positions an impressive improvement in the performance of the screened room can be obtained relatively cheaply (when compared to a full anechoic chamber).

8. DAMPING THE SCREENED ROOM RESONANCES USING MAGNETIC ABSORBER

8.1 Introduction

8.1.1 Introduction

It has been shown that the Q of resonances in a cavity resonator can be reduced using carbon loaded foam to absorb energy from the electric fields of the resonances. From the definition of Q in a cavity it can be seen that it is not necessary to absorb energy from the electric field only, as long as energy is dissipated by the system. If energy can be absorbed from the magnetic fields it should also be possible to get similar results with some advantages. This chapter and Chapter 9 describe work carried out to investigate the use of magnetic absorbers. The work described is of a pratical nature with very little theoretical work carried out. This is due to the time constraints which existed while this work was carried out.

The carbon loaded absorber is bulky and must be placed in positions of electric field maxima which means that the absorber is in the middle of the room and can be a nuisance as it can be a problem when setting a test up. The bulk of the absorber also means that by placing it in position the fields are perturbed so that it is not as effective as it might otherwise be. Magnetic fields in cavity resonators have maxima parallel and adjacent to the cavity walls. This means that a material which absorbs energy from magnetic fields can be placed on the walls where it does not get in the way. The fields will also be perturbed less by the presence of the absorber as the reflective surface is close to the walls so the position at which the initial waves are reflected is not moved significantly.

There are three possible loss mechanisms with magnetic absorbers.

1. Conduction current at the surface of a material with a permeability which is not that of the adjacent material. The change in parallel magnetic field across the boundary is proportional to the current sheet flowing on the boundary [Plonus 1978]. This may be a conduction current, in which case there will be loss, or a displacement current with no energy dissipation.
2. Hysteresis losses within the magnetic material. These losses are a function of the material and the magnitude of the fields [Plonus 1978].
3. Loss due to the movement of the individual magnetic dipoles within the material (as for dielectric losses in an Electric field). This and the hysteresis loss are usually accounted for together as the complex permeability of the material [Tebble and Craik 1969].

There are two major types of magnetic materials which are used in magnetic absorbers for plane waves.

1. Ferromagnetic materials such as iron have a high relative permeability which gives rise to a current sheet on the surface of the material. If the material is bound in a rubber or resin binder the conductivity of the material is reduced to zero so the surface current is displacement current only and that energy is dissipated only by the hysteresis effect.
2. Ferrites have a lower permeability than ferrous materials but also have a lower permittivity which gives them a wave impedance with is closer to that of free space so that they are used in plane wave absorbers. Ferrites in general have a very low conductivity and any energy loss is due to hysteresis effects.

Most magnetic absorbers operate as plane wave absorbers. By reducing the wavelength of the wave within the material energy that is passed into the material is dissipated relatively rapidly so that little is reflected from the back. The input impedance of the absorbers varies with frequency, the response being a function of the material and its thickness. These absorbers can work very well over a narrow band or can be relatively broad band with an increased reflectivity.

It was proposed to examine the effectiveness of using ferrite loaded absorbers to reduce the resonances within a screened room.

8.1.2 Literature search

A literature search was carried out on the University's on-line system. This search was confined to the INSPEC database. There was very little recent work (last 10 years) on the use of ferrites in electromagnetic absorbers. A few papers looked possible but were found to contain very little in the way of theory of ferrites. The same was the case of older papers (i.e 1970s). Papers which were published before this have not been included in the database. The few papers which did look more useful were published in Japanese.

A search of text books on magnetics in general and ferrites in particular was also not very useful as most concentrated on the atomic properties of ferrites. Others were concerned with their use in microwave devices such as isolators where a DC magnetic field is applied to control the properties of the ferrite. Neither of these branches is of much use when considering the effect of ferrites on electromagnetic fields in the frequency range of interest.

Two papers which consider the use of carbon loading of ferrite absorbers were obtained [Shimizu and Nishikata 1985: Naito and Mizumoto 1986]. These were requested as a result of initial measurements carried out on materials provided by Emerson and Cuming Ltd.

The most useful works have been general electromagnetics books which usually consider waves in infinite or semi-infinite media. It has been possible to apply some of this to ferrites by considering the complex permeabilities and assuming real permittivities. No modelling was carried out due to time limitations.

8.1.3 Method of investigation

The screened room at the University of York has been described earlier in this thesis and was used to develop the electric field loading. However, the type of absorber under investigation in this section is more expensive than the carbon loaded absorber and the room is also under constant use for other projects. It was therefore decided to construct a one-fifth scale model of the room for the investigative work. This gives a frequency range of about 360 MHz (1st resonance) to 1GHz to cover the same modes as in the larger room. Ferrites do not have the same properties at all frequencies so that after the initial work to investigate the idea it was also necessary to examine the effect of the ferrites at the lower frequencies in the full sized room.

The model room was constructed from mild steel and had two walls which could be removed for access (one small, one large). These walls were attached by means of bolts with wing nuts placed every 25cm which had been found previously to give a good rigid bond. Beryllium copper finger stock soldered to the walls were used to provide good electrical contact between these two walls and the rest of the box (Fig. 8.1.1 a & b).

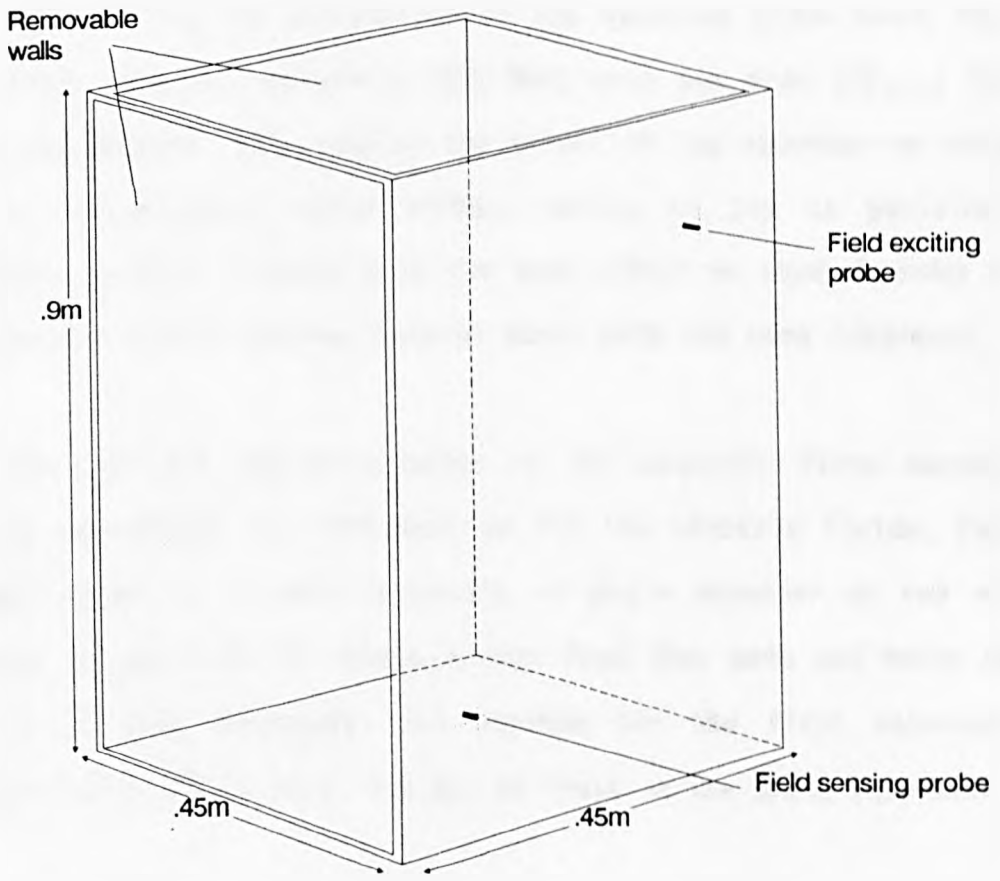

Fig. 8.1.1 Model screened room showing position of probes and removable walls

The room was excited and the fields sensed by means of two short electric probes on one of the longer walls (Fig. 8.1.1). The probes were each about 5mm long so that the fields were perturbed as little as possible and were placed so that they did not fall on an electric field minimum or maximum at any resonance frequency in the range of interest. Comparison of the modes measured in the screened room with the two loops and the model with two electric probes shows a good relationship for the lower modes but the higher ones are not as close. This is due to the supports and the wooden floor in the screened room which perturb the fields and to the different positioning of the probes.

The position and orientation of the exciting probe meant that at the first resonant frequency (360 MHz) only one mode (TE_{011}) in the room was excited. This enabled the effect of the absorber on one mode to be investigated easily without having to try to position the absorber so that it would have the same effect on several modes or to try to distinguish between several modes with the same frequency.

The position and orientation of the magnetic field maxima are easily calculated for each mode as for the electric fields. For the higher modes it is only necessary to place absorber on one of the maxima of each mode to remove energy from that mode and hence reduce the Q of that resonance. The maximum for the first resonance is particularly simple (Fig. 8.1.2), at least in the empty resonator.

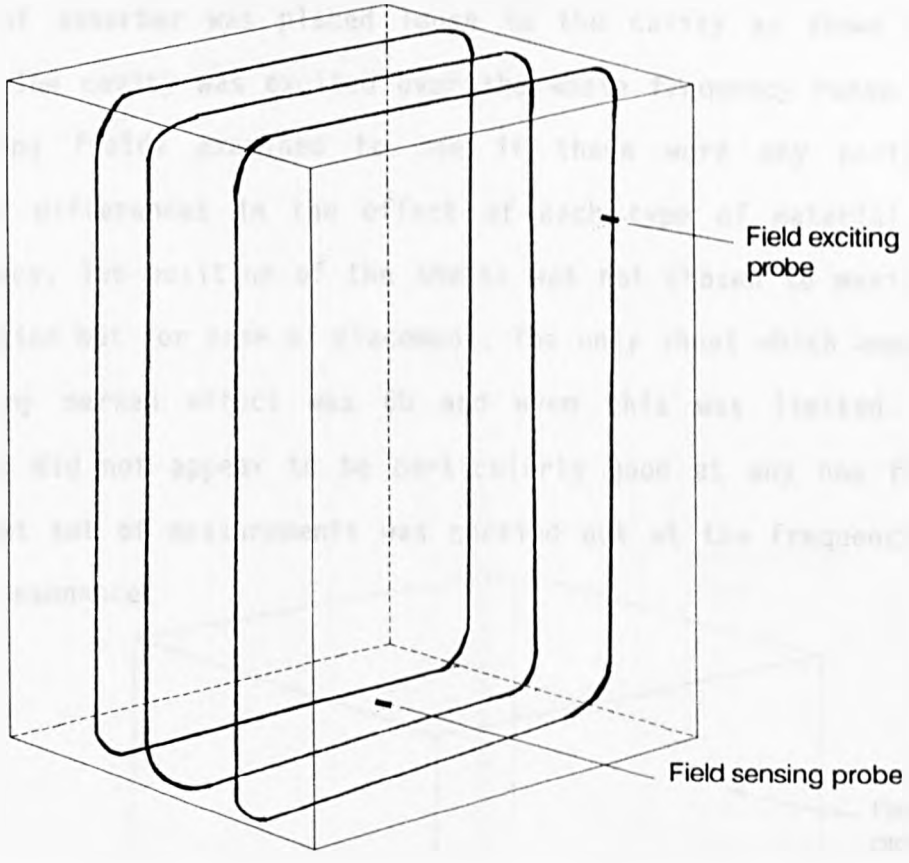

Fig. 8.1.2 The positioning of the magnetic fields for the first resonance

8.2 Initial Measurements in a 1/5 th Scale Room

Twelve squares of absorber were supplied by Emerson and Cuming for the first measurements. They were each approximately 30cm square and varied in thickness from approximately 2 mm to 6 mm. As well as different thicknesses the absorbers were loaded with different types and quantities of ferrite and also with iron. The sheets were labled 1a, 1b, 2a, 2b, 3a, 3b, 4a, 4b, 5a, 5b, 6a and 6b. Initially the whole sheet of absorber was placed loose in the cavity as shown in Fig. 8.2.1. The cavity was excited over the whole frequency range and the resulting fields examined to see if there were any particularly obvious differences in the effect of each type of material at any frequency. The position of the sheets was not chosen to maximise the absorption but for ease of placement. The only sheet which appeared to have any marked effect was 6b and even this was limited. As the results did not appear to be particularly good at any one frequency the next set of measurements was carried out at the frequency of the first resonance.

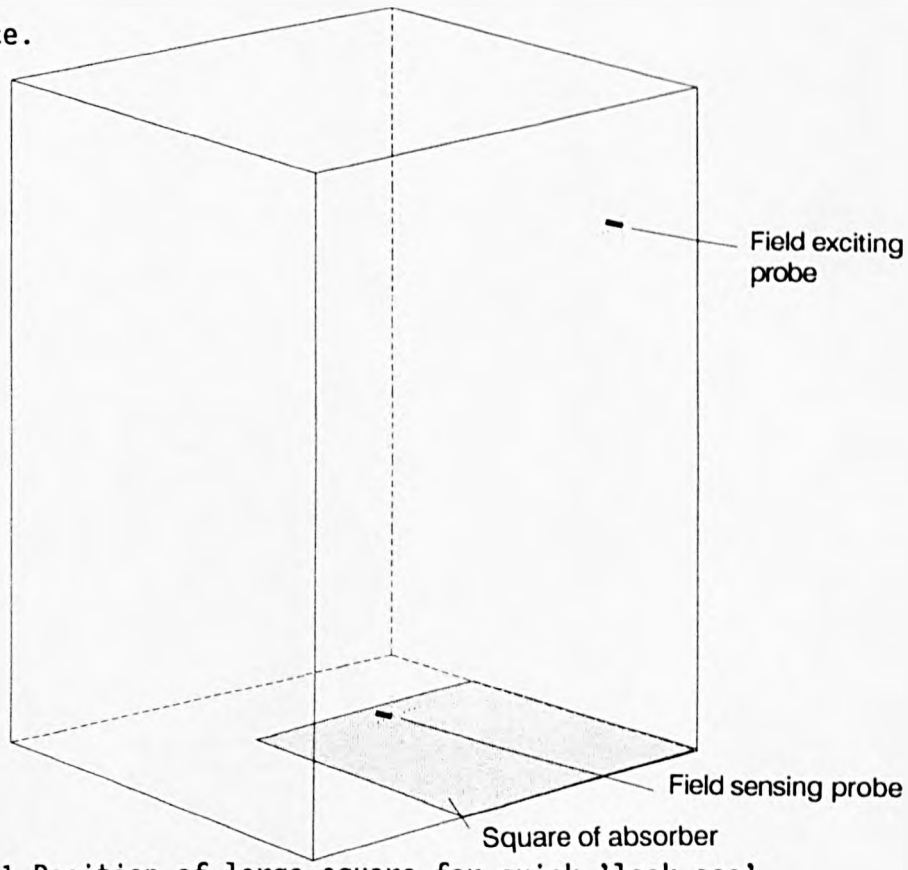

Fig. 8.2.1 Position of large square for quick 'look see'

Two strips of each type of absorber were placed as shown in Fig. 8.2.2 along part of the line of maximum magnetic field. Each strip was 2cm wide. The effect on the first resonance was then observed. As with the initial measurement type 6b was by far the most effective and reduced the resonance peak by about 10dB (Fig. 8.2.3). It reduced the Q of the resonance from about 1800 to about 760. The second most effective type was 6a but this reduced the resonance peak by approximately 3dB. The rest of the sheets gave a reduction which was within the limits of experimental error.

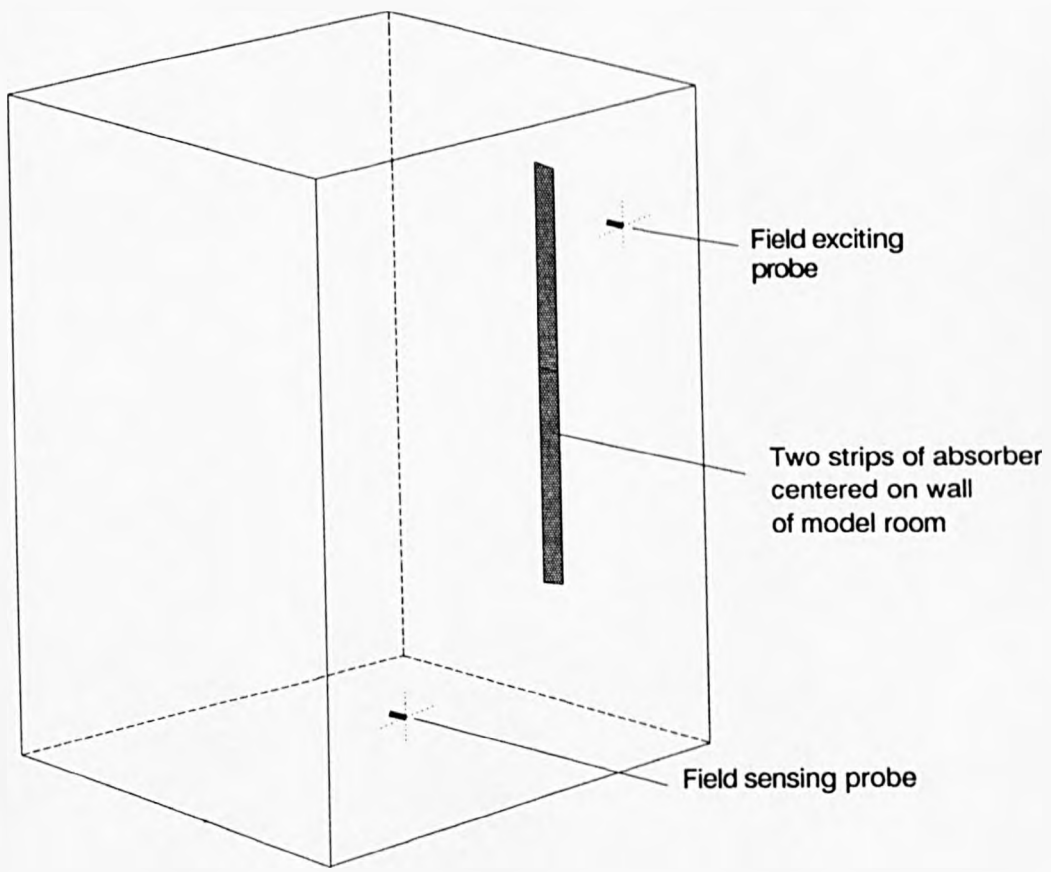

Fig. 8.2.2 Positioning of two strips in the model room

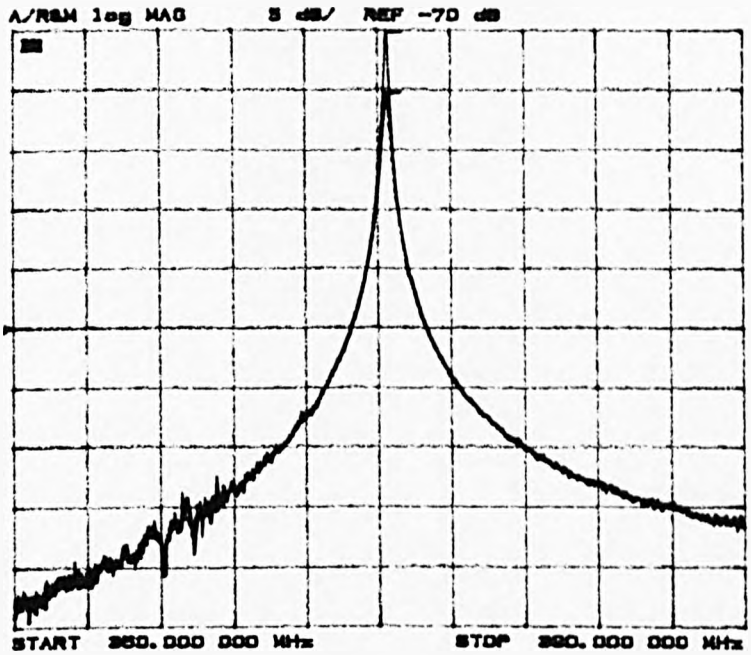

Fig. 8.2.3 Reduction of Q of the first resonance for type 6b

Type 6b was a ferrite loaded absorber (some of them contained an iron loading) with the heaviest loading of those supplied. It was also the thickest being about 4mm thick. It was a resonance type absorber with its lowest reflectivity at about 8GHz. This type of absorber has limited attenuation of the wave and relies on waves reflected from the front and back faces being out of phase and cancelling. It works best over a fairly narrow range of incidence angle [Emerson 1977].

8.3 Positioning of Absorber

The fields within an empty rectangular cavity can be calculated as described in Chapter 6. Equations 8.1 and 8.2 describe the magnetic field distribution for the magnetic fields of the $TE_{0,1,1}$ mode which is the resonance that was used to compare the absorbers. The positioning of the magnetic field maxima can also be calculated. As with the loading of the electric fields with carbon loaded absorber the ferrite absorber will dissipate the most energy when it is placed in a position of maximum magnetic field. If it is assumed that the addition of a small amount of absorber will not disturb the field patterns by a significant amount, the best place to position the absorbers is at the field maxima calculated for the empty room. All resonant modes in the room have magnetic field maxima around the sides of the room which enables the absorber to be attached to the walls, ceiling and floor of the room where it is not going to get in the way of people or equipment.

Equations 8.1 and 8.2 below gives the magnetic field distribution for the $TE_{0,1,1}$ mode.

$$H_X = - \frac{jE_0}{\eta} \frac{\lambda}{2d} \sin\frac{\pi X}{a} \cos\frac{\pi Z}{d} \qquad 8.1$$

$$H_Z = \frac{jE_0}{\eta} \frac{\lambda}{2a} \cos\frac{\pi X}{a} \sin\frac{\pi Z}{d} \qquad 8.2$$

$$\text{where } \eta = \sqrt{\frac{\mu}{\epsilon}} \qquad 8.3$$

The orientations of H_X and H_Z are shown in Fig. 8.3.1

Considering the $TE_{0,1,1}$ mode equation 8.2 gives the distribution of the magnetic field in the Z direction (Fig. 8.3.1). This shows that a

maximum for the field lies along the line marked 'a' and if the absorber is placed along here the Q should be reduced most.

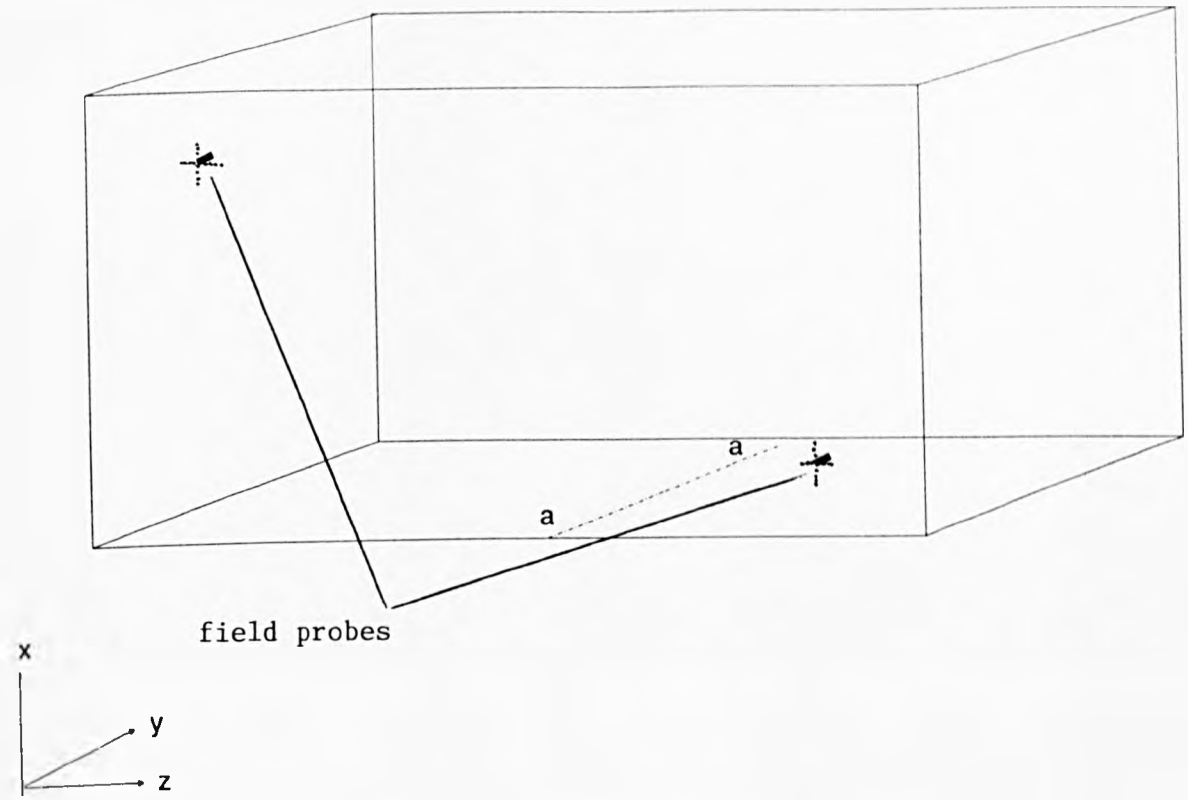

Fig. 8.3.1 Showing the orientation described in the text

To test this two strips of absorber (30 × 2 cm) were placed in various positions and the Q of the first resonance was measured. The positions of the absorber and the Q of the resonance with the absorber in that position are shown in Fig. 8.3.2.

The results show that placing the absorber in the position shown in Fig. 8.3.1 does not give the best reduction in Q although for this particular mode there is little difference in the reduction in Q for several positions. The optimum position is that shown in Fig. 8.3.2 b. For this mode the magnetic field changes relatively slowly along the length of the absorber when it is placed in this position and it is not surprising that the reduction in Q should be close to that for

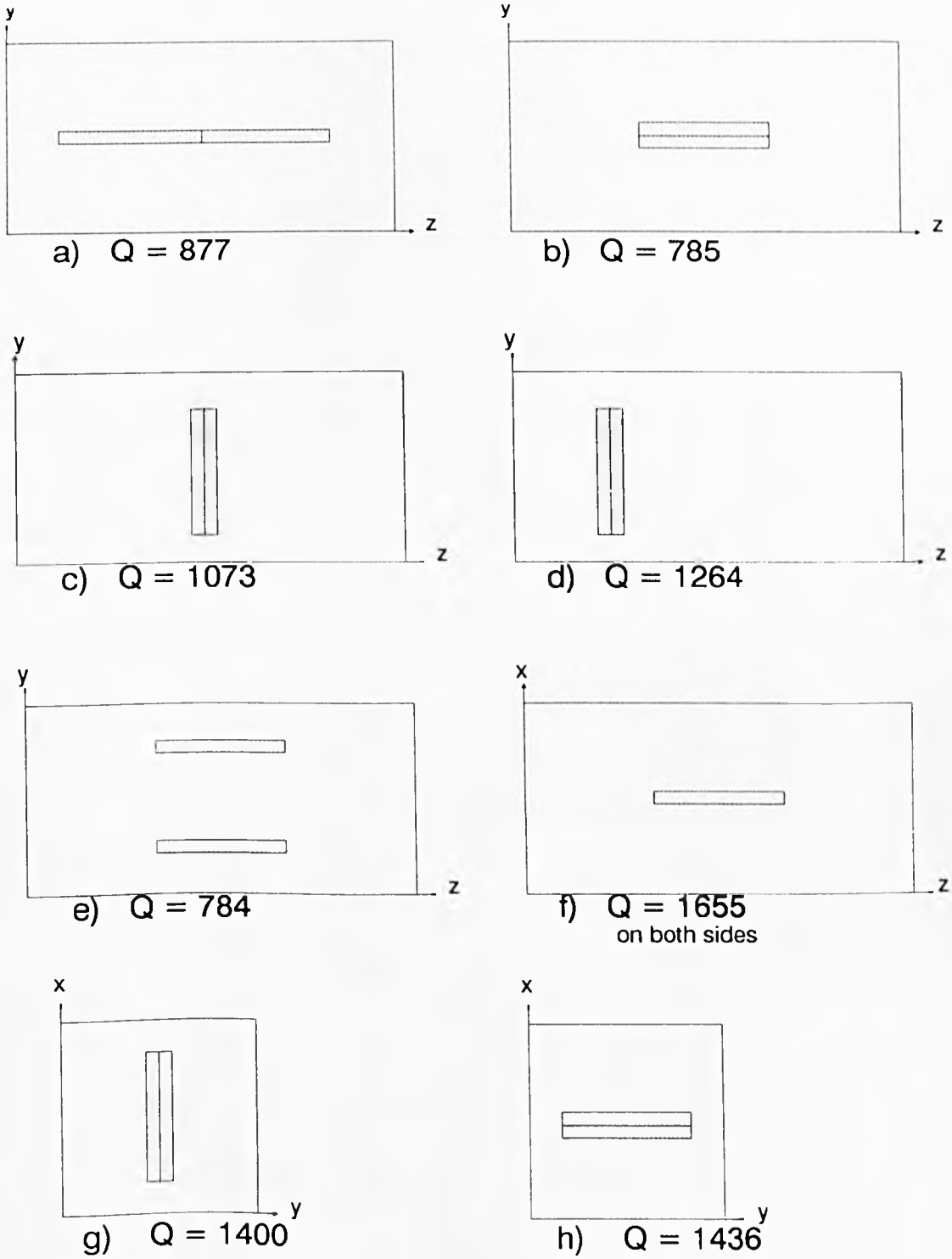

Fig. 8.3.2 The Q of the first resonance for various positions of absorber

the calculated maximum field position although it could be expected to be slightly lower. This difference could be due to the distortion of the field at the edges of the strips. When the strip is narrow and placed across the direction of the field there will be a very short length of field which is parallel to the surface of the absorber and hence it will be less efficient. It would be expected that this would be the best position (Fig. 8.3.2.b) for the absorber for the $TE_{1,1,1}$ mode as a given length strip of absorber will have a greater field strength along the length of the absorber. For higher modes the field changes faster and the positioning of the absorber will need to be more accurate. The result of the positioning for this mode will not change the positioning of a full load as it will need to have absorber in both directions to ensure that all modes are loaded.

This positioning of the absorber also means that the absorber is perpendicular to the currents which flow on the walls of the room. When the current flow is parallel to the strip of absorber the current may flow around the absorber having little effect on the fields within the room. However, when the strip is across the current flow the current may be diverted around the strip and have a greater effect on the fields within the room.

When the same amount of absorber is placed along the field lines but on the ends of the cavity the reduction in Q is smaller which can be expected as the field is lower in this direction by a quantity which is a function of the box dimensions (see equations 8.1 and 8.2).

8.4 Carbon Loading of the Ferrite Absorbers

8.4.1 Introduction

There are three mechanisms of energy loss in magnetic materials:-

1) Hysteresis loss within the material
2) Dissipation by conduction currents
3) Loss due to the complex nature of the permeability

The hysteresis loss is usually included with the complex permeability as it is difficult to separate the effects of the two mechanisms when measuring the parameters of magnetic materials. Conduction currents can be either on the surface of the material where a change in the permeability causes a change in the magnetic field or within the material where the conductivity of the material causes attenuation of the fields which are propagating within it. Where no conduction current can flow because of the insulating properties of the material all loss is due to hysteresis and the complex permeability.

Considering a TEM wave propagating within an infinite block of material the attenuation of the wave can be increased by increasing the conductivity of the material [Chen 1985]. This will reduce the thickness of material which is required to give a particular attenuation such as with wave absorbers. However, increasing the conductivity by adding a component such as carbon to the absorber will alter the wave impedance of the material which with wave absorbers could reduce their effectiveness as there may be an increase in the reflected waves. An impedance matching layer may then be needed to

improve it again. However, for the use under consideration this would not be a problem. It could even be an improvement as the absorber could be thinner and would not perturb the fields by as much so that adding more absorber to the room would not be counter productive as occurs with the electric field absorber described in Chapter 7.

Carbon has been added to plane wave ferrite absorbers [Naito and Mizumoto 1987] to reduce the thickness of the absorber sheets necessary for a particular centre frequency. The reduction in the thickness gives a reduction in the weight of the absorber but the paper does not describe the effect of the carbon on the loss experienced by the wave.

8.4.2 Measurements on carbon loaded ferrite rubber

Sheets of absorber with various ratios of carbon to ferrite (by volume) were suggested as a starting point. However, it was found during manufacture of these absorbers that the addition of the carbon prevented the absorber from binding together properly and the quantity of ferrite had to be reduced. Thus it is not possible to compare the absorbers with the carbon loading with those with no loading without accounting for the relative levels of ferrite in the different absorbers.

The various levels of carbon loading were compared in the same way as the original absorbers (i.e placing two strips down the centre of one side) and measuring the Q of the first resonance. The results of this comparison are shown in Table 8.1.

absorber number	Q
1	850
2	895
3	1008
4	1049
5	1459
6	1545
7	1620
6b	862

Table 8.1 The Q of the first resonance with two strips of absorber along one wall

The relative quantities of ferrite, carbon and binder (by volume) were supplied for the carbon loaded absorber and the original 6b. The ratios of carbon to ferrite and ferrite to total volume are shown in Table 8.2. These values were used to calculate what volume of each

absorber would be required to keep the quantity of ferrite the same as that for type 1. The Q for this volume of each absorber was then calculated (assuming the increase in volume does not change the field distribution) and also measured (also in table 8.2). The volume was increased by increasing the width of the strips in the same ratio as that of ferrite in type 1 to ferrite in the absorber under consideration.

sheet number	ferrite per unit volume	carbon / ferrite	ferrite in 1 / ferrite in n	Q_1	Q_x	
					calc	measured
1	.3223	.0226	1	850	850	850
2	.3132	.0466	1.03	895	881	885
3	.2712	.1069	1.19	1008	930	910
4	.2546	.2239	1.27	1049	943	988
5	.096	.4583	3.36	1459	1008	1308
6	.0797	1.074	4.04	1545	1080	1350
7	.0445	1.932	7.24	1620	998	1200

Q_1 is the Q measured for the standard strip (2 × 30 cm)
Q_x is the Q calculated or measured for the adjusted volume with the same quantity of ferrite as type 1.

Table 8.2 Calculated and measured Q for various ratios of carbon to ferrite

The quantity of ferrite in absorber type 6b and the carbon loaded absorber number 1 is fractionally different (approx 1.5%) but it is not possible to cut the sheets sufficiently accurately to account for this difference. The absorbers are ferrite bound in rubber which gives a fairly soft flexible material which is difficult to mark and difficult to hold securely while cutting which limits the accuracy of the cutting.

8.4.3 Discussion of results

The results for the carbon loaded absorber show that the type 1 gives a Q which is a little lower than that obtained with type 6b. As the relative quantities of ferrite in the two absorbers are very close (32 in 1 : 32.5 in 6b) there will not be much improvement in the energy absorption by increasing the ferrite in 1 to the same as the ferrite in 6b. A close inspection of the sheets of absorber also shows that the carbon loaded absorbers are about 0.5 mm thinner than the original type 6b. This would also decrease the reduction in Q observed with type 1 when the same area of absorber was used so that the improvement may be greater than it appears at first. If the quantity of type 1 were increased by 12.5% to account for this the Q of the first resonance would be decreased to approximately 720 (by calculation) which is a significant improvement although still not good enough.

For this first mode a small change in the positioning of the absorber does not give a significant change in the Q of the resonance. The quantity of each absorber was adjusted to give the same amount of ferrite in the cavity for each of the carbon loaded absorbers. This shows that with the ratio of carbon to ferrite at 2.25% the reduction in Q is the greatest for those examined. The calculated and measured values of Q are close for the lower levels of carbon (and small change in volume) but for the higher carbon content the two values are not as close. This can be put down to the change in absorber positioning for the larger volumes of absorber as the absorber was not stacked on top of itself but was left as a single layer which would cause some of it to be away from the field maxima. Also to the difficulty in cutting the absorber accurately as described in the previous section.

8.5 Extra Absorbers

8.5.1 Introduction

After the initial set of measurements was carried out and found to give slightly disappointing results Emerson and Cuming supplied three extra types of absorber to investigate.

1. Type FSD which is a thin ferrite loaded rubber sheet similar to those supplied originally.
2. Two pressed ferrite tiles with different compositions (no data on the compositions was supplied) which were labelled 9 and 10.

8.5.2 FSD

This sheet of absorber is much thinner than those investigated previously. It was compared with type 6b in two ways:-

1. Two single strips (30 × 2 cm) positioned as before
2. Strips (30 × 2 cm) built up to same thickness as type 6b positioned as previously.

In both cases the Q of the first resonance was measured. The results are given below:-

1. single strips	Q = 1423
2. multiple strips	Q = 704

The measurements carried out on the FSD type absorber shows that the Q for the thin strips is not particularly low, but when the strips are built up to the same thickness as type 6b the Q is reduced to significantly lower than for 6b. Therefore as an absorber with no changes this type gives the largest reduction in the Q of the first resonance and would be the most effective composition to use although it would need to be thicker. However, as it stands it is still does not give a good enough reduction in the Q to give a smooth frequency response when the cavity is fully loaded.

8.5.3. Ferrite tiles

Two ferrite tiles were supplied by Emerson and Cuming. One was labelled 10, the other 9. The tiles each have dimensions of 10 × 10 × 0.8 cm. They were individually placed in the centre of the test wall and the Q measured. A section of absorber type 6b was also cut to the same dimensions (2 layers to get the same thickness) and tested in the same way. The results are shown in Table 8.3

absorber type	Q
10	124
9	110
6b	673

Table 8.3 Comparison of the Q of the first resonance for absorber type 6b and the ferrite tiles

The levels of Q obtained with the ferrite tiles are far lower than those obtained by any of the other magnetic absorbers used. They are within an order of magnitude of that obtained for the first resonance in the screened room when a single column of the carbon loaded foam is used as the absorbing medium. This level of Q for the individual block of absorber is probably sufficiently low for the individual resonances to merge into each other when the absorber is positioned so that all modes are effected.

8.6 Addition of Conductive Layers

8.6.1 Introduction

The results shown so far do not indicate a high enough level of energy dissipation by the (rubber) magnetic absorbers to give a reasonable degree of damping for a fully loaded room. It was suggested that conductive coatings to the surface of the absorber may increase the energy dissipation by allowing conduction currents to flow on the surface of the material. Without carrying out an exhaustive theoretical study it is not possible to predict the surface conductivity required to give the best results and there was insufficient time to carry out such a study. If the conductivity is too great the fields will not permeate into the absorber and this energy absorption mechanism will not function as well, little energy is dissipated by very good conductors. If the surface is not conductive enough the surface current levels will not be high and again little extra energy will be dissipated.

Three types of conductive coating were investigated with various numbers of coats and patterns. These were :-

1. Aluminium foil
2. Nickel paint (aerosol)
3. Silver paint (brush on)

8.6.2 Aluminium foil

Two strips of absorber 6b were placed down the centre of one side as before. Also a single strip of foil was placed in this position with no absorber. Then the strips of foil and absorber were placed in various configurations. The positions and values of Q measured are shown in Tables 8.4 and 8.5. Table 8.4 shows measurements made on absorber type 6b. Table 8.5 shows measurements made on the new absorbers.

layout of absorber and foil	Q
just foil (foil = 95 × 6cm)	1493
6b on foil	802
foil on 6b (edges fastened with sellotape)	744
as above with all edges trimmed level with absorber	791
as above with 2 layers of foil	764
1 layer of foil between two layers absorber	541
2 layers of absorber - no foil	545
2 layers absorber with 1 layer of foil on top	518
2 layers absorber with 2 layers foil on top	530

Table 8.4 The effect of different foil layouts on the Q of the first resonance

		Q	
		edges stuck to room wall	edges level with absorber
New absorber	type 1 carbon loaded	781	860
	FSD thin sheets × 2	1162	1376
	FSD thick sheets × 2	438	700
	Ferrite tile 10	940	57
	Ferrite tile 9	625	97

Table 8.5 The effect of the conductive layer on the Q of the first resonance for the extra absorbers

8.6.3 Nickel paint (aerosol)

Again two pieces of absorber (6B) were placed in the usual position down the centre of one side. These were then sprayed with 1 or 2 layers of paint at a time. This was done in situ to try to prevent the paint cracking when the absorber was flexed. This also prevented the paint from flaking and gave a conductive path from the paint to the walls of the cavity. The results are shown in Fig. 8.6.1.

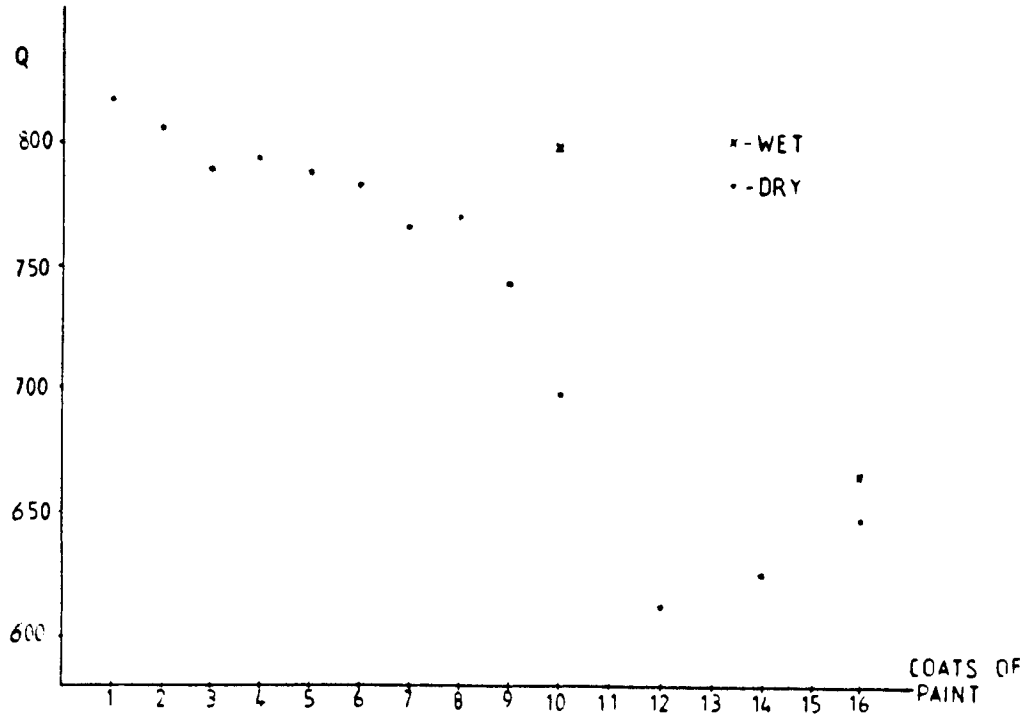

Fig. 8.6.1 The variation in Q of the first mode for varying thicknesses of nickel paint on type 6b

The Q of the cavity was also measured when the painted absorber (16 coats of paint) was raised and a second layer of 6b was inserted underneath. This meant that the paint was not in contact with the walls of the cavity and gave a Q of 514. As already stated the Q for 2 layers of 6b on their own is 545 so the extra reduction in the Q with the painted layer which is not in contact with the walls is not significant.

8.6.4 Silver paint (brush on)

This paint is a silver based paint usually used to mend broken tracks on printed circuit boards. Some measurements were made while the paint was still damp, others once it was dry. To reduce the amount of paint required the measurements were carried out on one strip of absorber and the equivalent Q for 2 strips of absorber was then calculated (see Appendix E for method). The first set of results given are those for the damp paint (Table 8.6). The average thickness of the layers of paint could not be determined as the paint cracked apart when the strip of absorber was removed from the cavity.

	Q	
	1 sheet	2 sheets
lines approx 1 inch apart - no contact to room walls	1190	888
with lines inserted between others	1183	881
as above connected down long edges	676	416
total cover with silver no contact with sides	1146	840
as above + contact down short edges	1160	856
as above + contact points apprx 2" apart on long edges	923	621
as above with solid contact down sides	1230	934

Table 8.6 The effect of a silver based paint on the Q of the first resonance (paint damp)

The measurements shown in Table 8.7 were made when the paint had been allowed to dry for several days.

	Q	
	1 sheet	2 sheets
solid paint on top with solid connection down sides	1830	——
as above with gaps in sides	1680	1575
strips on top joined all down sides	1460	1228

Table 8.7 The effect of allowing the silver paint to dry

8.6.5 Discussion of results

It can be seen from the measurements carried out that the conductivity of the surface does have an effect on the energy dissipated by the absorber and hence the Q of the cavity. Nickel is a magnetic material so that some of the extra losses with this may be coming from magnetic losses within the material itself. However, silver is not magnetic and all the extra losses will be from the conduction currents. The results for both the nickel and silver paints show the effect of different conductivities as the paints dry. The silver paint in particular shows that too good a conductor actually reduces the energy dissipated by the absorber as it prevents any level of magnetic field entering the absorber so that absorber might as well be removed from the cavity. The Q with the solid dry silver paint is very similar to that for the empty room which has been taken as 1800 for the calculations.

The aluminium foil on its own does dissipate some energy (Q of an empty cavity is approximately 1800) but even so it is possible to see the reduction in the Q when it is placed across the absorber and connected to the cavity walls.

The experiments with the aluminium foil also show that

1. the conductive layer must be on the top surface, it has no effect in the middle of the absorber.
2. a conductive layer on the carbon loaded absorber does not give a significant improvement. Although the DC resistance of the absorber is too high to measure there is probably some

finite value of AC resistance which dissipates energy without the extra layer.

3. the effect of the conductive layer is different for absorbers made with different materials (the change in Q with the conductive coating was different for the two ferrite tiles).

4. for all the ferrite rubber absorbers the conductive surface has a greater reduction in the Q if the edges of the conductor are in contact with the metal walls of the cavity itself. However, for the ferrite tiles the opposite is true and if the conductor is in contact with the cavity walls the Q is greatly increased. Even when it is not connected to the walls of the room the foil has very little effect on the Q of the resonance for the ferrite tiles.

8.7 Electrical Contact of Ferrite Loaded Absorber With Walls

Carbon loaded plane wave absorbers are designed so that they operate best when the absorbers are backed with a metal wall such as the walls of the screened room. However, the carbon loaded absorber used to damp the resonances in chapters 6 and 7 are used as resistive loads away from the walls. The ferrite loaded absorbers are also not being used as plane wave absorbers so should not need to be in direct electrical contact with the walls of the room.

As a confirmation that the absorbers are operating in this manner and not as plane wave absorbers the Q of the first resonance in the model room was again measured with a ferrite tile placed in close contact with the metal and not in contact with the wall. The ferrite tile was held away from the metal of the room by placing it on a 5mm thickness of paper. There was no difference which could be observed in the two measurements, even that which could be expected to be caused by the slight movement of the tile away from the magnetic field maximum adjacent to the walls.

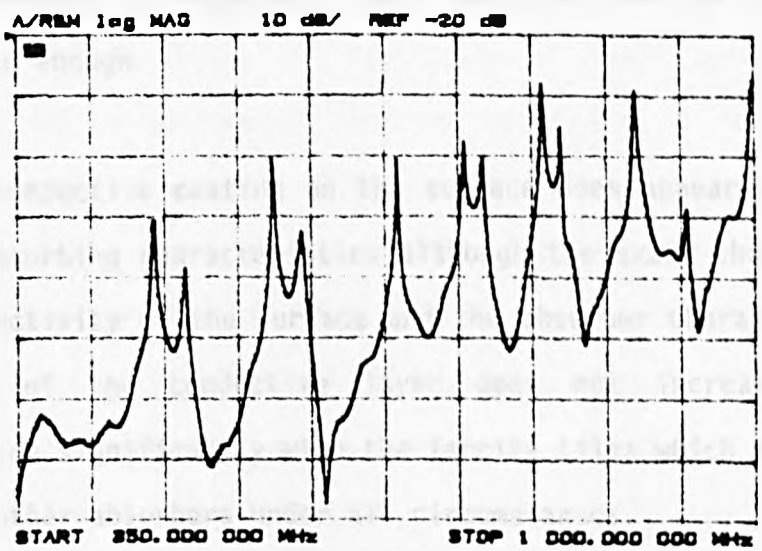

Fig. 8.7.1 Frequency response for tile against wall and on paper

8.8 Conclusions For Loading TE_{101} Mode

The theoretical positioning of the absorber has been checked for the first resonance and has been shown to agree with the theory. The positioning for the higher modes cannot be verified until a good suitable absorber is obtained in large enough quantities to load all the modes in the chamber. This is due to the degenerate nature of rooms with the relative dimensions of the one used. This means that even if the Q of one particular mode is reduced it may not be visible due to other modes existing with the same frequency.

The ferrite tiles prove that enough energy can be absorbed from the magnetic fields to reduce the Q of the resonances to the same order as that obtained using the carbon loaded foam to absorb energy from the electric fields.

The investigations show that the most effective carbon loaded ferrite absorbers are those with approximately 2.5% of carbon to ferrite. This level gives a lower Q than for the original type 6b but the improvement is relatively small and the level of Q is still not nearly low enough.

The conductive coating on the surface does appear to improve the energy absorbing characteristics although the exact change depends on the conductivity of the surface and the absorber characteristics. The addition of the conductive layer does not increase the energy dissipation significantly with the ferrite tiles which are better than all the other absorbers under all circumstances.

9 FULL MAGNETIC LOADING AND COMPARISON WITH CARBON LOADING

9.1 Introduction

Chapter 8 describes the reasons for work carried out with magnetic absorbers and the results of measurements carried out using various absorbers on mode TE_{011}. The electric field absorber has been shown to load all modes to give a frequency response with a variation of less than +/- 10 dB about a smooth curve with a box shaped load (Chapter 7). It should also be possible to design a layout for the ferrite loaded absorber which will load every mode possible in the frequency range of interest and obtain a similar response.

Equations describing the field distribution within the resonant cavity have been quoted in Chapters 5 and 8. Chapter 8 describes measurements carried out which show that for the first resonance the position of maximum energy absorption for the magnetic absorber is to lie it along the line of the field such that it cuts across the currents which flow on the surface of the wall. If this is done for all possible modes a shape will build up as is shown in Fig. 9.1.1. This shows the positions and directions of field maxima for several modes and the corresponding absorber positions. It is necessary to place absorber on at least 2 orthogonal walls to absorb energy from every mode but to be complete absorber can be placed on 3 orthogonal walls. Unlike the electric field which can exist in one direction only for the lowest modes there will always be a magnetic field adjacent to two walls as a magnetic field always forms a complete loop. This means that for all modes there is loading on two walls which will increase the energy absorption.

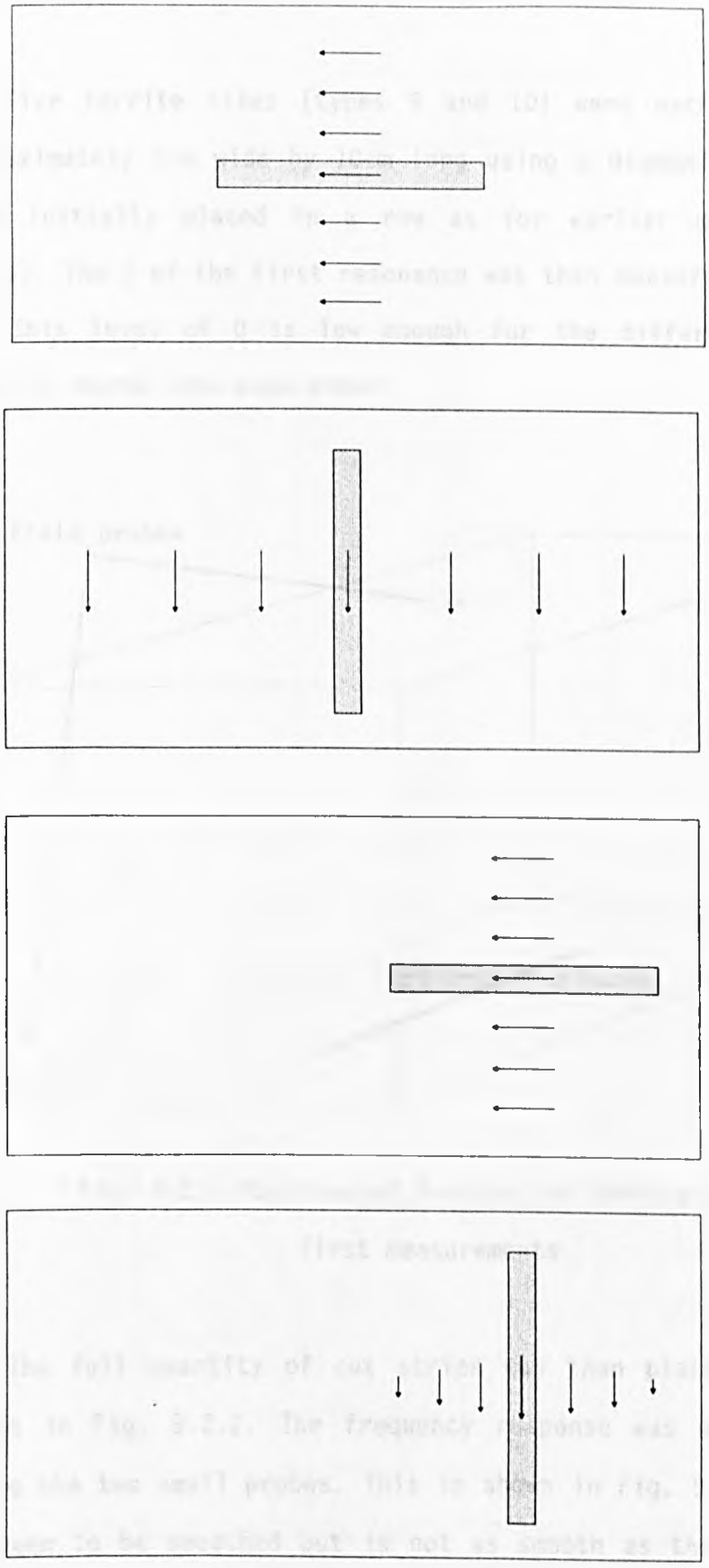

Fig. 9.1.1 Positions of magnetic field maxima and corresponding positions of absorbers

Five ferrite tiles (types 9 and 10) were each cut into strips approximately 2cm wide by 10cm long using a diamond saw. Five strips were initially placed in a row as for earlier measurements (Fig. 9.2.1). The Q of the first resonance was then measured and found to be 52. This level of Q is low enough for the different resonances to start to merge into each other.

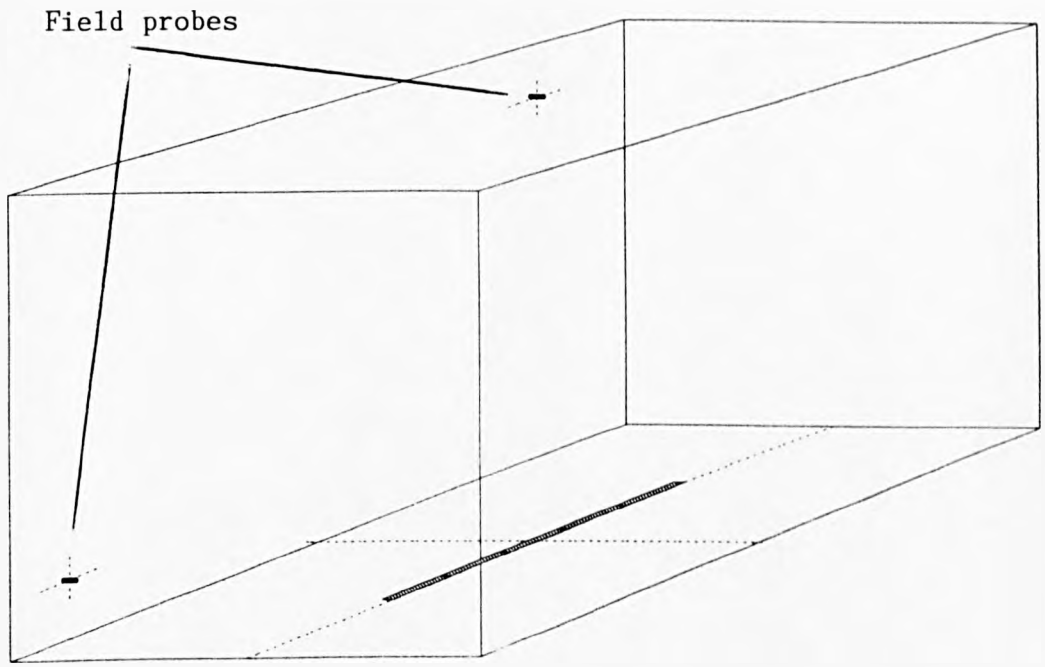

Fig. 9.2.1 Position of 5 strips of ferrite tile for first measurements

The full quantity of cut strips was then placed in the room as shown in Fig. 9.2.2. The frequency response was measured as before using the two small probes. This is shown in Fig. 9.2.3. The response is seen to be smoothed but is not as smooth as that obtained in the full sized room with the full carbon loaded foam as the energy dissipating material.

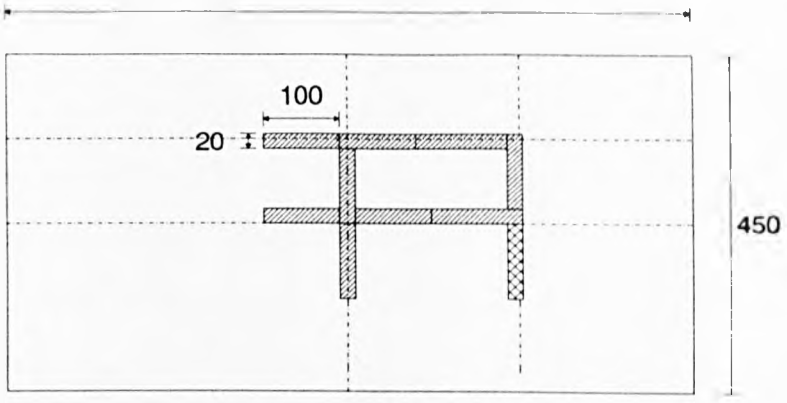

Base and Side

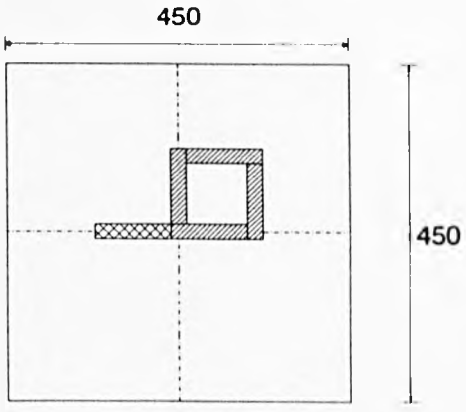

One end

Fig. 9.2.2 Positioning of ferrite strips for full room load

(hatched strips are referred to in section 9.6.2

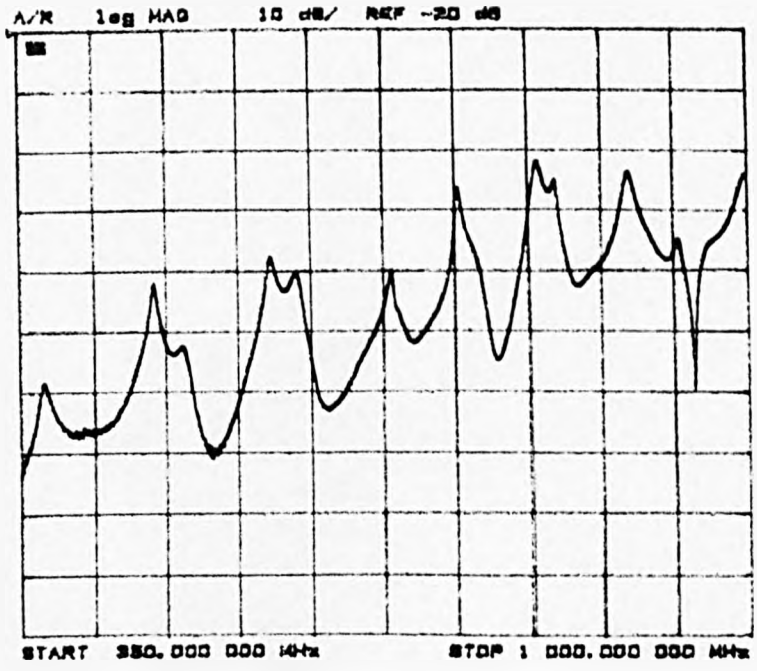

Fig. 9.2.3 Frequency response for load shown in Fig. 9.2.2

(electric probe source and sense)

Further uncut tiles were then placed as shown in Fig. 9.2.4 and the frequency response obtained for this is shown in Fig. 9.2.5. This shows that the response can be further improved by adding extra tiles although there is excess absorber included here which has not been positioned in the most effective places (i.e. at magnetic field maxima). If further tiles were cut into strips and positioned more carefully it should not require as much extra absorber to be included to obtain similar results. The easiest way to include more absorber will be to lengthen the lines of absorber which are already in position.

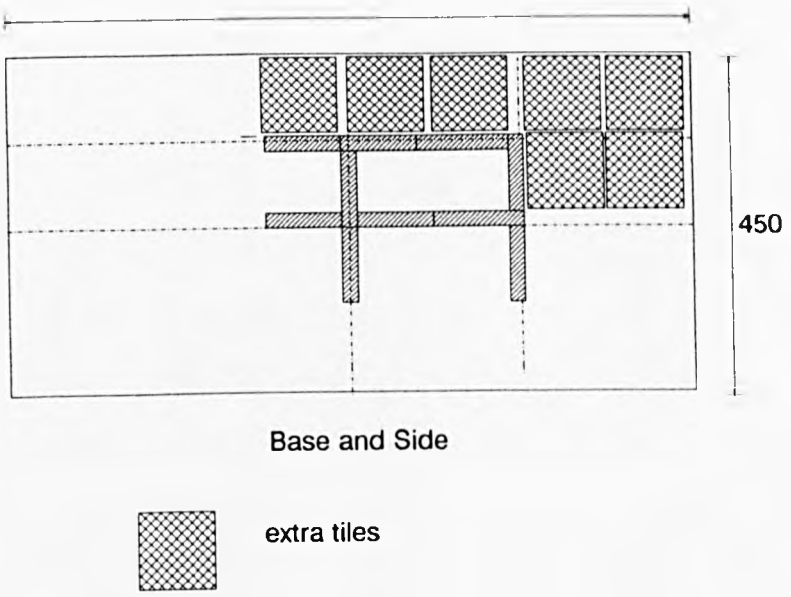

Fig. 9.2.4 Positioning of extra ferrite tiles

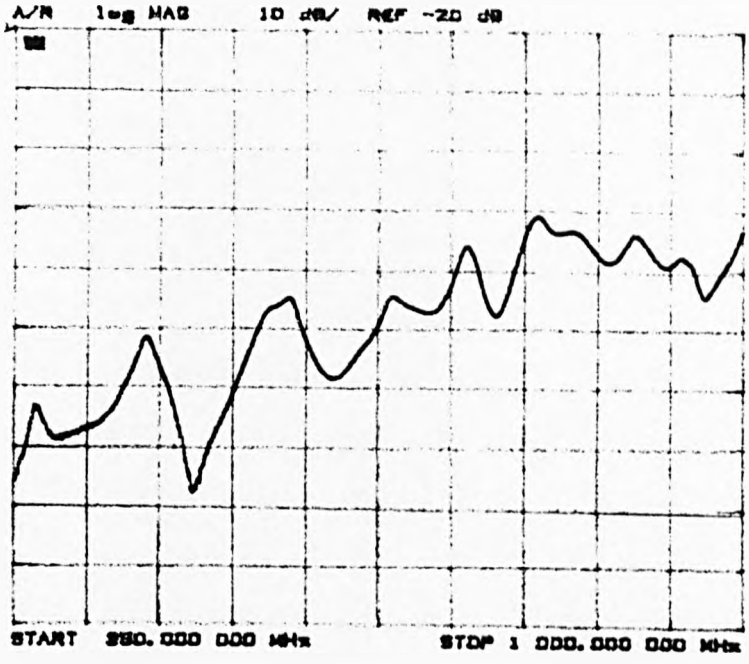

Fig. 9.2.5 Frequency response for load shown in Fig. 9.2.4 (electric probe source and sense)

9.3 Conductive Coating For Higher Modes

As stated in the previous chapter the effect of the conductive layer on the surface of the ferrite tiles was not the same as that observed for the other materials tested. With the tiles the addition of a conductive layer only improved the energy absorption if the edges of the conductive layer are not in contact with the walls of the cavity. The addition of the conductive layer for the other materials gave the best improvement in absorption when the edges of the conductor were in contact with the walls of the cavity. Measurements described in the previous chapter were only carried out on the first resonant mode as there was no point in further testing of materials which do not work well enough at the lowest frequency. Measurements were carried out on the ferrite tiles and are now described.

Ferrite tiles were placed in the model room in the positions shown in Fig. 9.3.1. The room was then excited and sensed using the two probes as before with the tiles uncoated and coated with one layer of aluminium foil which was not connected to the room walls but trimmed level with the edges of the tiles. The frequency response of the two set-ups are shown in Fig. 9.3.2. They show that except for the first mode the Q of each resonance is higher for the absorber coated with foil. This means that the tiles are more efficient dissipaters of energy without the conductive coating at higher frequencies and indicates that it is more useful not to have the coating. This does not show, however, whether the foil coating will improve the energy dissipation at lower frequencies which would be present in a larger cavity.

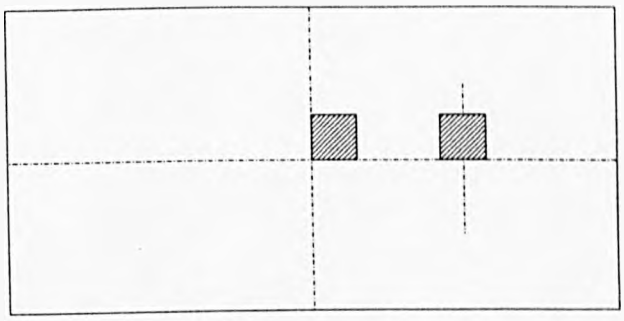

Base and Side

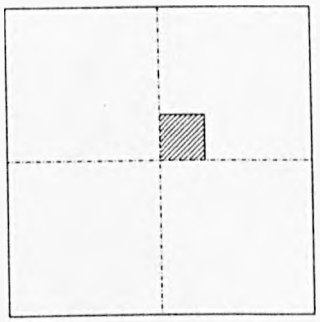

One end

Fig. 9.3.1 Positioning of ferrite tiles to investigate the effect of a conductive coating

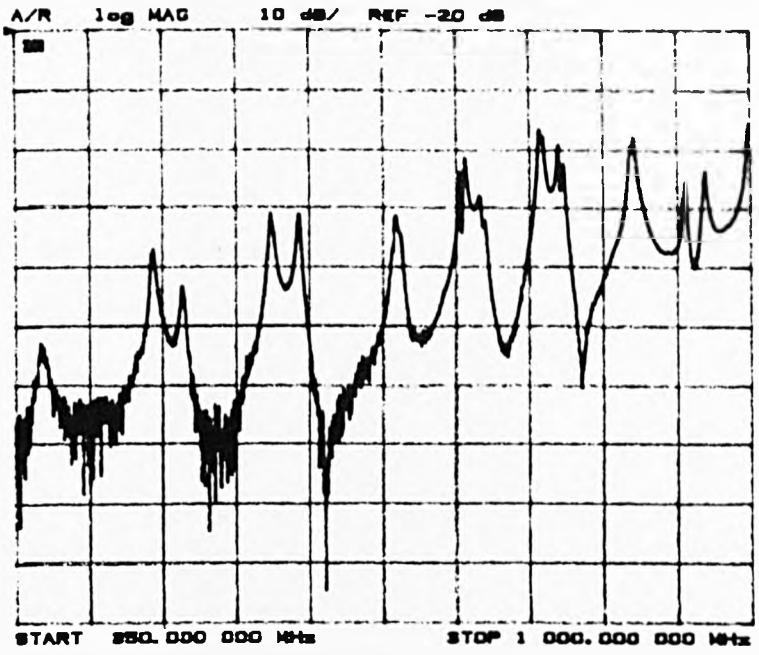

a) with conductive coating

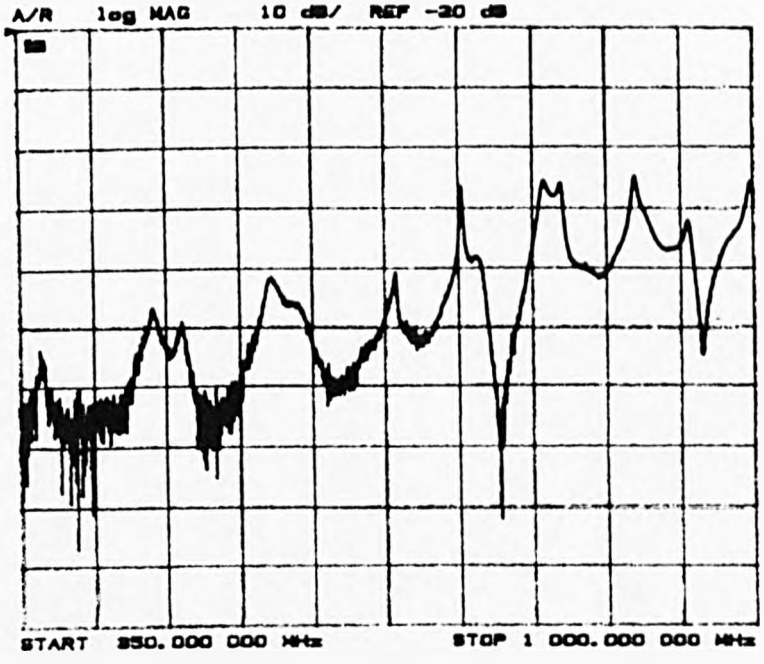

b) without conductive coating

Fig. 9.3.2 Frequency response for layout shown in Fig. 9.3.1 (with and without conductive coating)

The reduction in the energy dissipation at the higher frequencies is probably due to the reduced skin depth in the conductive coating which will reduce the levels of the magnetic fields which are penetrating the ferrite material itself.

9.4 Room 'Papered' With Ferrite Loaded Rubber

The ferrite tiles are expensive and are difficult to use due to their lack of flexibility and have to be fastened onto the walls securely due to their weight (they are heavy). The ferrite loaded rubber tiles which were initially tested are much lighter and more flexible so would be easier to use. However, the earlier measurements have indicated that this type of absorber is not as effective as the ferrite tiles. It is possible that placing more absorber in position will improve the response.

The model room was 'papered' with all the rubber absorbers available with the most effective absorbers in the positions where they are most effective (i.e where the magnetic fields are greatest). The room was sensed and exited with the two probes. The frequency response is shown in Fig. 9.4.1. The response shows that even with the majority of the room covered (19 sheets were available all together) the response was not as good as that obtained with just 5 ferrite tiles which were strategically placed (Fig. 9.2.3).

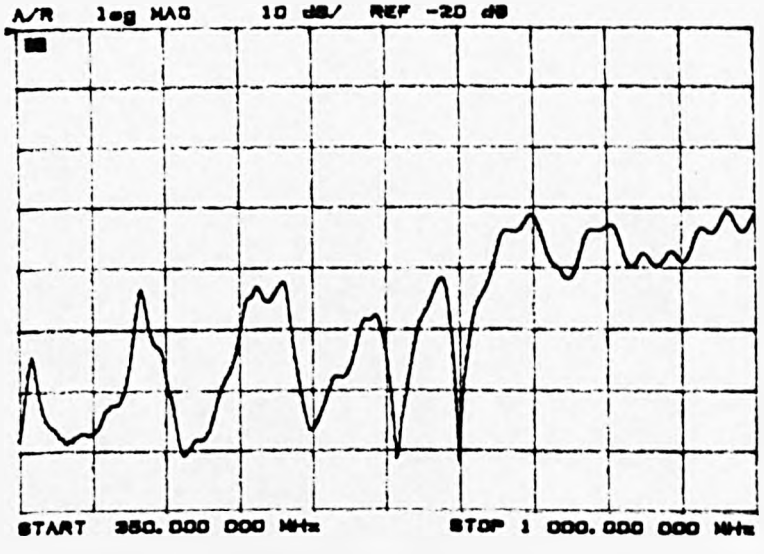

Fig. 9.4.1 Frequency response for 'papered room' (electric probes)

A fifth scale model of the carbon loaded foam absorber used for the original work was constructed from the foam with the highest carbon loading. To be perfectly accurate the blocks should have been layered from the different conductivities but it was found during the original work that the single absorber with the highest loading gave similar results. The model load was constructed in the same way as the original load and was supported on a card base instead of a wooden frame to position it in the correct place. The load was placed in the room as shown in Fig. 9.5.1.

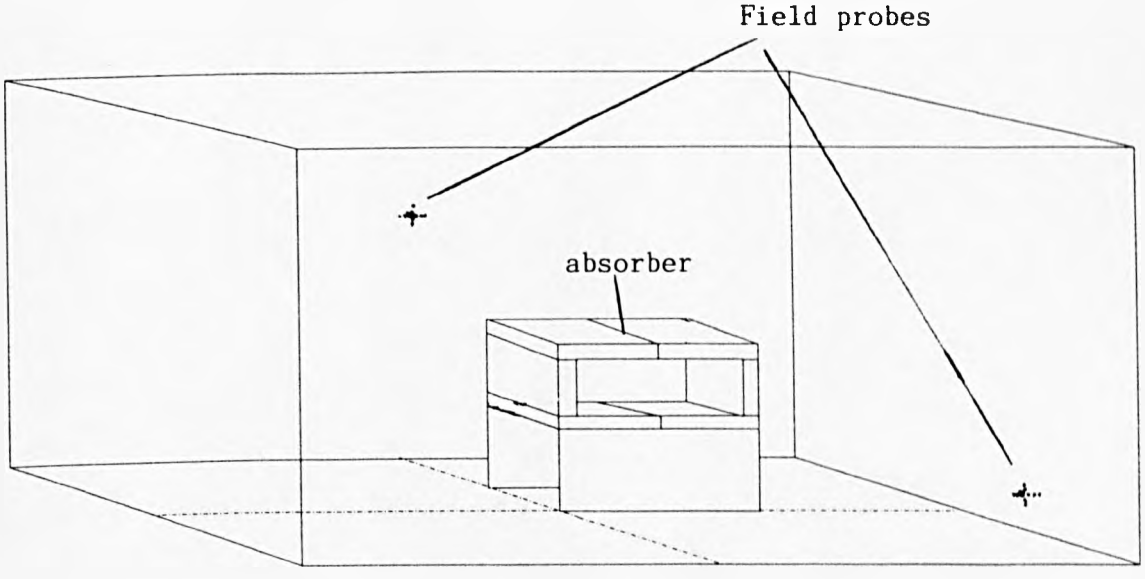

Fig. 9.5.1 Positioning of model carbon load

Fig. 9.5.2 shows the frequency response of the room with the carbon load with the room sensed and excited with the two small probes. The response is not as smooth as that obtained in the full sized screened room. This may be due to the change in the frequency range being used as the energy dissipated by the carbon loaded absorber is frequency dependent. For maximum dissipation for a given value of permittivity and frequency $\sigma = \epsilon\omega$.

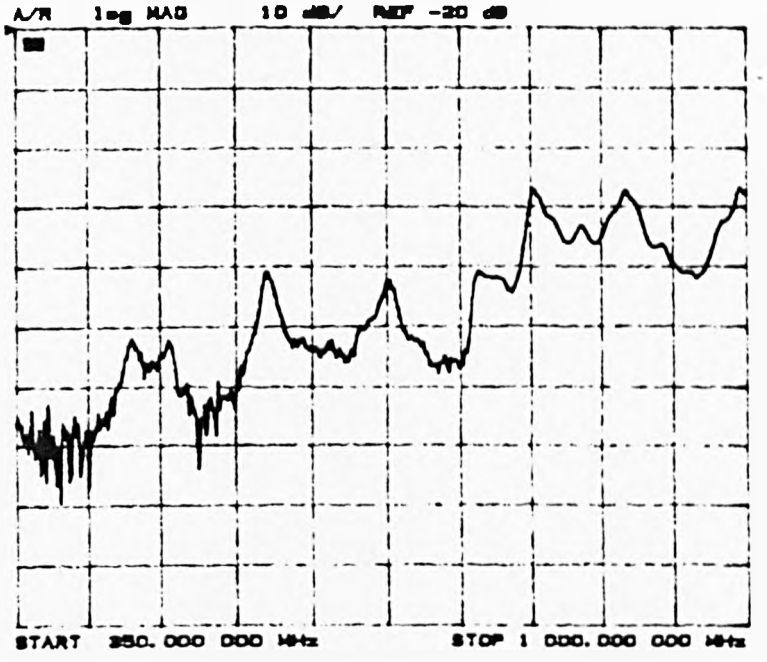

Fig. 9.5.2 Frequency response with model carbon load
(electric probe sense and source)

It was found in the original work that when the fields in the room were being sensed by the biconical dipole there was a further smoothing of the frequency response. A fifth scale model biconical was put in the room as a field sensor and the frequency response measured

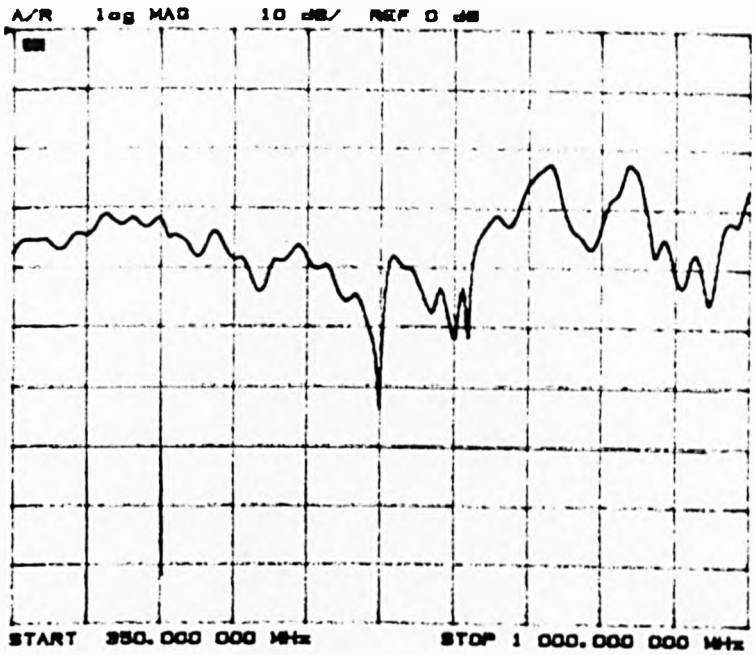

a) exciting probe close to load

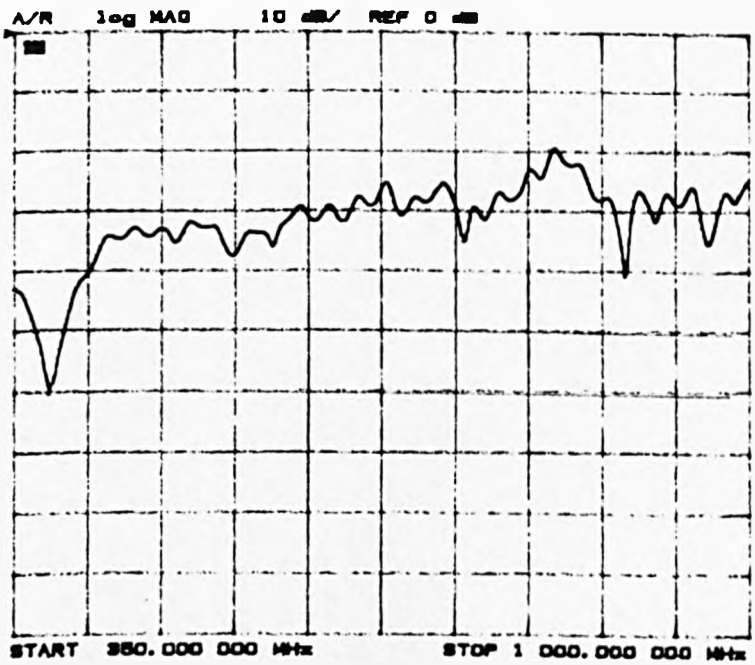

b)exciting probe remote from load

Fig. 9.5.3 Frequency response for model room with carbon load (electric probe source, biconical dipole sense)

with the room excited using the small probes (one at a time). Fig. 9.5.3a shows the response when the probe close to the load is the exciting device. Fig. 9.5.3b shows the response when the probe remote from the load is used to excite the fields within the room. For both measurements the antenna was horizontal. The response when the exciter is close to the load is not quite as smooth as that obtained when the exciter remote from the load is used. Having the absorber close to the source may perturb the mode structure of the room more than having it at the further end of the room. This would then mean that the absorber was not in the correct position to absorb the maximum energy and reduce the Q of the cavity resonances. Reflections of the initial wave by the absorber will also have the same effect.

9.6 Adding A Model Bench

Although the room resonances can be reduced in the empty room the addition of a conducting bench will introduce more resonances (TEM mode resonances on the bench; see Chapters 2 to 5) and will perturb the field positions within the room so that the positioning of the absorber may not be sufficient when the bench is present. A bench was placed in the model room in the same position as the full sized room. The bench was constructed from copper clad board used for making printed circuit boards bonded to the back wall of the model room with copper straps. It was found that, when the room was excited using the probes used for the rest of the model room investigations, the TEM transmission line formed by the bench in the room did not couple with the fields produced by the probes and the bench resonances could not

be clearly observed. Small magnetic loops were then mounted on the back wall of the room above the bench as in the full sized room to excite and sense the field (Fig. 9.6.1). As the loops couple closely with the transmission line formed by the bench and walls of the room the bench resonances can be clearly seen (Fig. 9.6.2).

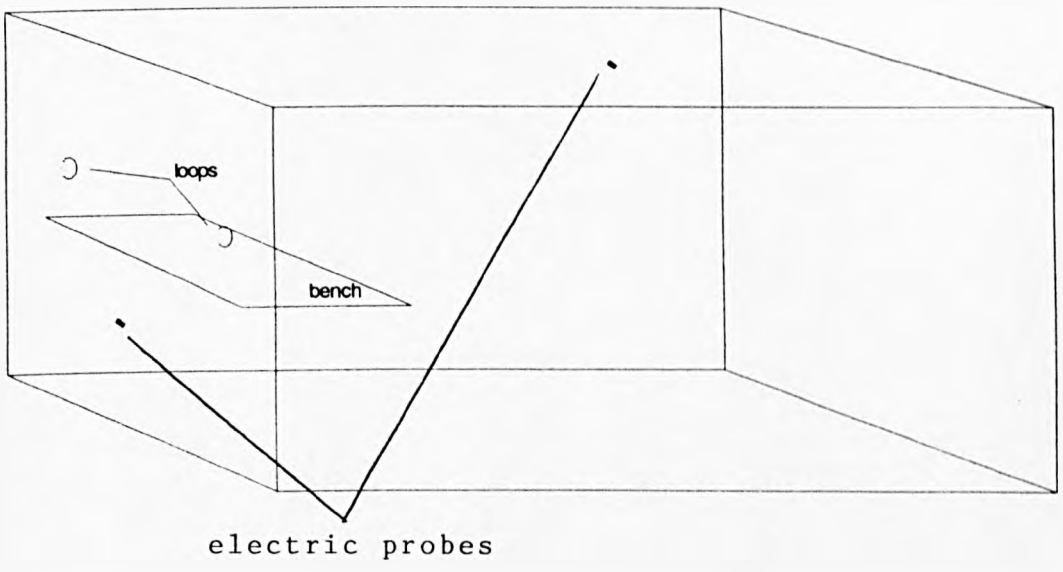

Fig. 9.6.1 Positioning of bench and magnetic loops in model room

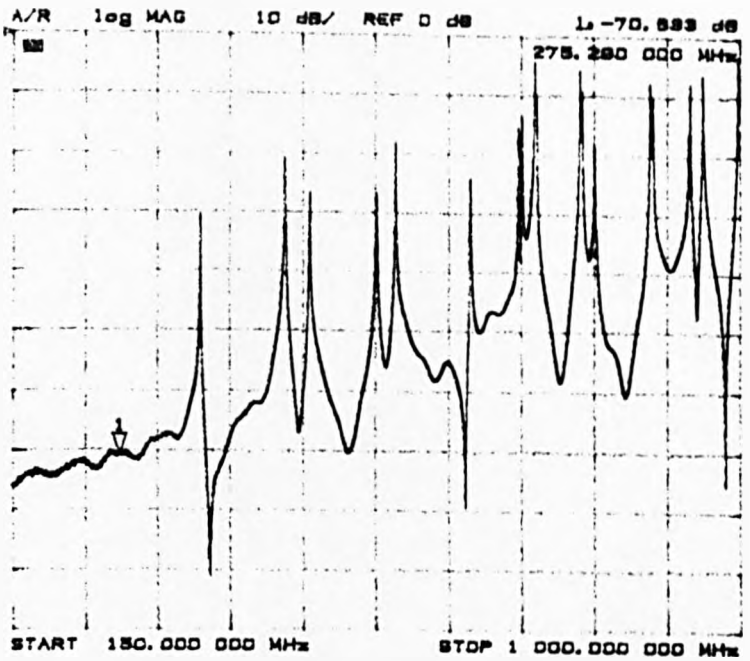

a) no bench

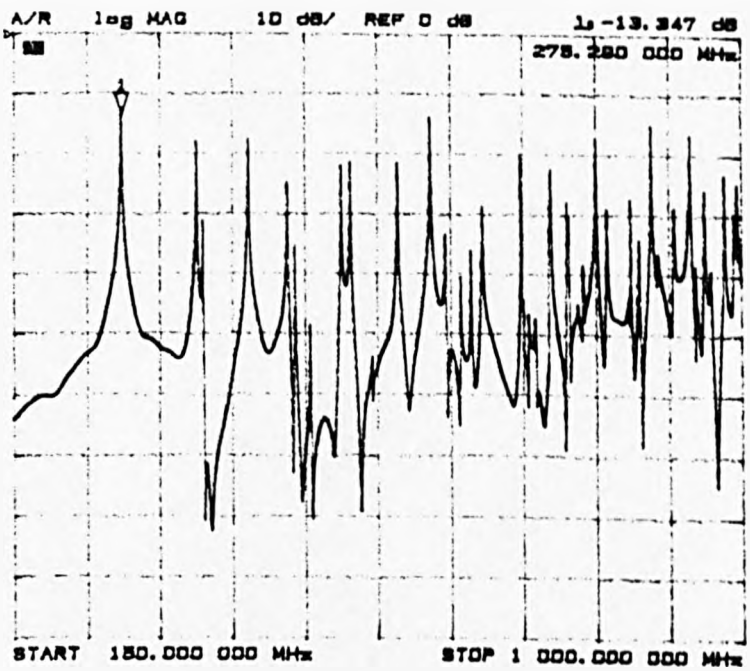

b) bench present

Fig. 9.6.2 Frequency response with and without bench (no loading) magnetic loop sense and source

9.6.1 Using ferrite to damp the bench resonances

Fig. 9.6.2 shows the response of the room with and without the bench when the fields are sensed and excited with the magnetic loops. The measurements are almost identical to those obtained from the full sized room (with the appropriate scaling in frequency). For the full sized room the bench resonances were reduced by loading the bench and making the transmission line lossy by bonding the sides of the bench to the walls of the room with conductive plastic sheet (60Ω per square). This absorber is easy to obtain but it is easily damaged and must be connected to the walls of the room. In order to remove the bench when necessary (e.g when testing a larger piece of equipment) the material must be clamped to the walls of the room which may mean that holes have to be made in order to fasten the clamps to the walls. This may not be possible in many rooms which are certified as any change to the room will invalidate the certification.

As it is possible to load the transmission line formed by the bench and walls of the room with the conductive sheet, so it should be possible to make the line lossy by loading it with the lossy ferrite tiles. The strips of tile were placed in various positions to determine the most effective placing for the tiles. The most effective placing was found to be along the back edge of the bench (Fig. 9.6.3) with the tiles either flat on the bench or flat along the back wall. This is the 'short circuit' end of the transmission line formed by the bench and the walls of the room and is where the currents flowing on the bench will be at their greatest. The magnetic fields will therefore also be at a maximum so that the maximum energy may be dissipated by the absorber. Placing the absorber in this position reduced the bench resonances but not to the same level as the

conductive sheet in the full sized room. However, it did reduce the resonances by enough to be able to see the effect of the load in the room, but the first resonance could still be observed above the general response. This should be further investigated in the full sized room.

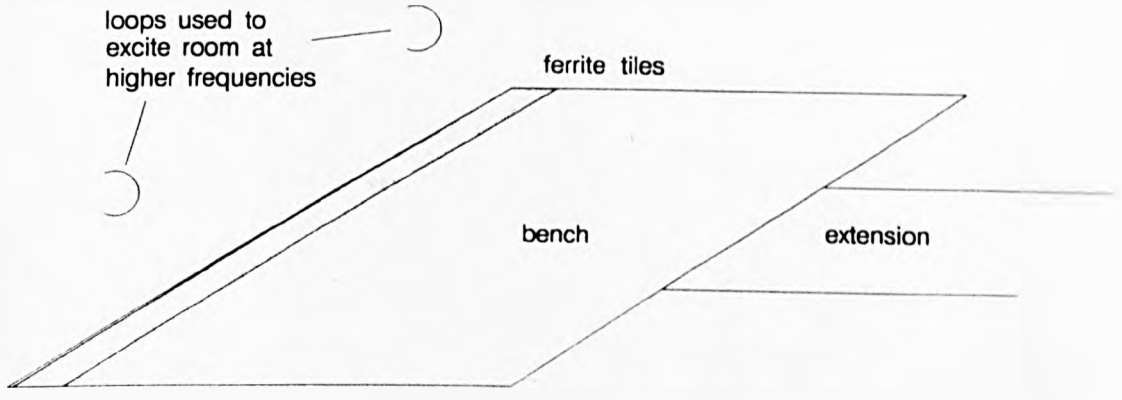

Fig. 9.6.3 The most effective positioning of ferrite for reducing the bench resonances

9.6.2 The effect of adding the bench on the measurements

It was found in the initial work on carbon loaded absorbers that the addition of the bench perturbed the fields so that the absorber was not necessarily positioned at the field maximum. However, it was found that providing the absorber was placed at the end of the room remote from the bench the frequency response was not greatly altered, i.e. it was still relatively flat. This is because the bench on its own also flattens the response at the higher frequencies as it introduces more resonances into the room (see Fig. 9.6.2 a and b).

The bench was added to the model room with the full ferrite load in place. The bench was not loaded in any way so the electric probes were used to excite and sense the fields. This is because the probes do not couple well with the transmission line formed by the bench so that the bench resonances are not dominant. When equipment is tested inside a screened room the EUT is placed on the bench and will couple strongly with the transmission line so the bench will resonate and will need to be damped.

The response of the room was recorded with the loading at the end of the room remote from the bench and close to the bench. The measurements are shown in Fig. 9.6.4. It can be seen that in general the response is flatter with the load remote from the bench although the difference is not as marked as that obtained with the carbon load used in the full room.

Fig. 9.6.5 shows the response when the fields are sensed by the model biconical dipole. The bench is loaded with 3 strips of ferrite tile against the back wall of the room (Fig. 9.6.3). Fig. 9.6.5 a shows the response when the room is excited by the small electric dipole close to the bench and Fig. 9.6.5 b shows the response when the room is excited by a magnetic loop. The ferrite loading of the bench means that the 3 strips have been removed from the room load (those hatched in Fig. 9.2.2). Fig. 9.6.6 a and b are the same measurements carried out with the carbon load.

The carbon load (Fig. 9.6.6) gives a slightly smoother response but a modest quantity of extra ferrite should improve this. Even without any improvement Fig. 9.6.5 shows a good reduction in the variability of the frequency response (+/- 10dB about a smooth curve instead of +/- 30dB).

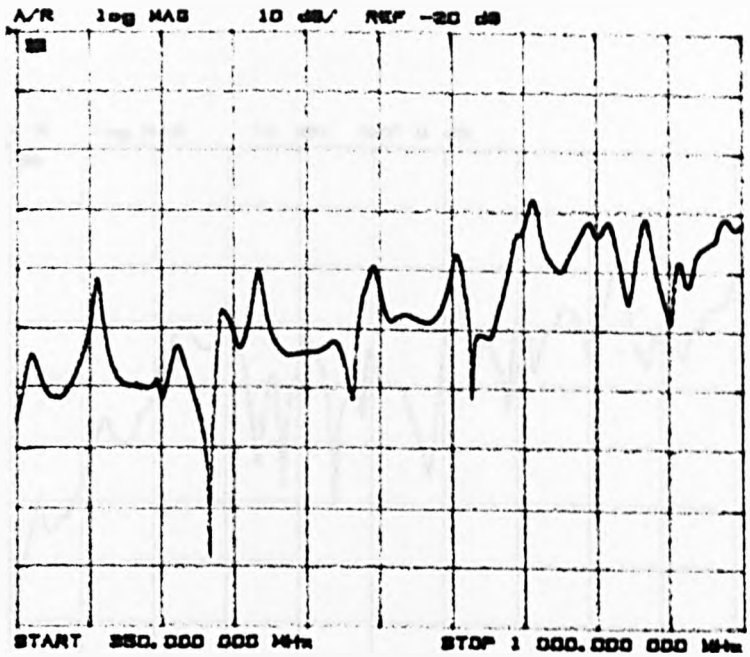

a) load near bench

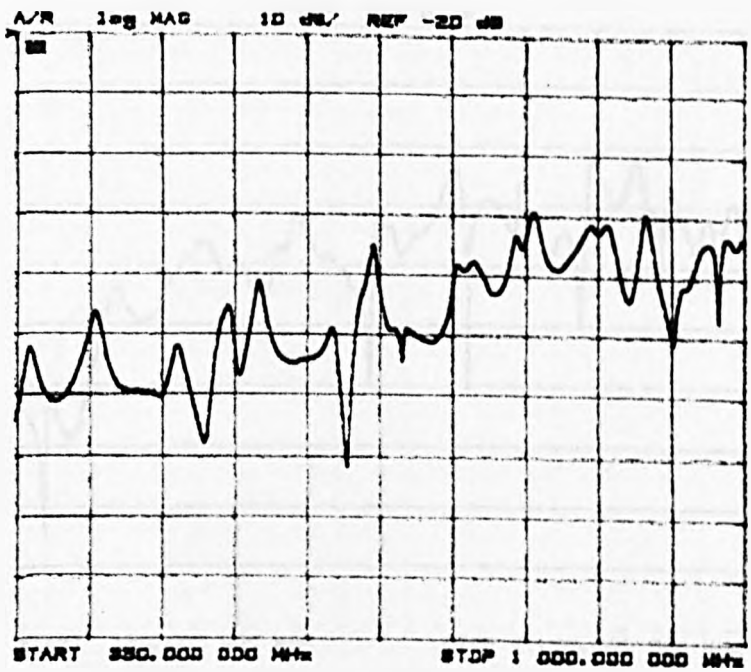

b) load remote from bench

Fig. 9.6.4 Frequency response of ferrite loaded room with bench (electric probe source and sense)

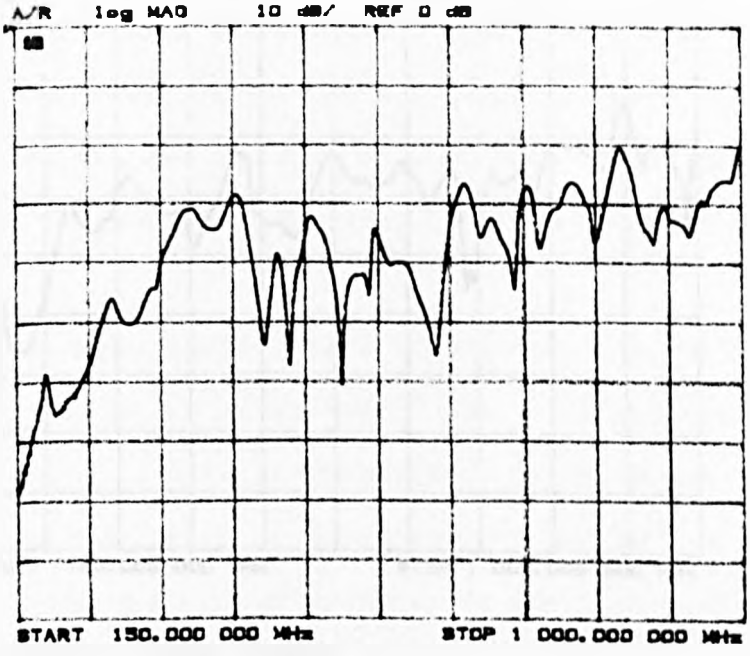

a) electric probe source

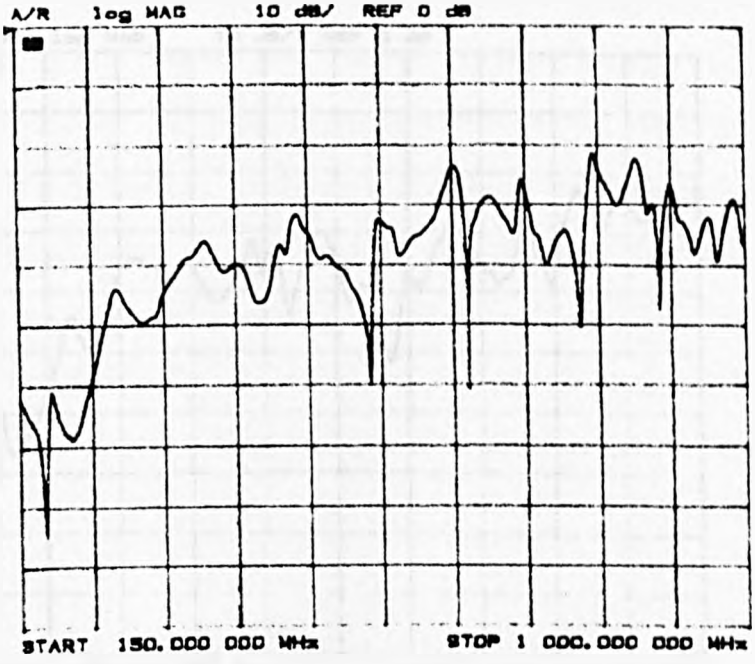

b) magnetic loop source

Fig. 9.6.5 Frequency response with ferrite load remote from bench (biconical dipole sense)

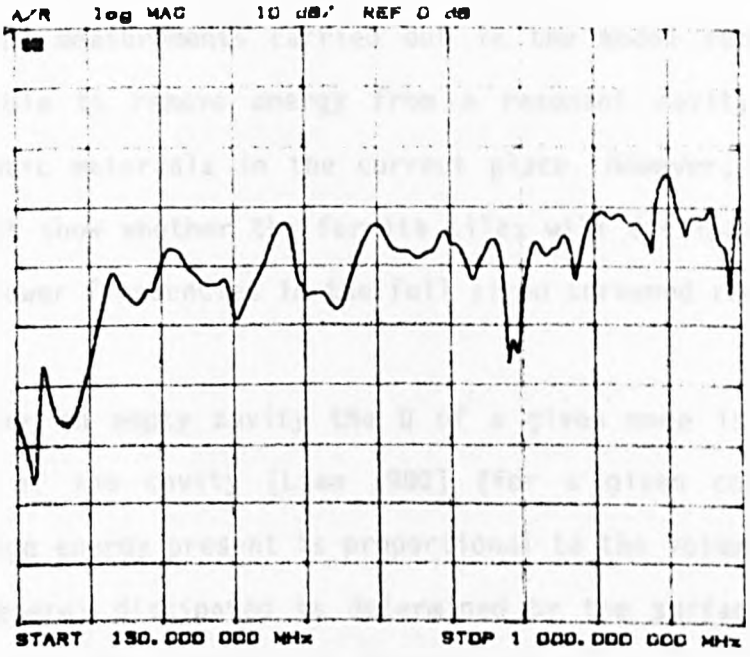

a) electric probe source

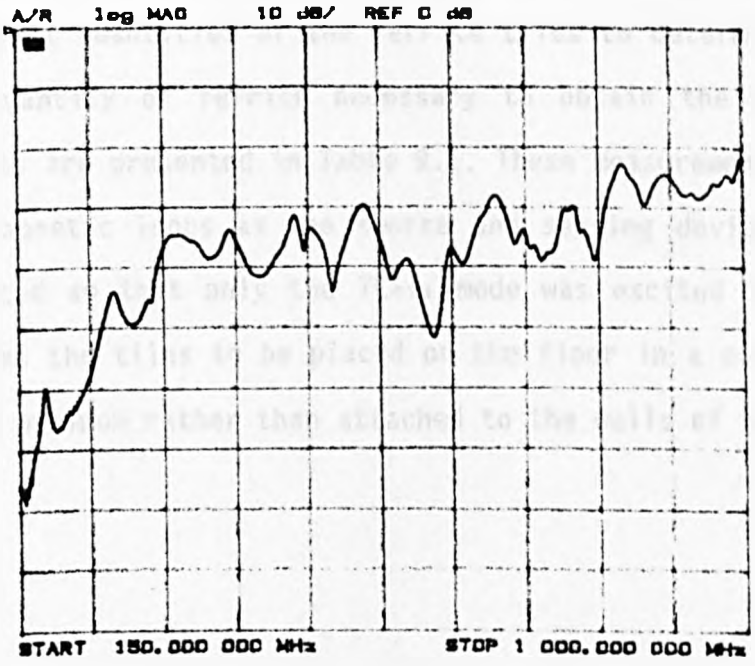

b) magnetic loop source

Fig. 9.6.6 Frequency response with carbon load remote from bench (biconical dipole sense)

9.7 Ferrite In The Full Sized Room (First Mode Only)

The measurements carried out in the model room show that it is possible to remove energy from a resonant cavity by placing lossy magnetic materials in the correct place. However, these measurements do not show whether the ferrite tiles will dissipate enough energy at the lower frequencies in the full sized screened room.

For an empty cavity the Q of a given mode is determined by the size of the cavity [Liao 1980] (for a given construction) as the average energy present is proportional to the volume of the cavity and the energy dissipated is determined by the surface area. This could mean that the quantity of absorber in the room needs to be increased with the volume of the cavity instead of the area.

The first resonance in the full sized room was investigated with different quantities of the ferrite tiles to determine the scaling of the quantity of ferrite necessary to obtain the same results. The results are presented in Table 9.1. These measurements were made using the magnetic loops as the source and sensing devices with the loops oriented so that only the TE_{011} mode was excited (Fig. 9.7.1). This enables the tiles to be placed on the floor in a position of magnetic field maximum rather than attached to the walls of the room.

layout of absorber	Q
empty room	5130
1 ferrite tile placed in centre of floor	4280
5 tiles placed in a line (Fig. 9.7.2a)	540
25 tiles in a square in the centre of floor	180
15 tiles in line on floor (Fig. 9.7.2b)	90
15 tiles in line on floor (Fig. 9.7.2c)	90
25 tiles in symmetrical line on floor (Fig. 9.7.2d)	52

Table 9.1 The Q of the first resonance in the full sized room for various quantities and layout of ferrite tile

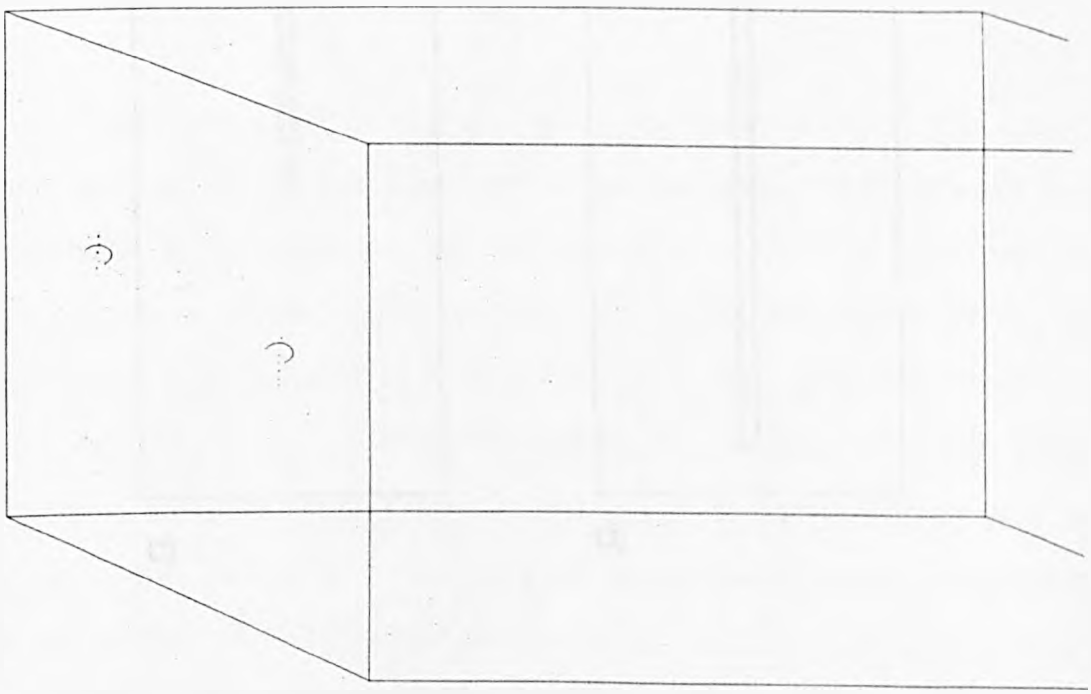

Fig. 9.7.1 Orientation of loops to excite TE_{011} only

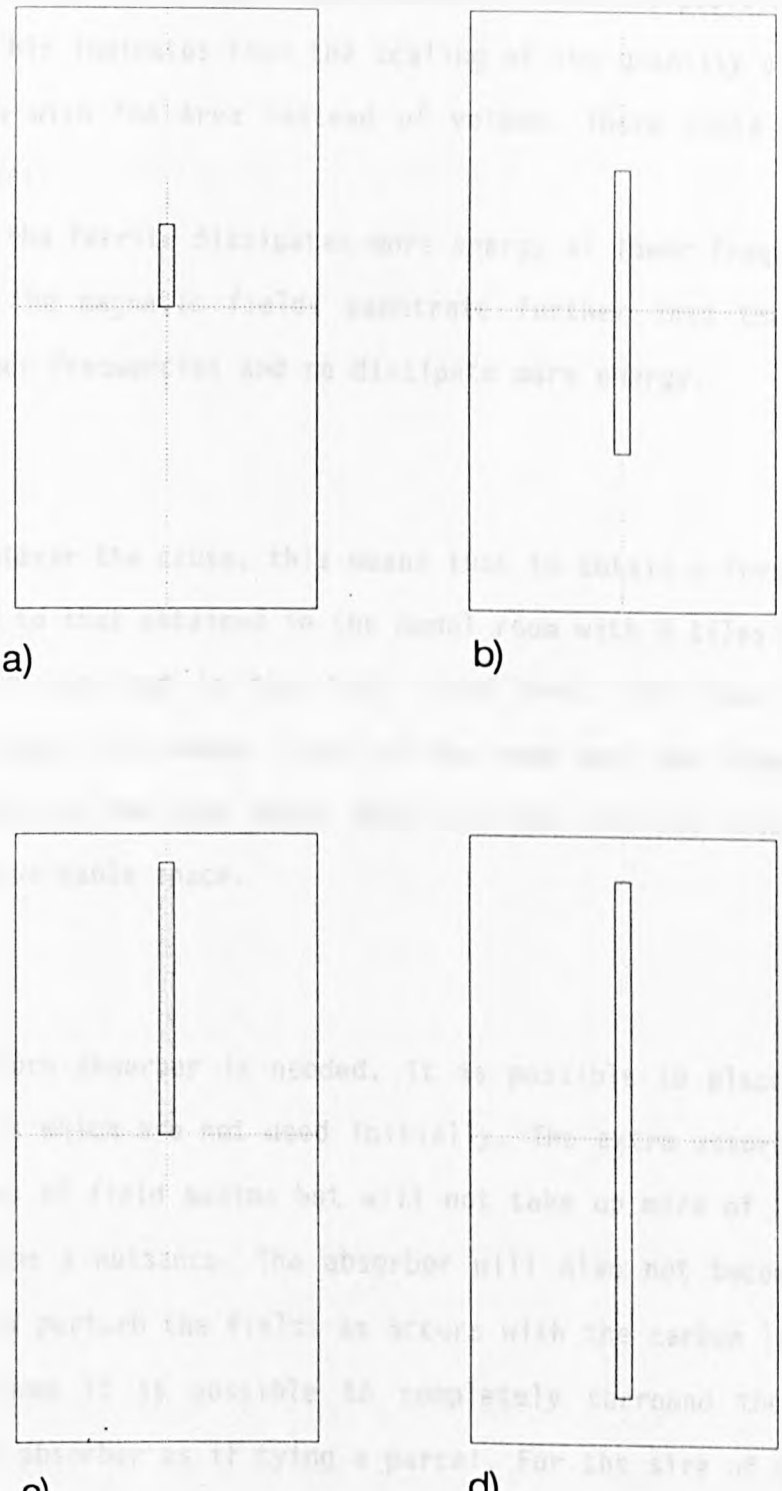

Fig. 9.7.2 Positioning of ferrite tiles on floor of full sized room

The results shown in Table 9.1 show that 25 tiles placed in a line on the floor give a Q of 52 which is only 2 higher than that obtained when the 5 small strips were placed in the same position in the model room. This indicates that the scaling of the quantity of absorber need only be with the area instead of volume. There could be two reasons for this:-

1) the ferrite dissipates more energy at lower frequencies.

2) the magnetic fields penetrate further into the tiles at the lower frequencies and so dissipate more energy.

Whatever the cause, this means that to obtain a frequency response similar to that obtained in the model room with 5 tiles only 125 tiles would be required in the full sized room. The floor tiles can be placed under the wooden floor of the room and the others attached to the walls of the room where they will not intrude into the room and take up valuable space.

If more absorber is needed, it is possible to place the extra on the walls which are not used initially. The extra absorber will be in positions of field maxima but will not take up more of the room space and become a nuisance. The absorber will also not become excessively bulky and perturb the fields as occurs with the carbon loaded foam. In the extreme it is possible to completely surround the room with a strip of absorber as if tying a parcel. For the size of room used here even if the strips of tiles need to be extended around the room the total number of tiles required is only 720. To fully line the room would take just over 5000 tiles.

9.8 Full Load in the Full Sized Room

The results of a measurement carried out in the full sized room are shown in Fig. 9.8.1. The absorber was positioned in strips one tile wide as was shown in Fig. 9.2.2. The conductive bench was in the room and was damped using the conductive cloth as with the carbon load described in Chapter 7. Again the source was a small electric dipole placed 10cm from the front of the bench. The sensor was the biconical dipole 1m from the source (vertically orientated).

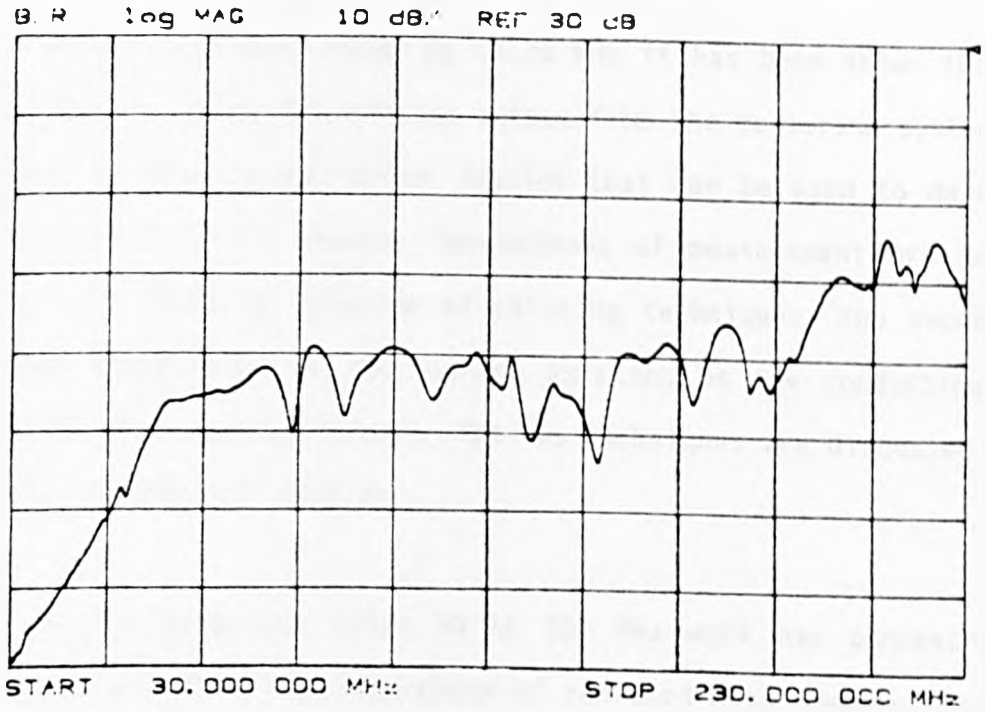

Fig. 9.8.1 Fully loaded room (magnetic room load), electric dipole source, biconic dipole sense.

The results shown in Fig. 9.8.1 indicate that the ferrite tiles are effective at reducing the energy within the resonant cavity and should be useful where the bulk of the carbon loaded absorber may be a problem. The overall response is slightly flatter than that obtained for the E field damping, probably due to the perturbation of the fields by the carbon loaded absorbers.

10 CONCLUSIONS

10.1 Introduction

The aim of the research described in this thesis was to develop quantitive test methods for the measurement of radiated Electromagnetic emissions in a screened room in the frequency range up to 200 MHz. These methods were to be simple to carry out and not require expensive adaption of existing measurement facilities.

In the frequency range up to 30 MHz it has been shown that it is possible to relate the voltage output from the measuring system to the moment of the six equivalent dipoles that can be used to describe an electrically small source. Two methods of measurement are possible, the first being an adaption of existing techniques; the second using direct measurement of the voltage existing on the conducting bench, instead of a sensing antenna. The two techniques are discussed in more detail in the next section.

In the frequency range 30 to 200 MHz work has concentrated on reducing the frequency dependence of radiated measurements carried out in screened rooms. Two related methods of reducing the Q of cavity resonances have been investigated successfully. These use either carbon or ferrite loaded materials to absorb energy from the resonant system and reduce the Q of the resonances. The TEM mode resonances which exist on the conducting bench have also been reduced by bonding the bench to the walls of the room with resistive cloth. Work has not been specifically carried out on relating the measurement to the dipole moment but it is assumed that if the source is subresonant this may be done with little difficulty.

10.2 The Lower Frequencies

Within the lower frequency range it has been shown that there are two techniques which can be used to carry out emission tests on small pieces of equipment with a reduced degree of measurement uncertainty. In addition it has been shown that with each of these tests it is possible to distinguish between electric and magnetic dipole sources.

Each technique for the measurement of the potential emissions from a piece of electronic equipment has its own advantages and disadvantages.

10.2.1 Resistively loading the end of the bench extension

The easiest technique to carry out which needs no alteration to the room is to load the end of the bench with as low an impedance as possible. The easiest method of constructing such an impedance is to support the end of the conducting extension on a column of carbon loaded absorber (such as AN 79). For best results the base of the absorber should be electrically connected to the floor of the room. If this is not carried out the capacitive connection between the absorber and the floor adds an extra impedance to the load which reduces its effect.

A perfectly flat frequency response has not been obtained but it should be possible to get a flatter response for the electric dipole source if a lower impedance load could be constructed. The response for the magnetic source cannot be made perfectly flat however good the load. The fall off at lower frequencies is due to

the inductive coupling between the source and the TEM transmission line which does not operate as effectively at lower frequencies. However, if a good enough load is constructed the frequency response for the electric dipole source should become flat due to the capacitive coupling between the source and the sensing 'antenna' which dominates the measurements at the lower frequencies.

This method of testing distinguishes well between the electric and magnetic dipole sources. However, because the coupling to the bench of the two sources does not change in the same way with frequency it is not particularly easy to obtain the relative moments of the two sources if both are present.

The differentiation between the orientations of the magnetic dipole source is good. Although the differentiation for the electric dipole source is not as effective due to the potential which still exists between the bench and a horizontal dipole it is still possible to obtain the amplitude for the orientation with the greatest dipole moment.

10.2.2 Direct measurement technique

The second method is to measure the voltage at the end of the transmission line (the bench when the extension has been removed). This is slightly more difficult to carry out and it is also necessary to sum the voltages measured from the two straps to be able to separate the waves due to different orientations of magnetic dipole. Very careful construction is necessary to ensure that the same phase shift occurs through each arm of the circuit.

The change in measured voltage with source position is very easy to use to distinguish between the source dipole types because for an electric source the received voltage goes up and for the magnetic it goes down as the source is moved back. The measured voltage for both electric and magnetic source change in the same manner with frequency so that it is easier to obtain the relative moments of two dipole sources across the frequency range.

The measured voltage falls off with reducing frequency for both electric and magnetic dipole sources so that this method is less sensitive than the first for the electric source. However, it does mean that if both sources are present the electric source will not mask the magnetic source if they are at the same level.

For both of the techniques above it is assumed that the equipment under test is electrically small so that it can be placed on the bench and moved back towards the wall. However, it is unlikely that equipment will be small enough for it to be moved back so that the front of the EUT is 10cm from the back of the bench. This may

introduce errors when the measured signal with the source at the back of the bench is used to determine the magnitude of the moment of the source dipole. It is also assumed that the source of emissions is the equipment itself and not the cables connecting the unit under test to other equipment or power supplies. As emissions from cables are distributed the results given in this thesis will not give the correct results for cables. This is the subject of a separate investigation.

10.3 The Higher Frequencies (30 to 200 MHz)

It has been shown that the strategic placing of carbon loaded and ferrite absorbers can be used to reduce the Q of resonances within a screened room used for emission measurements. The reduction in Q of the individual resonances enables the individual modes to blend into each other to give a relatively flat frequency response. In turn this will enable the measurements made in the screened room to be calibrated so that the results can be compared with those made on an open field test site. Even if this is not carried out it means that initial 'look see' measurements which are carried out to determine which frequencies are present will not miss some emissions at frequencies which occur at nulls in the frequency response of the room.

The reduction in the Q of the resonances also reduces the change in field with position, so that a small change in the positioning of the source or sensing antenna gives a reduced change in the measured field. This means also that the positioning of the source and sensing antenna is not so critical and measurements can be repeated and compared.

The use of the two types of absorber each has its own advantages and disadvantages which are described below.

1. The carbon loaded absorber is easily available and is relatively cheap. For a room of the size used only 6 blocks are required. However, the blocks are bulky and the whole load is not small and can get in the way of people and equipment. In particular if the room is any smaller than that used it will be difficult to position the sensing antenna 1m from the source

without it touching the absorber, particularly when the EUT is positioned .1m from the front of a 1m deep bench. If a frame is constructed to hold the absorber it should not be difficult to position the absorber with reasonable accuracy each time it is used.

2. The magnetic absorbers are more expensive than the carbon loaded absorbers but they do have advantages. The thin tiles are positioned around the walls of the room and under the wooden floor where they do not get in the way of people or equipment. The response obtained so far is not quite as smooth as that obtained with the carbon loaded absorbers but it is easy to add further absorber by increasing the length of the strips of absorber. With the magnetic absorber the addition of extra tiles does not perturb the fields within the room to the same extent as the carbon loaded foam does and the extra tiles will absorb more energy. The tiles can be positioned behind the carbon loaded absorbers which are used to make screened rooms anechoic at higher frequencies so that the room can be used for emission measurements over the whole range of frequencies from 10 KHz upwards. The carbon loaded absorbers will absorb some energy at frequencies below which it is anechoic and the response should be further flattened. The carbon loaded absorbers will absorb energy from the electric fields which are perpendicular to the walls as well as absorbing the initial wave from the source at frequencies where the depth of absorber is sufficient to present an impedance of 377 Ω to the plane wave from the source. The ferrite tiles can be left in position for all measurements whereas in an anechoic chamber the carbon loaded absorber would need to be removed for measurements carried out at frequencies where the room was anechoic as it would otherwise

cause reflections which could disturb the 'quiet zone'.

The bench resonances can be reduced by using either the ferrite tiles along the back of the bench or the conductive plastic connected between the walls and the edges of the bench. The conductive plastic reduces the resonances further than the ferrite tiles but it is not so easily used as it can get in the way when setting up equipment and is easily damaged. The tiles are also easily damaged but this is less likely to occur as they are firmly fixed along the back of the bench against the back wall.

This technique is designed assuming small sources. It has not been investigated in any detail using larger sources which will distort the field distributions and may reduce the smoothing effect of the absorber (the bench may not be needed for large free standing objects). This technique has also not been tried in larger rooms but should still work as the arguments are the same. In larger rooms the fields will be distorted by a proportionally smaller amount by the source etc than in a small room where the source and antenna could be near to the walls of the room.

10.4 Merging The Methods For The Two Frequency Ranges

It should also be possible to use both the low and high frequency techniques at the same time (i.e. to arrange the tests so that only the bench extension -if used- and the antennas need be moved between the measurements). This would reduce the time taken between measurements in the two frequency ranges.

The ferrite loading of the room (i.e. tiles on the walls) in particular can be left in position for the lower frequency measurements although the carbon loaded absorber may get in the way in small rooms. The ferrite loading of the bench was not as successful as the resistive loading for reducing the bench resonances: the resistive loading (i.e loss) can be left on the bench for the lower frequency measurements although this will reduce the sensitivity of the measurements carried out at frequencies below 30 MHz.

10.5 Suggestions for Further Work

10.5.1 Different sized rooms

Although these techniques have been shown to work in the screened room available at York they have not been tried in rooms with different dimensions. In particular the loading of the room with the carbon loaded foam or the ferrite tiles should be investigated further with different rooms so that the quantity of absorber needed in different sized rooms can be determined.

10.5.2 Merging the methods

It should be possible to merge the techniques for the two frequencies as stated above but detailed measurements need to be made to confirm that this can be carried out, particularly in different sized rooms to check that the sensitivity of the lower frequencies would not be reduced so far that measurements could not be carried out.

10.5.3 Size of equipment under test

The work carried out in this thesis has been carried out using electrically small sources. Further investigation should be carried out on the effect of larger sources, particularly for floor standing equipment in the frequency range 30 to 200 MHz as the larger equipment will perturb the field distributions within the room reducing the effect of the absorbers. Also work has not been carried out on

relating the measured voltage to the dipole moment of the source in the higher frequency range. Although it is assumed that if the source is subresonant the output of the measuring antenna will be proportional to the dipole moment of the source, this should be investigated more thoroughly.

REFERENCES-B-

W.S.Bennet
'Comment on calculation of site attenuation from antenna factors'
IEEE Trans EMC, vol.EMC-25, 1983, pp 121

E.L.Bronaugh
'Comparison of 4 open area test sites'
7th International Symposium on EMC, Zurich, March 1987, pp 339-345

BS 6572 :1984
'Specification for limits and measurement of spurious signals generated by data processing and electronic office equipment'

BS 800 :1983
British Standard Specification for Radio interference limits and measurements for household appliances, portable tools and other electrical equipment causing similar types of interference'

REFERENCES-C-

D.C.Chang and M.T.Ma
'A method of determining the emission and susceptibility levels of electrically small objects inside a TEM cell'

H.C.Chen
'Theory of electromagnetic waves'
McGraw Hill, 1985, pp 123-175

P.Corona, G.Latmiral, E.Paolini and L.Piccioli
'Use of a reverberating enclosure for measurements of radiated power in the microwave range'
IEEE Trans EMC vol 18, May 1986

P.Corona, G.Latmiral and E.Paolini
'Performance and analysis of a reverberating chamber with variable geometry'
August 1980, pp 2-5

M.L.Crawford
'Generation of standard EM fields using TEM transmission cell'
IEEE trans EMC vol 16, November 1974, pp 189-195

M.L.Crawford et al
'Predicting free space radiated emissions from electronic equipment using TEM cell and open field site measurement'
IEEE Symposium on EMC, Baltimore, 1980

M.L.Crawford, J.L.Workman and C.L.Thomas
'Expanding the bandwidth of TEM cells for EMC measurements'
IEEE trans EMC, vol.EMC-20, 1988, pp 368-375

M.L.Crawford and J.L.Workman
'Using a TEM cell for EMC measurments of electronic equipment'
NBS Technical note 1013, April 1979

G.K.Deb, M.Mukherjee

'EM susceptability studies and measurements on electro-explosive devices'

IEEE 1985

Defence Standard 59/41

Electromagnetic compatibility

part 1 / issue 3 1986 General requirements

part 3 / issue 2 1986 Technical requirement, test methods and limits

part 4 / issue 1 1987 Open site testing

E.E.Donaldson, W.R.Free, D.W.Robertson, J.A.Woody,

'Field measurements made in an enclosure'

Proc IEEE, vol 66, no.4, April 1972, pp 464-472

L.N.Dworsky

'Modern transmission line theory'

Willey,NY, 1979, pp 38-39

REFERENCES-E-

W.H.Emerson
'Electromagnetic wave absorbers - a useful tool for engineers'
Commun Int, vol.4, 1977, pp 22-31

W.H.Emerson
'Electromagnetic wave absorbers and anechoic chambers throughout the years'
IEEE Trans Antennas and Propag, vol.ap-21, 1973, pp 484-490

REFERENCES-F-

A.N.Faught, J.T.Dowell and R.D.Scheps
'Shielding material insertion loss measurement using a dual TEM cell measuring system'
IEEE International Symposium on Electromagnetic Compatibility
Washington, 1983

FCC, OST 55, 1982
'Characteristics of open field test sites'

FCC, OST MP-4, 1983
'FCC methods of measurement of radio noise emissions for computing devices'

FCC, 47 CFR 15 (Code of Federal Regulations part 47)
'limits for computing devices'

'Calibration of a radiation measurement site - site attenuation'
FCC docket 21371, Appendix A, Bulletin OCE44, Sept 1977

A.Feh and D.Bianchi
'Dipoles' EM field attenuation versus distance in near field
and above reflecting ground'
EMC Symposium, Rotterdam, 1979, pp 63-66

R.G.Fitzgerrell
'Site attenuation'
IEEE Trans EMC vol 28, Feb 1986, pp 38-40

R.G.Fitzgerrell
'E-Fields over ground'
IEEE symposium on EMC (Arlington, VA), 1983

W.R.Free
'Radiated EMI measurements in shielded enclosures'
IEEE Int Symposium on EMC, Washington DC, 1967, pp 43-53

R.F.German

'Comparison of semi-anechoic chambers and open field site attenuation measurements'

IEEE Int EMC Symposium, Santa Clara CA, 1982,

K.H.Gonschorek and A.Kohling

'The microwave anechoic chamber - a prerequisite for testing electromagnetic compatibility'

Siemens Power Eng. (Germany), vol.6, 1984, pp 292-295

S.Goodwin and A.C.Marvin

'A transmission line model of cable to antenna coupling inside a screened room'

IEEE Trans EMC, Vol.11 (to be published)

L.G.Gruner

'High order modes in rectangular coaxial waveguides'

IEEE Trans Microwave Theory, Vol.MTT-15, 1967, pp 483-485

R.F.Harrington

'Time harmonic electromagnetic fields'

McGraw Hill, 1961, pp 66-81

D.S.Heisman

'Investigating open area test site measurement differences'

7th International Symposium on EMC, Zurich, March 1987, pp 335-338

D.A.Hill

'Bandwidth limitations of TEM cells due to resonances'

J. Microwave power, vol 18 no2,1983, pp 181-195

F.L.Hofman

'Correlation of theoretical and measured site attenuation in an absorber lined chamber'

IEEE Int EMC Symposium, Washington DC, 1983

P.A.Hyde and M.S.Leak

'A case study - living with high power broadcasting transmitters'

IERE International conference on EMC, York 1986

JAN-1-222, Joint Army-Navy specification, June 14, 1945
'Interferance measurements, radio methods of, 150 kilocycles to
20 Megacycles (for components and complete assemblies)'

E.C.Jordan and K.G.Balmain
'Electromagnetic waves and radiating systems'
Prentice-Hall, 1968, pp 545-548

T.Kawana and S.Miyajima
'Theoretical investigation of site attenuation by means of
mutual impedance between antennas'
Proc 3rd symposium and technical exhibition
on EMC (Rotterdam), 1979, pp 83-88

B.Keiser
'Principles of EMC'
Artech, 3rd edition, 1987, pp 353-355

G.H.Koepke and M.T.Ma
'A new method for determining the emission characteristics of
an unknown interferance source'
IEEE Int Symposium on EMC, Santa Clara CA, 1982

D.Konigstein and D.Hansen

'A new family of TEM cells with enlarged bandwidth and optimised working volume'

7th International Symposium on EMC, Zurich, March 1987, pp 127-132

Kraus

'Electromagnetics'

McGraw Hill, 1985, pp 597 - 604

REFERENCES-L-

S.Y.Liao

'Microwave devices and circuits'

Prentice-Hall, 1980, pp 134-135

B.H.Liu,D.C.Chang and M.T.Ma

'Eigenmodes and the composite quality factor of a reverberating chamber'

NBS technical note 1066, August 1983

M.Ma, M.Kamda, M.Crawford and E.Larsen
'A review of Electromagnetic Compatibility/Interferance measurement methodologies'
IEEE trans EMC vol 7, March 1985, pp 388-411

R.A.Magnuson
'An experiment in reducing reflections in a shielded room'
IEEE International Symposium on EMC, Santa Clara, 1982, pp 237-243

A.C.Marvin
'The use of screened rooms for the identification of radiation mechanisms and the measurement of free space emissions from electrically small sources'
IEEE trans EMC vol.26, Nov.1984, pp149-153

G.Meyer
'The TEM measuring line - a critical overview'
4th Symposium on EMC, Zurich, 1981

Military Standard 461
April 1980, Department of Defence,
Washington, DC 20360, USA

D.Mis and A.J.Visek
'FCC/VDE radiated measurements - potential differences in test results between test sites as a function of extrapolation and the use of published antenna factors'
IEEE Symposium on EMC, San Diego, 1986

S.R.Mishra and S.C.Kashyap

'Measurement of Electromagnetic field distribution in an absorber lined chamber'

7th International Symposium on EMC, Zurich, March 1987, pp 115-120

REFERENCES-N-

Y.Naito and K.Suetake

'Applications of ferrite to electromagnetic wave absorber and its character'

IEEE trans microwave theory and tech, vol.MTT19, 1971, pp 65-72

Y.Naito and T.Mizumoto

'Effect of doping carbon in an electromagnetic wave absorber rubber ferrite'

Electron and commun JPN, vol.70, 1987, pp 12-17

'Construction of a large transverse TEM cell'

NBS tech note 1011, Feb 1979

T.J.F.Pavlasek and S.R.Mishra
'Ground plane influence on EMC measurement'
7th International Symposium on EMC, Zurich, March 1987, pp 353-358

M.A.Plonus
'Applied electromagnetics'
McGraw Hill, 1978, pp 569-573

Saad
'Microwave engineers handbook, vol 1'
Artech, 1971

G.H.Schildt
'Influence of man made noise on the reception of standard frequency transmission at VLF'
EMC Symposium, Rotterdam, 1979, pp 181-185

A.A.Smith, R.F.German and J.B.Pate
'Calculation of site attenuation from antenna factors'
IEEE Trans EMC vol 24, August 1982, pp 301-316

A.A.Smith
'Standard site method for determining antenna factors'
IEEE Trans EMC, vol.EMC-24, 1982, pp 316-322

I.Sreenivasiah, D.Chang and M.Ma
'Emission charateristics of electrically small radiating sources from tests inside a TEM cell'
IEEE trans EMC vol 23, Aug 1981, pp 113-121

A.Sugiura and M.Okamura
'Evaluation of interferance generated by microwave ovens'
7th International Symposium on EMC, Zurich, March 1987, pp 267-269

REFERENCES-T-

T.Tang and M.W.Gunn
'Terminal voltage of a receiving antenna above a conducting plane'
7th International Symposium on EMC, Zurich, March 1987, pp 347-352

R.S.Tebble and D.J.Craik
'Magnetic materials'
John Willey 1969, pp 402-410

J.Tippet and D.Chang
'Radiation characteristics of electrically small devices in a TEM transmission cell'
IEEE Trans EMC vol 18, Nov.1976, pp 134-140

A.Tsaliovich
'Anechoic room versus open area test site - a case for EMC study'
7th International Symposium on EMC, Zurich, March 1987, pp 359-364

VDE 0875 part2 1985
'Measurement of radio interferences, measurement of radio interference field strength'

VDE 0871/6 1978
'Radio frequency interference suppresion of radio frequency equipment for industrial, scientific and medical (ISM) and similar purposes'

W.C.Webb
'Managing and coping with electromagnetic environments- pioneering perspectives'
AESS newsletter, April 1985, pp 5-8

P.F.Wilson, M.T.Ma
'Simple approximate expression for higher order mode cutoff and resonant frequencies in TEM cell'
IEEE trans EMC, vol 28, 1986, pp 125-130

P.F.Wilson and M.T.Ma (a)
'A study of techniques for measuring the electromagnetic shielding effectiveness of materials'
NBS technical note 1095, May 1986

A.D.Yaghjiam

'Efficient computation of antenna coupling and fields within the near field region'

IEEE Trans Antennas and Propagation, vol 30, 1982, pp 133-138

APPENDIX A MATRIX ANALYSIS

Matrix analysis can be used to analyse a cascade of two terminal networks. Each element in the circuit is described by an ABCD (transmission) matrix which relates the input and output currents and voltages as shown in equation A.1. The currents and voltages are shown in Fig. A.1.

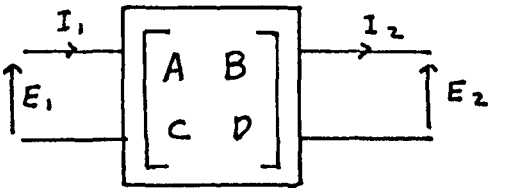

Fig. A.1 The relationship between the currents and voltages

$$\begin{bmatrix} E_1 \\ I_1 \end{bmatrix} = \begin{bmatrix} A & B \\ C & D \end{bmatrix} \times \begin{bmatrix} E_2 \\ I_2 \end{bmatrix}$$

A series impedance is described by the matrix

$$\begin{bmatrix} 1 & Z \\ 0 & 1 \end{bmatrix}$$

where Z is the impedance.

A shunt addmittance is

$$\begin{bmatrix} 1 & 0 \\ Y & 1 \end{bmatrix}$$

where Y is the addmittance

A length of transmission line of normalised impedance is

$$\begin{bmatrix} \cosh \gamma l & Z0 \sinh \gamma l \\ Y0 \sinh \gamma l & \cosh \gamma l \end{bmatrix}$$

where l is the length of the line and γ is the propogation term

$$\gamma = \sqrt{(R + j\omega L)(G + j\omega C)}$$

which can be simplified to the following for a lossless line

$$\begin{bmatrix} \cos \frac{2\pi l}{\lambda} & jZ0 \sin \frac{2\pi l}{\lambda} \\ \frac{j}{Z0} \sin \frac{2\pi l}{\lambda} & \cos \frac{2\pi l}{\lambda} \end{bmatrix}$$

where λ is the wavelength

The transmission matrix can be transformed to an admittance matrix so that two parallel networks with a common return can be modelled (the sum of the admittance matrices for each network gives the admittance matrix for the whole circuit). The total admittance matrix can then be transformed back to the transmission matrix for completion of the circuit analysis.

The relationships between the two sets of parameters are given below.

$$Y_{11} = \frac{D}{B} \qquad Y_{12} = -\frac{\Delta T}{B}$$

$$Y_{21} = -\frac{1}{B} \qquad Y_{22} = \frac{A}{B}$$

$$A = -\frac{Y_{22}}{Y_{21}} \qquad B = -\frac{1}{Y_{21}}$$

$$C = -\frac{\Delta Y}{Y_{21}} \qquad D = -\frac{Y_{11}}{Y_{21}}$$

The input impedance of a circuit is given by

$$Z_i = \frac{(A \times ZL) + B}{(C \times ZL) + D}$$

where ZL is the load impedance

The voltage across the output load is given by

$$V_o = \frac{I_i}{\frac{D + C}{ZL}} \qquad \text{or} \qquad V_o = \frac{V_i}{\frac{B + A}{ZL}}$$

were I_i is the input current
and V_i is the input voltage

The individual tranmission matrices are used to model a complete circuit by multiplying the individual matrix elements together in the order in which the relevant elements occur in the circuit as is shown in Fig. A.2.

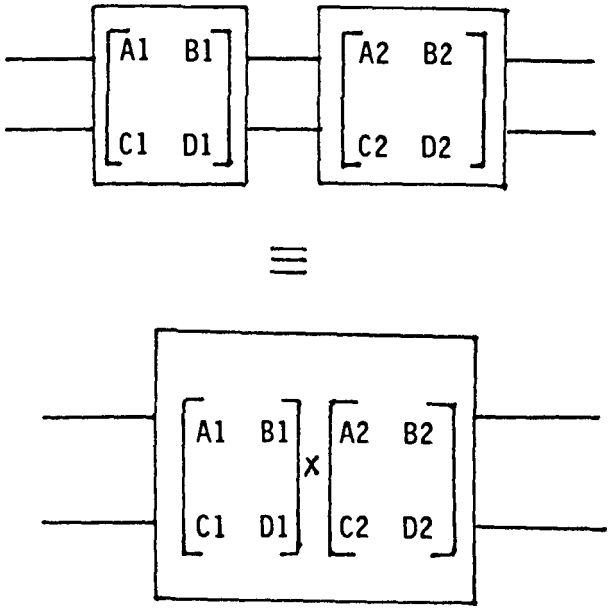

Fig. A.2 The cascading of circuit elements

It is necessary to ensure that the matrices are multiplied in the correct order although it is possible to carry out the multiplication for parts of the circuit at a time providing the overall order is maintained.

APPENDIX B PROGRAM TO MODEL THE STANDARD TEST SETUP

```
C      PROGRAM TO MODEL DIPOLE COUPLING IN A SCREENED ROOM FOR TEM MODES
C      PLOT RESULTS AS A FUNCTION OF FREQUENCY WITH CONSTANT POSITION
C      RESULTS FOR EACH DIPOLE AND THE DUAL
C
       IMPLICIT REAL (I-N)
       INTEGER J,M,K
       DIMENSION VE(5,100),VM(5,100),CMU(5),VD(5,100),PM(5,100),PE(5,100)
      2  ,PMR(5,100),PMI(5,100),PER(5,100),PEI(5,100),FA(100)
       COMPLEX VD,ZDM,IO,ZSM,ZA,A,B,C,D,ZI,VI,TOP,BOT,A1,B1,C1,D1,
      2   ZOE,ZSE,YSE,A2,B2,C2,D2,A3,B3,C3,D3,Y11C,Y12C,Y21C,Y22C,
      3   Y11,Y12,Y21,Y22,Y11T,Y12T,Y21T,Y22T,AP,BP,CP,DP
      4  ,A4,B4,C4,D4,A5,B5,C5,D5,BM,DM,ZB,ZE,GB,G,GE,X1,X2,X3
      5,CCOSH,CSINH,CTANH,ZS,AM,CM,COM0,COM1
C
       DATA U,EPS/12.47E-7,8.854E-12/
C
       OPEN(UNIT=1,FILE='DATA.DAT', STATUS='OLD')
       X = 20.0
       Y = 135.0
       W = 0
       COM0 = CMPLX(0.0,0.0)
       COM1 = CMPLX(1.0,0.0)
C
C     ENTER REQUIRED FREQUENCY ETC
       WRITE(5,5)
5      FORMAT(' ENTER 1 OR 2 TO READA FILE OR KEYBOARD')
       READ(5,*)E
       IF (E.EQ.1) GOTO 60
         WRITE(5,10)
10       FORMAT(' ENTER LOWER AND UPPER FREQUENCY  (MHZ)')
         READ(5,*)F1,F2
         WRITE(5,30)
30     FORMAT(' ENTER ZBENCH,ZEXT,RSORS (OHMS) AND CDIS,CAMP (PF)')
         READ(5,*)ZBR,ZER,RS,CD,CAMP
       WRITE(5,40)
40     FORMAT(' ENTER MUTUAL CAPACITANCE TO INNER AND OUTER CONDUCTOR
      2  FOR TX AND RX DIPOLES')
       READ(5,*)CP2,CP1,CA2,CA1
       WRITE(5,45)
45     FORMAT(' ENTER COUPLING CAPACITANCE IN PF')
       READ(5,*)CMU(1),CMU(2),CMU(3),CMU(4),CMU(5)
       WRITE(5,50)
50     FORMAT(' ENTER MUTUAL AND DIPOLE INDUCTANCE IN NH')
       READ (5,*)ML,LP
       WRITE(5,55)
55     FORMAT(' ENTER R AND C FOR LOSS ON BENCH AND EXTENSION')
       READ(5,*)RB,CBL,RE,CEL
       GOTO 53
60     READ(1,*)F1,F2,ZBR,ZER,RS,CD,CAMP,CP2,CP1,CA2,CA1,CMU(1),CMU(2 ),
      2CMU(3),CMU(4),CMU(5),ML,LP,RB,CBL,RE,CEL
       GOTO 53
53     WRITE(5,56)
56     FORMAT(' ENTER R AND C FOR LOAD ON END')
       READ(5,*)RR,CR
       WRITE(5,57)
57     FORMAT(' ENTER I AND R WHERE VIM=(R+JI)*VIE')
       READ(5,*)I,R
C
C     START CALCULATING PARAMETERS
```

```
      CB=SQRT(J*EPS)/ZBR
      CE=SQRT(J*EPS)/ZER
      LB=SQRT(J*EPS)*ZBR
      LE=SQRT(J*EPS)*ZER
      DF = (F2-F1)/99.0
C
C
C
C
      DO 100 M=1,100
      DO 100 J=1,5
      LS=1.1-(J*0.2)
      F = F1 + (M-1)*DF
      FA(M) = F
C
C LOAD IMPEDANCE
       AZ = -1000000.0/(6.284*F*(CAMP+CA2))
       ZA = CMPLX(0.0,AZ)
C
C INDUCED IMPEDANCE FOR MAGNETIC SOURCE
      ZI = (39.5*(F**2)*(ML**2)/1000000)/
     2   CMPLX(RS*2,6.284*F*LP/1000)
C
C LENGTH OF BENCH TO OPEN END
       LO = 1.0 - LS
C
C
C
C     CALCULATE GAMMA AND THE COMPLEX IMPEDANCE FOR EACH PORTION OF THE BENCH
C
C
      X1=CMPLX(0.0,6.284*F*LB*1000000)
      X2=CMPLX(RB,-1000000.0/(6.284*F*CBL))
      X3=CMPLX(0.0,6.284*F*CB*1000000)
      GB=CSQRT(X1*((1/X2)+X3))
      ZB=CSQRT(X1/((1/X2)+X3))
C
      X1=CMPLX(0.0,6.284*F*LE*1000000)
      X2=CMPLX(RE,-1000000.0/(6.284*F*CEL))
      X3=CMPLX(0.0,6.284*F*CE*1000000)
      GE=CSQRT(X1*((1/X2)+X3))
      ZE=CSQRT(X1/((1/X2)+X3))
C
C
C
C     CALCULATE Z SHORT FOR ELECTRIC AND MAGNETIC CASES
C
      ZS=ZB*CTANH(GB*LS)
      ZSM=ZS+ZI
C
C
C
C     MODEL THE TRANSMITION LINE AND DISCONTINUITY CAPACITANCE
C
       CALL TXLN(F,LO,ZB,1.0,ZE,CD,A,B,C,D,GB,GE)
C
C
C
C     CALCULATE Z OPEN FOR THE MAGNETIC CASE
C
      BOT = CMPLX(1.0,6.284*RR*F*CR/1000000)
      C1 = CMPLX(0.0, 6.284*CR*F/1000000) /BOT
      CALL MATRIX(A,B,C,D,COM1,COM0,C1,COM1,A2,B2,C2,D2)
      B3 = 1/CMPLX(0.0,6.284*CA1*F/1000000)
      CALL MATRIX(A2,B2,C2,D2,COM1,B3,COM0,COM1,AM,BM,CM,DM)
        ZOM =((AM*ZA)+BM)/((CM*ZA)+DM)
```

```
C
C     CALCULATE I OPEN FOR THE ELECTRIC CASE
C
      Y11C = CMPLX(0.0,6.284*CMU(J)*F/1000000)
      Y12C = CMPLX(0.0,-6.284*CMU(J)*F/1000000)
      Y21C = CMPLX(0.0,-6.284*CMU(J)*F/1000000)
      Y22C = CMPLX(0.0,6.284*CMU(J)*F/1000000)
      BOT = CMPLX(0.0,6.284*F*CP1/1000000)
      CALL MATRIX(COM1,1/BOT,COM0,COM1,COM1,COM0,1/ZS,COM1,A1,B1,C1,D1)
      CALL MATRIX(A1,B1,C1,D1,A,B,C,D,A2,B2,C2,D2)
      BOT = CMPLX(1.0,6.284*RR*CR*F/1000000)
      C4 = CMPLX(0.0,6.284*F*CR/1000000)/BOT
      CALL MATRIX(A2,B2,C2,D2,COM1,COM0,C4,COM1,A3,B3,C3,D3)
      BOT = CMPLX(0.0,6.284*F*CA1/1000000)
      CALL MATRIX(A3,B3,C3,D3,COM1,1/BOT,COM0,COM1,A4,B4,C4,D4)
      Y11=D4/B4
      Y12 = ((C4*B4)-(A4*D4))/B4
      Y21 = -1.0/B4
      Y22 = A4/B4
30    Y11T =Y11+Y11C
      Y12T = Y12+Y12C
      Y21T = Y21+Y21C
      Y22T = Y22+Y22C
35    AP = -Y22T/Y21T
      BP = -1.0/Y21T
      CP = ((Y12T*Y21T)-(Y11T*Y22T))/Y21T
      DP = -Y11T/Y21T
      C1 = CMPLX(0.0,6.284*F*CP2/1000000)
      CALL MATRIX(COM1,COM0,C1,COM1,AP,BP,CP,DP,A,B,C,D)
      ZOE = ((A*ZA)+B)/((C*ZA)+D)
      IO = 1.0/(ZOE+RS)
C
C
C
C
C     CALCULATE VE AND VM
C
C INDUCED VOLTAGE FOR MAGNETIC SOURCE
      TOP = CMPLX(0.0,6.284*F*ML/1000)* CMPLX(R,I)*(-1)
      BOT = CMPLX(RS*2,6.284*F*LP/1000)
      VI = TOP/BOT
      VO =(ZOM/(ZOM+ZSM))*VI
      VM(J,M) = CABS(VO/(AM + (BM/ZA)))
      VE(J,M) = CABS(IO/(CP+(DP/ZA)))
      VO(J,M) = CABS((VO/(AM+(BM/ZA))) + (IO/(CP+(DP/ZA))))
C
C
C
C    CALCULATE ANGLES OF THE ELECTRIC AND MAGNETIC ELEMENTS
C
C
90    PMR(J,M) = REAL(VO/(AM+(BM/ZA)))
      PMI(J,M) = AIMAG(VO/(AM+(BM/ZA)))

      PER(J,M) = REAL(IO/(CP+(DP/ZA)))
      PEI(J,M) = AIMAG(IO/(CP+(DP/ZA)))
C
      PM(J,M) = PMI(J,M)/PMR(J,M)
      PE(J,M) = PEI(J,M)/PER(J,M)
      PM(J,M) = ATAN(PM(J,M))
      PE(J,M) = ATAN(PE(J,M))
C
```

```
C
C
C    SET ANGLES INTO CORRECT QUADRANT
C
      PMR(J,M)=REAL(VD/(AM+(BM/ZA)))
      PMI(J,M)=AIMAG(VD/(AM+(BM/ZA)))
      PER(J,M)=REAL(ID/(CP+(DP/ZA)))
      PEI(J,M)=AIMAG(ID/(CP+(DP/ZA)))
C
      CALL ANGL(PMR(J,M),PMI(J,M),PM(J,M))
      CALL ANGL(PER(J,M),PEI(J,M),PE(J,M))
C
100   CONTINUE
C
C
C
      DO 150 M = 1,100
      DO 150 J=1,5
      K=6-J
      VM(K,M) = 20.0*ALOG10(VM(K,M))
      VD(K,M) = 20.0*ALOG10(VD(K,M))
150     VE(K,M) = 20.0*ALOG10(VE(K,M))
C
C
```

results stored in files for plotting later

```
      STOP
      END
C
C
      COMPLEX FUNCTION CSINH(G)
      COMPLEX G
      CSINH = 0.5 *(EXP(G)-EXP(-G))
      RETURN
      END
C
C
C
      COMPLEX FUNCTION CCOSH(G)
      COMPLEX G
      CCOSH = 0.5*(EXP(G)+EXP(-G))
      RETURN
      END
C
C
C
      COMPLEX FUNCTION CTANH(G)
      COMPLEX G
      CTANH = (EXP(G)-EXP(-G))/(EXP(G)+EXP(-G))
      RETURN
      END
```

```
      SUBROUTINE TXLN(F,L1,Z1,L2,Z2,CD,A,B,C,D,GB,GE)
      REAL L1,L2
      COMPLEX A,B,C,D,B1,B2,C1,C2,A3,B3,C3,D3,YC,Z1,Z2,GB,GE,CCOSH,CSINH
      A1 = CCOSH(GB*L1)
      B1 = Z1*CSINH(GB*L1)
      C1 = CSINH(GB*L1)/Z1
      YC = CMPLX(0.0,6.284*F*CD/1000000.0)
      A3 = A1+(B1*YC)
      B3 = B1
      C3 = C1+(A1*YC)
      D3 = A1
      A2 = CCOSH(GE*L2)
      B2 = Z2*CSINH(GE*L2)
      C2 = CSINH(GE*L2)/Z2
      A =(A3*A2)+(B3*C2)
      B = (A3*B2)+(B3*A2)
      C = (C3*A2)+(D3*C2)
      D = (C3*B2)+(D3*A2)
      RETURN
      END


      SUBROUTINE ANGL(R,I,A)
      REAL R,I,A
      IF(R.LT.0.AND.I.LT.0) A=A-3.142
      IF(R.LT.0.AND.I.GT.0) A=A+3.142
      RETURN
      END


C
C
C
      SUBROUTINE MATRIX(A1,B1,C1,D1,A2,B2,C2,D2,A3,B3,C3,D3)
      COMPLEX A1,A2,A3,B1,B2,B3,C1,C2,C3,D1,D2,D3
      A3 = A1*A2 + B1*C2
      B3 = A1*B2 + B1*D2
      C3 = C1*A2 + D1*C2
      D3 = C1*B2 + D1*D2
      RETURN
      END
```

data input as for 'standard' program

```
C
      DO 100 M=1,100
      DO 100 J=1,3
      LS=1.1-(J*0.2)
      F = F1 + (M-1)*DF
      FA(M) = F
C
C LOAD IMPEDANCE
       ZL = RR/CMPLX(1.0, (6.284*CR*RR*F/1000000))
C
C INDUCED IMPEDANCE FOR MAGNETIC SOURCE
      ZI = (39.5*(F**2)*(ML**2)/1000000)/
     Z   CMPLX(RS*2,6.284*F*LP/1000)
C
C LENGTH OF BENCH TO OPEN END
       LO = 1.0 - LS
C
C
C
C    CALCULATE GAMMA AND THE COMPLEX IMPEDANCE FOR BENCH
C
C
      X1=CMPLX(0.0,6.284*F*LB*1000000)
      X2=CMPLX(RB,-1000000.0/(6.284*F*CBL))
      X3=CMPLX(0.0,6.284*F*CB*1000000)
      GB=CSQRT(X1*((1/X2)+X3))
      ZB=CSQRT(X1/((1/X2)+X3))
C
C
C   CALCULATE Z SHORT FOR ELECTRIC AND MAGNETIC CASES
C
      ZS=ZB*CTANH(GB*LS)
      ZSM=ZS+ZI
C
C
C
C    MODEL THE TRANSMISSION LINE AND DISCONTINUITY CAPACITANCE
C
        CALL TXLN(F,LO,ZB,1.0,ZE,CD,A,B,C,D,GB,GE)
C
C
C
C    CALCULATE Z OPEN FOR THE MAGNETIC CASE
C
      ZOM =((A*ZL)+B)/((C*ZL)+D)
C
C
C
C    CALCULATE Z OPEN FOR THE ELECTRIC CASE
C
      BOT = CMPLX(0.0,6.284*F*CP1/1000000)
      CALL MATRIX(COM1,1/BOT,COM0,COM1,COM1,COM0,1/ZS,COM1,A1,B1,C1,D1)
      CALL MATRIX(A1,B1,C1,D1,A,B,C,D,A2,B2,C2,D2)
      C1 = CMPLX(0.0,6.284*F*CP2/1000000)
      CALL MATRIX(COM1,COM0,C1,COM1,A2,B2,C2,D2,A,B,C,D)
      ZOE = ((A*ZL)+B)/((C*ZL)+D)
      ZO = 1.0/(ZOE+RS)
```

```
C     CALCULATE VE AND VM
C
C INDUCED VOLTAGE FOR MAGNETIC SOURCE
      TOP = CMPLX(0.0,6.28*F*ML/1000) **-1
      BOT = CMPLX(RO**2,6.284*F*LP/1000)
      VI = TOP/BOT
      VO =(ZOM/(ZOM+ZSM))*VI
      VM(J,M) = CABS((VO/2)/(A + (B/ZL)))
      VE(J,M) = CABS(IO/(C+(D/ZL)))/2
      VO(J,M) = CABS((VO/(A+(B/ZL))) + (IO/(C+(D/ZL))))/2
C
C
C
C    CALCULATE ANGLES OF THE ELECTRIC AND MAGNETIC ELEMENTS
C
90      PM(J,M) = AIMAG(VO/(A+(B/ZL)))/REAL(VO/(A+(B/ZL)))
      PE(J,M) = AIMAG(IO/(C+(D/ZL)))/REAL(IO/(C+(D/ZL)))
      PM(J,M) = ATAN(PM(J,M))
      PE(J,M) = ATAN(PE(J,M))
C
C
C
C    SET ANGLES INTO CORRECT QUADRANT
C
      PMR(J,M)=REAL(VO/(A+(B/ZL)))
      PMI(J,M)=AIMAG(VO/(A+(B/ZL)))
      PER(J,M)=REAL(IO/(C+(D/ZL)))
      PEI(J,M)=AIMAG(IO/(C+(D/ZL)))
C
      CALL ANGL(PMR(J,M),PMI(J,M),PM(J,M))
      CALL ANGL(PER(J,M),PEI(J,M),PE(J,M))
C
100   CONTINUE
C
C
C
C
C
      DO 150 M = 1,100
      DO 150 J=1,5
      K=6-J
      VM(K,M) = 20.0*ALOG10(VM(K,M))
150     VE(K,M) = 20.0*ALOG10(VE(K,M))
C
```

results stored in files for plotting later

subroutines/functions same as 'standard' program

APPENDIX D

THE RELATIONSHIP BETWEEN THE POWER DISSIPATED BY A LOSSY DIELECTRIC, ω and σ

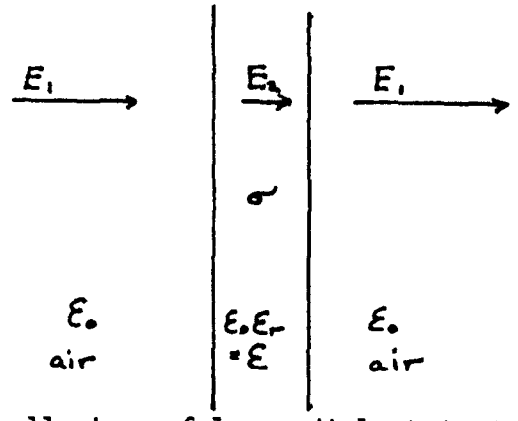

Fig. D1 A small piece of lossy dielectric in an electric field

The electric fields are shown as being perpendicular to the surface of the material, the effect of the fields which are parallel to the ends of the sample are ignored. If it is assumed that the piece of lossy material within the field is small and does not purturb the external fields, the power dissipated by the material is given by equation D1.

$$\text{Power dissipated} = \sigma|E_2|^2 \quad \text{per unit volume} \qquad \text{D1}$$

$$= \frac{\sigma|E_1|^2}{\epsilon_r^2\left|\left(1 - \frac{j\sigma}{\omega\epsilon}\right)\right|^2} \quad \text{per unit volume} \qquad \text{D2}$$

If it is assumed that the permitivity of the material is fixed and the the frequency is fixed, differentiation of the equation with respect to σ shows that the maximum power dissipation occurs when $\sigma=\epsilon\omega$. The power dissipated by the material will increase with increasing frequency so that it will be impossible to select a value of σ which will give a maximum dissipation for all frequencies.

APPENDIX E

CALCULATION OF Q FOR DIFFERENT QUANTITIES OF ABSORBER

$$Q \propto \frac{\text{average energy in the cavity}}{\text{energy dissipated during one cycle}} \qquad \text{E1}$$

$$= \frac{a}{b}$$

for the empty room Q 1800
if the energy absorbed in the walls = b
and the energy absorbed in one length of absorber is c
then $Q_1 = \frac{a}{b+c}$ when one length of absorber is included in the room

$$b + c = \frac{a}{Q_1} \qquad \text{E2}$$

$$c = \frac{a}{Q_1} - b = \frac{a}{Q_1} - \frac{a}{1800} \qquad \text{E3}$$

for a room with x times the volume of absorber (assuming the extra absorber dissipates the same energy per unit volume as the original strip).

$$Q_2 = \frac{a}{b + xc} \qquad \text{E4}$$

substituting for b and c from the above equations

$$Q_2 = \frac{Q_1 \times 1800}{(x \times 1800) - Q_1(1 - x)} \qquad \text{E5}$$

IMPROVED TECHNIQUES FOR THE MEASUREMENT OF RADIATED EMISSIONS INSIDE A SCREENED ROOM

Indexing terms: Microwave circuits and systems, Radiation and radiation effects

It is shown that the use of simple equivalent-circuit models enables the characteristics of radiated emission measurements of electrically small sources performed in a screened room to be predicted. The models indicate a method of reducing the frequency dependence of the measurements and identifying the dominant dipole type (electric or magnetic).

When fields emitted by a piece of electronic equipment are measured in a screened room the resulting field strength measurements are difficult to relate to the corresponding field strengths measured in free space. This is due to the effective frequency response of the room caused by the various propagation mechanisms that exist in the frequency range up to 200 MHz for which the room cannot be made anechoic. For electrically small electric or magnetic dipoles, with constant excitation over the frequency range below the first cavity resonance of the room, the signal measured by an active electric field sensing antenna has an amplitude range of up to 80 dB (see Figs. 1 and 2), depending on the type of source present

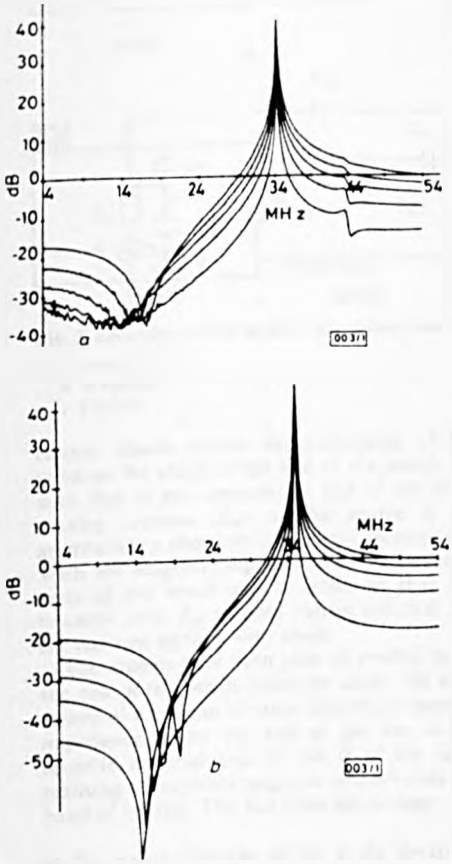

Fig. 1 *Frequency response of electric dipole source in a screened room*
a Measured
b Predicted

(i.e. electric or magnetic). A measurement will determine whether any radiation is being emitted but will not give any indication of the type of source present or a reliable value of its intensity. Simple models were put forward in Reference 1 for the set-up shown in Fig. 3*a*, typical of many EMC specifications, e.g. Reference 2, to try to identify the radiation mechanism present and to decrease the frequency dependence of the measurements. These models are for the frequency region below the first cavity resonance where the source is electrically small and the screened room is acting as a TEM transmission line. They did not predict, however, the deep null that occurs in the case of electric dipole excitation (Fig. 1*a*). The models have been improved, and now predict this null

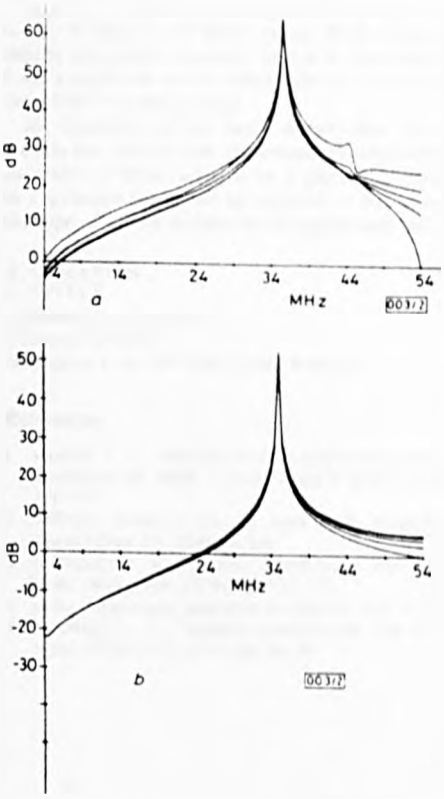

Fig. 2 *Frequency response of magnetic dipole in a screened room*
a Measured
b Predicted

The improved models (Figs. 3*b* and *c*) are based on a coaxial TEM transmission line comprising of the conducting bench which supports the source and its extension which supports the sensing antenna as the centre conductor, and the walls and ceiling of the room which form the outer conductor. The back wall is a short-circuit between the two with the other end open-circuit. The characteristic impedance of the bench and extension sections were calculated from the room dimensions.[3] The reactance of the discontinuity where the two meet is accounted for by a parallel capacitance C_{dis}.[4] The sensing antenna is modelled as a pair of capacitances to the inner and outer conductors, as is the electric dipole source. The magnetic dipole source (a loop antenna) is coupled to the TEM circuit by their mutual inductance.

With the electric source the dominant mode of operation at the lower frequencies in this range, below the first null in Fig. 1, is the direct capacitive link between the source and sensing antenna. The null in the response occurs when the signals via this and the TEM mode are of equal amplitude and opposite phase. The direct capacitance does not exist between the magnetic source and the sensing antenna. Calculations using these circuits are carried out using standard chain parameter techniques.[5]

It can be seen from Figs. 1 and 2 that these equivalent circuits give an accurate prediction of the measured values, particularly in the frequency range below 30 MHz. In each Figure the family of curves gives the response as the source is moved back from the front of the conducting bench towards the back wall (the sensing antenna remains stationary). Each set of curves is plotted relative to the result at the highest frequency (54 MHz in this case) with the source at the front of the bench.

The graphs also show that (except at the nulls) the measured field strength drops by 20 to 25 dB for the electric source but by less than 5 dB for the magnetic source. This can be used as a simple test to determine which type of source is

the dominant one except at the nulls which cover a fairly large proportion of the frequency band.

The difference in the effect on the measured field strength of moving the two types of source towards the back of the bench can be explained by examining the two circuits. With the

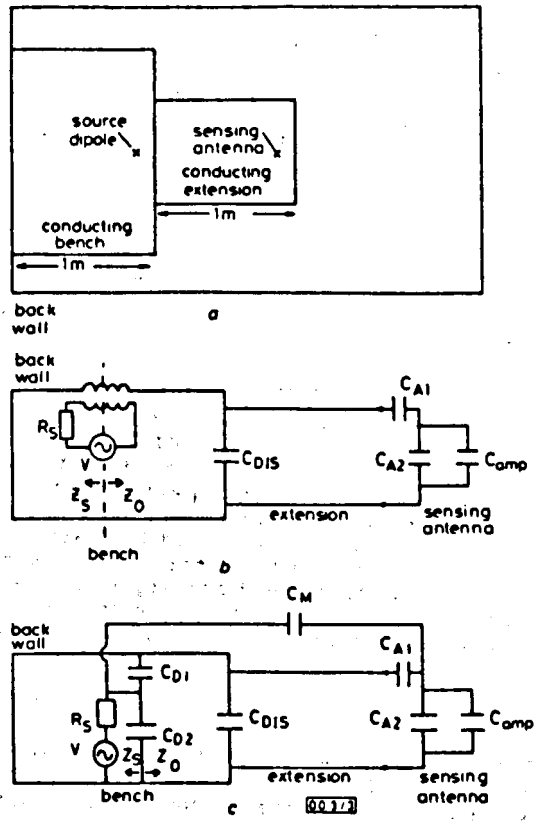

Fig. 3 *Equivalent-circuit models and screened room plan*

a Room plan
b Magnetic
c Electric

electric dipole source the impedance of the line looking towards the short-circuit end of the bench (Z_S) is in parallel with that of the open-circuit end of the line supporting the sensing antenna (Z_O); as the source is moved back, Z_S approaches a short-circuit and the received signal level drops. With the magnetic dipole source the impedances of the two ends of the bench are in series so that as Z_S is reduced towards zero, Z_O remains almost constant and the effect on the received signal is very small.

The models have been used to predict the effect of loading the end of the bench extension under the sensing antenna by means of a column of radio absorbant material (by adding an impedance across the end of the line in the models). The resistive material reduces the Q of the resonances, thereby realising a frequency response which varies only slowly in the band of interest. This has three advantages:

(i) The signal strengths all fall as the electric source is moved back, which enables the source type to be determined over the whole range.
(ii) The dipole moment of the source can be measured after a room calibration.
(iii) The difference in the response of different rooms will be diminished, enabling results from different rooms to be compared more realistically. Individual rooms can be calibrated against known sources.

From the predictions, the best method is to load the end of the extension with a resistance of about 10 Ω, which gives a frequency-independent response for the electric source up to about 40 MHz, with the magnetic source also changing by less than 5 dB from 4 to 30 MHz. The best result so far in practice is a response similar to that of 50 Ω in the predictions, a good improvement on the unloaded case. The dynamic range of the responses drops from 28 to 13 dB and from 48 to 4 dB for the magnetic and electric cases, respectively, in the 4 to 30 MHz range. With these values the null depths are greatly reduced, and it is therefore possible to tell from a family of curves which type of source is present across the whole frequency range.

In summary, it has been shown that the use of simple models has shown how the frequency dependence in the measurement of fields radiated by a piece of electronic equipment in a screened room can be reduced; it has also indicated how the type of source present in the equipment can be predicted.

A. C. MARVIN
L. STEELE

Department of Electronics
University of York
Heslington, York YO1 5DD, United Kingdom

25th October 1985

References

1 MARVIN, A. C.: 'Identification of mechanisms from emission measurements of small sources.' *IEE Proc. EMC, 1984, Vol. 26, pp. 149–153*
2 Military standard 461, 1st April 1980, Department of Defense, Washington, DC 20360, USA
3 DWORSKY, L. N.: 'Modern transmission line theory and applications' (Wiley, NY, 1979), pp. 143–152
4 SAND: 'Microwave engineers handbook, Vol. 1' (Artech, 1971)
5 DWORSKY, L. N.: 'Modern transmission line theory and applications' (Wiley, NY, 1979), pp. 38–39

NEW SCREENED ROOM TECHNIQUES FOR THE MEASUREMENT OF RFI

L. Steele and A. C. Marvin*

SUMMARY

The electromagnetic field measured in a screened room is dependent on the size and geometry of the room, the type of source (electric or magnetic dipole) and the dipole moment. In this paper, computer models based on TEM wave propogation within a screened room are used to describe the fields measured from a source inside the room. The models are used to predict the results of changes in the test set-up which enable qualitative measurements of the dipole type and moment to be undertaken.

1 Introduction

The measurement of electromagnetic radiation emitted by electrically small sources is often carried out in screened rooms. Fig.1 shows a typical test set-up which is defined in various EMC specifications for use up to 30 MHz. The radiation from a small source can be described in terms of elemental dipole radiation [1] with the source being described as a set of three othogonal pairs of dipoles (one each of electric and magnetic to each pair). For this, the moment of each dipole must be measured but the output of the antenna in the sreened room is determined by the test set up and is not a direct measurement of the field that would be radiated if the source were situated elsewhere (eg. free-space). The measurement only indicates that a source is emitting at a particular frequency.

Ideally the measurement of emissions should be carried out under free-space conditions or in screened anechoic conditions if the weather or external interferance dictates. However, the lowest practical frequency of an anechoic chamber is 100 or 200 MHz and a different approach is needed for the measurement of lower frequency emissions.

Typical screened rooms have linear dimensions of around 10m so that the lowest order waveguide cavity resonance is around 30 MHz. In the waveguide propogation region the resonances can be smoothed out by mode stirring techniques where a large reflecting surface is rotated in the screened room [2]. The perturbator tunes the enclosure through many different modes at the test frequency and the total radiated power is calculated for that frequency. In the region below wave-guide cut-off interest has been shown in adapting the Crawford cell TEM transmission line to emission measurement [1]. In both these two cases the sreened room will need to be modified with both the resulting cost and loss of equipment flexibility. The techniques described below enable an unmodified screened room to be used for quantitative measurement of emissions in the frequency region below wave-guide cut-off and also enable the type of source (electric or magnetic dipole) to be determined; thus enabling the fields to be predicted at any distance away from the source and also providing diagnostic information on a piece of equipment which fails a test.

The work described below is the design of a test which will not only give a reasonable figure for the moment of the dipole source but will give this for both the electric and magnetic components. To be able to do this it is first necessary to understand the propogation mechanisms that exist at the various frequencies. The frequency range can be divided into two areas:-

1. Below the first cavity resonance where the source is electrically small and the screened room is acting as a TEM transmission line .
2. Above this frequency where the room also acts as a waveguide cavity.

It is the first area which this paper will cover.

*UNIVERSITY OF YORK

2 The computer models

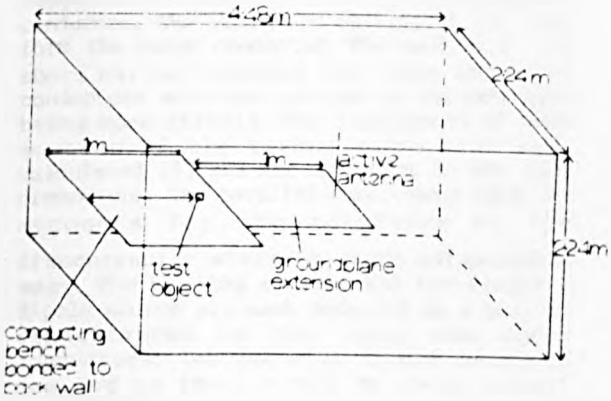

Fig.1 Typical test set up.

Simple equivalent circuit models were put forward [3] for the test setup shown in Fig.1 which is typical of many EMC specifications used at present [4]. These models tried to identify the mechanisms present and predict fields that would be measured when the source had constant excitation over the frequency range. They went some way to predicting the response but did have errors and did not describe the deep null that exists in the response of the electric dipole source (fig.2). These models have been improved and now also predict this null.

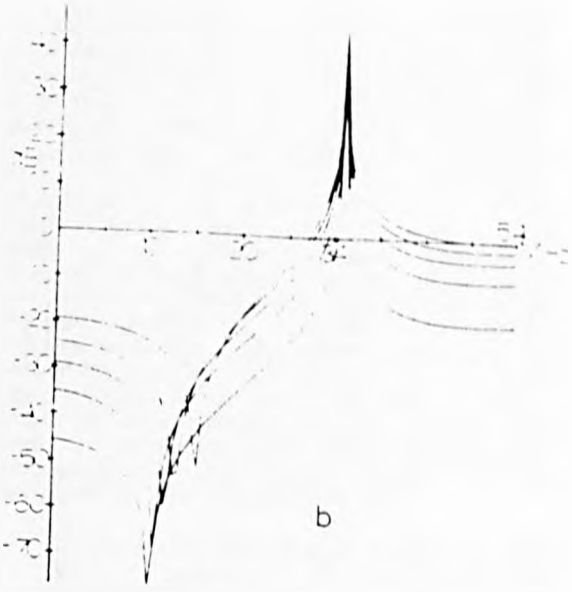

Fig.2 Frequency response of electric dipole
a) measured
b) predicted

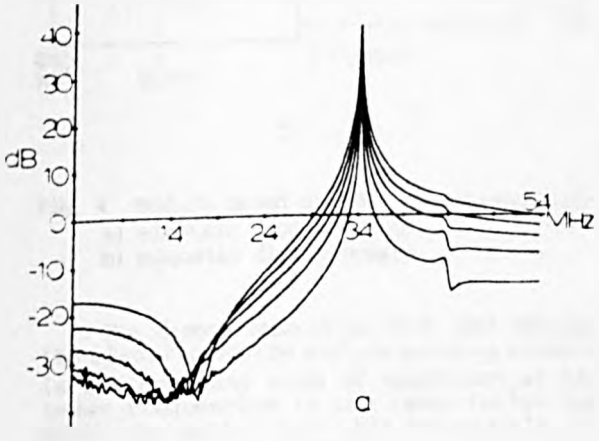

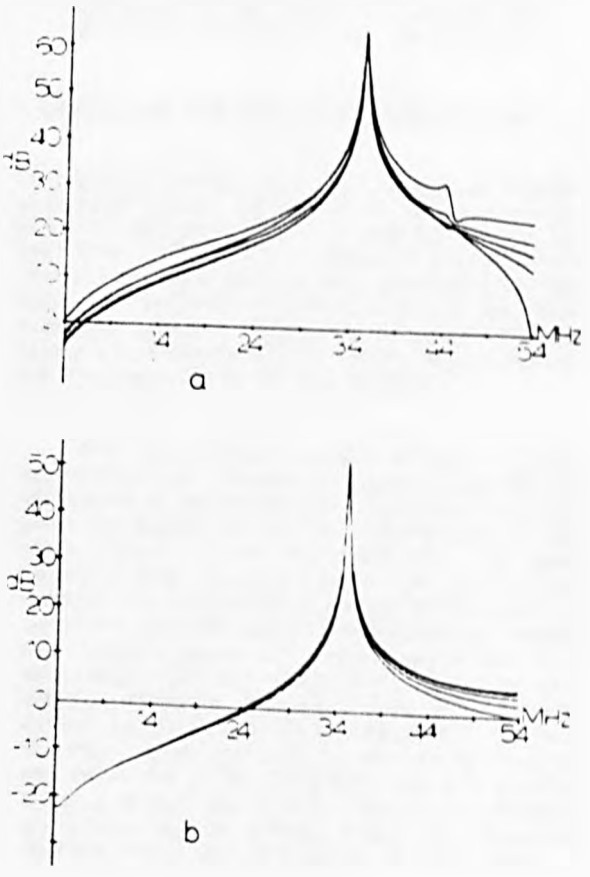

Fig.3 Frequency response of magnetic dipole
a) measured
b) predicted

The equivalent circuits (fig.4) are based on a coaxial TEM transmission line. This comprises of the conducting bench which supports the source and its extension, which supports the sensing antenna, as the center conductor. The walls and ceiling of the room form the outer conductor. The back wall is a short circuit between the inner and outer conductors with the far end of the extension being open circuit. The impedances of each section of the transmission line were calculated [5] and are dependent on the room dimensions. The parallel capacitance Cdis [6] accounts for the reactance of the discontinuity where the bench and extension meet. The sensing antenna and the electric dipole source are each modelled as a pair of capacitances to the inner and outer conductors. The magnetic dipole source is coupled to the circuit by their mutual inductance.

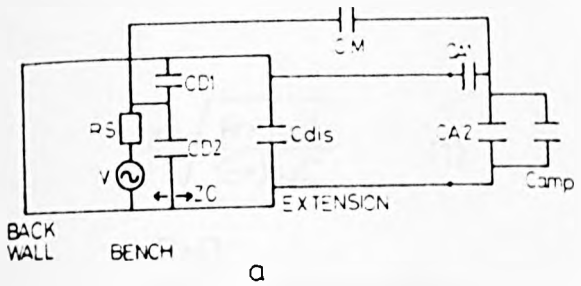

a

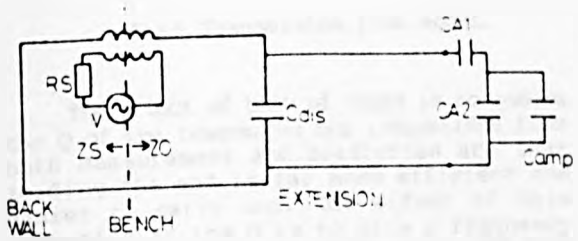

b

Fig. 4 Models based on TEM transmission line
a) electric dipole source
b) magnetic dipole source

The direct capacitive link (Cm) between the electric source and the sensing antenna is the dominant mode of operation at the lower frequencies in the range (below the null). The null occurs when the signals via this link and the TEM mode are of equal amplitude but opposite phase so the frequency at which the null occurs is detemined by the physical size of the dipole. This capacitive link does not occur with the magnetic source which has an electrostatic shield. Standard chain parameter techniques [7] are used with these circuits to calculate the measured fields.

It can be seen by comparing the measured and predicted fields (figs. 2 and 3) that these models give an accurate prediction of the measured fields and can therefore be used to predict the fields measured when the sources are moved or the bench is loaded. The large resonance that is present at about 36 MHz is caused by the quarter wavelength resonance of the transmission line. The discontinuity capacitance has some tuning effect on the resonant frequency. The family of curves on each graph give the response as the source is moved back from the front of the bench towards the back wall (the sensing antenna remains stationary). Each set of curves is plotted relative to the result at the highest frequency (54 MHz in this instance) with the source 100 mm from the front of the bench. Differences between the measured and calculated fields can be explained by the assumptions that:-

1) dipoles are lumped elements with point injection of currents and voltages.
2) there is no change in the mutual inductance between the bench and magnetic dipole as it is moved back.
3) there is no change in the capacitance between the electric dipole source and the bench as the source is moved back.
4) the transmission line is lossless.

3 Identifying The Type of a single source

The graphs show that the measured field strength drops by 20 to 25 dB with the electric source (except at the nulls) but by less than 5 dB with the magnetic source. This can be used as a simple test to determine the type of source present except in the frequency region covered by the nulls in the electric response which cover about 35% of the frequency band (below 30 MHz).

The difference in the effect on the measurement of moving the source back can be explained by examining the circuits. With the electric dipole source the impedances of the short circuit end of the bench (ZS), the open circuit end of the bench and extension supporting the sensing antenna (ZO) are in parallel so that as ZS is reduced by moving the source back it takes more of the available current which is limited by the source impedance (RS) and hence the received signal level drops. In the magnetic circuit the two impedances are in series so that as one falls the other increases and the current flowing around the circuit remains relatively constant which means that the measured voltage level does not alter by very much.

4 Loading The Circuits

As stated above the equivalent circuits can be used to investigate the effect on the measured fields of loading the end of the extension under the sensing antenna and of making the transmission line lossy. The first is done by adding an impedance across the end of the line in the models, the second is done by adding lossy elements into the transmission line equations (see fig.5 and equation 1).

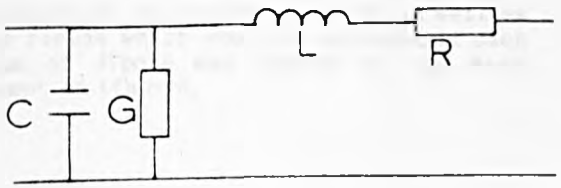

$$Z = \sqrt{\frac{R + j\omega L}{G + j\omega C}} \qquad (1)$$

$R = 0$

$G = 0$ for no loss

fig.5 Transmision line model.

The effect of both of these is to reduce the Q of the resonances but indications from both measurement and prediction are that loading the end is far more efficient and easier to carry out. The effect of this reduction in the Q is to give a frequency response that varies very slowly in the band of interest. This has three advantages:

1) The signal strengths fall as the source is moved back across the whole frequency band, which allows the source type to be determined across the whole band.
2) The dipole moment of the source can be determined after a room has been calibrated against a known source.
3) The difference in the response of different rooms will be reduced, thus enabling the results from different rooms be compared more realistically as the rooms can be calibrated against the same source. If the frequency response is flat the only difference in the fields measured in different rooms will be in their magnitudes.

The predictions indicate that the most effective load will be about 10 ohm which gives a frequency independent response for the electric source up to about 40 MHz (see fig.7) with the magnetic response also changing by less than 5 dB over the same frequency range. The best result so far in practice is equivalent to a predicted load of about 50 ohm (see fig.6) which is still a good improvement on the unloaded case.

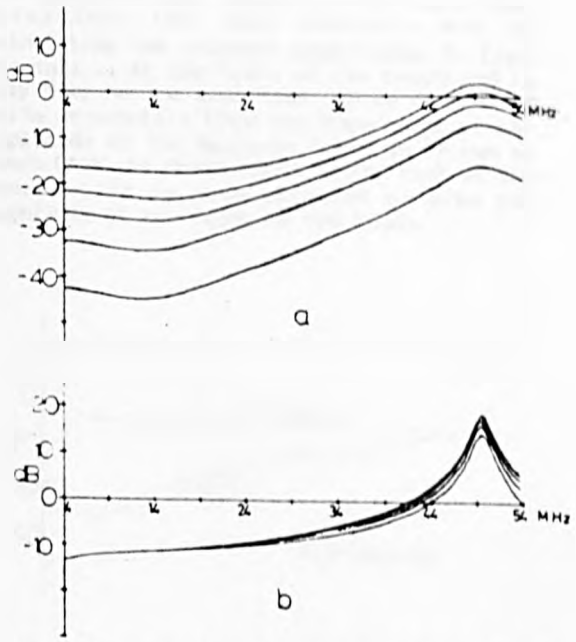

fig.6 The predicted response with a 50 ohm load
a) electric dipole source
b) magnetic dipole source

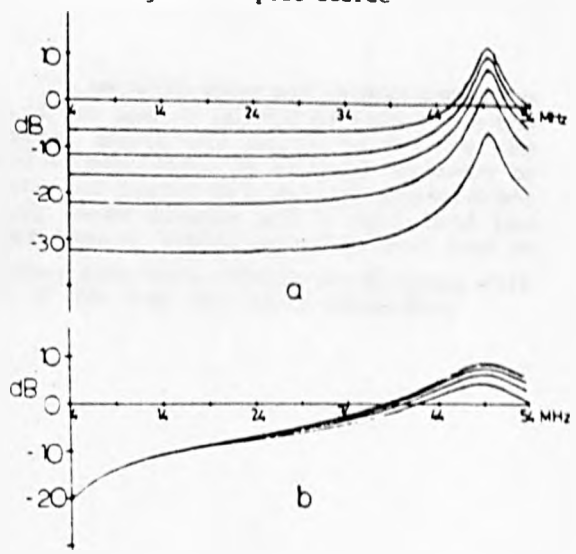

Fig.7 The predicted response with a 10 ohm load.
a) electric
b) magnetic

5 Identifying the moments in a dual source

Whilst it is easy to distinguish between purely magnetic and purely electric dipole sources , it is likely that a practical source will be a combination of the two with relative amplitudes that will not always be the same. It is possible to give relative amplitudes for the two sources as can be seen by examining two examples. It is easiest to see by looking at plots which give the measured field of a particular frequency as a function of distance along the bench. Fig.8 shows the predicted field of a source which consists of both types of dipole as well as the fields which would be measured if each type of dipole was present at the same moment on its own.

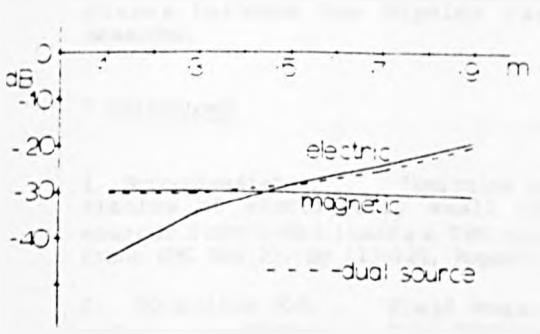

Fig.8 Predicted fields of a dual source.

In fig.8 it can be seen that where the electric and magnetic elements of the source are not of a similar magnitude the measured field strength is very close to that of the more dominant dipole (less than 2dB error). This is because the field strength measured due to the electric source changes so rapidly as the source is moved back that the two elements are of a similar magnitude for a very small portion of the bench. It is therefore possible to examine the way the measured field strength changes to distinguish between the two types of source. In fig.8 the field towards the front of the bench is following the pattern for the electric case and towards the back of the bench is following the pattern of the magnetic case so the relative amplitudes can be taken from the front (electric) and back (magnetic) of the bench and adjusted to allow for the change in amplitude as the source is moved back.

The relative amplitudes and phases can be such that the fields cancel each other out at some point along the bench (eg.fig.9). If the null then measured is very deep the fields are of equal amplitude and opposite phase but if the null is not so large either the phase difference is not so close to 180° or the amplitudes are not so close to each other. The position and depth of the null then determines the most accurate way of calculating the relative amplitudes. In fig.9 the null is at the front of the bench and is very deep so the amplitude can be determined quite accurately from the knowledge of the amplitude of the magnetic field which can be taken from the measurement at the back of the bench which is then adjusted to give the magnitude at the front of the bench.

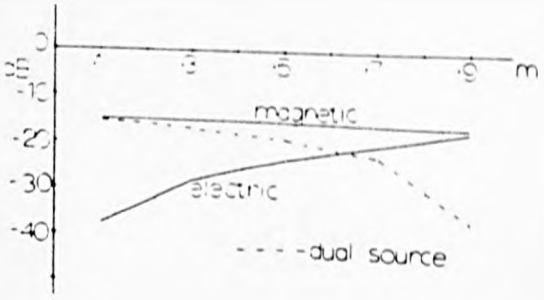

fig.9 Predicted fields of a second dual source.

The examples shown are predictions using the 10 ohm load on the end as this gives the easiest plots off which to derive the relative amplitudes. It is still necessary to verify the method by practical measurement using known sources and a real load but comparison of results using the best load at present available and the predictions with the 50 ohm load look quite favourable.

6 Conclusions

It has been shown that measurements of radiated fields in a screened room are subject to a large error which is a result of the various propogation mechanisms that exist inside the room at different frequencies. Analysis of the room as a simple TEM transmission line has been shown to be valid at frequencies below waveguide cut-off and to enable the developement of a measurement procedure which will give a far more accurate value for the dipole moment of a source as well as the relative moments of electric and magnetic dipole sources. The three orthogonal sets of dipoles can be measured although this is not generally called for in test specifications and will not give a complete description of the source as the relative phases between the dipoles cannot be measured.

7 References

1. Screenivasiah I. "Emission characteristics of electrically small radiating sources from tests inside a TEM cell." IEEE trans EMC Vol 23, pp 113-121, August 1981

2. Donaldson E.E. "Field Measurements made in an enclosure." Proc IEEE Vol 66, No 4, pp464-472, April 1978

3. Marvin A.C. "Identification of mechanisms from emission measurements of small sources." IEEE trans EMC Vol 26, pp149-153, 1984

4. Military standard 461 1st April 1980, Department of Defence, Washington, DC 20360, USA

5. Dworsky L.N. "Modern transmission line theory and applications." (Wiley, NY,1979) pp 143-152

6. Sand (Ed), "Microwave engineers handbook." Vol 1 (Artech, 1971)

7. Van Valkenburg, "Network analysis." (Prentice-Hall, 1974) pp 325-341

UDC 621.3.083.9 : 621.3.013.7
Indexing Terms: Radio interference, Electric measurements, Electromagnetic compatibility

New screened room techniques for the measurement of RFI

L. DAWSON (née Steele), BSc*

and

A. C. MARVIN, MEng, PhD*

Based on a paper by L. Steele and A. C. Marvin presented at the 5th International IERE Conference on Electromagnetic Compatibility held at the University of York in October 1986

* *Department of Electronics, University of York, York YO1 5DD*

SUMMARY

The electromagnetic field measured in a screened room is dependent on the size and geometry of the room, the type of source (electric or magnetic dipole) and the dipole moment. In this paper, computer models based on TEM wave propagation within a screened room are used to describe the fields measured from a source inside the room. The models are used to predict the results of changes in the test set-up which enable qualitative measurements of the dipole type and moment to be undertaken.

1 Introduction

The measurement of electromagnetic radiation emitted by electrically small sources is often carried out in screened rooms. Figure 1 shows a typical test set-up which is defined in various EMC specifications for use up to 30 MHz. The radiation from a small source can be described in terms of elemental dipole radiation[1] with the source being described as a set of three othogonal pairs of dipoles (one electric and one magnetic dipole to each pair). For this, the moment of each dipole must be measured but the output of the antenna in the screened room is determined by the test set-up and is not a direct measurement of the field that would be radiated if the source were situated elsewhere, e.g. in free-space. The measurement only indicates that a source is emitting at a particular frequency.

Ideally the measurement of emissions should be carried out under free-space conditions or in screened anechoic conditions if the weather or external interference so dictates. However, the lowest practical frequency of an anechoic chamber is 100 to 200 MHz and a different approach is needed for the measurement of lower frequency emissions.

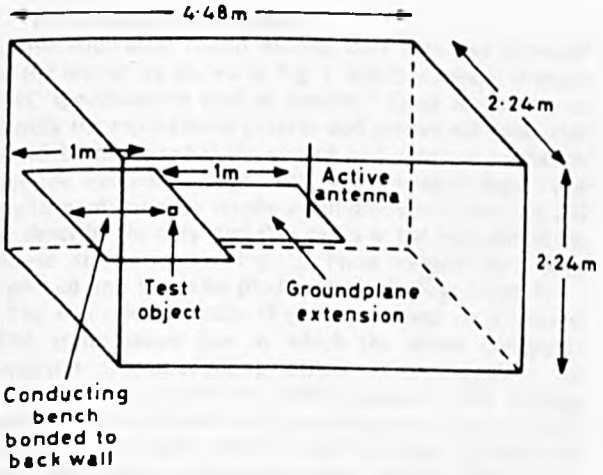

Fig. 1. Typical test set-up

Typical screened rooms have linear dimensions of around 10 m so that the lowest order waveguide cavity resonance is around 30 MHz. In the waveguide propagation region the resonances can be smoothed out by mode stirring techniques in which a large reflecting surface is rotated in the screened room.[2] The perturbator tunes the enclosure through many different modes at the test frequency and the total radiated power is calculated for that frequency. In the region below waveguide cut-off, interest has been shown in adapting the Crawford cell TEM transmission line to emission measurement.[3] In both these cases the screened room will need to be modified, resulting in cost increases and loss of equipment flexibility. The techniques described below enable an unmodified screened room to be used for quantitative measurement of emissions in the frequency region below waveguide cut-off and also enable the type of source (electric or magnetic dipole) to be determined, thus enabling the fields to be predicted at any distance away from the source and also providing diagnostic information on a piece of equipment which fails a test.

The work described below is the design of a test which will not only give a reasonable figure for the moment of the dipole source but will give this for both the electric and magnetic components. To understand the method it is first necessary to understand the propagation mechanisms that exist at the various frequencies. The frequency range can be divided into two regions:

(1) Below the first cavity resonance where the source is electrically small and the screened room is acting as a TEM transmission line.
(2) Above this frequency where the room also acts as a waveguide cavity.

It is the first region which this paper will cover.

Journal of the Institution of Electronic and Radio Engineers Vol 58 No 1 pp 28–32 January/February 1988

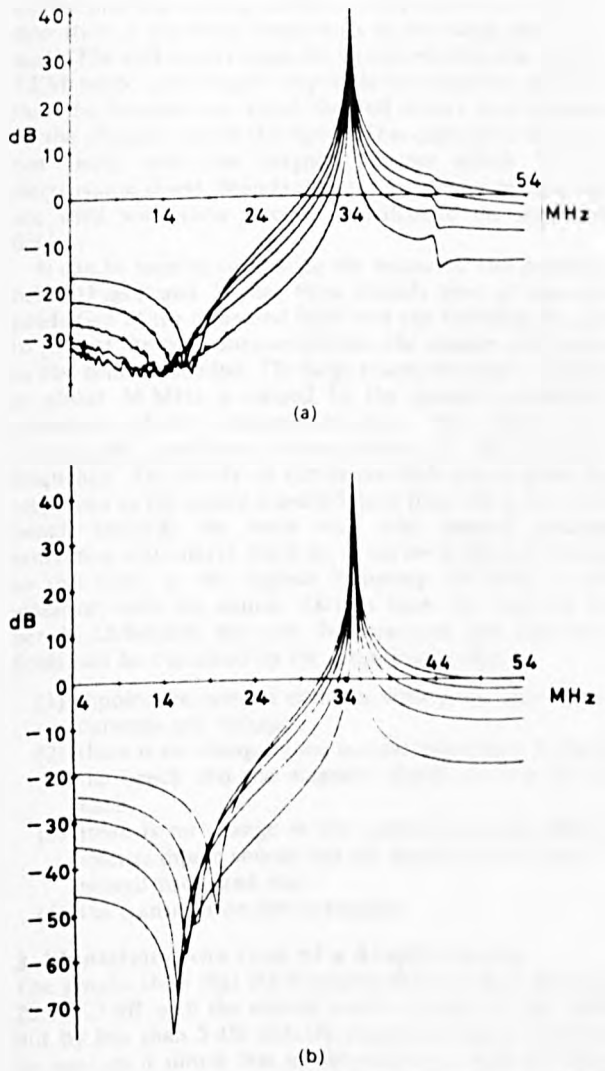

Fig. 2. Frequency response of electric dipole (a) Measured (b) Predicted

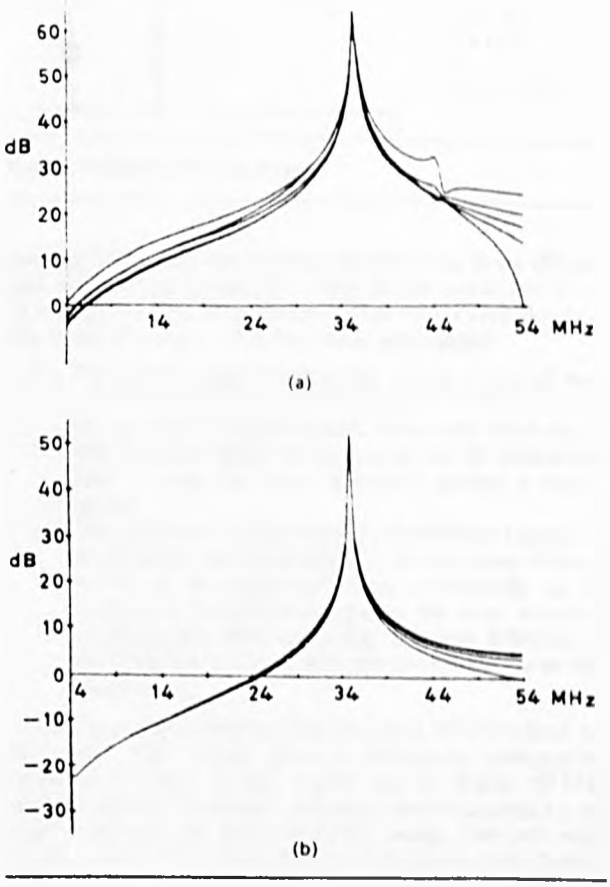

Fig. 3. Frequency response of magnetic dipole (a) Measured (b) Predicted

2 The Computer Models

Simple equivalent circuit models have been put forward[3] for the test set-up shown in Fig. 1, which is typical of many EMC specifications used at present.[4] These models try to identify the mechanisms present and predict the fields that would be measured if the source had constant excitation over the frequency range. The earlier models went some way to predicting the response but did have errors and did not describe the deep null that exists in the response of the electric dipole source (Fig. 2). These models have been improved and now also predict this null (Figs 2 and 3).

The equivalent circuits (Fig. 4) are based on a coaxial TEM transmission line in which the centre conductor comprises the conducting bench, which supports the source, and its extension, which supports the sensing antenna. The walls and ceiling of the room form the outer conductor. The back wall is a short circuit between the inner and outer conductors with the far end of the extension being open circuit. The impedances of each section of the transmission line were calculated[5] and are dependent on the room dimensions. The parallel capacitance[6] C_{dis} accounts for the reactance of the discontinuity where the bench and extension meet. The sensing antenna and the electric dipole source are each modelled as a pair of capacitances to the inner and outer conductors. The magnetic dipole source is coupled to the circuit by mutual inductance.

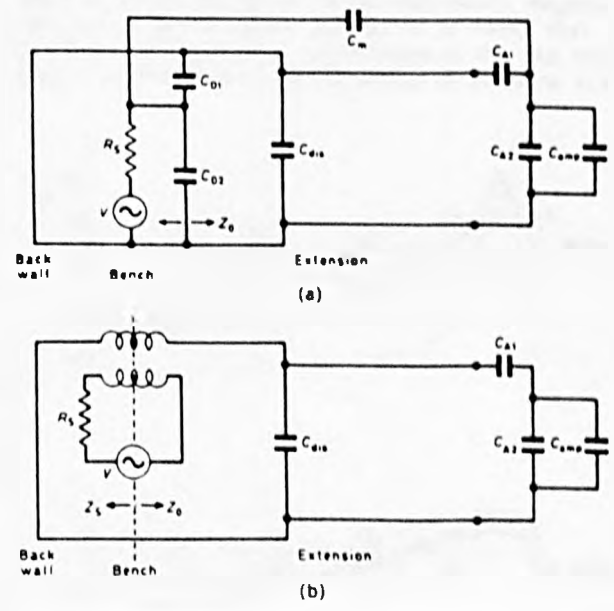

Fig. 4. Models based on TEM transmission line (a) Electric dipole source (b) Magnetic dipole source

The direct capacitive link (C_m) between the electric source and the sensing antenna is the dominant mode of operation at the lower frequencies in the range (below the null). The null occurs when the signals via this link and the TEM mode are of equal amplitude but opposite phase so that the frequency at which the null occurs is determined by the physical size of the dipole. This capacitive link does not occur with the magnetic source which has an electrostatic shield. Standard chain parameter techniques[2] are used with these circuits to calculate the measured fields.

It can be seen by comparing the measured and predicted fields (Figs 2 and 3) that these models give an accurate prediction of the measured fields and can therefore be used to predict the fields measured when the sources are moved or the bench is loaded. The large resonance that is present at about 36 MHz is caused by the quarter wavelength resonance of the transmission line. The discontinuity capacitance has some tuning effect on the resonant frequency. The family of curves on each graph gives the responses as the source is moved back from the front of the bench towards the back wall (the sensing antenna remaining stationary). Each set of curves is plotted relative to the result at the highest frequency (54 MHz in this instance) with the source 100 mm from the front of the bench. Differences between the measured and calculated fields can be explained by the assumptions that

(1) dipoles are lumped elements with point injection of currents and voltages;
(2) there is no change in the mutual inductance between the bench and the magnetic dipole as it is moved back;
(3) there is no change in the capacitance between the electric dipole source and the bench as the source is moved back; and that
(4) the transmission line is lossless.

3 Identifying the type of a Single Source

The graphs show that the measured field strength drops by 20 to 25 dB with the electric source (except at the nulls) but by less than 5 dB with the magnetic source. This can be used as a simple test to determine the type of source present except in the frequency region covered by the nulls in the electric response, which cover about 35% of the frequency band (below 30 MHz).

The difference in the effect on the measurement of moving the source back can be explained by examining the circuits. With the electric dipole source the impedances of the short circuit end of the bench (Z_S) and of the open circuit end of the bench and extension supporting the sensing antenna (Z_O) are in parallel so that as Z_S is reduced by moving the source back it takes more of the available current, which is limited by the source impedance (R_S), and hence the received signal level drops. In the magnetic circuit the two impedances are in series so that as one falls the other increases and the current flowing around the circuit remains relatively constant, which means that the measured voltage level does not alter by very much.

4 Loading the Circuits

As stated above the equivalent circuits can be used to investigate the effect on the measured fields of loading the end of the extension under the sensing antenna and of making the transmission line lossy. The former is done by adding an impedance across the end of the line in the models, the latter by adding lossy elements into the transmission line equations (Fig. 5).

The effect of both of these procedures is to reduce the Q of the resonances, but indications from both measurement

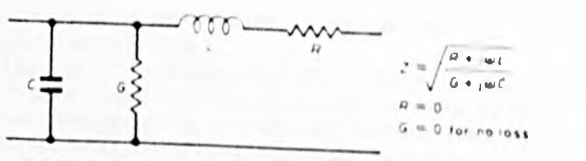

Fig. 5. Transmission line model

and prediction are that loading the end is far more efficient and easier to carry out. The effect of this reduction in the Q is to give a frequency response that varies very slowly in the band of interest. This has three advantages:

(1) The signal strengths fall as the source is moved back across the whole frequency band, which allows the source type to be determined across the whole band.
(2) The dipole moment of the source can be determined after a room has been calibrated against a known source.
(3) The difference in the response of different rooms will be reduced, thus enabling the results from different rooms to be compared more realistically as the rooms can be calibrated against the same source. If the frequency response is flat, the only difference in the fields measured in different rooms will be in their magnitudes.

The predictions indicate that the most effective load will be about 10Ω which gives a frequency independent response for the electric source up to about 40 MHz (Fig. 6) with the magnetic response also changing by less than 5 dB over the same frequency range. The best result so far in practice is equivalent to a predicted load of about 50Ω (Fig. 7), which is still a good improvement on the unloaded case.

5 Identifying the Moments in a Dual Source

Whilst it is easy to distinguish between purely magnetic and purely electric dipole sources, it is likely that a practical source will be a combination of the two with relative amplitudes that will not always be the same. It is

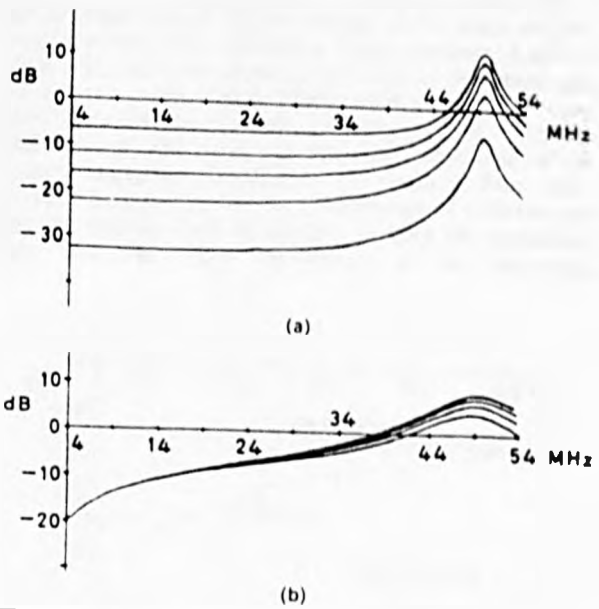

Fig. 6. Predicted response with a 10Ω load. (a) Electric dipole source. (b) Magnetic dipole source.

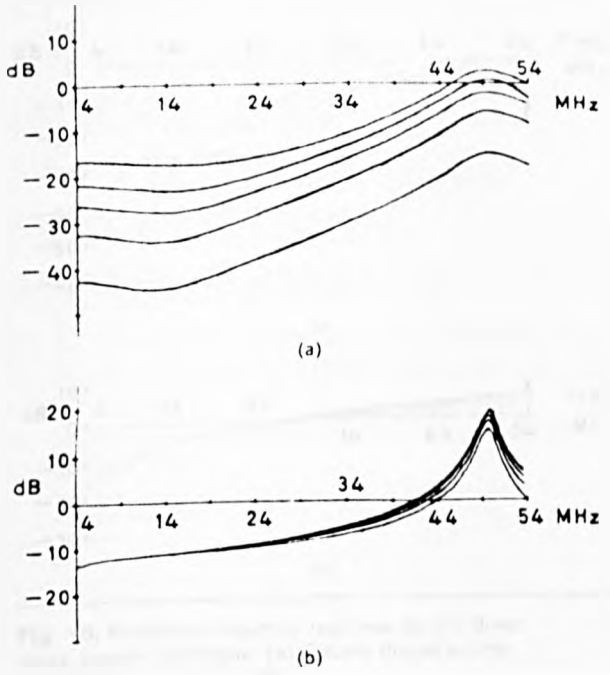

Fig. 7. Predicted response with a 50Ω load (a) Electric dipole source (b) Magnetic dipole source

possible to give relative amplitudes for the two sources, as can be seen by examining two examples represented by plots which give the measured field of a particular frequency as a function of distance along the bench. Figure 8 shows the predicted field of a source which consists of both types of dipole as well as the fields which would be measured if each type of dipole were present with the same moment on its own.

In Fig. 8 it can be seen that, where the electric and magnetic elements of the source are not of a similar magnitude, the measured field strength is very close to that of the more dominant dipole (with less than 2 dB error). This is because the measured field strength due to the electric source changes so rapidly as the source is moved back that the two elements are of a similar magnitude for only a very small portion of the bench. It is therefore possible to examine the way in which the measured field strength changes in order to distinguish between the two types of source. In Fig. 8 the field towards the front of the bench is following the pattern for the electric case and towards the back of the bench it is following the pattern of the magnetic case, so the relative amplitudes can be taken from the front (electric) and back (magnetic) of the bench and adjusted to allow for the change in amplitude as the source is moved back.

The relative amplitudes and phases can be such that the fields cancel each other out at some point along the bench, as for example in Fig. 9. If the null then measured is very deep the fields are of equal amplitude and opposite phase, but if the null is not so large either the phase difference is not so close to 180° or the amplitudes are not so close to each other. The position and depth of the null then determine the most accurate way of calculating the relative amplitudes. In Fig. 9 the null is at the front of the bench and is very deep, so that the amplitude can be determined quite accurately from a knowledge of the amplitude of the magnetic field, which can be taken from the measurement at the back of the bench which is then adjusted to give the magnitude at the front of the bench.

The examples shown are predictions for the case of a 10Ω load on the end, as this gives the easiest plots from which to derive the relative amplitudes. It is still necessary to verify the methods by practical measurement using known sources and a real load but comparison of results using the best load at present available and the predictions with the 50Ω load look quite favourable.

6 An Alternative Measurement Method

At the frequencies under consideration the measuring antenna used in the screened room is not acting as an antenna would in free space but as a capacitive probe of the voltage at the end of the extension. If the voltage at the end of the bench is measured by some means other than an antenna the frequency response could be flattened. The removal of the antenna will also remove the deep null which occurs in the electric dipole response due to the direct coupling between the electric dipole source and the sensing antenna.

Without the antenna there is no need for the extension which supports it and the open circuit transmission line formed by the bench in the room will resonate at about twice the previous frequency, which will put the resonance well out of the required frequency range. Also, if a transmission line is terminated in its characteristic impedance it will cease to resonate at any frequency. The impedance of the bench is calculated to be about 56Ω so that an impedance of 50Ω on the end of the bench will not match it perfectly but will not be highly resonant. A pair of straps from the two corners at the end of the bench can thus each be terminated in 100Ω to the walls of the room, which form the return of the transmission line, to give a total load of 50Ω assuming that the impedance of the straps is negligible compared to the resistors. Two straps are used to keep the line as symmetrical as possible and they are kept as short as possible to keep the impedance low. The 50Ω input impedance of the measuring

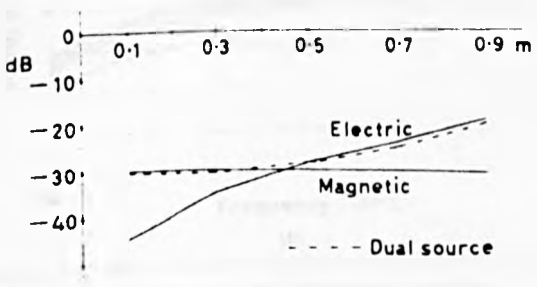

Fig. 8. Predicted fields of a first dual source

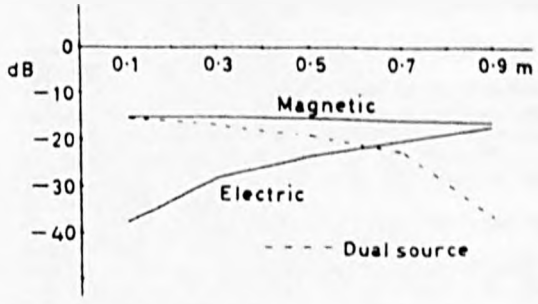

Fig. 9. Predicted fields of a second dual source

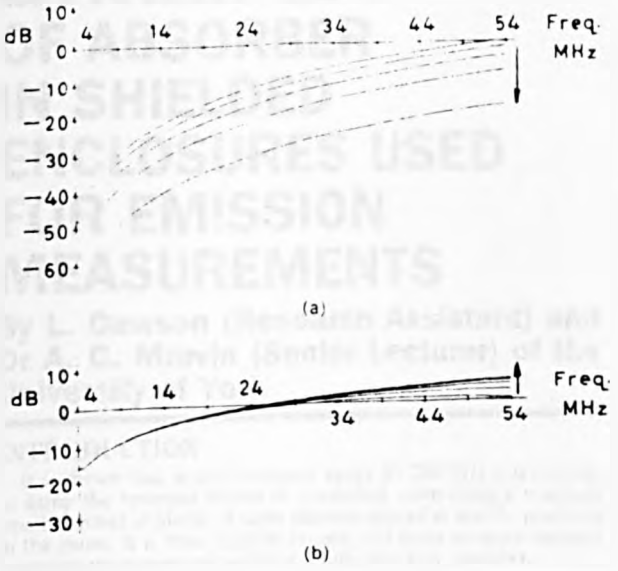

Fig. 10. Predicted frequency response for the direct measurement technique (a) Electric dipole source (b) Magnetic dipole source

instrument (network analyser) can form part of the 100Ω load on one strap.

This change is easily incorporated into the equivalent circuit models by removing the antenna extension, C_{ds} and the mutual capacitance between the electric dipole source and the sensing antenna. The load is included on the end of the bench and the measured voltage will be half that developed across the load.

The predicted response for this system of measurement is shown in Fig. 10. The arrows indicate the change in the measured voltage caused by moving the source back from the front of the bench. They predict that with this method of measurement the differentiation between the types of source will be similar to that obtained with the other measurement technique. The measured voltage for the magnetic dipole source is predicted to rise by up to 5 dB across the frequency range and the measured voltage for the electric dipole source is predicted to fall by 20 dB across the whole range. The response for both types of source is a steady change with frequency which is relatively easy to calibrate out of measurements. Practical measurements (Fig. 11) confirm the results except that the change in amplitude as the magnetic dipole source is moved back is a rise of 10 dB across the whole frequency range, which is even easier to use to distinguish between source types. The error will be due to the assumption that the coupling between the magnetic dipole source and the bench is constant across the frequency range for all positions on the bench and that the coupling occurs at a single point, which is not the case.

Although this technique is easier to use to distinguish between the types of dipole source and also gives a reasonably slow change in the amplitude of the measured voltage across the frequency range, below about 5 MHz it is less sensitive for measuring the electric dipole source than the earlier techniques. This is because the capacitive probe gives a flat response for the electric dipole source at the lower frequencies whereas with this technique the response falls off rapidly for both electric and magnetic dipole sources below about 5 MHz.

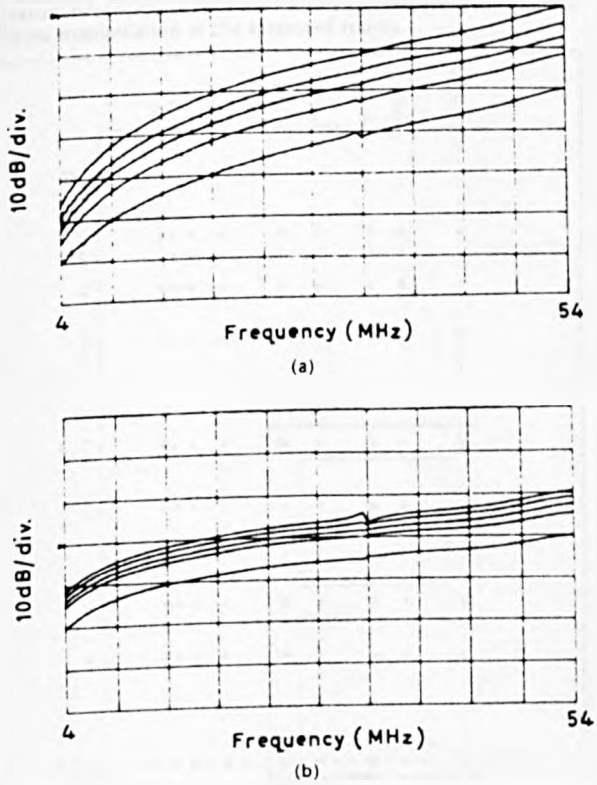

Fig. 11. Measured frequency response for the direct measurement technique (a) Electric dipole source (b) Magnetic dipole source

7 Conclusions

It has been shown that measurements of radiated fields in a screened room are subject to a large error, which is a result of the various propagation mechanisms that exist within the room at the different frequencies. Analysis of the room as a simple TEM transmission line has been shown to be valid at frequencies below waveguide cut-off and this makes it possible to develop test procedures which will give far more accurate values for the dipole moment of a source as well as the relative moments of electric and magnetic dipole sources. Three orthogonal sets of dipoles can be measured, although this is not generally called for in test specifications and will not give a complete description of the source as the relative phases between the dipoles cannot be measured.

8 References

1 Screenivasiah, I., Chang, D. C. and Ma, M. T., 'Emission characteristics of electrically small radiating sources from tests inside a TEM cell', *IEEE Trans. on Electromagnetic Compatibility*, **EMC-23**, no. 3, pp. 113–21, August 1981

2 Donaldson, E. E., 'Field measurements made in an enclosure', *Proc. IEEE*, **66**, no. 4, pp. 464–72, April 1978

3 Marvin, A. C., 'The use of screened rooms for the identification of radiation mechanisms and the measurement of free space emissions from electrically small sources', *IEEE Trans. on Electromagnetic Compatibility*, **EMC-26**, no. 4, pp. 149–53, November 1984

4 Military Standard 461, 1st April 1980, Department of Defence, Washington, DC 20360, USA

5 Dworsky, L. N., 'Modern Transmission Line Theory and Applications', pp. 143–52 (Wiley, New York, 1979)

6 Sand (Ed.), 'Microwave Engineers Handbook', Vol. 1 (Artech, 1971)

7 Van Valkenburg, M. E., 'Network Analysis', pp. 325–41, (Prentice-Hall, Englewood Cliffs, 1974)

Manuscript received by the Institution in final form on 10th November 1987
Paper No. 2329/M150

EFFICIENT USE OF ABSORBER IN SHIELDED ENCLOSURES USED FOR EMISSION MEASUREMENTS

By L. Dawson (Research Assistant) and Dr A. C. Marvin (Senior Lecturer) of the University of York

INTRODUCTION

It is shown that in the frequency range 30-200 MHz it is possible to damp the resonant modes in a screened room using a relatively small number of blocks of radio absorber placed at specific positions in the room. It is thus possible to carry out more accurate radiated emission measurements without a fully anechoic chamber.

Measurements of radiated emissions carried out in a screened room in the frequency range 30-200 MHz are subjected to large errors and uncertainties as each room acts as a waveguide cavity and therefore has a series of high Q resonances. Furthermore, measurements made on the same equipment in other rooms will not be the same because the resonant frequencies of rooms with different dimensions will differ.

A screened room can be made anechoic by placing absorber around the walls but in the frequency range of interest the depth of absorber required prevents this from being a practical solution in all but the largest and most expensive rooms.

Mode stirring techniques can be used at higher frequencies where the mode density of the room is high [1] but this technique requires the room to be specially adapted and also needs more computing power to analyse the resulting measurements. This paper describes the results of an investigation to provide a method of damping out the resonances without the need for costly adaptions to the room or complex manipulation of the measured results.

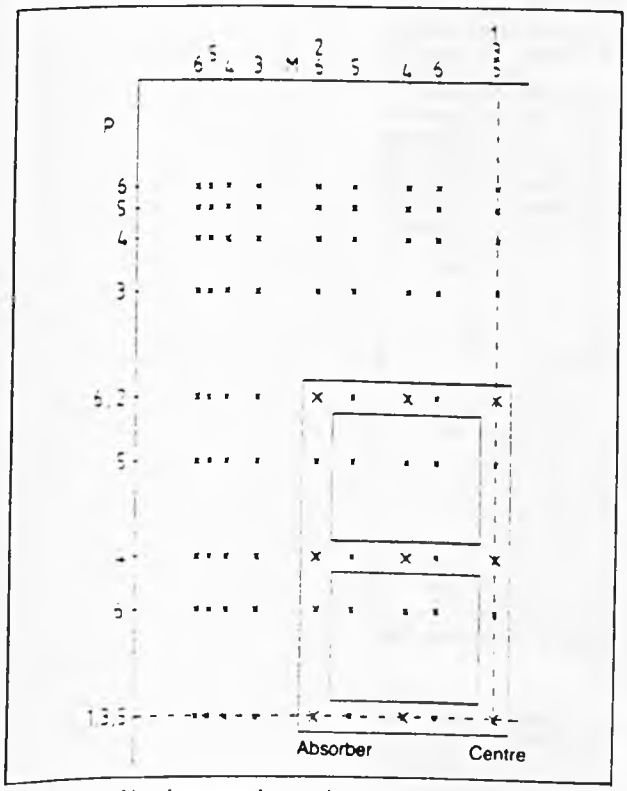

Fig 1. Plan of ¼ of a screened room showing the positions of the first 36 resonant modes in an empty rectangular cavity.

SAVING COST AND SPACE

An empty cavity of known dimensions has a series of resonant modes. The frequency of each of these modes can be calculated together with the positions of field maxima of each of the modes. Equation 1 describes the resonant frequencies for a rectangular cavity with dimensions a, b and d

$$F_{mnp} = \frac{1}{2\pi\sqrt{\mu}} \sqrt{\left(\frac{m}{a}\right)^2 + \left(\frac{n}{b}\right)^2 + \left(\frac{p}{d}\right)^2} \qquad 1.$$

Considering only TE modes with vertical electric fields, the first mode which resonates is the TE101 which has its electric field maximum in a line between the centres of the floor and ceiling. The TE201 and TE102 have their maxima half way between that and the side or end walls respectively. For modes where n=0 the field structure is more complex but still has maxima at positions on the floor of the room shown in fig.1.

Higher order modes have many electric field maxima but it is possible to show by symetry that there will be at least one maximum in each quarter of the floor area of the room or at least on one of the edges of that quarter. For each mode it is possible to reduce the Q of the resonance by placing some resistive material at the position of one of the maxima of that mode. It is therefore only necessary to place resistive material in one quarter of the room with the consequent saving in cost and space. Multilayer microwave absorber was used as the bulk resistive material for these experiments.

Fig. 2 shows the voltage received by a small magnetic loop placed on the back wall of the room to sense the surface magnetic field. The room is excited by a similar loop, fed with a constant amplitude swept voltage, also on the back wall (fig. 3). As well as cavity resonances some of the resonances shown in fig. 1 are TEM mode bench resonances [2], the frequency of these being determined by the bench dimensions. The Q of the bench resonances can be reduced by bonding the bench to the side walls of the room (fig.3) with a resistive material (60Ω/square) which loads the bench and attenuates waves propogating along it.

Fig 2. Surface current of a screened room, excited by a magnetic loop, as a function of frequency.

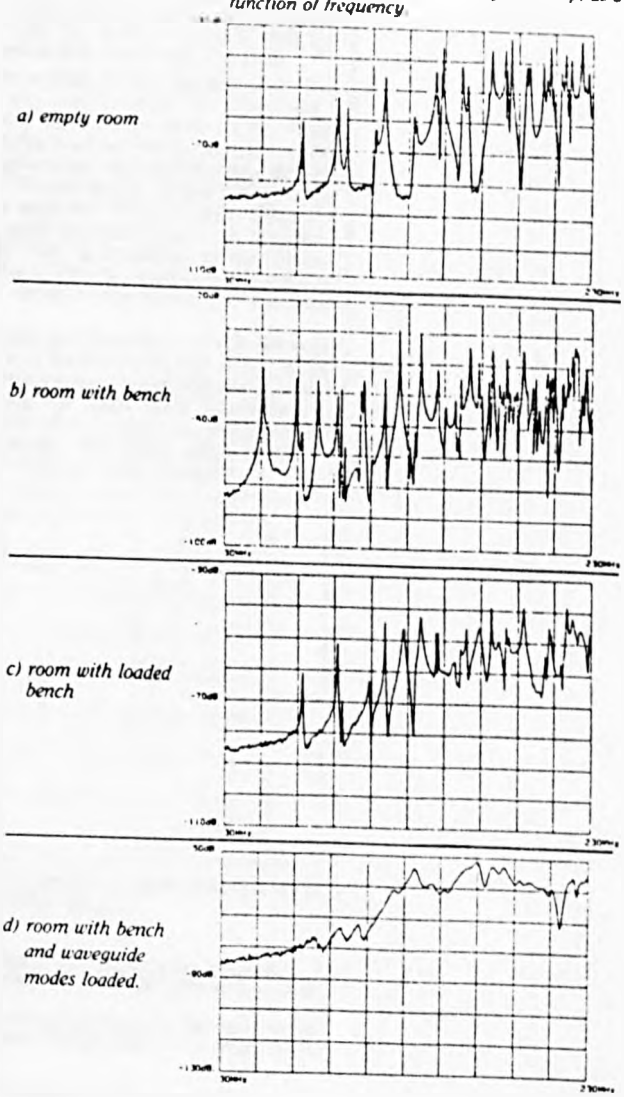

ABSORBER REQUIREMENTS

The bench alters the positions of the maximum E fields in each mode but in the half of the room remote from the bench they are moved by a very small amount and the absorber can be placed in the positions calculated and still give a very good degree of damping. The small room used for these experiments had absorber placed as shown in fig. 3. A larger room with more resonant modes will also need absorber to be placed in positions corresponding to the maxima of higher order modes which will fall within the frequency bands of interest as in fig. 2. It can be seen from fig. 2 that one maximum from each mode will be covered by absorber positioned as shown although for larger rooms more dividing sections will need to be added to the box shape.

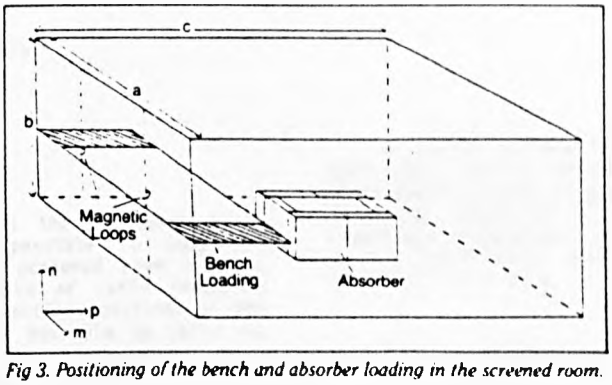

Fig 3. Positioning of the bench and absorber loading in the screened room.

The blocks of absorber are placed on edge so that as much of the absorber as possible is away from the metal walls where the tangential electric fields are zero. However they are not large enough to extend far enough into the room to coincide with the maxima of the TE0np or TEmn0 modes which can also exist.

Fig. 4 shows the results where a small electric dipole placed 10cm from the front of the bench was used to excite the room and a biconical dipole placed 1m away was used to measure the fields. Also, the absorber was raised off the floor so that the top edges of the blocks were half way up the height of the room and did coincide with the maxima of the TE0np and TEmn0 modes. Below 130 MHz the received signal strength shows relatively little deviation about the average increasing received signal predicted from the published antenna factor. The null at 140 MHz is dependent on the antenna position and as such it is possible to alter its depth and frequency by adjusting the position of the antenna, the tripod and the cable within the room.

The results shown in this paper are the results of a preliminary investigation. They show that it is possible to reduce the Q of the resonant modes in a screened room using a small number of blocks of absorber and without altering the room itself. Therefore it is possible, with suitable room calibration, to carry out more accurate emission measurements and predict the fields which would be radiated in free space without a fully anechoic chamber.

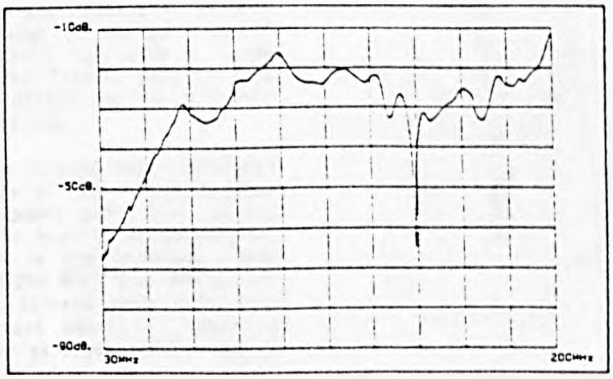

Fig 4. Fields measured by a biconical antenna in a screened room excited by a small electric dipole.

References

1. CORONA P., LATMIRAL G. and PAOLINI E.: 'Performance and analysis of a reverberating chamber with variable geometry', IEEE Trans EMC, 1980, vol 22, pp2-5.
2. MARVIN A.C. and STEELE L.: 'Improved techniques for the measurement of radiated emissions inside a screened room', Electronics letters, 1986, pp94-96.

Information: Dept of Electronics, University of York, YO1 5DD.

ALTERNATIVE METHODS OF DAMPING RESONANCES IN A SCREENED ROOM IN THE FREQUENCY RANGE 30 TO 200 MHz

L.Dawson and A.C.Marvin *

SUMMARY

It is shown that in the frequency range 30-200 MHz it is possible to damp the resonant modes in a screened room using a small number of blocks of radio frequency absorber placed at specific positions in the room. It is therefore possible to carry out more accurate emission measurements in a screened room without the need for a fully anechoic chamber.

1. Introduction

A screened room acts as a resonant cavity at frequencies with associated wavelengths of the same order as the dimensions of the room and less. For a typical room with dimensions of 2.5 × 2.5 × 5m this gives a fundamental resonance at about 75MHz. This frequency is below the lowest (about 200 MHz) at which it is easy to make such a room anechoic due to the depth of absorber required. Such absorber would fill a room this size and would need a large room to be practical. It would also be expensive due to the quantity of absorber required and the size of the empty room.

The resonances in such a room have a very high Q and give a great deal of uncertainty in an emission measurement carried out in the room (+/- 40dB). Due to the field distribution in a cavity resonator measurements are also not repeatable in such rooms as a small change in the position of the EUT or the antenna can give a large change in the measured fields. Results from various test houses differ due to different room sizes and positioning.

It is possible to use stirred mode techniques [1] to get a measure of the radiated power from a piece of equipment under test but for this the room must be heavily overmoded. For this to be possible in the frequency range under discussion (30-200 MHz) this would need a very large room. Stirred mode techniques also require a certain amount of computing power and take longer as measurements need to be averaged over a period of time.

The object of the research described in this paper was to determine a test method which could be used in a screened room in the frequency range 30 to 200MHz to give a repeatable measurement which can be related to the fields which would be measured on an open field test site.

2. The screened room as a resonant cavity

As stated in the introduction an empty screened room can be treated as a cavity resonator. As such it is possible to calculate the field distributions for the various resonant modes as well as the resonant frequencies [2] which are given by equation 1.

$$F_{mnp} = \frac{1}{2\sqrt{\varepsilon\mu}}\sqrt{\left[\frac{m}{a}\right]^2+\left[\frac{n}{b}\right]^2+\left[\frac{p}{d}\right]^2} \qquad 1.$$

where m,n,p are positive integers, one of which may be 0
and a,b,d are the room dimensions

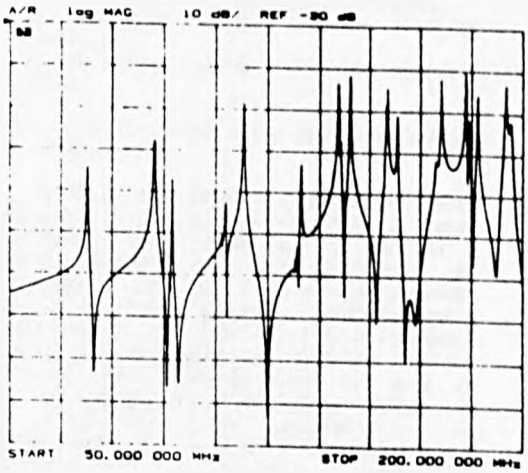

Fig.1 Frequency response of a room excited with a small magnetic loop.

* University of York

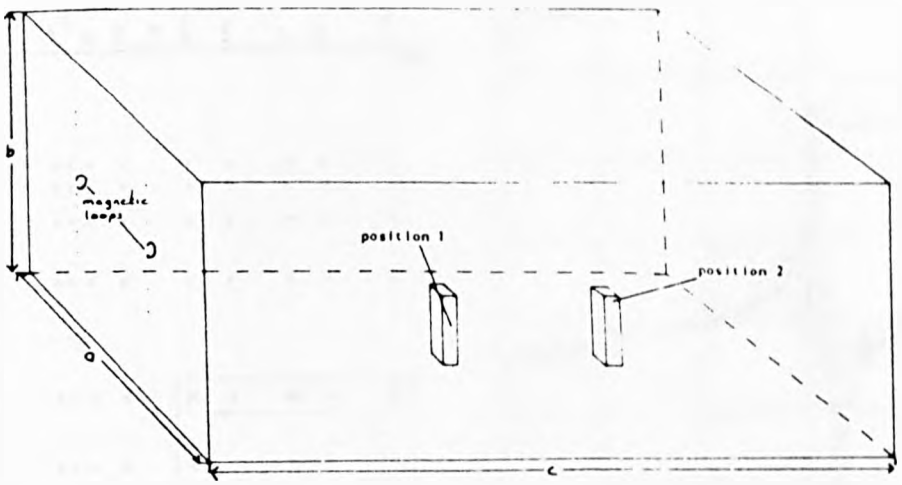

Fig.2 Layout of room showing positions of loops and positions 1 and 2 for absorber.

Fig.1 shows the frequency response of a room excited with a small magnetic loop on the back wall with the surface currents measured with a similar loop (fig.2). Comparison of the measured resonances with those calculated from equation 1 shows that the two sets are very close. Several of the modes which are calculated to be degenerate (have the same frequencies) can be seen to be slightly different. Differences which can be seen between the measured and calculated response can be explained by the following:-

a) The room has a series of ridges inside which give structural support (the model assumes a smooth internal surface).

b) There is a wooden floor in the room which acts as a dielectric slab and has been ignored in the calculations.

3. Reducing the Q of resonances

The Q of a resonance is given by equation 2.

$$Q = \frac{2\pi \times \text{the average energy in the room}}{\text{the energy dissipated in one cycle}} \qquad 2.$$

To flatten the frequency response of the room it is necessary to reduce the Q of the resonances. From equation 2 this can be done by removing energy from the resonances (from equation 2). This can be done in two ways as the energy in the resonator is alternately stored in the electric and magnetic fields:-

a) absorbing energy from the electric fields.

b) absorbing energy from the magnetic fields.

Initially a technique using the first method was investigated.

A lossy or conductive dielectric will absorb energy from a changing electric field [3]. Carbon loaded foam such as AN79 is a readily available conductive dielectric. It is normally used as a microwave absorber where it is placed against a conducting wall and presents a near free space wave impedance so that incident waves are absorbed and not reflected. This absorber does not work as well at frequencies below about 500MHz. At the frequencies under consideration the apparent wave impedance of the absorber when against a conducting surface is lower than that of free space so that waves will be reflected. However, in the cavity resonator energy is being absorbed from standing waves so this is not such a problem providing the presence of the absorber does not perturb the fields more than a minimum amount.

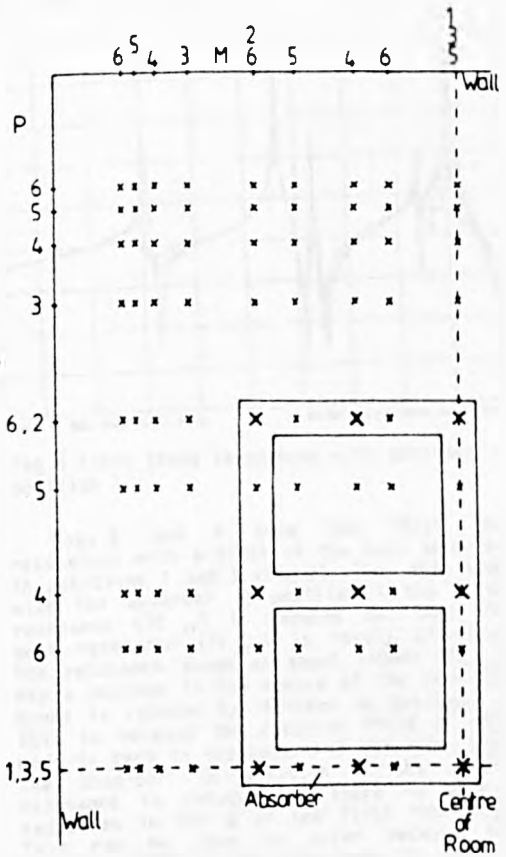

Fig.3 Positions of electric field maxima, of first 36 modes, on floor of room.

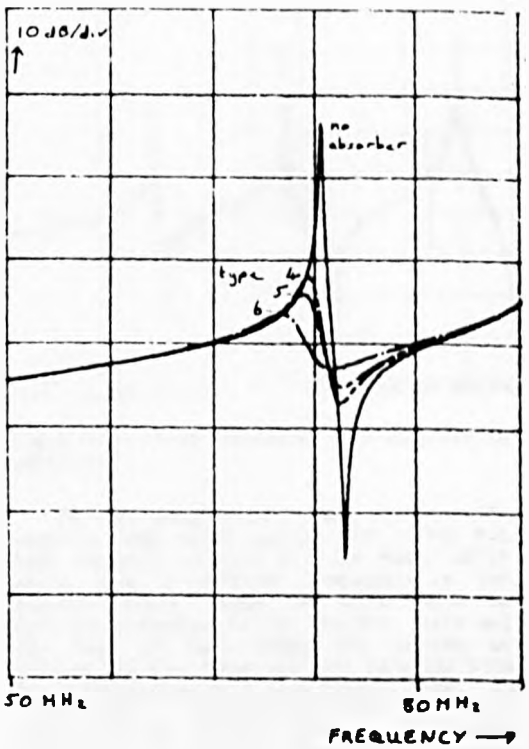

Fig.4 First resonance with increasing conductivity absorber column in centre of room.

To absorb the maximum energy from the fields the lossy material should be placed at field maxima, the positions of which are easily calculated [4]. The positions of the electric field maxima of the first 36 modes with vertical electric fields are shown in fig.3. This figure shows a map of one quarter of the floor area of the cavity as the system is symmetrical for a rectangular cavity. It can be seen that most modes have more than one maximum, but to remove energy it is only necessary to place the dielectric on one of them. This can be done by placing absorber in the positions shown in fig.3. When arranged this way the absorber is only positioned in one quarter of the room with a consequent saving in cost and space. Higher modes will have at least one maximum which falls within the overall area covered by the box shape and will need only one extra dividing section added so that the shape is easy to build up. Many higher modes will have maxima which coincide with the absorber positions as shown.

Six blocks of absorber with conductivities corresponding to the 6 different layers of AN79 were specially constructed for this work. They are labelled 1 to 6 in order of increasing conductivity. Fig.4 shows the first resonant mode with blocks of carbon loaded foam with different conductivities placed in the centre of the room. It can be seen that there is a reduction in the Q of the resonance for increasing conductivity. Maximum energy dissipation occurs when $\sigma = \omega\varepsilon$ which cannot be chosen for all frequencies due to the range of frequencies the loading must operate over. The conductivity must be chosen so that enough energy is absorbed at each frequency so that the Q of each resonance is low enough for the resonances to merge together and give a resonably flat response.

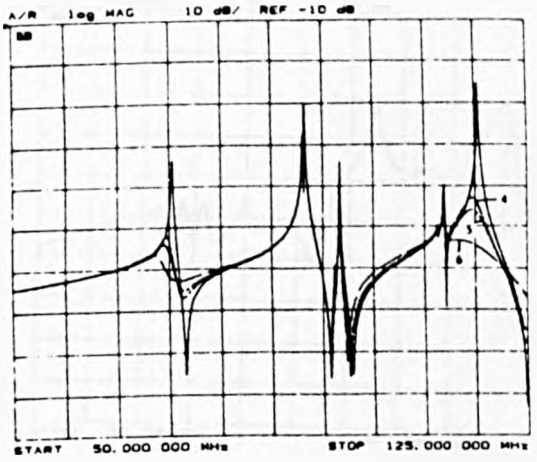

Fig.5 First three resonances with absorber in position 1.

Fig.6 First three resonances with absorber in position 2.

Figs.5 and 6 show the first few resonances with a block of the best absorber in positions 1 and 2 (fig.2). They show that with the absorber in position 1 the first resonance (TE_{101}) is reduced but that the next resonance (TE_{201}) is hardly affected. The resonance shown at about 110MHz (TE_{103}) has a maximum in the centre of the room and hence is reduced by absorber in position 1. This is because the electric field of this mode is zero in the centre of the room. With the absorber in position 2 the second resonance is reduced but there is also a reduction in the Q of the first resonance. This can be seen to occur because the electric field of the first mode is non-zero at position 2.

For the measurements shown so far, the magnetic loop which excites the fields has been arranged so that all the modes which exist have a vertical component to the electric field. Modes can exist with no vertical component to the electric field and for some of these modes the columns of absorber on the floor will not coincide with field maxima and will have little effect. To improve the performance of the absorber on these modes the absorber needs to be arranged so that it has the same effect in all directions. This can be done by constructing the whole load as is shown in fig.7 and raising it off the floor so that one corner is in the very centre of the room. Fig.8 shows the response with the full load raised off the floor. The loops were orientated so that all modes were excited.

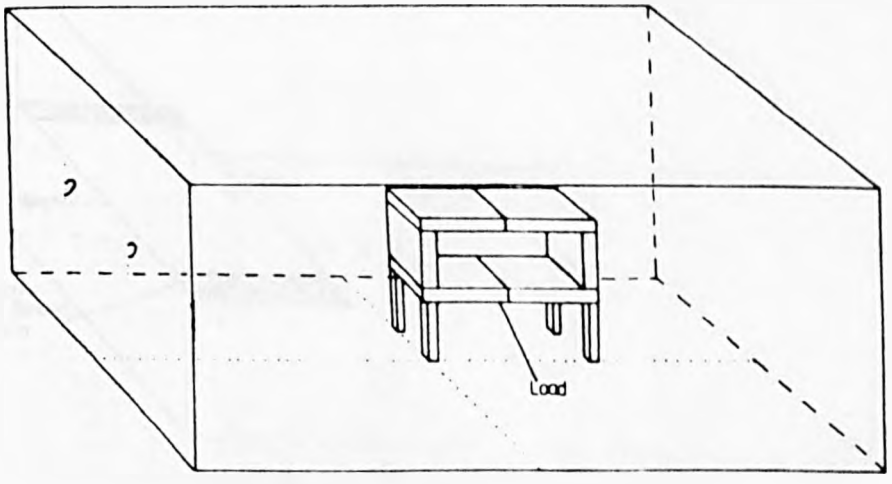

Fig.7 Position and layout of full load raised off floor.

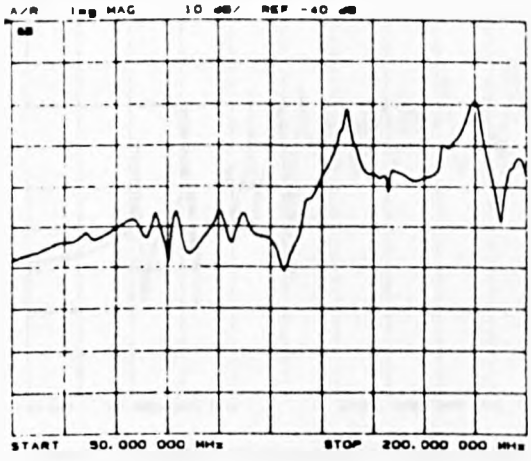

Fig.8 Frequency response with full load raised.

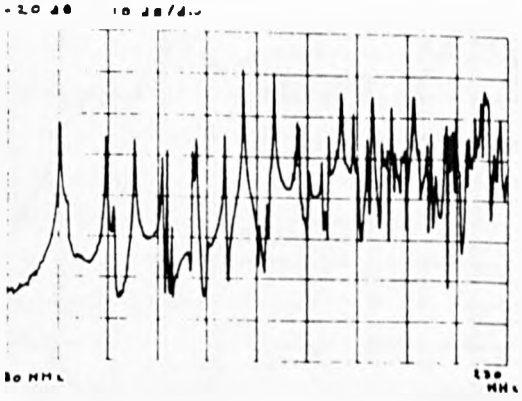

Fig.9 Frequency response with bench in room (no load).

4. Results in a room with a bench

When the conductive bench is included in the room (bonded to the wall below the loops) an extra set of resonances can be observed (fig.9). This is due to the bench acting as a TEM transmission line which is open circuit at one end and short circuit at the other [5]. Such a line has a series of resonances which can be reduced in two ways:-

a) terminate the line in its characteristic impedance.
b) load the line to make it lossy.

The bench is bonded to the back wall at three places so that waves can propagate on the bench in two directions. Bonding the bench to the walls with 60Ω/square conductive sheet (fig.10) reduces the resonances in both directions and examining the frequency response with this (fig.11) shows that it is now very similar to the empty room at the lower frequencies. The differences at the higher frequencies can be put down to the field perturbations caused by the bench itself.

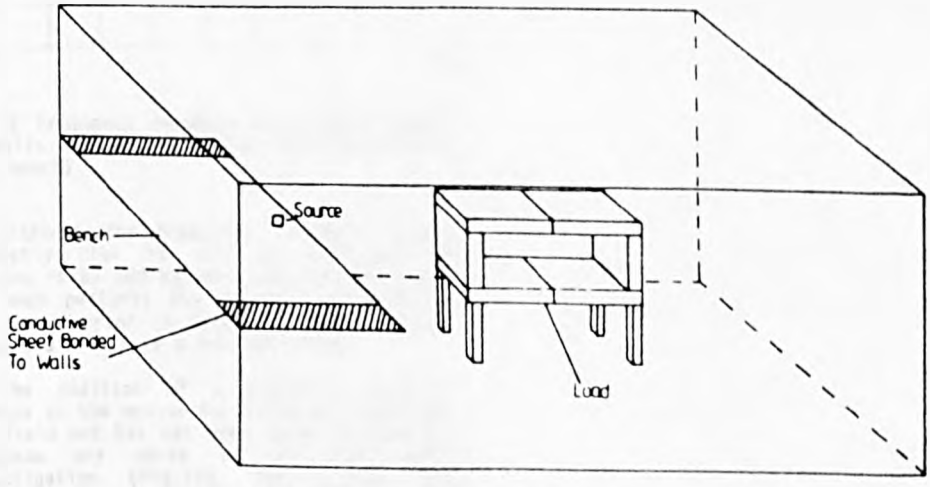

Fig.10 Position of conductive sheet bonding bench to walls.

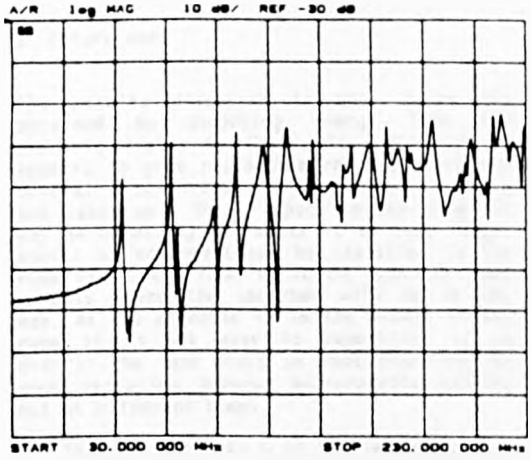

Fig.11 Frequency response with bench bonded to walls.

The bench perturbs the fields in the cavity, hence the positions of the electric field maxima will be different. However if the resistive load is placed in the portion of the room remote from the bench a reasonably flat response (fig.12) is still obtained as the field maxima are not far away from the original positions.

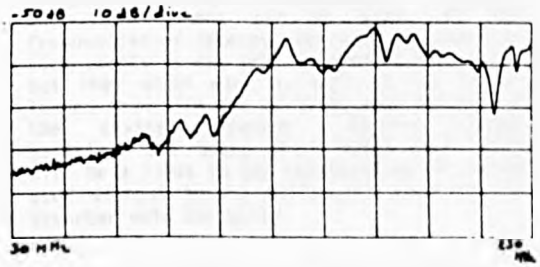

Fig.12 Frequency response with bench bonded to walls and full load in room (end remote from bench).

Although the frequency response is not perfectly flat it will be difficult to improve it by adding more absorber as adding too much perturbs the fields in the cavity and the absorber is then not in the optimum place and will have a reduced effect.

The addition of a standard biconical antenna as the measuring device also perturbs the field but has not been found to make the response any worse in the room under investigation (fig.13). The antenna was placed 1m from the source (a small electric dipole .1m from the front of the bench).

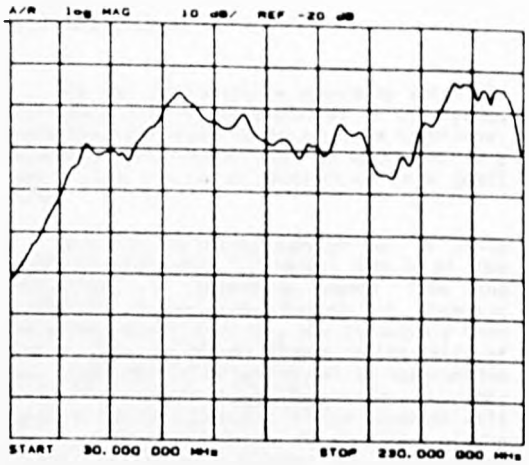

Fig 13 Frequency response with bench bonded to wall and full load in room with biconic antenna as field transducer.

In an unloaded room a small change in position of either the source or measuring device can give a large change in the voltage output by the antenna. With the bench and room loaded as described in this paper the test method is not as senstive to the positioning of the two elements, which therefore enables measurements which are made at different times to be compared more realistically.

5. Future work

The results discussed in this paper are obtained by absorbing energy from the electric fields in the cavity. Although it appears to give reasonable results there are several disavantages. The absorber is bulky and takes up a lot of space in the room. It may be necessary to remove it so that larger pieces of equipment can be installed in the room or if the room is to be used for some purpose where the absorber will be in the way. As the absorber is in the middle of the room it is not easy to reposition it in exactly the same place so that there may be some variation between measurements carried out at different times.

Theoretically the Q of the resonances can be reduced by absorbing energy from the magnetic fields. All the modes have magnetic fields which have maxima parallel and adjacent to the room walls. The positioning of the magnetic field maxima can be calculated in a similar way to that used for the electric field maxima . If a material can be produced which absorbs energy from varying magnetic fields it can be placed on the walls and ceiling of the room where it will not be an obstruction and can probably be left in position permanently.

Various magnetic materials exist. Ferrite materials are often used in wave absorbers which are generally used at higher frequencies where the wavelength is shorter and thin sheets can be used. At the frequencies of interest the wave impedance of such sheets is not well matched to free space but they might work as well as the carbon loaded foam with the standing wave pattern in the cavity resonator. Ferrite loaded materials are heavy which means that there will be a limit to the thickness which can be used without having difficulty securing the absorber onto the walls.

Several materials are under investigation to find one which will absorb enough energy to give a reasonably flat frequency response. Initial measurements indicate that energy can be absorbed this way and methods of increasing the energy dissipation using magnetic materials are under investigation.

6. Conclusions

The use of resistive absorbing materials to reduce the Q of resonances in a screened room has been shown to be a viable technique. However, the absorber used is bulky and in a small room can be an obstruction in a small room.

Work is now being carried out on using magnetic absorbers to reduce the Q of the resonances by absorbing energy from the magnetic fields. The nature of magnetic absorbers means that they are relatively thin and as they can be positioned on the walls of the room they will be less of an obstruction than the carbon loaded foam. Also, as they are thinner the presence of the absorber will have a reduced effect on the positions of the fields in the room so that the field maxima may be closer to that calculated than is the case with the electric field loading.

References

1. 'Performance and analysis of a reverberating with variable geometry' P.Corona, G.Latmiral, E.Paolini, IEEE trans EMC vol 22, August 1980, pp2-5

2. 'Microwave devices and circuits' S.Y.Liao, Prentice Hall 1980, pp130-137

3. 'Electromagnetics' J.D.Kraus, Mcgraw Hill 1984, pp346-349

4. 'Fields and waves in communication electronics' Ramo, Whinnery, Van Duzer, Whiley 1965, pp534-548

5. 'New screened room techniques for the measurement of RFI' L.Dawson, A.C.Marvin, Fifth international conference on EMC. October 1986

Acknowledgement

We would like to thank Emerson and Cuming for their help and the provision of materials which have been used for this work.

TECHNIQUES FOR DAMPING RESONANCES IN SCREENED ROOMS IN THE FREQUENCY RANGE 30 TO 200 MHZ

L. Dawson and A.C. Marvin, University of York

SUMMARY

It is shown that in the frequency range below 200 MHz it is possible to damp the resonant modes in a screened room using either a small number of blocks or dissipative dielectric material placed at specific positions within the room volume or a small area of dissipative permeable material placed on the room walls. A fully anechoic chamber is therefore not required for emission measurements.

1. Introduction

A screened room acts as a resonant cavity at frequencies with associated wavelengths of the same order as the dimensions of the room and less. For a typical room with dimensions of 2.5 x 2.5 x 5 m this gives a fundamental resonance at about 75 MHz. This frequency is below the lowest (about 200 MHz) at which it is easy to make such a room anechoic due to the depth of absorber required. Such absorber would fill a room this size and would need a large room to be practical. It would also be expensive due to the quantity of absorber required and the size of the empty room.

The resonances in such a room have a very high Q and give a great deal of uncertainty in an emission measurement carried out in the room (± 40 dB). Due to the field distribution in a cavity resonator measurements are also not repeatable in such rooms as a small change in the position of the Equipment under Test (EUT) or the antenna can give a large change in the measured fields. Results from various test houses differ due to different room sizes and positioning.

It is possible to use stirred mode techniques to get a measure of the radiated power from a piece of equipment under test but for this the room must be heavily overmoded. For this to be posible in the frequency range under discussion (30-200 MHz) this would need a very large room. Stirred mode techniques also require a certain amount of computing power and take longer as measurements need to be averaged over a period of time.

The object of the research described in this paper was to determine a test method which could be used in a screened room in the frequency range 30 to 200 MHz to give a repeatable measurement which can be related to the fields which would be measured on an open field test site.

2. The screened room as a resonant cavity

As stated in the introduction an empty screened room can be treated as a cavity resonator. As such it is possible to calculate the field distributions for the various resonant modes as well as the resonant frequencies which are given by Equation (1)

$$F_{mnp} = \frac{1}{2\sqrt{\epsilon\mu}} \sqrt{\left[\frac{m}{a}\right]^2 + \left[\frac{n}{b}\right]^2 + \left[\frac{p}{d}\right]^2} \qquad (1)$$

where m, n, p are positive integers, one of which may be 0, and a, b, d are the room dimensions.

Fig. 1 shows the frequency response of a room excited with a small magnetic loop on the back wall with the surface currents measured with a similar loop. Comparison of the measured resonances with those calculated from Equation (1) shows that the two sets are very close. Several of the modes which are calculated to be degenerate (have the same frequencies) can be seen to be slightly different. Differences which can be seen between the measured and calculated response can be explained by the following:

(a) The room has a series of ridges inside which give structural support (the model assumes a smooth internal surface).

(b) There is a wooden floor in the room which acts as a dielectric slab and has been ignored in the calculations.

3. Reducing the Q of resonances

The Q of a resonance is given by Equation (2).

$$Q = \frac{2\pi \times \text{the average energy in the room}}{\text{the energy dissipated in one cycle}} \qquad (2)$$

To flatten the frequency response of the room it is necessary to reduce the Q of the resonances. From Equation (2) this can be done by removing energy from the resonances (from Equation (2)). This can be done in two ways as the energy in the resonator is alternately stored in the electric and magnetic fields:

(a) absorbing energy from the electric fields

(b) absorbing energy from the magnetic fields

A lossy or conductive dielectric will absorb energy from a changing electric field. Carbon loaded foam such as AN79 is a readily available conductive dielectric. It is normally used as a microwave absorber where it is placed against a conducting wall and presents a near free space wave impedance so that incident waves are absorbed and not reflected. This absorber does not work as well at frequencies below about 300 MHz. At the frequencies under consideration the apparent wave impedance of the absorber when against a conducting surface is lower than that of free space so that waves will be reflected. However, in the cavity resonator energy is being absorbed from standing waves so this is not such a problem providing the presence of the absorber does not perturb the fields more than a minimum amount.

To absorb energy from the electric fields a dielectric load can be designed which ensures that some dielectric material is present at the position of at least one electric field maximum for each of the resonant modes present within the frequency range. The pattern of field maxima within a rectangular chamber means that the load, shown in Fig. 2, only occupies part of one-eighth of the room volume.

To absorb energy from the magnetic fields dissipative permeable material must be placed at positions of magnetic field maxima using the same criteria. In this case, unlike the electric field case, each mode has some of its magnetic field maxima adjacent to the conducting walls, with corresponding electric current maxima on the walls. In this way a minimum amount of ferrite material can be used. Typical wall coverages for acceptable results are in the order of 3% of the room surface area.

4. Results in a room with a bench

When the conductive bench is included in the room (bonded to the wall below the loops) an extra set of resonances can be observed (Fig. 3). This is due to the bench acting as a TEM transmission line which is open circuit at one end and short circuit at the other. Such a line has a series of resonances which can be reduced in two ways:

(a) terminate the line in its characteristic impedance

(b) load the line to make it lossy

The bench is bonded to the back wall at three places so that waves can propagate on the bench in two directions. Bonding the bench to the walls with 60 Ω/square conductive sheet (Fig. 4) reduces the resonances in both directions and examining the frequency response with this (Fig. 5) shows that it is now very similar to the empty room at the lower frequencies. The differences at the higher frequencies can be put down to the field perturbations caused by the bench itself.

5. Comparison of loading types

Results are presented for three cases.

(a) 2.5 m x 2.5 m x 5 m room with conducting bench loaded with conductive sheet, and with dielectric load (Fig. 6).

(b) 2.5 m x 2.5 m x 5 m room with conducting bench loaded with conductive sheet and with permeable load on walls (Fig. 7).

(c) 2.5 m x 2.5 m x 2.5 m room with permeable load on walls (Fig. 8).

In these experiments the EUT is simulated by a controlled source in the form of a short monopole antenna. The sense antenna is a standard biconical antenna placed 1 m from the EUT.

In each case it can be seen that the frequency response of the room is much smoother with excursions from the mean response of less than ± 10 dB compared with ± 30 dB for the unloaded rooms. This is achieved in small rooms with minimal amounts of lossy material at frequencies below that for which anechoic behaviour is possible.

6. Conclusions

We have demonstrated that it is possible to achieve pseudo-anechoic behaviour in a resonant screened room using small amounts of properly placed dissipative material. If the rooms were made anechoic for UHF frequencies in the conventional way, then our results would be improved further. In the case of the permeable material the technique is non-invasive and the absorption mechanism is different. Conventional anechoic material used for UHF could be overlayed on the tiles giving very wide frequency range anechoic performance.

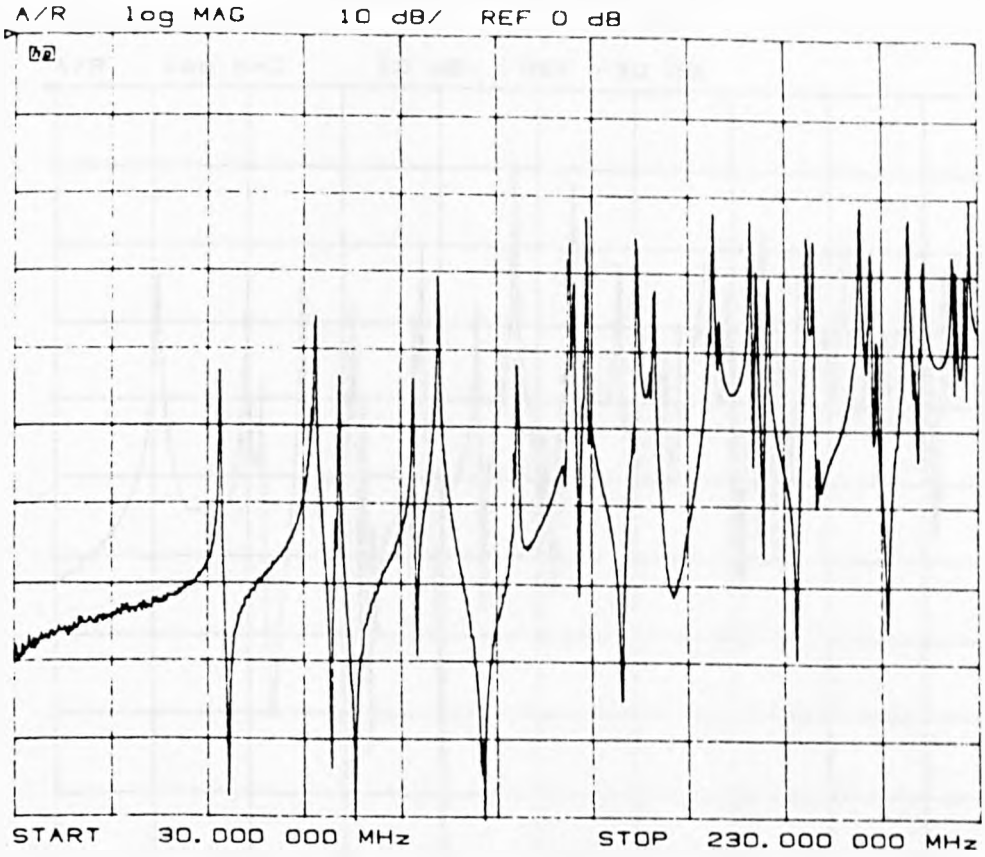

Fig. 1 Frequency response of empty room

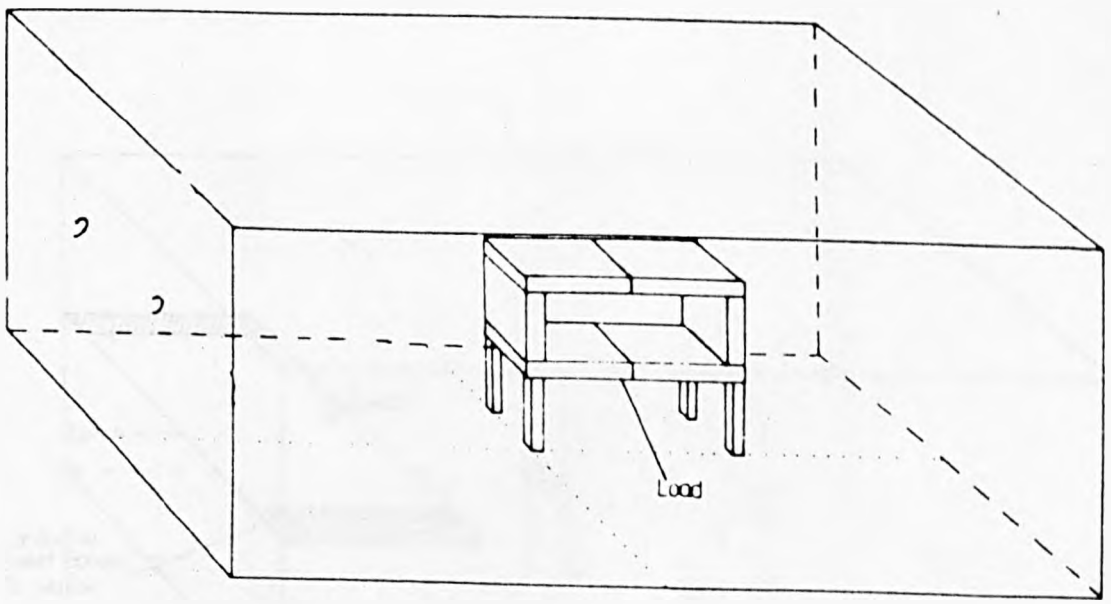

Fig.2 Positioning of dielectric absorber

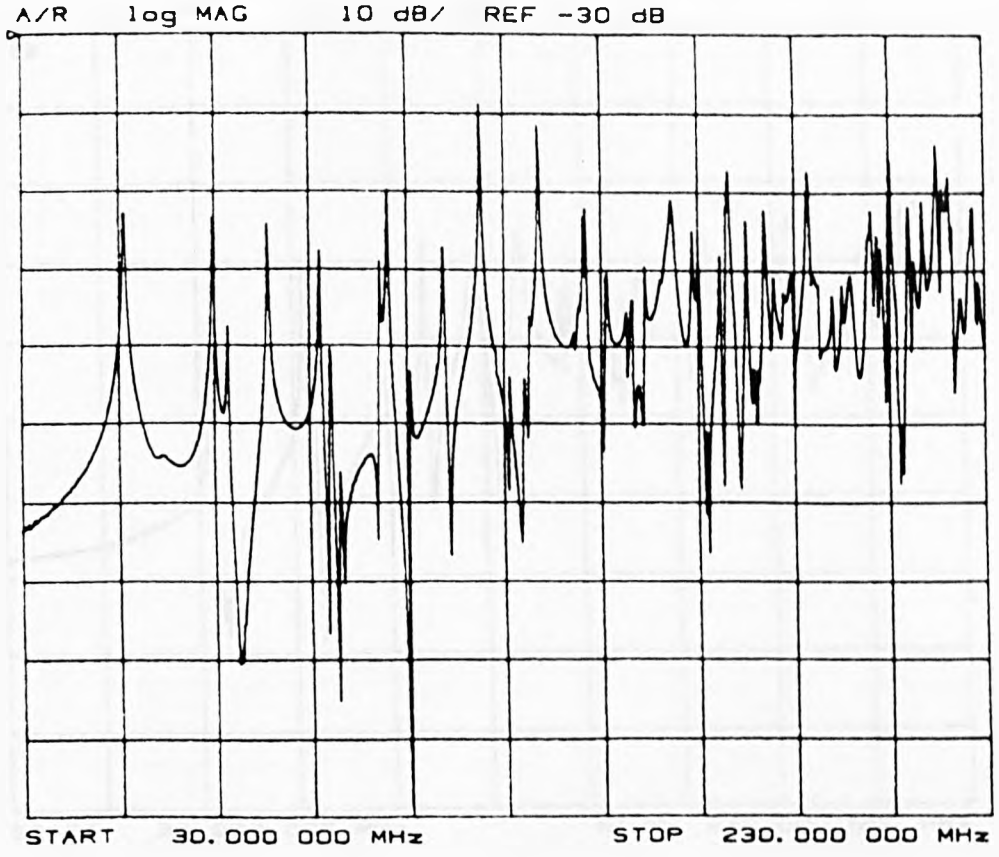

Fig.3 Frequency response with conductive bench in position

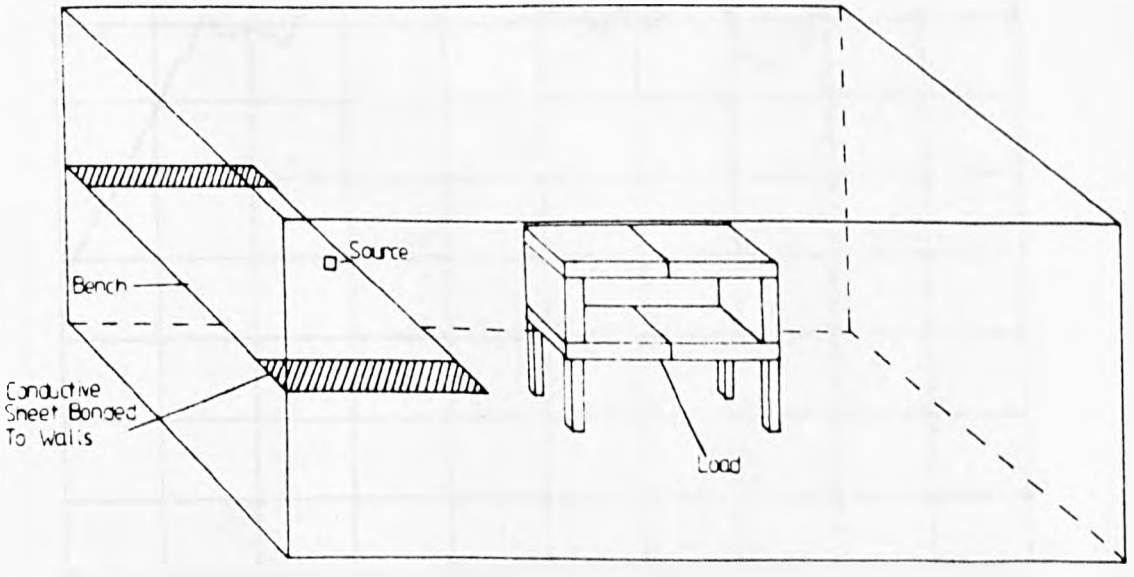

Fig.4 Method of bonding the bench to the walls

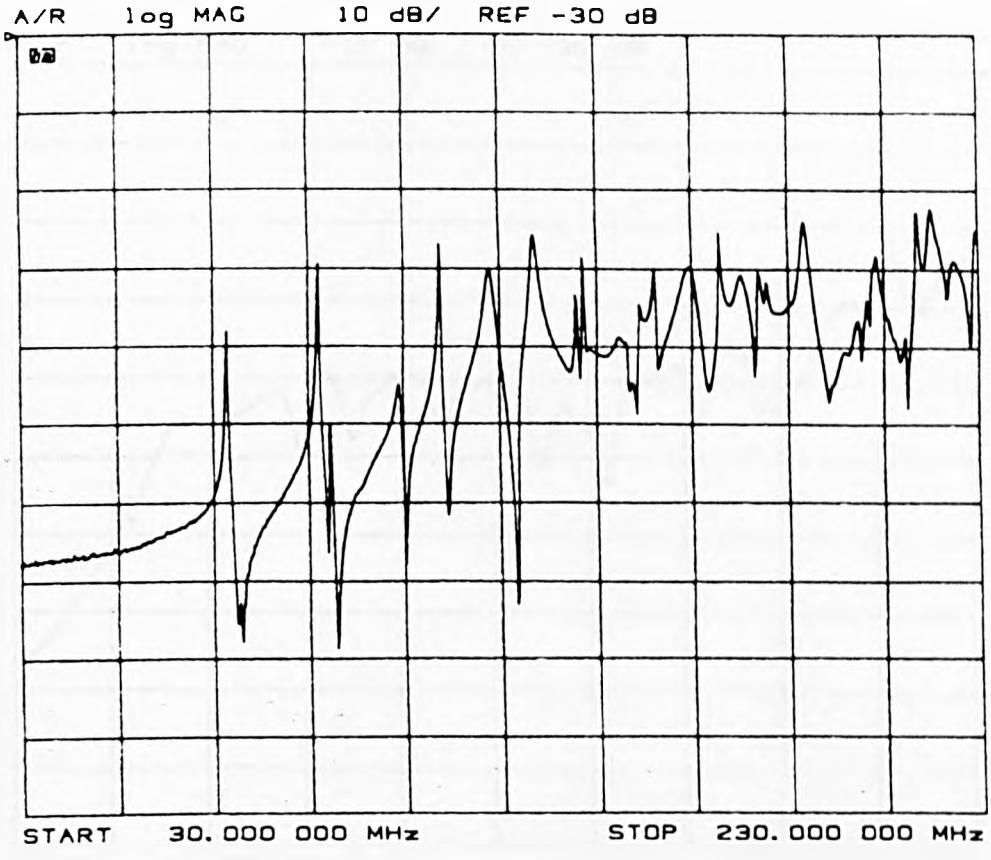

Fig.5 Frequency response with bench in place

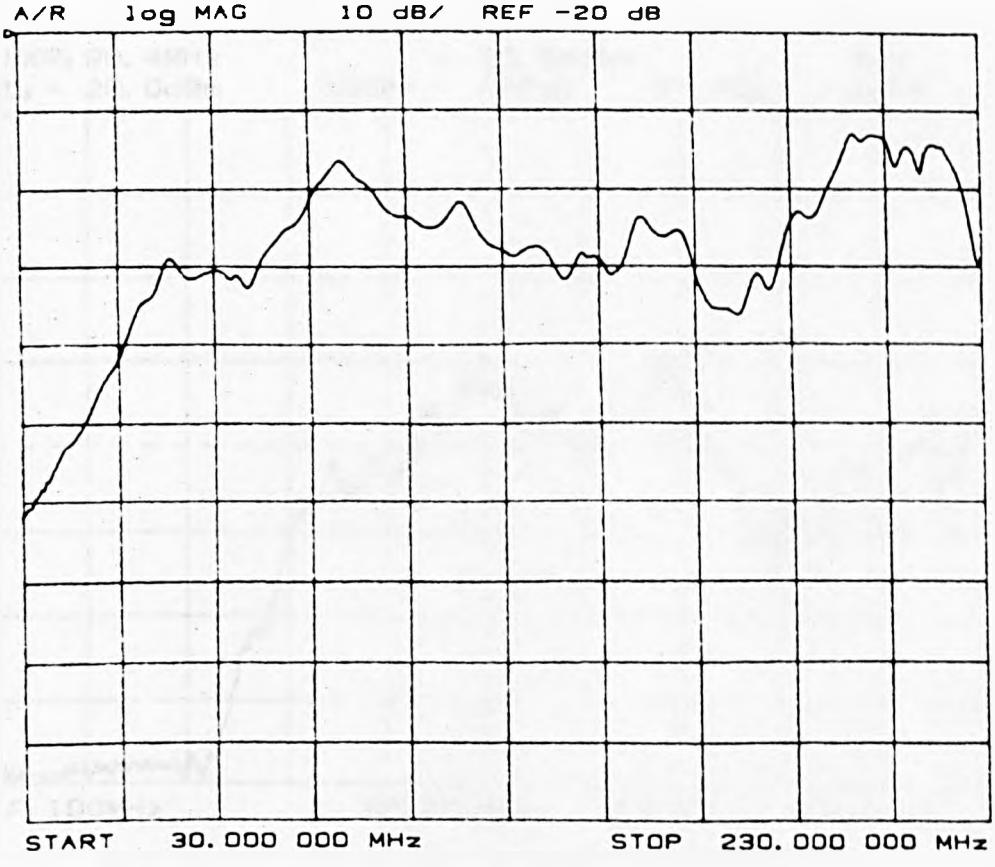

Fig.6 Larger room with full dielectric load

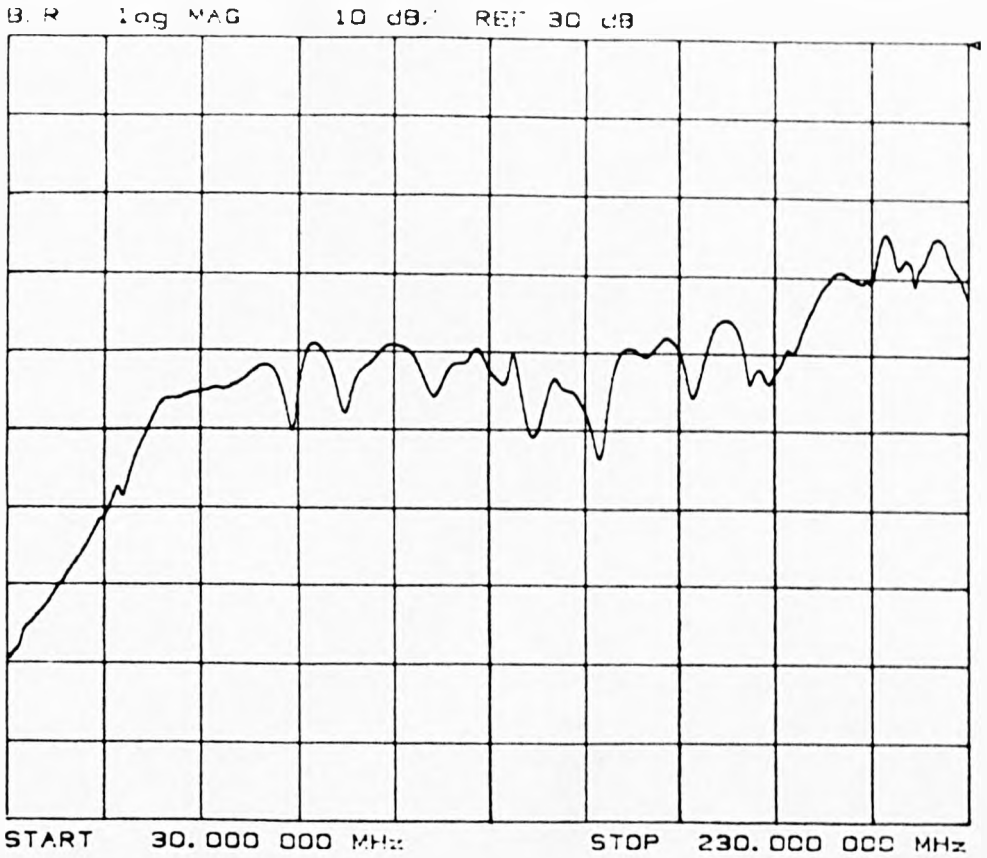

Fig.7 Large room with magnetic load

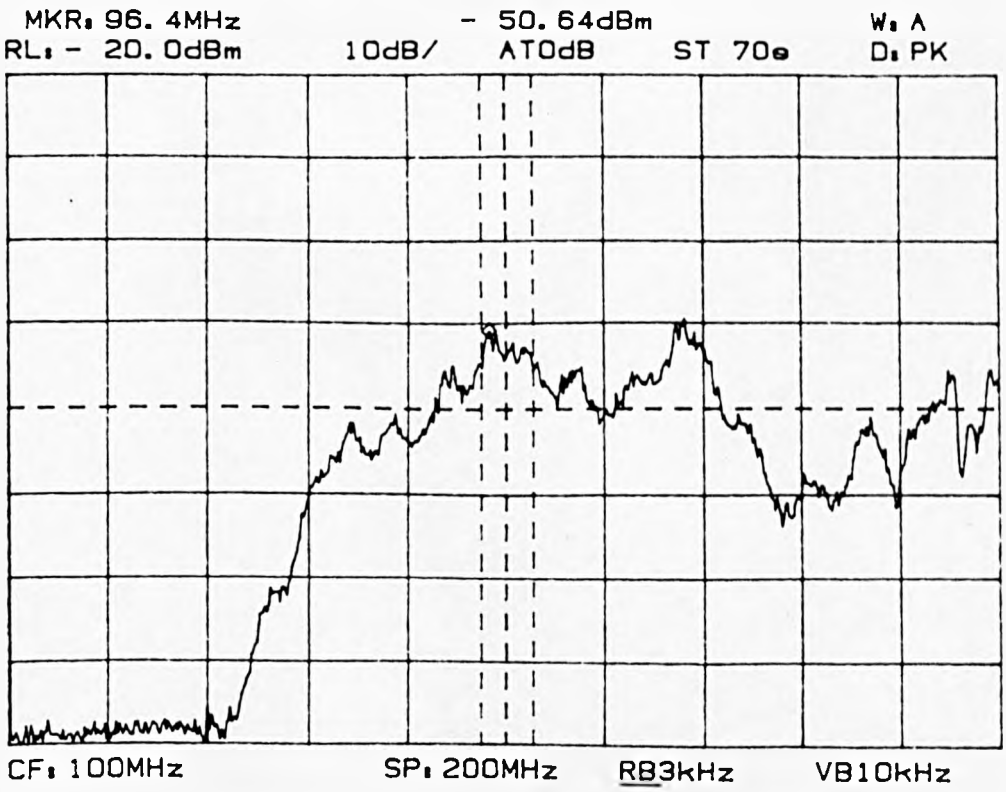

Fig.8 Small room with non-conducting bench (magnetic load)